ISSUE RESOLUTION STATUS REPORT

KEY TECHNICAL ISSUE:
STRUCTURAL DEFORMATION AND SEISMICITY

Division of Waste Management
Office of Nuclear Material Safety and Safeguards
U. S. Nuclear Regulatory Commission

Revision 2

AUGUST 1999

301---------------------------Q199908260003

MM 1402-471-910: IRSR KTI: Structural
Deformation and Seismicity

TABLE OF CONTENTS

Section

TABLE OF CONTENTS (cont'd)

Section

TABLE OF CONTENTS (cont'd)

Section

FIGURES

FIGURES (cont'd)

TABLES

ACKNOWLEDGMENTS

This and the previous reports were prepared jointly by the U.S. Nuclear Regulatory Commission (NRC) and the Center for Nuclear Waste Regulatory Analyses (CNWRA) staffs. Primary authors of this report are Philip S. Justus (NRC), John A. Stamatakos (CNWRA) [co-leads], and [in alphabetical order] David A. Ferrill (CNWRA), Abou-Bakr K. Ibrahim (NRC), H. Lawrence McKague (CNWRA), and Darrell Sims (CNWRA). Contributions were also made by William M. Dunne, Deborah Waiting, Peter La Femina, Ronald H. Martin, Alan Morris (University of Texas at San Antonio) and Mary Beth Gray (Bucknell University). The primary authors of appendix E are Gerry L. Stirewalt (MANDEX, Inc.), Darrell Sims (CNWRA), Alan P. Morris (University of Texas at San Antonio), under the direction of Abou-Bakr K. Ibrahim (NRC).

The authors thank C. William Reamer (NRC), David J. Brooks (NRC), Charles B. Connor (CNWRA), Goodluck Ofoegbu (CNWRA), Simon Hsiung (CNWRA), Amitava Ghosh (CNWRA), Randall Fedors (CNWRA), Gordon Wittmeyer (CNWRA), Budhi Sagar (CNWRA), and James R. Firth (NRC) for their useful reviews. Discussions with other technical staff at CNWRA was also appreciated. Editorial and document preparation assistance by Annette Mandujano (CNWRA) greatly improved the quality of the document. Mrs. Mandujano's skills in coordinating, word processing, graphics layout, and producing the manuscripts won the authors' admiration.

QUALITY OF DATA, ANALYSES, AND CODE DEVELOPMENT

Data: CNWRA-generated original data contained in this report meet quality assurance (QA) requirements described in the CNWRA QA manual. Sources for other data should be consulted for determination of the level of quality of those data.

ANALYSES AND CODES: The software 3DSTRESS, Version 1.3, was used for some analyses in this report. Version 1.3 fulfills the CNWRA Technical Operations Procedure (TOP-018) Development and Control of Scientific and Engineering Software. The TPA code, Version 3.2.3, was used for faulting analyses in this report. This code has also been placed under the CNWRA TOP-018 control.

1.0 INTRODUCTION

1.1 PURPOSE

Issue Resolution Status Reports (IRSRs) are written to provide the U.S. Department of Energy (DOE) with feedback regarding the adequacy of its program before the license application is submitted. IRSRs are the primary way that the staff provides DOE feedback on the subissues making up the Key Technical Issues (KTIs). IRSRs are comprised of: (1) acceptance criteria (AC) and review methods (RMs) (i.e., review guidance) that will be used by the staff to review the DOE license application and prelicensing submittals, and that indicate the basis for resolution of the subissue; and (2) a report of the status of resolution. Open meetings, site visits, and technical exchanges with the DOE provide opportunities to (1) discuss issue resolution, (2) identify areas of agreement and disagreement, and (3) develop plans to resolve such disagreements. In turn, DOE commented on Revision 1 of the IRSR.

In addition to providing feedback to the DOE, the IRSRs contain guidance for the staff's review of DOE license application and sufficiency report. The staff also plans to use the IRSRs in developing of the Yucca Mountain Review Plan (YMRP) for the repository license application for the repository license application. This revision of the Structural Deformation and Seismicity (SDS) IRSR was written during the initial development of concepts for the YMRP. It was recognized that some of the material in the IRSRs, specifically the AC and the RMs, will be incorporated into the YMRP when it is developed. Five uniform ACs (see section 4.1) are under consideration for the YMRP.

In this IRSR, staff decided that the ACs of SDS IRSR Revision 1 would form the basis for development of the RMs. These RMs would then be used to assess the uniform ACs. While it is anticipated that the format and structure for the development of ACs and RMs will change, technical basis for subissue resolution will change only when new information, data, interpretations and models become available. Full implementation of this methodology will follow in the YMRP and Revision 3 of the SDS IRSR.

Consistent with NRC regulations on prelicensing consultations and a 1992 agreement with the DOE, staff-level issue resolution can be achieved during the prelicensing consultation period. Such resolution at the staff level does not preclude the issue from being considered during the licensing proceedings. Issue resolution at the staff level during prelicensing is achieved when the staff has no further questions or comments, regarding how the DOE program is addressing an issue. There may be some cases where resolution at the staff level may be limited to documenting a common understanding regarding differences in NRC and DOE points of view. Pertinent additional information could raise new questions or comments regarding a previously resolved issue.

This IRSR documents the status of resolution of SDS subissues that are significant to performance evaluations of a candidate high-level radioactive waste repository at Yucca Mountain (YM). Parts of the subissues are resolved at the staff level, and the bases for resolution are provided. For parts of those subissues unresolved at the staff level, the bases for that status are provided along with at least one mechanism for achieving resolution. Further, this report ensures that: (1) all significant issues are related to tectonics, seismotectonics, faults, and fractures are identified and adequately characterized; and (2) their significance is sufficiently understood, fully considered, and appropriately used to evaluate long-term performance and as input to an adequate repository design by the DOE.

Regulatory attention is focused where KTIs and attendant technical uncertainties will have the greatest effect on the assessment by annual radiological dose. This risk-informed approach is implemented by identifying those events and processes that have sufficient probability of occurrence during the time period of interest and multiplying these probabilities by their dose-consequences. The significance of the risks during to post-closure performance can then be evaluated.

1.2 SCOPE OF KEY TECHNICAL ISSUE

The scope of the SDS K T I includes the geologic features, events, processes (FEP), and conditions in and around the candidate repository that result from tectonic activities (except igneous activity (IA) which is the subject of a separate KTI) and that may affect or do affect evaluation of long-term performance. Subissues that may affect or do affect evaluation of natural and engineered barrier systems (EBS) and performance include (1) faulting, (2) seismicity, (3) fracturing and structural framework, and (4) tectonic framework of the geologic setting. Matters that concern SDS effects on waste containment and isolation and repository design for the preclosure phase, and on flow and transport in the postclosure, are also within scope and will be included in subsequent reports.

1.3 CONTENT OF ISSUE RESOLUTION STATUS REPORT SECTIONS

This IRSR is organized to document the NRC staff's current position on resolution of the SDS KTI for the purpose of evaluating the postclosure performance of a repository at YM. The KTI will be considered resolved when all its ancillary subissues are resolved. Section 1, "Introduction," describes the purpose and scope of this KTI. Section 2, "Issue and Subissues Statements," states the objectives of the KTI and defines the key issue and the subissues. Section 3, "Importance of Subissues to Repository Performance," provides a perspective on the role each subissue has in the Total System Performance Assessment (TSPA). A quantitative analysis of significance of several subissue components to dose is based on sensitivity analyses using the NRC Total Performance Analysis (TPA) code (Version 3.2.3). The relationship of subissues to the DOE's Repository Safety Strategy (RSS) (U.S. Department of Energy, 1998a) is also discussed.

Section 4, "Review Methods and Acceptance Criteria," describes the minimum quantity, quality, and level of detail of information required of the DOE for NRC staff to evaluate the adequacy of the DOE proposed resolution of each subissue. The section explains why the information is required, and what methods NRC staff may use to determine whether the standard for resolution has been met. The ACs and RMs will be used to evaluate the DOE prelicensing and licensing submittals. Section 5, "Status of Subissue Resolution," explains the bases for resolution of fracture framework, effects of faulting on waste packages (WPs), viable tectonic models, seismic, and fault displacement hazard assessment, Geologic Framework Model 3.1, and provides paths to resolution of open items. Open items will be tracked by the staff, and resolution will be documented in subsequent revisions of this IRSR.

2.0 ISSUE AND SUBISSUES STATEMENTS

Resolution of this KTI entails evaluation of all aspects of the seismotectonic FEPs that have the potential to effect postclosure repository performance. Resolving this KTI also requires development of AC and RMs to evaluate the technical adequacy of the DOE characterization of key site- and regional-scale seismotectonic FEPs that may affect design or performance.

The KTI to be resolved, broadly stated, is that SDS (seismotectonic FEPs) issues that may significantly affect the design or performance of a repository at YM are: (1) identified and adequately characterized, (2) sufficiently understood and fully considered, and (3) used appropriately by the DOE to evaluate long-term performance and as input to repository design (e.g., uncertainties of abstractions remain transparent in results of process models).

Subissues considered important to the resolution of this KTI include:

(i) Faulting—What are the viable models of faults and fault displacements at YM?

(ii) Seismicity—What are the viable models of seismic sources and seismic ground motions (GMs) at YM?

(iii) Fracturing and Structural Framework of the Geologic Setting—What are the viable models of fractures and structural controls of flow at YM?

(iv) Tectonic Framework of the Geologic Setting—What are the viable tectonic models and crustal conditions at YM?

This IRSR addresses:

(i) Faulting Components—Type I faults, Fault Displacement Hazard, Faulting Causing WP Failure, Faulting Exhuming WP, Probability and Consequences (Risk) of Faulting Directly Rupturing WP

(ii) Seismicity Components—Seismic Hazard, GM, Probabilistic Seismic Hazard Methodology and results of Probabilistic Seismic Hazard Analyses (PSHA)

(iii) Fracturing Components—Viable Fracture Models; Fracturing and Structural Framework of the Geologic Setting

(iv) Tectonics Components—Viable Tectonic Models, DOE's Preferred Tectonic Models, DOE Geologic Framework Models, Crustal Strain at YM

This report summarizes the data and pertinent conclusions of numerous geologic and seismologic publications that are relevant to the seismotectonics and structural framework of YM. Also included are the interim results of the analysis of risks of faulting estimated from sensitivity studies using NRC's TPA code (Version 3.2.3).

3.0 IMPORTANCE OF SUBISSUES TO REPOSITORY PERFORMANCE

The YM site region (figure 3-1) has been seismically, tectonically, and volcanically active on the timescale of a geologic repository. Future seismotectonic activities could affect the stability of the repository and the geosphere part of the natural barrier system (NBS). For example, seismic and tectonic activities change the *in situ* stress field and generate faults and fractures (or change the properties and potential behavior of existing discontinuities) in ways that affect many aspects of flow of water, vapor, heat, and magma, including fluctuations in the elevation of the water table. Changes to the system of discontinuities in and around a repository may be beneficial (e.g., dilation of a fracture zone may promote drainage around WPs) or adverse (e.g., fault slip may focus flow quickly through a normally impermeable rock stratum) to waste containment and isolation; to repository design (e.g., drift stability); and to long-term performance (e.g., tectonic strain partitioning altering distribution of fracture permeability causing deviation from expected groundwater flow paths). Therefore, continuing faulting, fracturing, seismicity, and regional strain at YM and in the surrounding YM region could pose a potential risk of noncompliance with radiological safety, health, and environmental protection standards because of possible disruptions to surface facilities and underground openings, including emplacement drifts and flow pathways.

Uncertainties in long-term changes to the geologic system attributable to seismotectonic events and processes that contribute to risk make it difficult for the DOE to demonstrate that a repository system will perform in a reasonably predictable way. However, in the present regulatory framework of risk-informed performance-based standards (e.g., draft 10 CFR Part 63), only those events and processes that can be shown to make a significant contribution to risk, as measured by the expected annual dose to an individual in a critical group, need to be considered in an assessment of long-term repository performance. The processes of faulting causing disruption of WPs and earthquake-induced rockfall causing disruption of WPs are scenarios considered to be contributors to risk. These have been evaluated by the NRC and the Center for Nuclear Waste Regulatory Analyses (CNWRA) by means of a systematic quantitative analysis using reasonable and generally conservative assumptions that enable an estimation of incremental expected annual dose to an individual. Preliminary results of such analyses indicate that faulting disruption of WPs (this IRSR, section 3.3.1) and seismic disruption of WPs [Repository Design and Thermal-Mechanics Effects (RDTME) IRSR, U.S. Nuclear Regulatory Commission, 1999b] pose relatively low risk to long-term performance. The importance of fractures and fracturing in estimation of expected annual dose has not been systematically evaluated.

3.1 RELATIONSHIP OF SUBISSUES TO THE U.S. DEPARTMENT OF ENERGY'S REPOSITORY SAFETY STRATEGY

The DOE RSS (U.S. Department of Energy, 1998a) continues to rely on multiple barriers to limit radionuclide movement. Therefore, the integrity of the NBS needs to be understood. The subissues of faulting, seismicity, fracturing, and tectonic models focus on the NBS. In addition, the integrity of part of the EBS, WPs, may be affected by faulting, seismicity, and development of fractures. The objective of a potential repository system at YM is to ensure that annual doses to a person living near the site will be acceptably low. The effect on integrity of WPs by mechanical failure modes, such as direct disruption by faulting or by seismically induced rockfall (or fall of pieces of liner, drip shield, or ground support material, if used) onto WPs, therefore

Figure 3-1. LANDSAT thematic mapper image of the Yucca Mountain region showing the proposed repository relative to other geographic and geologic features

need to be examined by DOE within the content of total system performance. Preliminary results that show low risk from these processes need to be confirmed.

The DOE has identified four key attributes of the repository system as most important to assessments of postclosure performance of the EBS and the NBS (1) limited water contacting the WPs, (2) long WP lifetime, (3) low rate of release of radionuclides from breached WPs, and (4) radionuclide concentration reduction during transport. DOE and NRC analyses have shown that most of the water that will become available to contact WPs, breach WPs, or otherwise affect WP lifetime, and transport radionuclides, will do so by flow within rock discontinuities (i.e., fractures, fault zones, and stratigraphic boundaries). Interconnected fractures, including intensely fractured fault damage zones, are the primary source of hydraulic conductivity and groundwater flow paths at YM. Alternatively, intensely deformed fault zone cores may be relatively impermeable (i.e., are barriers to flow), due to grain size reduction and cementation and might lead to perching of groundwater or anisotropic hydraulic conductivity. Therefore, the SDS subissues that evaluate models of discontinuities are related to RSS through the process models of unsaturated zone (UZ), saturated zone (SZ), and near-field environment that abstract or otherwise consider discontinuities.

The DOE stated that its RSS addresses disruptions to the system that potentially could release radionuclides directly to the human environment or otherwise adversely affect the characteristics of the system (U.S. Department of Energy, 1998a). The DOE strategy to address tectonic processes is based on their likelihood and potential effects. The DOE stated that it has initiated analyses through the PSHA and Probabilistic Fault Displacement Hazard Analysis (PFDHA) expert elicitation process to support assessment of the potential effects of such disruptions (U.S. Department Of Energy, 1998b). The DOE has enumerated two hypotheses to be tested: (1) (Hypothesis No. 16)—the amount of movement on faults through the repository horizon will be too small to bring waste to the surface and too small and infrequent to significantly impact containment during the next few thousand years [U.S. Department of Energy, 1998a, Hypothesis 16 was simply stated as, fault displacement impacts will not be significant]; and (2) (Hypothesis No. 17)—the severity of GM expected in the repository horizon for tens of thousands of years will only slightly increase the amount of rockfall and drift collapse (U.S. Department Of Energy, 1998a) (U.S. Department of Energy, 1998a, Hypothesis 17 was simply restated as, GM impacts will be minimal).

3.2 RELATIONSHIP AND IMPORTANCE OF SUBISSUES TO U.S. DEPARTMENT OF ENERGY'S VIABILITY ASSESSMENT

In December 1998, DOE completed its viability assessment (VA) for a potential high-level radioactive waste repository at YM (U.S. Department of Energy, 1998a). The NRC reviewed the VA and supporting documents[1]. The staff agreed with DOE's recommendation to continue site characterization; however, the staff identified several areas that need to be addressed more fully in a future license application, and the staff identified areas in which it had no questions at this time.

[1]Letter from C.J. Paperiello to L.H. Barrett, U.S. Nuclear Regulatory Commission Staff Review of the U.S. Department of Energy Viability Assessment for a High-Level Radioactive Waste Repository at Yucca Mountain, Nevada, dated June 2, 1999.

SDS provided input to two Integrated Subissues (ISI) that NRC staff found to be inadequately developed in TSPA-VA: (1) flow rates in water production zones (SZ flow and transport; appendix A, GS-4), and (2) volcanic disruption of WPs (appendix A, GS-6). The SDS analysis of SZ flow and transport indicated the need for the DOE to investigate structurally controlled anisotropic permeability within the SZ (Farrell, et al., 1999) and heterogeneities in the alluvium along the SZ flowpath. The staff's analysis is fully developed in the Unsaturated and Saturated Flow Under Isothermal Conditions (USFIC) IRSR, (U.S. Nuclear Regulatory Commission, 1999c). The SDS analyses of volcanic disruption of WPs indicated the need for the DOE to assess the relationship between global positioning system (GPS) measurements of the potential onset of anomalously high extensional strain-rate and the initiation of basaltic volcanism (Wernicke, et al., 1998; Savage, et al., 1998a; Connor, et al., 1999, in review). The staff's analysis is fully developed in this IRSR, section 4.4; and Igneous Activity (IA) IRSR (U.S. Nuclear Regulatory Commission, 1999a).

The SDS analyses of three ISIs in which staff had no questions at this time supported the general agreement that DOE's planned work appears adequate in these key element areas: (1) mechanical disruption of WPs (appendix A, EBS-2), (2) spatial and temporal distribution of flow (appendix A, GS-1), and (3) distribution of mass flux between fracture and matrix (fracture versus matrix flow, appendix A, GS-2). The SDS analysis of mechanical disruption of WPs indicated the need for the DOE to assess the effect of increased seismically induced rockfall onto WPs as a result of the potential onset of anomalously high *in situ* strain rate (Wernicke, et al., 1998; Connor, et al., 1998; this IRSR, section 4.4; and RDTME IRSR, U.S. Nuclear Regulatory Commission, 1999b). The DOE is investigating this potential relationship. The SDS analyses of spatial and temporal distribution of flow and fracture versus matrix flow indicated the need for the DOE to better propagate the uncertainties associated with the characteristics of fractures and their distribution and the need to account for the differences in fracture-flow systems in the various hydrogeologic units (this IRSR, section 4.3; and USFIC IRSR, U.S. Nuclear Regulatory Commission, 1999c).

3.3 RELATIONSHIP AND IMPORTANCE OF SUBISSUES TO TOTAL SYSTEM PERFORMANCE

The staff is developing a strategy for evaluating the performance of a proposed repository at YM. As currently visualized by the staff, key elements of this strategy are defined as those necessary for the DOE to demonstrate repository performance. These elements are illustrated in appendix A. Acceptance criteria for abstracting each of these elements into an NRC determination of compliance are under development [Total System Performance Assessment and Integration (TSPA&I) IRSR, U.S. Nuclear Regulatory Commission, 1999d].

Structural deformation and seismicity, as defined by the prevailing (i.e., ambient) tectonic, lithostatic, pore-fluid, and thermal stresses interacting with the fractured rocks at YM, are important factors in evaluating repository design and performance because they can cause premature WP failures and alter the flow regime—key elements of the total system performance model. Premature WP failures may be caused by direct rupture from faulting or seismicity-induced rockfall. Faults that are parallel or oblique to groundwater flow may act as barriers or conduits to flow. SDS KTI input is also important to assumptions about the future integrity of the NBS. Therefore, the acceptance and review criteria for the resolution of SDS KTI and subissues are designed to complement the broader-level acceptance criteria for the abstraction of the key elements of the repository subsystems in the TSPA flowdown diagram (appendix A; U.S. Nuclear Regulatory Commission, 1999d).

As highlighted in the flowdown diagram (appendix A), SDS subissues are integrated within eight ISIs of the EBS and NBS subsystems (figure 3-2). The SDS subissues are related to the following ISIs: (1) Mechanical Disruption of WPs; (2) Water Contacting WP; (3) Spatial and Temporal Distribution of Flow; (4) Mass Flux Between Fracture and Matrix: UZ; (5) Retardation in Fractures, UZ; (6) Flow in SZ; (7) Retardation in SZ; and (8) Volcanic Disruption of WP. SDS subissues are also integrated with preclosure design and performance assessment (PA). In this version of the SDS IRSR (Revision 2), only postclosure issues are considered. Preclosure considerations will be discussed in subsequent documents including review of Topical Report #3 and later revisions of the IRSR.

Additionally, the FEPs of faulting, seismicity, fracturing, and the tectonic framework of YM contribute to the long-term stability and integrity of the natural and engineered barriers. These may need to be considered in the defense-in-depth analysis of the total system.

3.3.1 Faulting—What Are the Viable Models of Faults and Fault Displacements at Yucca Mountain?

A paramount observation of the geological setting of YM is the presence of numerous faults, including many with evidence of Quaternary displacement (United States Geological Survey, 1996). The staff has determined that because of the likelihood of future slip on faults in the area and potential consequences, faults and faulting need to be abstracted into numerical PA codes, specifically with regard to the following two key elements of the engineered and natural barrier subsystems: (1) mechanical disruption of WPs; and (2) volcanic disruption of WPs (appendix A).

SDS will continue to provide input regarding faults and faulting to the ISIs—mechanical disruption of WPs in two ways: (1) by evaluating the probability of faulting through the waste-emplacement drifts, estimating the average annualized number of WPs sheared by such events, and calculating the incremental changes to the expected annual dose to an individual from this disruptive event scenario (this IRSR, section 3.3.1.1); and (2) by proposing a prudent and reasonably conservative range of fault zone characteristics and fault displacement hazard parameters necessary for RDTME KTI to investigate the effects of earthquake-induced rockfall onto WPs (U.S. Nuclear Regulatory Commission, 1999b). This information needs to be considered because faults have the potential to directly intersect emplacement drifts and WPs or act as loci of rock failure and associated rockfall. However, the DOE has asserted that fault displacement impacts will not be significant (U.S. Department of Energy, 1998a, hypothesis 16). Nevertheless, the DOE indicated its intention to set back WPs from known faults (not just to avoid potential for shearing, but to avoid potential for focusing seepage onto WPs). SDS is conducting confirmatory investigations of the nominal widths of fault damage zones at repository depths that should be considered in evaluating (1) adequacy of set back distances, and (2) models of flow where fracture permeability in and around faults may be an important parameter.

Also, SDS will continue to provide input regarding faults and faulting to the ISIs—volcanic disruption of WPs by providing prudent and reasonable ranges of fault displacement hazard

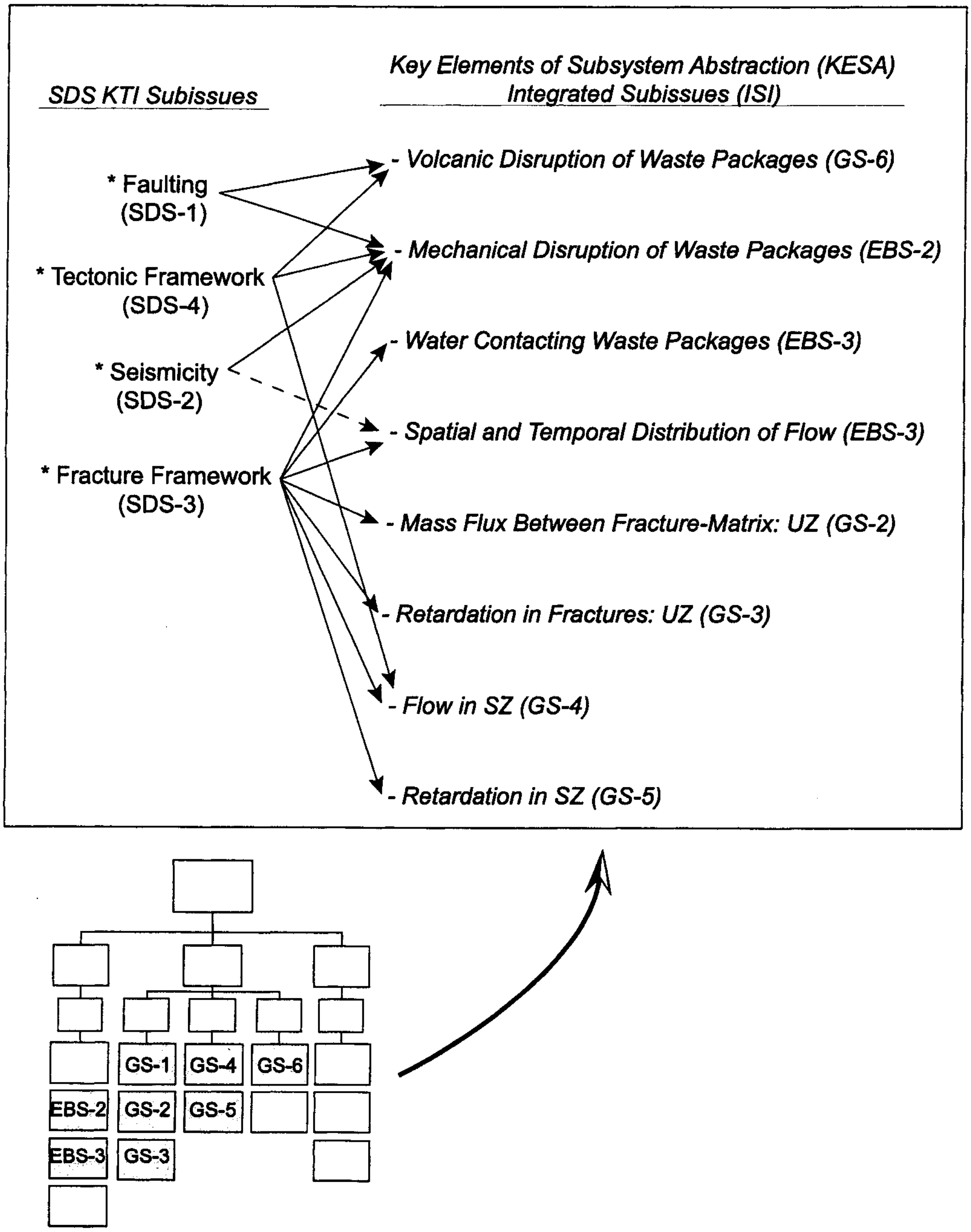

Figure 3-2. Integration of Structural Deformation and Seismicity key technical issue subissues and the integrated subissues. See appendix A for explanation of abbreviations and the relation of each integrated subissue to the Engineered and Geosphere Systems. The contributions of faulting, seismicity, tectonic, and fracture frameworks to total system performance (individual dose or risk) are captured within the respective integrated subissues and calculated in the total system performance code. Details of the performance calculations are described in the Issue Resolution Status Report, Total System Performance Assessment and Integration Key Technical Issue (U.S. Nuclear Regulatory Commission, 1999d).

parameters necessary for the IA KTI to investigate the flow of magma through fault zones and the transport of radionuclides from disrupted WPs through faults to the surface (see IA IRSR, U.S. Nuclear Regulatory Commission, 1999a).

Faults can also act as conduits or barriers to flow of water, vapor, magma, or heat, as evidenced or suggested by the many consistent orientation of washes and spring lines that follow surface fault traces (USFIC IRSR, U.S. Nuclear Regulatory Commission, 1999c), and preferential magma conduits such as dikes intruded along faults and alignments of the Quaternary or older volcanoes in Crater Flat and the Amargosa Desert (IA IRSR, U.S. Nuclear Regulatory Commission, 1999a; Ferrill, et al., 1997; Connor, et al., 1997; Connor, et al., 1999, in review). Faults occur in a wide range of lengths and widths and so are inherent features of the geologic setting at all scales of interest. Therefore, faults will also be discussed, in conjunction with fracturing and the geologic and tectonic framework of the geologic setting in the following sections.

3.3.1.1 U.S. Nuclear Regulatory Commission/Center for Nuclear Waste Regulatory Analyses Sensitivity Studies of Faulting

Of the three potential consequence effects of faulting abstracted into PA codes listed in section 3.2.1, SDS is responsible for investigations of the sensitivity to dose of faults and fault slip that directly rupture WPs. The investigation of WP failure from faulting presented in this report was based on PA studies using the FAULTING Module computer code, Version 1.0 (Ghosh, et al., 1997), as adapted for use within the NRC and the CNWRA TPA Version 3.2 code (Mohanty and McCartin, 1998). Version 3.2.3 of the TPA code was used for the analyses presented in this report. This investigation bears on DOE's Hypothesis No. 16 (U.S. Department of Energy, 1998a). Detailed studies that address the two other consequences of faulting listed in section 3.2.1 are ongoing, and results and conclusions from those studies were incorporated into the IA IRSR (U.S. Nuclear Regulatory Commission, 1999a) and USFIC IRSR (U.S. Nuclear Regulatory Commission, 1999b) respectively. The following sections summarize SDS consequence modeling of faulting through June 1999.

Conceptual Model

The FAULTING module was developed to assess the potential for direct disruption of WPs from fault displacements in the proposed repository block. The module evaluates the potential for direct WP rupture from fault displacement along planar decoupled fault zones. It is assumed that, in repository design, WP emplacement in the proposed repository will be appropriately set back from those faults known to present a potential hazard (U.S. Department of Energy, 1995a). Thus, the FAULTING module essentially evaluates hazards related to faults not accounted for in the repository design such as: (1) new faults, those that may form during the period of concern; (2) hidden faults, those within the repository that are presently unknown and unmapped; or (3) underestimated faults, those mapped faults not considered significant during design or construction (e.g., Type III Faults) that turn out to pose a significant risk over the lifetime of the repository. For simplicity, faults that fall in Categories 2 and 3 above will be referred to in this report as underappreciated faults.

To model faulting, the FAULTING module (FAULTO) generates a fault within the repository block (figure 3-3) based on a set of independent fault parameters whose range is described by

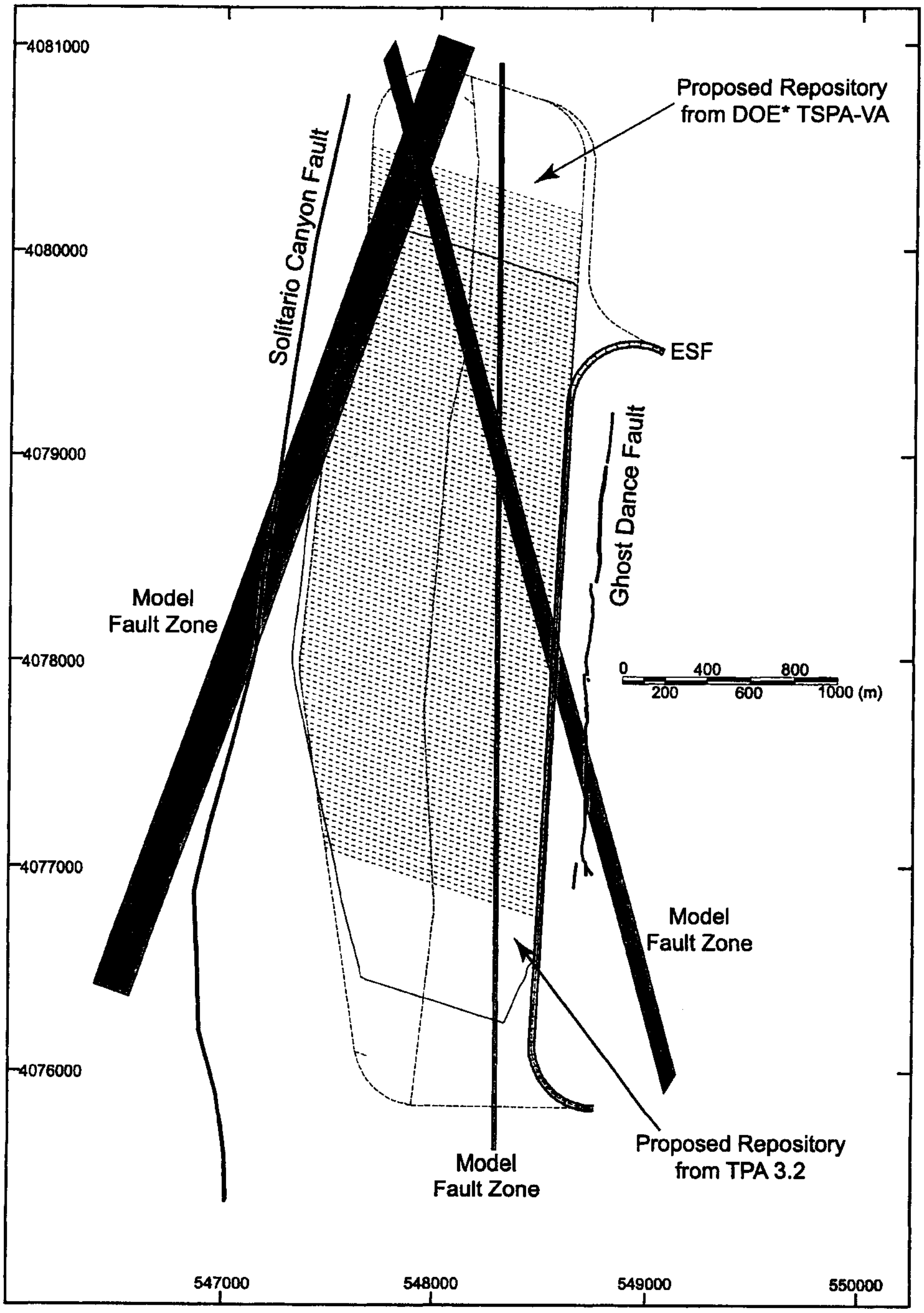

* DOE - U.S. Department of Energy

Figure 3-3. Map of the proposed Yucca Mountain repository showing the Exploratory Studies Facility and the proposed repository boundary. Three hypothetical fault zones used in consequence analyses are shown as dark gray bands. Note the differences in the proposed footprints of the repository used in (TSPA-VA) (U.S. Department of Energy, 1998b) and the Nuclear Regulatory Commission/Center for Nuclear Waste Regulatory Analyses TPA code (version 3.2.3). Base map and other repository features shown were adapted from figure 2-2 of U.S. Department of Energy (1998b).

probability density functions (PDFs) (table 3-1). The PDFs represent faulting characteristics such as fault-zone location, orientation, length, width, amount of fault displacement per faulting event, time of faulting event, and cumulative displacement rate. Fault dip is not considered because nearly all faults at YM dip moderately to steeply (45° to 90°). Under current designs, the emplacement drifts are horizontal, and thus the modeling of faulting can be simplified to a two-dimensional (2D) problem, in which new faults cut vertically across horizontal WPs. If new information shows that horizontal or low-angle faults are also important, then additional consequence analyses will be required.

Table 3-1. Probability Distribution Functions (PDF) for FAULTO Module

Parameter	Parameter Name in Code	PDF Type	Values
Time of Faulting Event	TimeOfNextFaultingEventinRegionOf-Interest[yr]	Uniform	100 yr to 10,000 yr
Threshold Displacement	ThresholdDisplacementForFault-DisruptionOfWP[m]	User Defined	0.25 cm
X Location Fault Zone Center	XLocationOfFaultingEventInRegionOf-Interest[m]	Uniform	547400-548600 UTM, Zone 11
Y Location Fault Zone Center	YLocationOfFaultingEventInRegionOf-Interest[m]	Uniform	4076200-4079040 UTM, Zone 11
Probability of Northwest Faulting	RNtoDetermineFaultOrientation	Not Used	None
Strike of Northwest Faults	NWFaultStrikeOrientationMeasured-fromNorthClockwise[degrees]	Not Used	Not Used
Strike of Northeast Faults	NEFaultStrikeOrientationMeasured-fromNorthClockwise[degrees]	Uniform	-50 to 50 degrees
Length of Northwest Faults	NWFaultTraceLength[m]	Not Used	None
Length of Northeast Faults	NEFaultTraceLength[m]	Constant	4000 m
Width of Northwest Fault Zones	NWFaultZoneWidth[m]	Not Used	None
Width of Northeast Fault Zones	NEFaultZoneWidth[m]	Log-normal	1.2793e-2, 6.522806e1
Displacement Per Event for Northwest Faults	NWAmountOfLargestCredible-Displacement[m]	Not Used	None
Displacement Per Event for Northeast Faults	NEAmountOfLargestCredible-Displacement[m]	Log-normal	1.39654e-1, 1.833439e0
Cumulative Displacement for Northwest Faults	NWCumulativeDisplacementRate [mm/yr]	Not Used	None

Table 3-1. **Probability Distribution Functions (PDF) for FAULTO Module (cont'd)**

Parameter	Parameter Name in Code	PDF Type	Values
Cumulative Displacement for Northeast Faults	NECumulativeDisplacementRate [mm/yr]	Not Used	None

For each realization, the code samples faulting characteristics from each of the faulting PDFs initiates a faulting event based on those sampled parameters, and determines number, location, and time of WP failures (if any). The resulting WP failures are then incorporated into downstream modules of the TPA code, which combine the results with failures from other processes (e.g., corrosion) to calculate a single estimate of dose consequence. Multiple realizations (generally 250), in which combinations of parameters are sampled stochastically, allow a statistical representation of repository performance to be developed. To be efficient, each realization assumes one faulting event (conditional probability). The resulting consequence (WP failure, peak dose, etc.) is then multiplied by the probability of faulting to determine the risk faulting poses to repository performance. The outcome (risk) is equal to what would be obtained if probability were directly incorporated into the TPA code. The difference is in the number of TPA runs necessary to obtain a meaningful statistical average. Incorporation of the probability into the TPA code would require a twenty-fold increase in the number of TPA realizations; in other words, to get 250 realizations with a faulting event would require 5,000 realizations.

FAULTO Input Parameters

PDFs and other parameters and constants used in the FAULTING module of the TPA code (Version 3.2.3) for these analyses are listed in Figure 3-1. Several parameters or groups of parameters were simplified from the version of FAULTO given in Mohanty and McCartin (1998). Technical rationale for FAULTO parameters and changes to the parameters since Mohanty and McCartin (1998) are given in the following.

Time of Faulting Event. No data currently exist to allow an accurate prediction of the time of a faulting event within the next 10,000-yr. Therefore, it was assumed that faulting could occur with equal probability any time during the next 10,000 yr. In addition, because the probability of faulting is small (see section on Probability of Faulting that follows), multiple faulting events were not considered. We assumed that a faulting event would occur only once during each realization.

Threshold Displacement. No empirical or model-derived values exist to indicate how much displacement along a fault is necessary to cause WP failure. In the current repository design, 1.8-m-diameter WPs are roughly centered in 5.0-m-diameter drifts without backfill. Thus, 1.6 m of fault offset will be sufficient to bring repository wall rock in contact with the WPs. The dynamics of faulting during a faulting event, however, are largely unknown. Dynamic forces coupled with rockfall could cause WP failure from faulting events with resulting fault displacements less than 1.6 m. To be conservative, it was assumed in these analyses that 25 cm of fault displacement would cause WP failure. As discussed in the following, both partial and complete breach of the WPs were analyzed by using both the "bathtub" and "flowthrough" models in the TPA code Version 3.2 (Mohanty and McCartin, 1998).

Location of Fault Within Repository. The center point of the fault was assumed to vary uniformly throughout the repository footprint. This allowed a complete range of geometrical possibilities to be analyzed, including cases in which faults cut parallel to the central axis, obliquely across, or along the edges of the repository (these three examples are shown in figure 3-3). Note that, for these analyses, the TPA code (Version 3.2.3) assumes a repository footprint similar to the one presented in TSPA-95 (U.S. Department of Energy, 1995b) and not the one given in TSPA-VA (U.S. Department of Energy, 1998b). These differences have little effect on the calculations presented here because the overall area of the repository in the two design options is nearly the same.

Fault Orientation. The distribution of fault zone strike was derived from the detailed scan line mapping of the ESF[2] (herein referred to as the ESF data). For FAULTO analyses, all mapped faults and shears were gleaned from the ESF data and the distribution checked for possible scan line bias using the method of Terzaghi (1965). The distributions of fault orientations Terzaghi-corrected, data compared to uncorrected data, were similar and thus, for these analyses, the uncorrected data set was assumed representative of the repository. A stereonet and rose diagram plot of the faults (figure 3-4a) shows a nearly uniform distribution between azimuth 310° and 50°. This is in contrast to fault orientations used in previous versions of FAULTO, (e.g., Ghosh, et al., 1997), in which two sets of faults were assumed, those that had northwest strikes and those that had north-northeast strikes. Thus, in these analyses, and the parameters designated for the north-northeast striking faults were modified to represent all faults (see table 3-1), the parameters designated for the northwest striking faults were not used.

Fault Length. Fault length was assumed to be 4 km because this length ensures that all faults generated in the Faulting Module would cut across the entire repository. This assumption is conservative in the sense that smaller faults or faults that do not completely transect the repository are possible. This assumption is used here because it allows for a straightforward calculation of the number of WPs failed by a faulting event without considering complications posed by the fault tips, which can have intricate and irregular terminations (e.g., Cartwright and Mansfield, 1998).

Fault Zone Width. Fault zone widths were also derived from the ESF data set. All fault zones in the Exploratory Studies Facility (ESF) data for which widths were recorded were used in these analyses. Several additional fault zones were derived from auxiliary analyses of the ESF scan lines included with the ESF data. The resulting distribution of fault zone widths is shown in figure 3-4b, both as a histogram and a cumulative curve. This distribution is best modeled as a lognormal distribution (table 3-1). For comparison and verification, the distribution of fault zone widths for a TPA (Version 3.2.3) run with 250 realizations is shown in figure 3-4c.

---

[2]Exploratory Studies Facility data transmitted from the U.S. Department of Energy to the Center for Nuclear Waste Regulatory Analyses, August 1998, U.S. Department of Energy Data Tracking Number numbers GS960708314224.008, .101, 011, .014, .003, .008, .010,.012, .020, .021, .022, .023, .024, .025, .026, and .028; Technical Data Information Form numbers 305556, 305554, 305624, 306645, 306017, 306284, 306298, 306299, 306509, 306510, 306511, 306512, 306513, 306514, 306515, 306517.

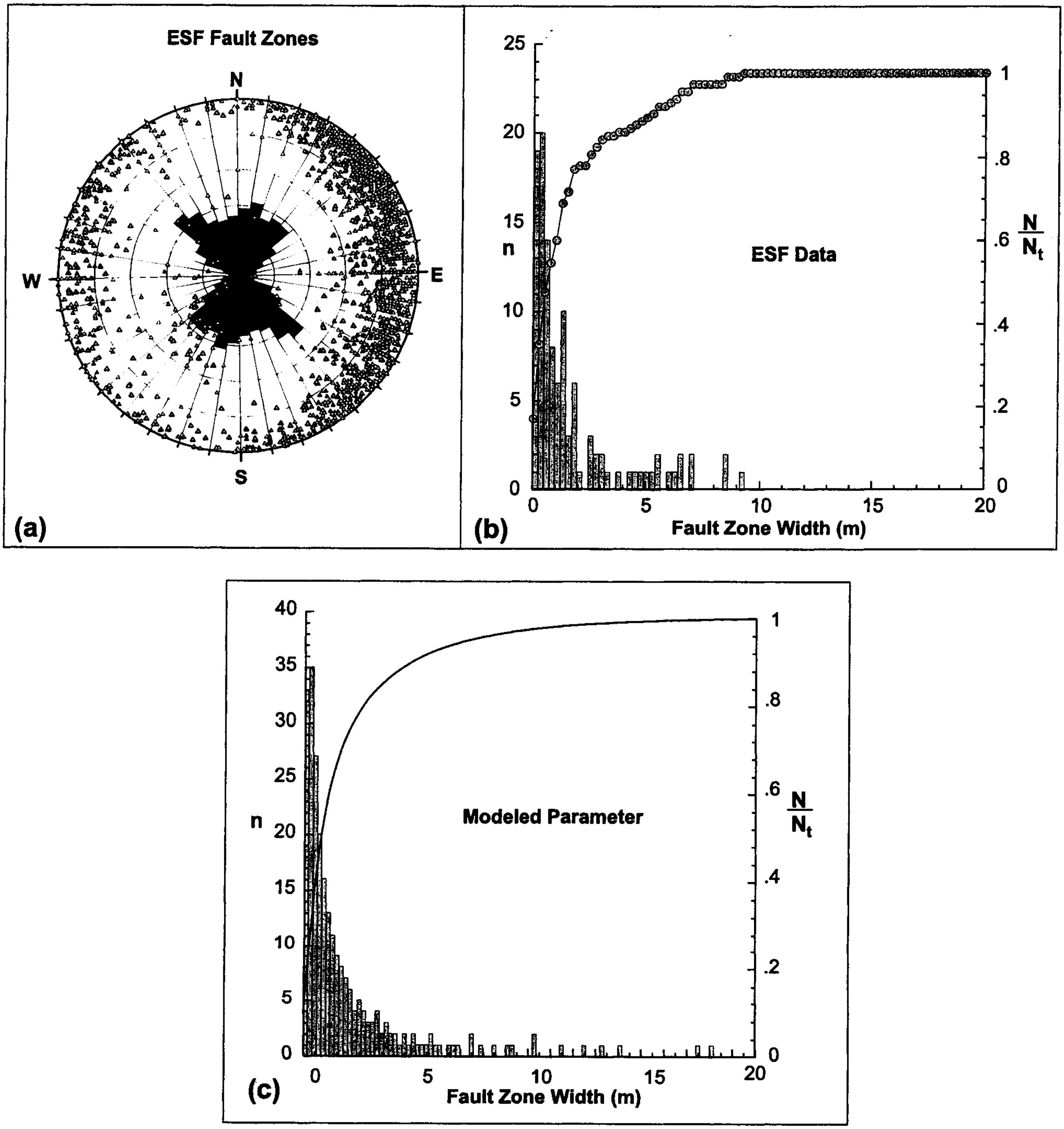

Figure 3-4. Fault width and fault orientation data used to develop parameter distributions for the Faulting Module of the Total Performance Assessment (TPA) code (Version 3.2.3). (a) Equal-angle stereonet and rose diagram showing the distribution of faults and shears from the Exploratory Studies Facility (ESF) data set. (b) Histogram and cumulative curve showing the distribution of fault zone widths from the ESF data set. (c) Distribution of fault zone widths from a 250-realization run of the TPA (Version 3.2.3) code. For cumulative curves, N/N_t is normalized to (b) total number of faults and (c) total number of realizations.

Displacement. At present there are insufficient data from the ESF to completely define the distribution of displacements for individual faulting events. Data of faults mapped from the ESF only present cumulative displacements with no information on displacement per event or recurrence. In addition, displacement values were not measured in the plane normal to the fault zone and thus, only apparent displacement values are given, and displacement values larger than the tunnel diameter could not be accurately measured. Therefore, for the consequence analyses presented here, displacement per faulting event data were derived from the paleoseismic record (figure 3-5a; U.S. Geological Survey, 1998). The distribution of fault zone displacement from trenching studies in and around YM is shown in figure 3-5b, both as a histogram and a cumulative curve. This distribution is best modeled as a lognormal parameter (table 3-1). For comparison and verification, the distribution of fault zone widths for a TPA (Version 3.2.3) run with 250 realizations is shown in figure 3-5c.

Cumulative Displacement. This parameter was first proposed in the code to test for possible exhumation of WPs to the surface along faults. As discussed in the section titled Faulting Exhuming WPs, this process is not considered credible and, thus, this parameter was not used in the performance computations.

Model Assumptions

Key assumptions in the consequence analyses of faulting presented here are

(1) Faults are considered as process zones or bands of deformation with finite width. All WPs within these zones are considered damaged (failed), provided the fault slip exceeds a user-input threshold displacement value.

(2) Faults are generated randomly, independent of the notion of linked faulting between intrabasin secondary faults, principal block-bounding, and basin-bounding faults (see section 4.1.2 for description of principal and secondary faults).

(3) For simplicity, the parameters describing fault characteristics are assumed to be statistically independent. In nature, many of these geometric and recurrence properties may be related (e.g., longer faults seem to correlate with wider deformation zones or longer faults tend to be more active).

(4) TPA (Version 3.2.3) assumes 6,427 uniformly distributed WPs.

(5) The compliance period for postclosure performance is 100 to 10,000 yr.

(6) The critical group is located 20 km from the repository.

Consequence Model Results

WP Failures. The number of WP failures from faulting correlates with fault zone width (figure 3-6a). Exceptions include (1) cases where the fault zone was wide and cut across the repository but in which fault displacement did not exceed the threshold displacement. Those cases show no WP failures and plot along the x-axis in figure 3-6a. (2) Cases in which the

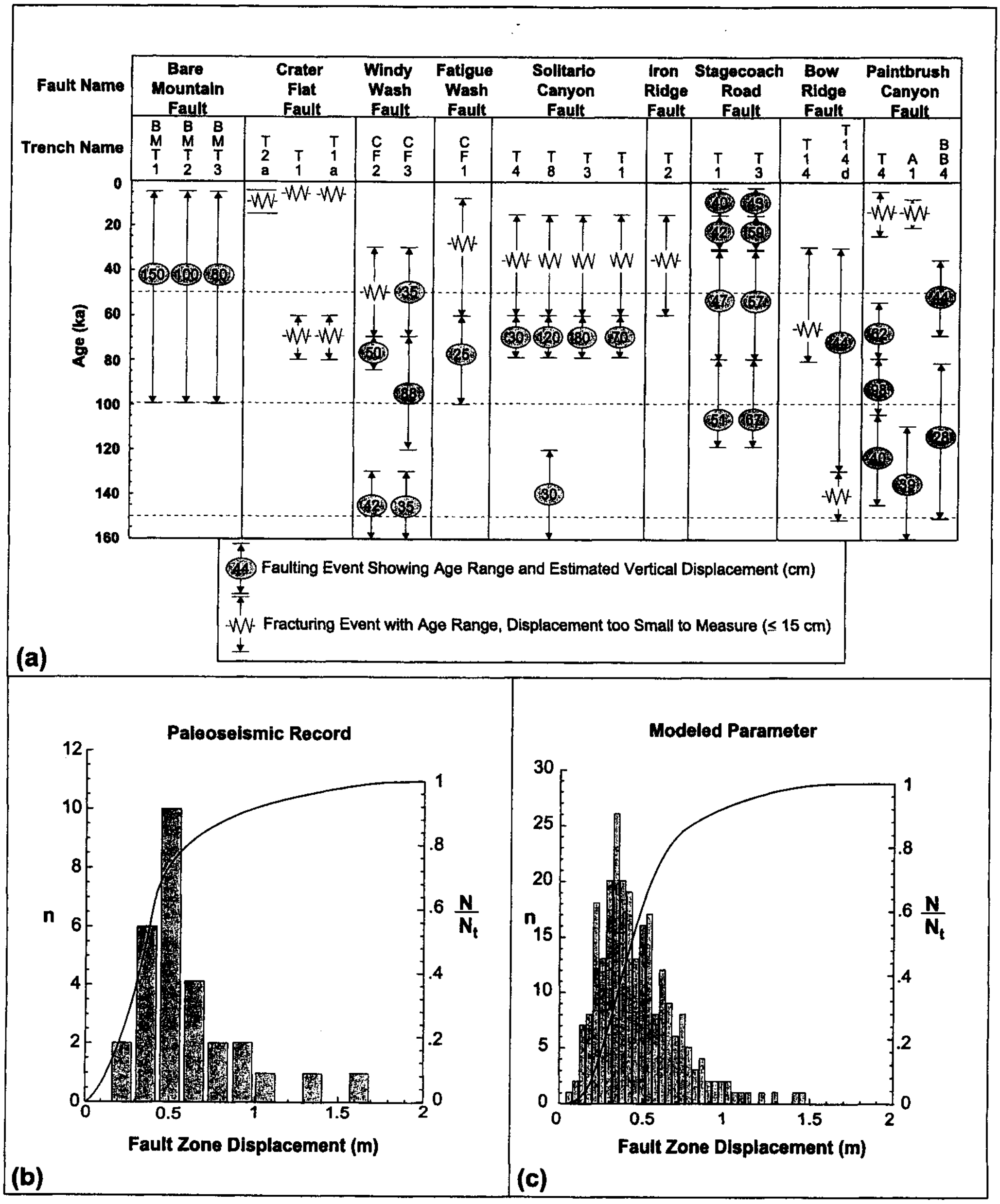

Figure 3-5. Fault displacement data used to develop parameter distributions for the Faulting Module of the Total Performance Assessment (TPA) code (Version 3.2.3) (a) Plot summarizing the paleoseismic data from Yucca Mountain region. The plot was generated from paleoseismic data presented in the U.S. Department of Energy Probabilistic Seismic Hazard Analyses (DOE PSHA) (U.S. Geological Survey, 1998) and was adapted from a similar plot presented by Larry Anderson to the DOE PSHA seismic source characterization workshop held in Salt Lake City, Utah, October 1997. (b) Histogram and cumulative curve showing the distribution of fault displacements from the paleoseismic data. (c) Distribution of fault zone displacements from a 250-realization run of the TPA code (Version 3.2.3). For cumulative curves, N/N_t is normalized to (b) total number of paleoseismic events and (c) total number of realizations.

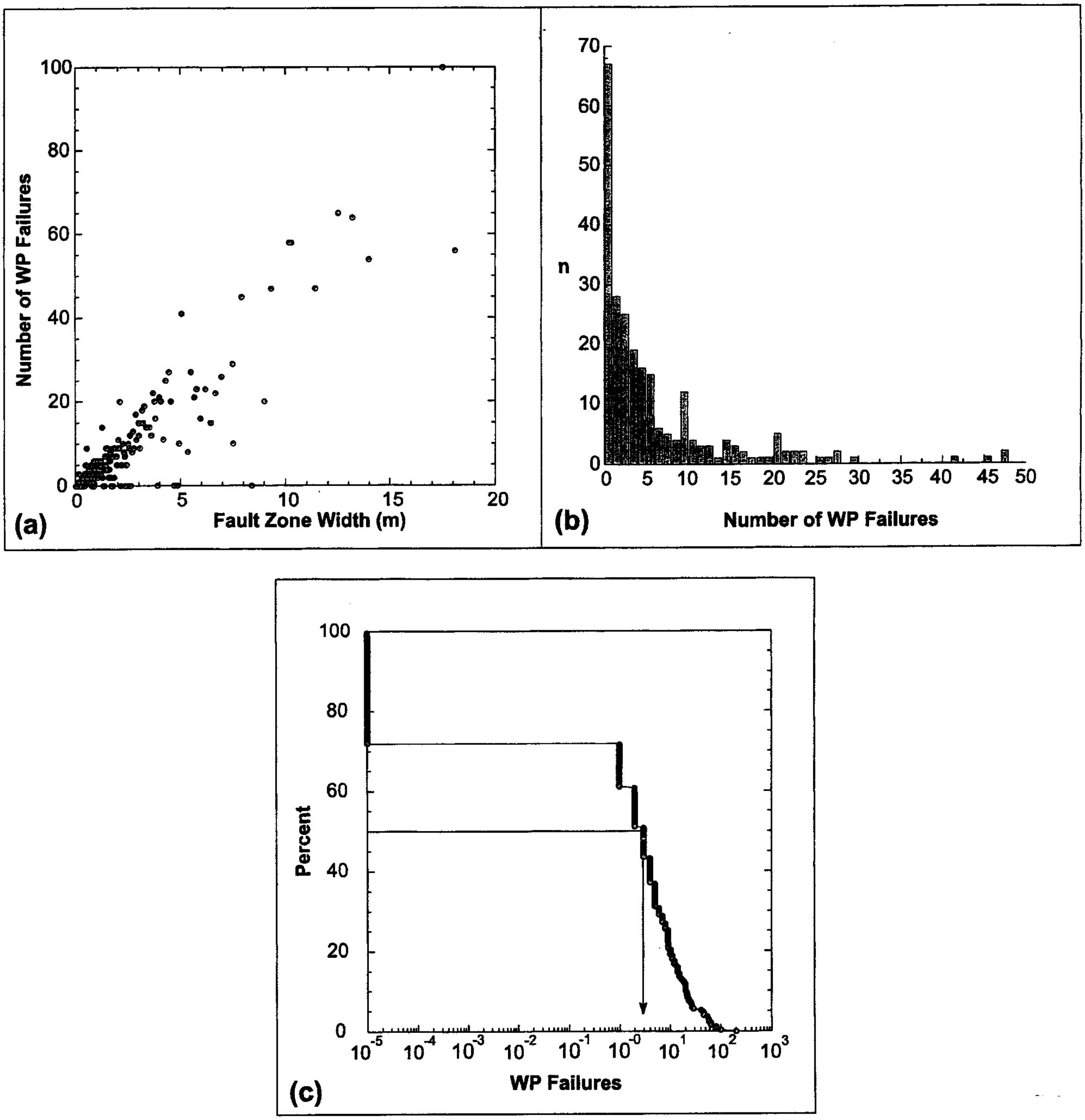

Figure 3-6. Consequence modeling results showing the effects of faulting on waste packages. (a) Histogram showing the distribution of number of waste package failures for 250 realizations is the number of realization in which a given number of WP failures occurred. (b) Scatter plot showing the correlation between fault zone width and number of waste package failures. (c) Complementary cumulative distribution function showing waste package failures, assuming a conditional probability that the faulting event takes place once during the 10,000-yr performance period.

fault zone was wide but cut across the edge of the repository (see figure 3-3a for a hypothetical example). Those cases resulted in fewer WPs per unit width of fault zone compared to faults that arose entirely within the repository footprint.

The distribution of the number of WPs failed by faulting follows a lognormal distribution as shown in the histogram of figure 3.6b. As shown if figure 3-6c, failures range between 0 and 200, but more than half of the realizations produce 3 or fewer WP failures, and 30 percent of the realizations produce no WP failures at all. The mean number of WPs failed is 8.5. The median number is 3. These values are conditional, (i.e., they assume the event occurred in each realization). The probability-weighted number of WP failures are approximately 5 percent of these values given an upper bound for the probability of faulting at 5×10^{-6}. This is equal to a frequency of faulting of once every 200,000 yr, or 1 chance in 20 over the 10,000 yr of regulatory concern of the repository. Thus, the probability-weighted mean values of WP failures is 0.43. The probability-weighted median value of WP failures is 0.15.

Draft 10 CFR Part 63 suggest that the measure of interest should be the peak expected dose. To calculate peak expected dose requires a large number of TPA runs in which the faulting event is forced to occur at specified times, following consequence analyses method reported in the TSPA IRSR (U.S. Nuclear Regulatory Commission, 1999d). In contrast to volcanic disruption, faulting consequences always reach peak dose at year 10,000 owing to the ground water pathway. Therefore, to bound the effects of faulting, peak dose and average dose were used instead of peak expected dose.

Dose. Peak and average dose from faulting were examined for two different end-member models of WP failure, (i) the bath tub model, in which the assumed breach of the WP is partial and the WP must fill up to the level of the breach with water before release can occur; and (ii) the flow-through model, in which the assumed breach is such that the flow out of the WP is equal to the flow in for all times (Mohanty and McCartin, 1998). For these consequence analyses of faulting, the flow through model is deemed more appropriate (and more conservative) given the conceptual model of faulting. Faults are considered to have moderate to steep dip angles (45° to 90°) and thus to cut across the horizontal drifts at high angles. If a fault intersects a WP to the extent that the WP fails, it is highly likely the WP will be entirely breached.

Comparisons of these models show a minimal increase in peak dose from faulting over the base case if the bath tub model is assumed and a slightly greater increase in peak dose over the base case if the flow through model is assumed (figure 3-7a; table 3-2). The peak doses, however, are, small compared to the base case. For peak doses at their mean values, the faulting contribution of 1.5×10^{-4} mrem adds less than 8 percent to the base case peak dose of 2.3×10^{-3} mrem (table 3-2). Moreover, this 8-percent value is highly conservative, not only because it uses an upper bounding value for the probability of faulting (see section of Probability of Faulting that follows), but because once the flow-through model is selected in the code, all WPs that fail, including initial failures and seismic-rockfall failures, are assumed to release radionuclides using the flowthrough model release parameters.

Table 3-2. Peak Dose for Consequence Modeling of Faulting

	Base case (mrem)	Faulting Bath Tub (mrem)	Probability Weighted Difference Bath-Base (mrem)	Faulting Flow-Through (mrem)	Probability Weighted Difference Flow-Through–Base (mrem)
Peak Dose (mean)	2.3×10^{-3}	2.6×10^{-3}	1.5×10^{-5}	5.2×10^{-3}	1.5×10^{-4}
Peak Dose (median)	3.1×10^{-4}	3.9×10^{-4}	4.0×10^{-6}	1.8×10^{-3}	7.5×10^{-5}

Dose Through Time. Estimates of expected dose through time from faulting for the base case, bath tub, and flowthrough show a similar pattern to the peak dose curves (figure 3-7b). In all cases considering a 10,000-yr period of repository performance, the peak dose occurred at year 10,000. Peak doses are higher in later years beyond year 10,000, but repository performance after year 10,000 was not considered in these FAULTO analyses.

In the mean curve, no significant dose occurs prior to approximately year 2,000, due primarily to the long groundwater travel times from the repository to the critical group. Dose through time values are also shown for all 250-realizations in which the faulting event was forced to occur at year 1,000 (figure 3-7c). The large spread in dose through time for the individual realizations reflects the large uncertainties in release and groundwater flow conditions. The distribution shows that releases can occur as early as year 1,500 and as late as year 7,000. Conditional peak doses range between 10^{-7} and 10^{-1} mrem.

Comparison of the dose-through-time curves, in which the faulting event is forced to occur at a specified year, are shown in figure 3-7d. Average expected dose values are greatest when the faulting event is initiated at year 500 and decrease systematically toward the base case curve as the faulting event is initiated at later years. The slightly higher dose values at year 500 versus year 100 appears to be an artifact of how the TPA (Version 3.2.3) code and, specifically, the NEFTRAN subroutine, time-step through their respective calculations. These differences are trivial, however, compared to the base case values, and this code-execution artifact does not significantly affect SDS conclusion regarding the significance (or insignificance) of faulting to repository performance.

A second important simplification of the FAULTING module is that faults are generated randomly, independent of the notion of linked faulting between intrabasin secondary faults, principal block-bounding, and basin-bounding faults (see section 4.1.2 for description of principal and secondary faults). This conceptualization is used because its implementation is straightforward and because no adequate model of how secondary faulting related to motion on principal faults had been developed when the code was first implemented. Planned revisions to the FAULTING module will incorporate recent concepts about en echelon faulting at YM (Ferrill, et al., 1999a, b) and recent numerical modeling results (Stamatakos, et al., 1997b).

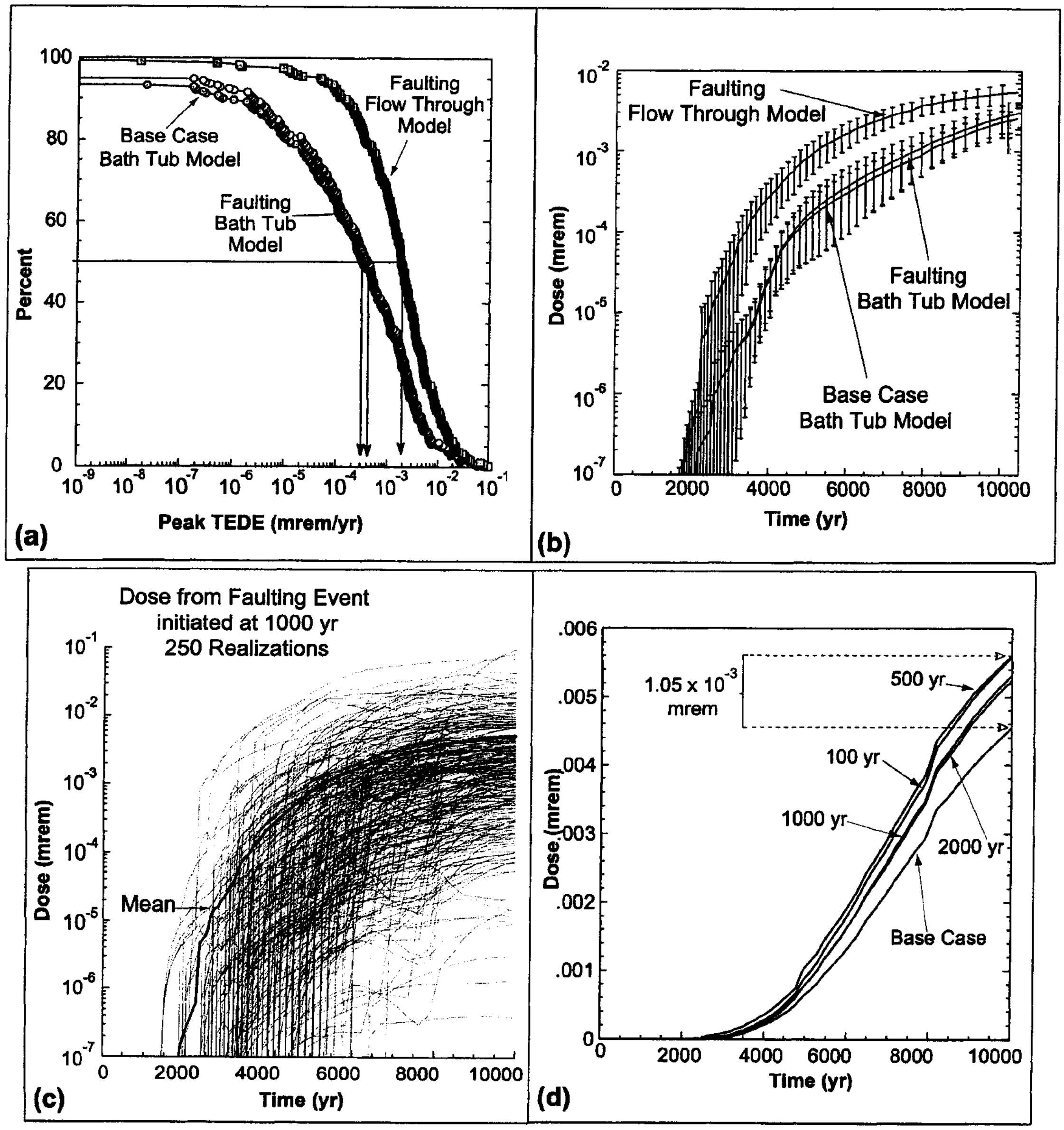

Figure 3-7. Consequence modeling results showing the effects of faulting on repository performance. (a) Complimentary Cumulative Distribution Factor comparing the peak total effective dose equivalent for the base case, faulting assuming the bath tub model, and faulting assuming the flowthrough model. (b) Dose-through-time plot showing the mean dose of 250-realization run that compares the base case, bath tub, and flowthrough models. Error bars are two standard errors about the mean curves. (c) Dose-through-time plot showing the individual results of each realization in a 250-realization run and the mean curve. In this example, the faulting event was forced to occur at year 1,000. (d) Dose-through-time curves comparing the mean dose values of the base case to ones in which the faulting event was forced to occur at year 100, 500, 1,000, and 2,000.

Probability of Faulting

An important abstraction for the methodology in the FAULTING module is the calculation of recurrence—the estimated frequency of faulting events within the boundary of the repository. Calculating the recurrence interval within the repository boundary is not straightforward because faults that initiate outside the boundary of the repository may still have a portion of their process zone intersect the repository itself. Thus, to estimate a recurrence rate, three additional values had to be determined: (1) the critical faulting region—that area that houses all faults capable of intersecting the repository; (2) the recurrence rate of faulting in the critical faulting region; and (3) the percentage of faults in the critical faulting region that also intersect the repository. Based on these three values, the recurrence rate for the repository was estimated from the following five steps.

(1) The critical faulting region is developed from the range of mapped fault lengths and orientations at YM (Scott and Bonk, 1984; Simonds, et al., 1995). From that data, nearly all faults have lengths of 30 km or shorter, or half lengths of 15 km or shorter. Fault orientations range between N55° W (azimuth 305°) and N25° E (azimuth 25°). Given these constraints, the size of the critical faulting region is defined as 15.2 × 32.8 km, centered about the midpoint of the proposed repository.

(2) Paleoseismic studies (e.g., U.S. Geological Survey, 1998) in the YM region (a region of approximately 15 × 15 km, with an area about 45 percent as large as the critical faulting region), document approximately 23 unique surface disrupting events in the last 150,000 yr (figure 3-5a). This number leads to a recurrence interval of about 6,520 yr (150,000 divided by 23).

(3) This recurrence interval (6,250 yr) is for all faulting, principal and secondary. In the absence of data about how this faulting should be partitioned between the two types, it is simply and conservatively assumed that half of this faulting occurs on new or underappreciated faults. This assumption leads to a recurrence rate for secondary faults of 13,000 yr (6,250 yr divided by 0.50).

(4) This 13,000-yr recurrence interval is for the 15 × 15 km^2 area covered by the paleoseismic studies. Because the area of the critical faulting region is approximately 2.2 times as large as the area covered by the paleoseismic studies, the recurrence interval for the critical faulting region scales to approximately 6,000 yr (13,000 yr divided by 2.2). This scaling assumes that faulting activity in the critical faulting region is similar to that in the area covered by the paleoseismic studies.

(5) The stand alone version of FAULTING (Ghosh, et al., 1997) was then used to empirically estimate what percentage of faults generated in the critical faulting region would actually intersect the repository, given the 6,000-yr recurrence interval for the critical faulting region. Preliminary modeling results indicated that an average of 3 percent of all simulated faults intersect the repository, based on up to 1,000,000 realizations. Thus, the recurrence for faults within the repository

itself is about 200,000 yr (6,000 divided by 0.03) or an annual probability (which can be referred to as absolute probability) of 5.0×10^{-6}/yr.

Risk of Faulting to Repository Performance

Estimates of the risk posed by faulting on repository performance were determined by multiplying the probability of faulting times the consequences. As shown by these analyses, peak dose for any set of parameters always occurs at year 10,000. Thus, unlike estimates of risk for other more complex processes, such as volcanism (IA IRSR, U.S. Nuclear Regulatory Commission, 1999a), estimates of the upper bound of risk associated with faulting were calculated by simply multiplying the peak dose at 10,000 yr by the probability of faulting in the repository for the next 10,000 yr. The dose contribution of faulting over the base case is 1.0×10^{-3} mrem (figure 3-7d). Multiplying that conditional dose by the probability of faulting $[(1 \times 10^{-3}) \times (5 \times 10^{-6}) \times (10{,}000\ \text{yr})]$ yields an upper bound value of 5×10^{-5} mrem, which is nearly two orders of magnitude below the base case value of 3.0×10^{-3} mrem (Mohanty, et al., 1999). Therefore, based on current analyses, faulting does not appear to pose a significant risk to repository performance.

Model Conservatism

Assumptions leading to overestimation of consequences of faulting:

(1) Absolute probability of faulting assumes up to 50 percent of faulting at the repository will occur on new or underappreciated faults. Most geological observations suggest that nearly all faulting will reactivate existing faults, [i.e., those that are known and mapped (see Morris, et al., 1996)]. This conservative assumption is made to ensure that some package failures occur and to evaluate the consequences when some faults might not be avoided.

(2) WP failure mechanism assumes that, after a minimum threshold displacement is exceeded (in this case 25 cm), the entire WP fails. WP failure is not linked to a common WP failure mechanism used in other modules of the TPA code, for example, in EBSFAIL. In addition, all WPs intersected by the fault zone are considered failed instantaneously and completely. This conservative assumption is made, at present, because the forces that WPs would encounter in an active fault zone are poorly understood.

(3) Emplacement of WPs is assumed to be random. Current design, however, shows the emplacement drifts oriented roughly east-west, perpendicular to the dominant trend of YM faults. Thus, the actual number of WPs impacted by a faulting event may be smaller than modeled here.

Assumptions leading to underestimation of consequences of faulting:

(1) Lack of a link between faulting, seismicity and volcanism. In nature, volcanic eruptions are always accompanied by numerous pre- and syn-eruption earthquakes (Luhr and Simkin, 1993; Fedotov and Markhinin, 1983). Similarly,

all faulting events that will affect the proposed repository would be accompanied by significant seismicity. Such earthquakes would have a high-frequency component and strong GM component because the earthquakes would be centered very close to, if not directly underneath, the proposed repository. Also, current TPA code does not account for the cumulative effects of these repetitive processes.

(2) Unaccounted for co-seismic slip on a new or an underappreciated fault generated by rupture on other existing faults. A new fault or an underappreciated fault is generated by the module without considering the faults and fractures that already exist. In FAULTING, displacement on an existing fault does not affect other faults and fractures in the repository block. In nature, a slip on a fault may have the potential to cause sympathetic slips on other existing faults and fractures.

In summary, a number of critical assumptions and simplifications are inherent in the abstraction of the geological process of faulting in the TPA code. In most cases, these assumptions and simplifications are conservative, in the sense that they overestimate the individual dose. These conservatisms add confidence to these analyses, given that these results show that faulting is not significant to dose.

The following caveats, if borne out by further work, could alter this conclusion:

(1) The regulatory period of performance of the proposed facility is significantly longer than 10,000 yr (e.g., more than 20,000 yr).

(2) Recurrence interval of faulting is significantly underestimated. For example, recent global positioning satellite (GPS) results (Wernicke, et al., 1998) suggest that the strain rate for the YM region may be underestimated by an order of magnitude. Current analyses indicate these results are not indicative of current crustal conditions (see section 4.4). However, additional GPS measurements and analyses are ongoing, and, if the Wernicke, et al. (1998) result is established (in the sense that future faulting at the site is expected to be greater than that predicted by the geological record) and it can be shown to directly influence the rate of faulting, then new faults can be expected to offset emplacement drifts and WPs in the repository during the lifetime of the facility.

(3) Significant low-angle faulting is found in the repository. Recent excavation of Alcove 5 of the ESF revealed at least three subhorizontal fault zones[3]. Subhorizontal faulting, if the faults are Type I and faulting occurs at the repository horizon level, could impact a significant number of WPs.

(4) Scoping analyses indicate that the effects on performance of the coupling of faulting and seismicity or volcanism are greater than when each event is considered separately.

---

[3]Gray, M.B., Personal Communication to J. Stamatakos, May 6, 1998.

(5) Significant changes are proposed for WP strength, layout in drifts, quantity, and distribution within the repository.

Faulting Exhuming Waste Packages

Inherent in the DOE RSS is the proposition that cumulative slip on a fault through the repository could not bring WPs to the surface (for example, see Hypothesis No. 16 of U.S. Department of Energy, 1998a). Evaluations of cumulative slip of faults by staff show that this proposition is correct; it is highly unlikely that WPs in the emplacement drifts will be exhumed to the surface by faulting. First, the repository block lies between two large block-bounding faults (the Solitario Canyon and Bow Ridge faults). Transport of the WPs to the surface would require a new block bounding fault to form within the repository block and for that new fault to accommodate all the extension (accumulate all the slip) at YM over the lifetime of the repository. Second, even if such a fault were to form, 10^6 to 10^7 yr would be required to exhume the WP, given current estimates of slip rates of 0.1 to 0.01 mm/yr [based on paleoseismic data summarized in table 4.2.1 of U.S. Geological Survey (1996)]. Even higher rates of about 1.0 mm/yr, as proposed by Wernicke, et al. (1998) based on GPS results, would require 10^5 to 10^6 yr to exhume WPs from the 300-m-deep repository. Therefore, the staff does not regard the possibility of WP exhumation a credible scenario for repository failure and considers this question resolved.

3.3.2 Seismicity—What Are the Viable Models of Seismic Sources and Seismic Motion at Yucca Mountain?

Because YM lies within a seismically active region of the Basin and Range province, moderate to large earthquakes (magnitude 6.0 and larger) are likely to occur over the life span of the repository (U.S. Geological Survey, 1998). The principal effect of earthquakes in the region are vibratory GMs at the repository site, (possibly in excess of 0.5 g), causing potential damage to facilities and structures, including WPs and emplacement drifts. The staff have determined that likelihood of earthquakes of various sizes occurring in the next 10,000 years and the potential consequences, effects of seismicity needs to be abstracted into numerical PA codes, specifically with regard to the following key elements of the engineered and natural barrier subsystems: (1) mechanical disruption of WPs either by induced rockfall, secondary faulting, or repeated vibratory GM; and (2) fracture dilation and redistribution of local stress field affecting flow. DOE and NRC consider seismicity to be an operative process at YM and have abstracted the process in their base case total system performance models.

The main consequence of seismicity is earthquake-induced rockfall in the emplacement drifts. In the current TPA code (Version 3.2), rockfall is assessed by the SEISMO module. Consequence assessment is currently being investigated by the RDTME KTI. SDS provides information on the input parameters, including the seismic hazard curve and the distribution of fractures used to calculate the size of rockfall blocks. Essentially, the SEISMO module generates a history of seismic events over the time period of interest from the seismic hazard curve. The input required for generating event history includes ground acceleration sampling points and the corresponding recurrence times, both derived directly from the probabilistic seismic hazard curve. The history of seismic events is then used by the code to determine two values, the area extent of rockfall throughout the entire repository and the yield-zone height of the repository blocks that can fall on WPs. Both correlate directly with ground acceleration.

SDS will continue to provide input regarding earthquakes and seismic hazard to the ISIs-mechanical disruption of WPs by proposing a prudent and reasonably conservative range of probabilities of occurrence of earthquakes of any size, the range of probabilities that any rock acceleration or velocity will be exceeded in any given year, recurrence rates of earthquakes, and related information. This information needs to be considered because seismicity-induced rockfall has the potential to directly rupture breach WPs, exposing its contents, and, thus, allow enable premature release of radionuclides from the repository (RDTME IRSR, Revision 2, U.S. Nuclear Regulatory Commission, 1999b). DOE has hypothesized that this is of little importance (U.S. Department of Energy, 1998, Hypothesis No. 17, "The severity of GM expected in the repository horizon for tens of thousands of years will only slightly increase the amount of rockfall and drift collapse"). The scenario of seismicity inducing existing faults to slip, or to initiate new faults is considered to be encompassed by the fault displacement hazard subissue.

The scenario whereby vibratory GM, by itself caused by a single moderate to large earthquake, or perhaps by repeated smaller earthquakes, might cause WPs to prematurely break or deform (by shaking, rattling, or rolling) will be analyzed at a future date. Changes in the flow of groundwater to and from the emplacement drifts also caused by 'seismic pumping' has the potential to alter WP stability, the direction and travel time of groundwater, and the release of radionuclides to the accessible environment. This scenario is addressed and resolved in the USFIC IRSR, Revision 2 (U.S. Nuclear Regulatory Commission, 1999c).

Consequence modeling of seismicity is now under the direction of the RDTME KTI, and the reader is referred to the RDTME KTI IRSR Revision 2 (U.S. Nuclear Regulatory Commission, 1999b) for consequence analyses of this process.

3.3.3 Fracturing and Structural Framework of the Geologic Setting—What Are the Viable Models of Fractures at Yucca Mountain?

Observations and tests at the repository level of the ESF show that the site is highly fractured. Pneumatic testing indicates that fractures are open and connected from depth to surface. ^{36}Cl data indicate that some fractures conduct water to repository depths. Fracture flow is recognized by the NRC and the DOE as an operative process at YM. Given that fractures can conduct water, vapor, heat, and perhaps magma, it is necessary to understand the fracture systematics and characteristics.

Depending on the geometric characteristics of individual fractures (e.g., size, aperture, and roughness) and fracture populations (e.g., population distributions and interconnectedness), extent and type of fracture filling, and associated deformation and alteration along fracture or fault zones, fractures, and faults may be either pathways or barriers with respect to flow. Similarly, the role of fractures and faults in repository stability is dependent on the fracture characteristics. Documentation of general fracture patterns and characteristics and analysis of potential future changes to fractures are important to assessment of flow- and stability-related performance parameters at YM.

Staff determined that, because of the presence and significance of fractures, the probability of physical changes in the next 10,000 yr and potential consequences, fractures or their effects on performance need to be abstracted into the following seven key elements of the EBS and NBS subsystems: (1) mechanical disruption of WP, (2) quantity and chemistry of water contacting WPs, (3) spatial and temporal distribution of flow, (4) distribution of mass flux between fracture and matrix (5) retardation in fractures in the UZ, (6) flow rate in water production zones, and (7) retardation in water production zones and alluvium (appendix A).

SDS will continue to provide input regarding fracturing and structural framework to the seven ISIs (appendix A) by proposing prudent and reasonably conservative ranges of fracture parameters. This information needs to be considered because fractures are likely to be loci of rock failure (e.g., rockfall) and serve as pathways or barriers (low permeability zones) to flow of fluids and heat (different hydraulic and thermal conductivity relative to rock matrix).

3.3.3.1 U.S. Nuclear Regulatory Commission/Center for Nuclear Waste Regulatory Analyses Sensitivity Studies of Fracturing

SDS will continue to provide input regarding fracturing and the structural framework to the seven ISIs described in the preceding and shown diagrammatically in figure 3-2. Sensitivity studies that assess fracture and fault zone effects on these processes will be documented in IRSR's for the USFIC, RDTME, Evolution of the Near Field Environment (ENFE), Thermal Effects on Flow (TEF) and Radionuclide Transport (RT) KTIs.

3.3.4 Tectonic Framework of the Geologic Setting—What are the Viable Tectonic Models at Yucca Mountain?

Tectonic models are prerequisites for evaluation of tectonic events and processes that have occurred in southern Nevada in the past 2,000,000 yr (Quaternary Period) and, therefore; may occur at or near YM in the period of interest. The tectonic FEPs relevant to a repository at YM include: (1) range-bounding faults, such as Bare Mountain (BM), Solitario Canyon, and Paintbrush Canyon faults, all considered currently active; (2) earthquakes associated with those and other faults; (3) basaltic volcanism, represented by the chain of million-year-old volcanoes in Crater Flat, and the 76 kyr-old volcano at Lathrop Wells; and (4) crustal extension rates up to 2 mm/yr-horizontal, caused by ongoing plate tectonics. The staff determined that tectonic strains in the vicinity of YM and the potential consequences have a high probability of continuing through the time period of interest (TPI). Tectonic models or their effects need to be abstracted into the following two ISIs of the EBSs and NBSs: (1) mechanical disruption of WPs, and (2) volcanic disruption of WPs (appendix A). The DOE and the NRC consider tectonic strain to be an operative process at YM.

SDS will continue to provide input regarding tectonic events and processes of interest to the ISIs—mechanical disruption of WPs, and volcanic disruption of WPs by proposing prudent and reasonably conservative ranges of tectonic events or processes, including the probability, distribution, and magnitude of their occurrence (see this IRSR, section 4.4 for discussion of tectonic models and faulting; see RDTME IRSR (U.S. Nuclear Regulatory Commission, 1999b) for discussion of tectonic models and seismicity; see IA IRSR for discussion of tectonic models and magmatism (U.S. Nuclear Regulatory Commission, 1999a). Tectonic framework information needs to be considered because it could provide geological and geophysical limits on, and alternative scenarios for, tectonic hazards and risks.

3.3.4.1 U.S. Nuclear Regulatory Commission/Center for Nuclear Waste Regulatory Analyses Sensitivity Studies of Tectonics

The NRC staff's ongoing sensitivity studies on seismicity that affect WPs consider the range of maximum earthquakes most likely to be generated by the strains implied by the various viable tectonic models (sections 3.2.2.1, 4.4.2.2, and 5.4.3.4).

3.4 Importance of Subissue to Repository Design and Preclosure Performance

DOE presented an approach for assessing seismic hazards and seismic design of the proposed YM geologic repository operations area in two Topical Reports #1 and #2. Topical Report #1 describes the DOE methodology for probabilistic assessment of vibratory ground motion and fault displacement hazards. Topical Report #2 describes the design methodology and criteria that DOE intends to implement to provide reasonable assurance that vibratory ground motions and fault displacements will not compromise the pre-closure safety functions of structures, systems, and components (SSC). Using the results of the hazard assessments discussed in PSHA (U.S. Geological Survey, 1998) pre-closure seismic ground motion and fault displacement will be determined. The seismic ground motion and fault displacement results will be documented in Topical Report #3, planned for completion late in 1999, and will be used to design the facilities at YM. SCC important to safety must be designed and built to meet these design values and all the requirements of preclosure performance. SDS Subissues are integrated with pre-closure design and performance assessment. In this version of the SDS IRSR (Revision 2.0), however, only post closure considerations are discussed. Pre-closure issues will be discussed in subsequent documents, including the review of Topical Report #3 and subsequent revisions of the SDS IRSR. Pre-closure design, as it relates to seismicity, is also discussed in the RDTME IRSR (U.S. Nuclear Regulatory Commission, 1999b).

4.0 REVIEW METHODS AND ACCEPTANCE CRITERIA

Resolution of the SDS KTI requires data on and estimates of: (1) the prevailing hydrostatic, lithostatic, thermal, and seismotectonic stresses; (2) future states of such stresses and seismicity; and (3) the corresponding behavior of fractured, faulted, and layered rocks in continual interactions with the variable stresses and strains and the hydrogeologic and potential igneous systems. These data enable performance of the structural framework portion of the NBS to be evaluated. Also needed for resolution of the SDS KTI are data on, and estimates of, construction and thermally induced changes to the structural framework of the rocks of the repository operations area. The DOE is in the process of obtaining data on, and estimates of, all the relevant FEPs and tectonic conditions. Such data or estimates, followed by issue resolution, will enable performance of the NBS and the EBS within it to be evaluated for any phase or period of performance.

NRC staff determined that the seismotectonic activities that may significantly affect the future (10,000 to 100,000 yr or more) performance of a repository at YM can be adequately identified and assessed by existing methods, models, and codes. With prudent projections of changes of processes and conditions and analyses of uncertainties attendant upon performance of engineered and natural systems, forward-modeled concepts of seismotectonic hazards and their effects can be reasonably applied to the analysis of risk.

Insights into the future SDS of the YM region will continue to emanate from field observations and measurements (including analogous systems around the globe), seismic and geodetic monitoring, scale-model experiments, and three-dimensional (3D) conceptual geologic and geophysical modeling. The NRC staff's review of DOE's conclusions about future seismotectonic behavior of the site will be based on the staff's professional judgment regarding the completeness and acceptability of DOE's data and interpretations and independent analyses.

The staff will determine whether the DOE has complied with the acceptance criteria described in the following for resolution of the SDS issue and subissues. The staff will evaluate DOE's demonstration that it has identified and adequately characterized seismotectonic activities, has sufficiently understood and fully considered its significance, and appropriately used relevant interpretations (abstractions and models) to evaluate long-term performance. The staff will evaluate DOE's assumptions and projections by applying its standards of completeness, quality, consistency, and consideration of uncertainties. Application of such standards of review is expected to result in NRC evaluations (and DOE assessments) that are technically defensible and, when uncertainties are appropriately considered, would be deemed to be reasonable and prudent.

4.1 UNIFORM ACCEPTANCE CRITERIA

The staff is developing a license application review plan specific to YM. At this time, a working set of uniform AC applicable to each area of review in NRC's current TSPA, TPA 3.2 (Mohanty and McCartin, 1998), is available for use by the KTIs. This IRSR reflects those preliminary criteria, anticipating their approval. One outcome of adapting the generally applicable criteria to the review of SDS subissues is that the SDS AC in Revision 1 have been reconstituted as RMs. These RMs provide staff with guidance on how to evaluate DOE's license application. These methods or means to resolve a subissue, or any acceptable substitute for them, are called RMs. This change of emphasis was facilitated by the fact that the ACs in revision 1 were more specific than what staff anticipates to be included in the Yucca Mountain Review Plan (YMRP). If ACs are not adequately met, then the subissue is not resolved at the staff level [i.e., it is categorized as an open item (RMs and ACs for each subissue are discussed in this section, and all resulting open and resolved items are compiled in section 5 of this report)].

The preliminary ACs for each of SDS's four subissues follow from the draft YMRP. They are:

AC 1: Physical phenomena and couplings, and consistent and appropriate assumptions have been incorporated into the [fault displacement hazard/seismic hazard/fracture framework/tectonic framework] abstraction in the PA, and the technical bases are provided.

AC 2: Sufficient data (field, laboratory, and/or natural analog data) are available to adequately define relevant parameters and conceptual models necessary for developing the [fault displacement hazard/seismic hazard/fracture framework/tectonic framework] abstraction in TSPA.

AC 3: Parameter values, assumed ranges, probability distributions, and/or bounding assumptions used in the [faulting hazard/seismic hazard/fracture framework/tectonic framework] abstraction, such as probability of occurrence of earthquakes or distribution of fracture spacing in the ceiling of emplacement drifts, are technically defensible and reasonably account for uncertainties and variabilities. The technical basis for the parameter values used in the PA needs to be provided.

AC 4: Alternative modeling approaches consistent with available data and current scientific understanding are investigated and results and limitations appropriately factored into the [fault displacement hazard/seismic hazard/fracture framework/tectonic framework] abstraction in TSPA.

AC 5: Output of the [fault displacement hazard/seismic hazard/fracture framework/tectonic framework] abstraction is verified through comparison to output of detailed process models and/or empirical observations (laboratory testings or natural analogs, or both).

The SDS issue will be resolved when the AC for each subissue have been met, because the subissues have a cause and effect interdependency.

Two additional generic AC relating to Quality Assurance (QA) and expert elicitation have been removed from SDS IRSR. A task force is being developed within the NRC to examine DOE's QA program and expert elicitations. Resolution of these criteria will be addressed when the task force completes its evaluation.

4.1 FAULTING

In previous versions of the SDS IRSR, the general concept of faulting has been subdivided into two components: (1) Type I faults, and (2) fault displacement. Type I faults and fault displacement are generally investigated by deterministic methods. It is state of the art to determine fault displacement hazards by probabilistic methods of analysis. In this report, Type I faults have been included under seismic source characterization (section 4.2). Also in this report, the NRC has combined the AC and review methods developed for: (1) identification of Type I faults and the catalog of known faults that could potentially affect repository design and performance, (2) fault displacement and the probability of direct fault rupture of WPs (section 4.1.2); and (3) seismicity and the estimates of peak GMs at the site from earthquakes (section 4.2). The AC are enumerated in section 4.0.

4.1.1 Fault Displacement Hazard

The objective of fault displacement analyses is to evaluate the potential hazards of an intersection of an active fault with vital components of the repository system, especially WPs. YM lies within the central Basin and Range Province of the North American Cordillera [for example, see figure 1 of Wernicke (1992), p. 554]. The region is characterized by complex interactions of strike-slip and extensional deformation, active since the onset of the Cenozoic 65 Ma. The region remains tectonically active as indicated by numerous Quaternary faults (including Holocene) and volcanism and historic seismicity (including the 1992 Little Skull Mountain earthquake) (Ferrill, et al., 1996a).

For this evaluation of faulting, both principal (including sympathetic) and secondary (or distributed) faulting must be considered (as defined in dePolo, et al., 1991). Principal faulting refers to displacement along the main fault zone responsible for the release of seismic energy (i.e., an earthquake). At YM, principal faulting is assumed to occur only on primary faults, mainly block-bounding faults. In contrast, secondary or distributed faulting is defined as rupture of smaller faults that occurs in response to the rupture in the vicinity of the principal fault. These two subsets of faults are not mutually exclusive. Faults capable of principal rupture themselves can undergo secondary faulting in response to faulting on another primary fault. Because principal and secondary faults pose a potential risk to repository performance, both types must be considered by the DOE in its analyses.

The simplest approach for the evaluations of principal faulting, and one which was used predominantly before 1998 for siting of nuclear reactors and other critical facilities, is a deterministic analysis. In that approach, capable faults (10 CFR Part 100, appendix A) are avoided by adequate setback distances. This approach may not be appropriate for YM (as noted in Coppersmith, 1996) because of the different performance requirements between a reactor and the repository and the proposed repository is too large to reasonably expect that virtually all faults of concern can be avoided.

Methods similar to the PSHA have also been developed to evaluate fault displacement hazards, especially for principal faults for which detailed paleoseismic data are available. These methods construct individual fault displacement hazard curves, analogous to probabilistic seismic hazard curves, for each principal fault (Youngs and Coppersmith, 1985; U.S. Geological Survey,1998).

Few techniques, however, exist to evaluate the probability of secondary faulting (e.g., Coppersmith and Youngs, 1992). Because of the complexity of fault analyses, DOE experts had to make assumptions and develop estimates of the future behavior of faults based on a variety of data and models (U.S. Geological Survey, 1998). The staff is currently evaluating the DOE assumptions and projections by examining the completeness, quality, consistency, and appropriate consideration of uncertainty. Further, this evaluation includes assessment of deterministic and probabilistic analyses of principal fault displacement, as well as integration of these analyses with structural and tectonic models used to assess secondary faulting. Fault displacement hazard in postclosure PA is treated as an event or series of events (as in FEPs) that has a probability of occurrence derived from a geologic analysis of its recurrence rate. The critical aspect of the staff's current review is the significance of faulting (if any) to overall repository performance during the postclosure period. Review of the faulting hazard with respect to preclosure regulations will be addressed separately in later documents.

4.1.1.1 Review Methods for Fault Displacement Hazard

The RM used to evaluate the preliminary Uniform AC (section 4.1) for the Faulting subissue is focused to provide the reviewer with guidance on evaluation of the DOE treatment of faulting as it relates to WP failure and post-closure repository performance. It also serves to highlight a path to resolution for the mechanical disruption of WP ISI. The RM addresses technical bases for adequate and conservative bounding analyses, and for the approximation of adequate and conservative parameters. Staff reviewed DOE's analyses of faulting to determine the adequacy of DOE's conclusions, especially with regard to the DOE probabilistic fault displacement hazard analysis, which was part of the DOE PSHA (U.S. Geological Survey, 1998a). Staff applied the following review method with three steps to determine whether the preliminary Uniform Acceptance Criteria (section 4.1) were met for this subissue. These steps are:

Step 1—Nature of Faulting at YM

Staff will ascertain that the DOE has adequately evaluated the nature of faulting, and the appropriate faulting hazard sources within the repository block, and both principal and secondary from the range of possible interpretations. For example, staff will ascertain that DOE's interpretations of faulting from surficial and underground mapping are geologically consistent and reasonable, and that they are compatible within the range of viable interpretations of YM tectonics. Faulting should be noted as primary or secondary as these classifications pertain to the PFDHA.

Step 2—Consistency of Faulting Models

Staff will ascertain that the DOE has adequately determined models of faulting from fault geometry, kinematics, and mechanical behavior as applicable to development of the PFDHA. For example, staff will ascertain that models used to describe primary and secondary faulting or distributed faulting are adequate as they relate to development of the faulting hazard assessment in the PSHA.

Step 3—Faulting Recurrence

Staff will ascertain that the DOE has adequately evaluated faulting activity as it relates to the development of the PFDHA. For example, staff will ascertain that faulting recurrence models based on slip rate, displacement, or earthquake data are consistent with the PSHA, site structural geology, YM tectonics, and geological theory.

4.1.1.2 Technical Bases for Review Method

Nature of Faulting at Yucca Mountain

YM consists of a thick accumulation of volcanic tuff deposited on an irregular surface of eroded and deformed Paleozoic and Precambrian basement composed of highly faulted and folded sedimentary and metasedimentary rocks. These tuffs were erupted from a series of Middle to Late Miocene (15 to 9 Ma) calderas that collectively form what has been defined as the southwestern Nevada volcanic field [see Sawyer, et al. (1994) for the most recent regional stratigraphy of the Miocene volcanic rocks in the YM region. Rocks of the Paintbrush Group, principally ash flows of the Topopah Spring Tuff (12.8 Ma) and Tiva Canyon Tuff (12.7 Ma), make up the main surface exposures of YM (figure 4-1). The Paintbrush Group tuffs rest on a sequence of older tuffs, including the Prow Pass and Bullfrog Members of the Crater Flat Group. Younger tuffs related to the Timber Mountain Group are locally exposed at YM in topographic lows between large block-bounding faults. This observation, along with evidence for growth faults in the Paintbrush rocks in Solitario Canyon (e.g., Carr, 1990; Day, et al., 1997), suggests that faulting and tuff deposition were synchronous at YM. Trenching studies of the Solitario, Paintbrush Canyon, and Bow Ridge faults show sufficient evidence for multiple-faulting events in the Quaternary (see sections 4.6 and 4.7 of U.S. Geological Survey, 1996). Contemporaneous faulting and basaltic volcanism have been suggested by the presence of ash in Quaternary faults in the Crater Flat—YM area (U.S. Geological Survey, 1996).

The majority of faults at YM are either north trending normal faults or northwest trending dextral strike-slip faults. The larger faults in these two orientations bound the fault blocks that underlie the study area. These two sets of faults are interpreted to be contemporaneous, based on mutual terminations and secondary structures between them, such as pull-apart basins (Day, et al., 1997, 1998). Some northwest trending faults are dominantly normal faults, accommodating extension in relay ramps between overlapping normal faults (Ferrill, et al., 1999a). Only four reverse faults with north-south or northeast-southwest strikes have been identified, but they are potentially key features for constraining the kinematic history of the region (Day, et al., 1998) and for identifying infiltration pathways (Levy, et al., 1997). Much of the detailed fieldwork to study faults in the central block focused on the Ghost Dance and Sundance faults, which are close to the subsurface trace of the ESF (Spengler, et al., 1994; Potter, et al., 1996).

YM consists of a sequence of north to north-northeast trending, fault-bound ridges crossed by occasional northwest trending, dextral strike-slip faults. Faults dip almost uniformly to the west and separate blocks of gentle to moderate east-dipping tuff strata. From north to south, both fault displacement and stratal tilt increases indicate progressively greater extension of the Crater Flat basin southward (Scott, 1990; Stamatakos, et al., 1997b). This pattern is most profound on the west flank of YM, which is defined by a series of left-stepping and north trending en echelon faults. The southward increase in fault offset is coupled with greater block rotation, both horizontal and vertical (Scott, 1990). Work by the USGS (Hudson, et al., 1994; Minor, et al., 1997) suggests that this pattern of faulting, along with rotated paleomagnetic direction in the tuffs, resulted from a discrete period of extension followed by a discrete period of dextral shear, akin to an oroclinal bending model. More recent reanalyses of these data suggest an alternative explanation. The north-to-south displacement gradient and rotation of fault blocks is simply a result of increased rollover deformation in the hangingwall above a listric

Miocene Volcanic Section
Yucca Mountain, Nevada

	Thirsty Canyon Group	Gold Flat Tuff	
		Trail Ridge Tuff	
		Pahute Mesa Tuff	
		Rocket Wash Tuff	9.4 Ma
	Fortymile Canyon assemblage	Beatty Wash Fm.	
	Timber Mountain Group	Ammonia Tanks Tuff	11.5 Ma
		Rainier Mesa Tuff	11.6 Ma
		Rhyolite of the Loop	12.5 Ma
	Paintbrush Group	Tiva Canyon Tuff	12.7 Ma
		Yucca Mountain Tuff	
		Pah Canyon Tuff	
Repository Horizon →		Topopah Spring Tuff	12.8 Ma
		Calico Hills Fm.	12.9 Ma
		Wahmonie Fm.	13.0 Ma
	Crater Flat Group	Prow Pass Tuff	
		Bullfrog Tuff	13.25 Ma
		Tram Tuff	
	Belted Range Group	Dead Horse Flat Tuff	13.5 Ma
		Grouse Canyon Tuff	13.7 Ma
		Comendite of Split Ridge	
		Lithic Ridge Tuff	14.0 Ma
	Older Tuffs	Lava of Tram Ridge	
		Tunnel Fm.	
		Tub Spring Tuff	
		Tuff of Yucca Flat	
		Redrock Valley Tuff	15.25 Ma

Figure 4-1. Summary chart of the Miocene volcanic stratigraphy at Yucca Mountain, derived from Sawyer, et al., 1994

BM fault (section 4.4.1.2; Ferrill, et al., 1996b; Ferrill and Morris, 1997; Stamatakos and Ferrill, 1998; Morris and Ferrill, 1999).

An en echelon pattern of faulting is best expressed along the western edge of Yucca Crest and the fault line escarpment that follows the west-dipping Solitario Canyon, Iron Ridge, and Stagecoach Road faults (see, for example, Simonds, et al., 1995). The geometry of faults and ridges defines a scallop trend, composed of linear, north trending fault segments connected by discrete curvilinear northwest trending fault segments. For example, the ends of the northwest trending curvilinear Iron Ridge fault bend to the northwest near its overlap with both the Stagecoach Road and Solitario Canyon faults. YM also contains numerous swarms of small northwest trending faults that connect the large north trending faults. One example is at West Ridge, which is cut by numerous small faults that connect segments of the Windy Wash and Fatigue Wash faults. This geometry strongly suggests that the entire YM fault system is an en echelon branching fault system (Ferrill, et al., 1999a), in which faulting on the large block-bounding fault triggers relatively widespread, but predictable, secondary faulting on connecting and linking faults. Linkage of the en echelon system is either by lateral propagation of curved fault tips or formation of connecting faults that breach the relay ramps (figure 1 of Ferrill, et al., 1999a; Peacock and Sanderson, 1994; Trudgill and Cartwright, 1994). More importantly, from this interpretation of en echelon faulting, it follows that locally developed faults and fractures were produced by local variations of the stress field (section 4.3.1) rather than dramatic swings of the regional extension direction (Throckmorton and Verbeek, 1995). The amount, orientation, and degree of faulting directly depend on the relative position of the rock within the en echelon fault system, either in relay ramps that connect overlapping en echelon fault segments or in the hangingwall or footwall blocks of the block-bounding faults.

Faulting Models from Tectonic Models

As discussed in section 4.4.1 and summarized in appendix C, numerous tectonic models have been proposed to explain the structural evolution of YM. Faults at YM, for example, have been interpreted as the result of: (1) hangingwall deformation related to normal fault motion on a listric B M fault (Ferrill, et al., 1996b), (2) hangingwall deformation above a regional low-angle detachment system (Scott, 1990; Hamilton, 1988), (3) deformation of the margin of a pull-apart basin (Fridrich, 1998), (4) listric faulting from a transtensional nappe deforming above the Amargosa Desert strike-slip shear system (Schweickert and Lahren, 1997), and (5) domino-style block deformation related to extension of an elastic-viscous Crater Flat graben (Janssen, 1995). These tectonic models can be used to estimate future fault activity at YM. For example, because a regional detachment system of the kind envisioned by Scott (1990) is assumed to have been truncated by a more recent uplift of BM, faulting at YM is assumed to be relatively inactive. Alternatively, very active strike-slip motion along the Amargosa Desert fault would predict relatively active faulting at YM.

In addition, the style (strike-slip or dip-slip) of faulting in the alternative tectonic models is important to evaluations of faulting data from the paleoseismic investigations. In trenches, typically only the vertical component of separation can be deduced from offset stratigraphic marker beds. If the style of faulting is dominantly dip-slip, then actual fault displacements, at least for the strand of the fault exposed in the trench, can be deduced from the paleoseismic data. In contrast, strike-slip separation is not readily apparent in trenches. If this style of faulting dominates, then the trenching data may grossly underestimate actual fault activity.

Deformation Mechanism and Fault Width

Fault zone deformation in the upper crust produces a wide variety of textures that affect the overall characteristics of fault zones. Idealized faults consist of two textural zones, a fault core and a damage zone (Sibson, 1977; Caine, et al., 1996; Seront, et al., 1998). The fault core is a zone of high strain and accommodates most the fault displacement by flow in gouge, cataclasite, breccia, or mylonite. The surrounding damage zone is less deformed, accommodates less displacement, and may contain subsidiary structures such as veins, fractures, and minor faults (see figure 4-2).

Deformation mechanisms govern the behavior of the fault zone with time. At YM, the protolith (undeformed volcanic tuff) has undergone brittle deformation by cataclasis at shallow levels in the upper crust. Changes in deformation mechanisms with time and deformation, the presence of fluids in the fault zone, mineral transformations, and syndeformational mineralization affect the rheology of the fault zone that caused them to widen or narrow with increasing displacement. Two end-member possibilities exist: (1) If the products of the deformation produced fault rocks that inhibited continued cataclasis then additional fault displacement would have caused the protolith to fracture, and the fault zone would have widened with time (i.e., strain harden); (2) In contrast, if the fault rocks became progressively easier to deform, then deformation would have localized within a narrow portion of the fault zone (i.e., strain localization or strain softening) resulting in an intensely deformed fault core with no increase in fault zone width. Investigations of faulting at YM, especially studies of ESF faults, reveal that all these deformation processes and related features are present (Gray, et al., 1998). Based on detailed field and microscope analyses of the ESF faults, four stylized fault types are recognized (figure 4-3). Of the faults exposed in the ESF, only the Solitario Canyon fault has a well-developed fault foliated gouge. The orientation of the foliation is indicative of dip-slip displacement on the fault. Detailed x-ray analyses of the Solitario Canyon fault gouge are given in Farrell, et al. (1999).

More general to YM are faults characterized by brecciation without development of fault gouge. A critical observation is that fault zones appear to narrow with depth from the surface to their subsurface exposures in the ESF. Wide fault zones at the surface, such as the exposure of the Ghost Dance fault zone at the UZ-7A drill pad that is more than 10 m wide, narrows to a meter or less in exposures in the ESF. The exact cause of this observed change in fault width is not known and is currently being investigated by ongoing SDS studies. Changes in fault width probably reflect differences in fault orientation and environmental conditions of faulting, including confining stress, lithology, and water content. Direct observation of fault zones in the ESF has led staff to reevaluate fault zone parameters used in PA calculations (see section 3.3.1.1).

Recurrence

Recurrence relationships of faulting are generally derived from paleoseismic data of faults exposed in alluvial trenches. The objective of the trenching studies is to find datable stratigraphic markers offset by the fault and, from the age and amount of offset, determine the recurrence relationship for the fault.Recurrence data for faults are then used in conjunction with regional seismicity parameters such as frequency of earthquakes to develop probabilistic fault displacement hazard curves for each fault of interest. The curves are derived from two different

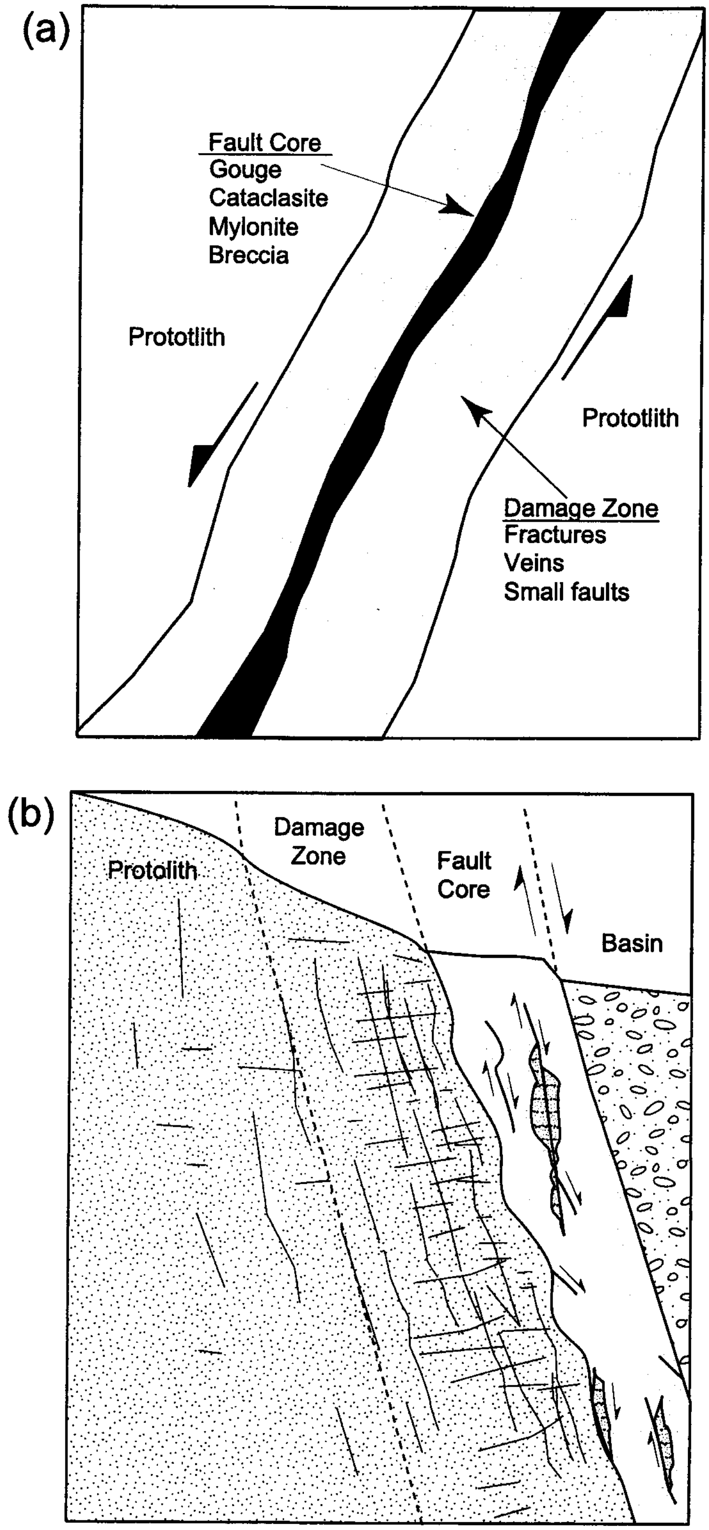

Figure 4-2. Definition of fault zone characteristics showing (a) conceptual model of fault zone showing the fault core and surrounding damage zone and (b) the Stillwater fault in Dixie Valley, Nevada (Seront, et al., 1998)

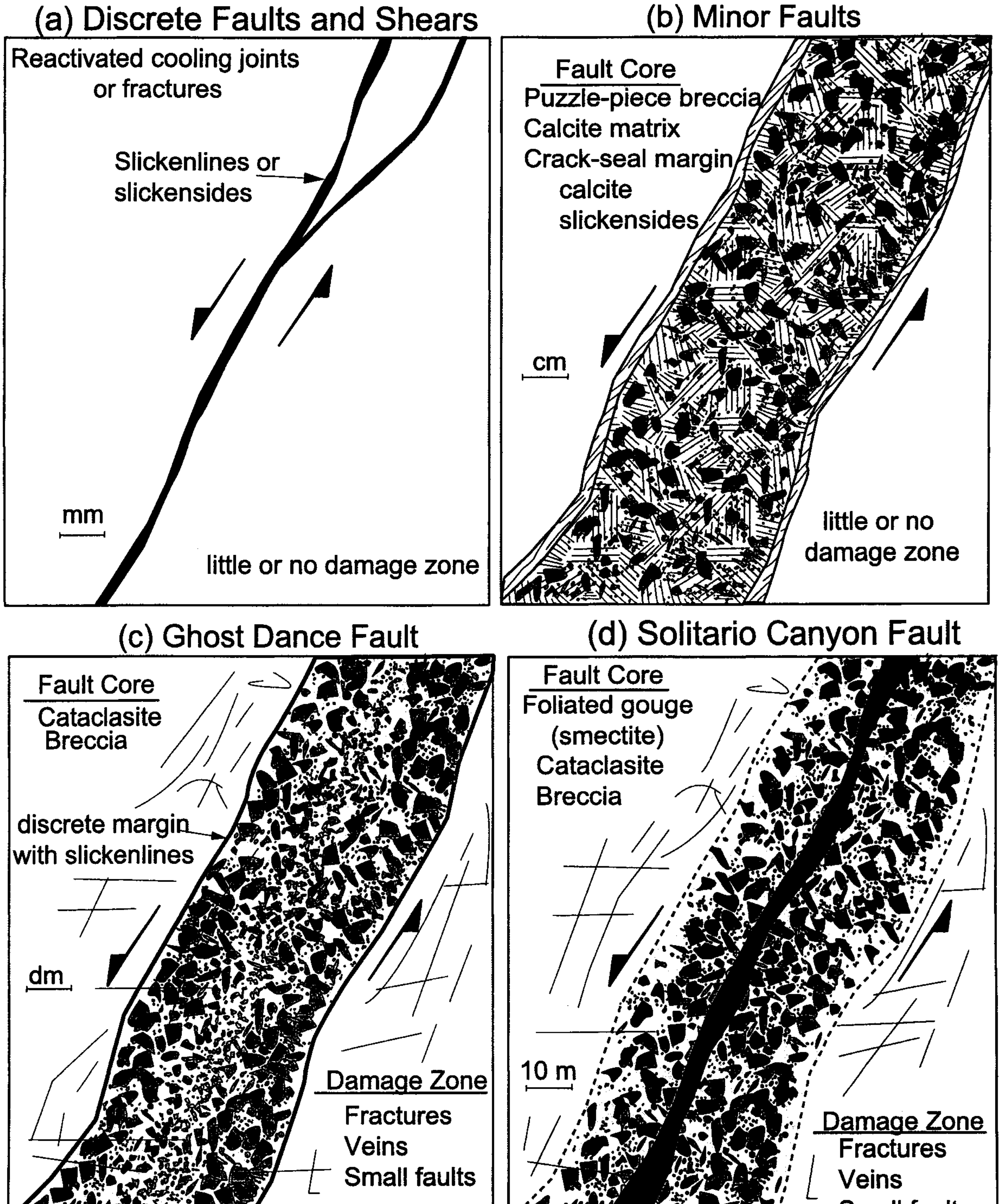

Figure 4-3. Types of fault zones observed from the Exploratory Studies Facility at Yucca Mountain. The four fault zones were identified from detailed field and laboratory studies of fault zone deformation (Gray, et al., 1998; Farrell, et al., 1999).

approaches, defined as the faulting-occurrence and magnitude-occurrence models (Cornell and Toro in Hunter and Mann, 1990). These methodologies, as applied in the DOE PSHA (U.S. Geological Survey, 1998), have been referred to respectively as the displacement approach and earthquake approach. The first approach uses fault-specific data, such as cumulative displacement, fault length, paleoseismic data from trenches, and historic seismicity. The second relates the frequency of the fault's slip events to the frequency of earthquakes on the seismic sources defined in the seismic source models developed for the corresponding seismic hazard analysis.

There are numerous potential sources of uncertainty associated with interpretations of fault slip histories from trenching studies (Ferrill, et al., 1996b) including: (1) distributed faulting, in which the trench captures only a fractional component of the total slip; (2) blind faulting, in which the offset is restricted to the fault below the surface and, thus, no surface data are available for study; (3) oblique or horizontal slip, in which the trench offset records only a small component of actual displacement; (4) inaccurate age estimates of the marker beds; and (5) variability of slip from event to event and along the strike of the fault. The accurate probabilistic fault displacement analyses need to account for these uncertainties.

Evaluation of the U.S. Department of Energy's Fault Displacement Hazard

The DOE (U.S. Geological Survey, 1998) developed a PFDHA using both the displacement and earthquake approaches. The assessment was constructed through the PSHA expert elicitation, which had six expert teams each consisting of three geoscientists.

In the expert elicitation (U.S. Geological Survey, 1998), probabilistic fault displacement hazard curves were developed for nine representative sites at YM (table 4-1), referred to as demonstration points. Of these, three points are on primary faults, three are on larger inter-block (secondary) faults, two are on small fault zones within the repository footprint, and one is in Midway Valley (4, 5, and 6) near the proposed surface facility site. Only three of the nine points are important to postclosure repository performance (points 5, 7, and 8). The other points are either outside the repository footprint or on faults that will be accounted for in repository design.

Table 4-1. Summary of U.S. Department of Energy Fault Displacement Results Demonstration Points for Fault Displacement Hazard Analyses

Point	Demonstration Point	Comment	Mean Displacements (cm)	
			10^{-4} yr	10^{-5} yr
1	Bow Ridge fault	Primary fault outside repository	< 0.1	7.8
2	Solitario Canyon fault	Primary fault outside repository	< 0.1	32
3	Drill Hole Wash fault	Primary fault outside repository	< 0.1	< 0.1

Table 4-1. Summary of U.S. Department of Energy Fault Displacement Results Demonstration Points for Fault Displacement Hazard Analyses (cont'd)

4	Ghost Dance fault	Secondary fault outside repository	< 0.1	< 0.1
5	Sundance fault	Secondary fault within repository	< 0.1	< 0.1
6	Small fault in Dune Wash	Secondary fault outside repository	< 0.1	< 0.1
7	100 m east of Solitario Canyon fault	Within repository; four conditions assessed: (a) small fault with 2 m of displacement (b) shear with 10 cm of displacement (c) fracture (d) intact rock	 < 0.1 < 0.1 < 0.1 < 0.1	 < 0.1 < 0.1 < 0.1 < 0.1
8	Center of Repository	Within repository, four conditions (a) small fault with 2 m of displacement (b) shear with 10 cm of displacement (c) fracture (d) intact rock	 < 0.1 < 0.1 < 0.1 < 0.1	 < 0.1 < 0.1 < 0.1 < 0.1
9	Midway Valley	Outside repository footprint	< 0.1	0.1

For both earthquake and displacement approaches, two critical parameters were developed by the expert teams, one describing the amount of fault displacement for each faulting event and one describing how frequently those events will occur. It is important to note that, unlike the seismic hazard assessment, methods to develop these parameters are not well established in the scientific literature; the probabilistic methodology was essentially developed by the experts within the DOE PSHA (U.S. Geological Survey, 1998). Thus, the expert teams relied on a wide variety of data and models to develop these two parameters.

Of these two methodologies, the displacement approach is more straightforward because it relies on direct observational evidence of faulting. The two required parameters can be derived directly from paleoseismic displacement and recurrence rate data, geologically derived slip rate data, or scaling relationships that relate displacement to fault length and cumulative fault displacement.

The earthquake approach uses earthquake recurrence models from the seismic hazard analysis. Three probabilities were assessed: (1) the probability that an earthquake will occur, (2) the probability that this earthquake will produce surface rupture on the fault generating the earthquake (the primary fault where the earthquake occurs), and (3) the probability that the earthquake will produce distributed surface displacement on other faults, primary or secondary.

(1) The probability that an earthquake will occur was derived from the seismic hazard assessment. In that assessment, the frequency distribution of

earthquake for each source (fault or area) was derived from available geologic, historical seismic, or paleoseismic data.

(2) The probability of surface rupture was determined by the expert teams in two ways: (a) logistical regression of historical earthquake and surface rupture data from the Basin and Range (see figure 4-11 of U.S. Geological Survey, 1998) and (b) focal depth calculations. In the focal depth calculations, the size and shape of the fault rupture for each earthquake (generally considered circular or elliptical) was estimated from empirical scaling relationships (e.g., Wells and Coppersmith, 1994). Depending on focal depth, the surface displacement (if any) along the fault was determined. Because the maximum surface displacement may not coincide with the demonstration point, an additional variable that randomized the rupture along the fault length was also introduced. Thus, for both the historical earthquake and focal depth methods, the amount of surface displacement at the demonstration point for each event was determined based on the location of the demonstration point relative to the surface rupture (figure 4-4).

(3) The probability of secondary or distributed faulting was determined by the experts in two ways: (a) by a logistical best fit to data from Basin and Range historical ruptures in which secondary or distributed faulting was mapped after the earthquake (see Pezzopane and Dawson in U.S. Geological Survey, 1996) and slip tendency analysis (Morris, et al., 1996).

Results of the DOE PSHA (U.S. Geological Survey, 1998) indicate that, except for the Bow Ridge fault, Solitario Canyon fault, and Midway Valley points, mean fault displacements are expected to be less than 0.1 cm over the next 100,000 yr (table 4-1). Mean displacements for the demonstration points important for repository performance (points 5, 7, and 8 that are within the repository footprint) do not exceed 0.1 cm in 100,000 yr. Except for demonstration points 5 and 7 (condition a; table 4-1), none of the hazard results predicts more than 10 cm of displacement for the next 10^8 yr. For demonstration points 5 and 7 (condition a; table 4-1), displacements of greater than 25 cm (the threshold value used in the PA calculations presented in section 3.3.1.1) can occur in the next 2×10^7 yr.

Sensitivity results provided in the PSHA (U.S. Geological Survey, 1998) show that neither earthquake nor displacement methods on average produces a greater hazard than the other. For example the Ake, Slemmons, and McCalpin team generally estimated the greatest faulting hazard (largest displacement for 10^{-5} yr) for each of the nine demonstration points. This team relied exclusively on the earthquake approach. The Smith, Bruhn, and Knuepfer team generally estimated the second greatest hazard using the displacement approach. Teams that used both approaches produced similar estimates of the hazard using both the earthquake and displacement approaches.

Staff has not fully reviewed all aspects of the DOE fault displacement methodologies. These methodologies are new and untested compared to existing and established techniques for analyses of GM. These methods should be published in the peer review literature and tested

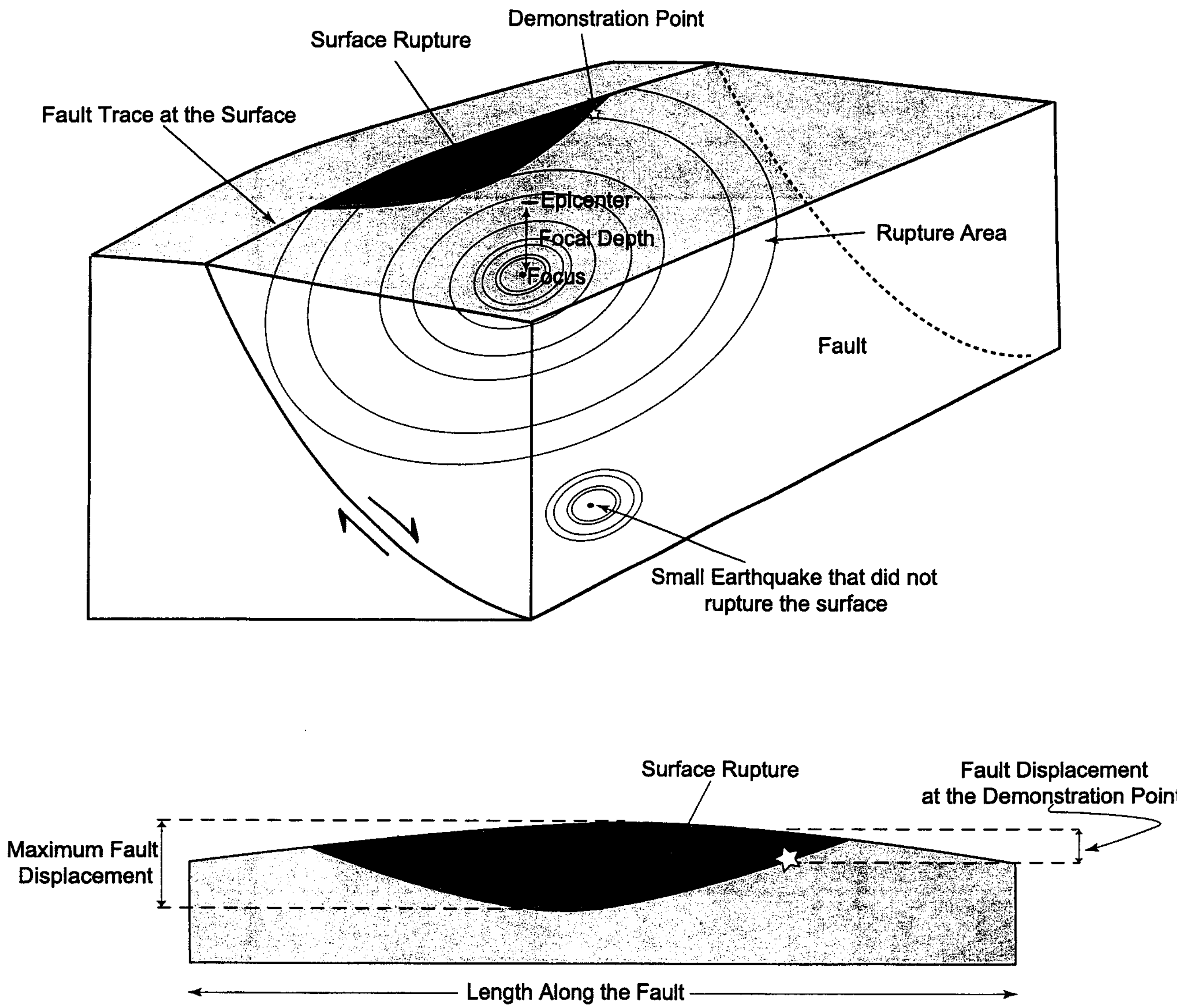

Figure 4-4. Schematic diagram illustrating possible rupture areas on a fault and their relative distribution to a demonstration point on the surface trace of the fault. The diagram shows that fault displacement at the demonstration point can vary depending on its location along the rupture surface.

accordingly by the scientific community at large. The staff assessment provided here and in section 5.1.3.3 examines the results of the fault displacement hazard in terms of staff's independent analysis of the effects of faulting on repository performance given in section 3.3.1.1.

Faulting in the repository is a low-probability, low-consequence event. The risk to performance is low even when very conservative assumptions are used about probability of occurrence and the effects on WPs (section 3.1.1.1). The DOE did not analyze faulting in the VA. The probability, however, that faulting exceeds 10 cm of displacements in the repository that might be sufficient to disrupt WPs is greater than 10^{-8}/yr threshold for consideration in PA. The DOE will, therefore, have to conduct a transparent and traceable analysis that demonstrates it has considered risk from faulting and defend their conclusions that fault disruption of WPs can be neglected in PA calculations.

4.2 SEISMICITY

YM lies within the central Basin and Range Province of the North American Cordillera [see, for example, figure 1 of Wernicke (1992), p. 554]. The region is characterized by complex interactions of strike-slip and extensional deformation, active since the onset of the Cenozoic 65 Ma. The region remains tectonically active, as indicated by numerous Quaternary faults (including Holocene), volcanoes, and historic seismicity (including the 1992 Little Skull Mountain earthquake).

In general, two approaches are considered acceptable by the staff to evaluate seismic hazards. These approaches are based on deterministic and probabilistic methodologies. Until January 1997, deterministic methodology has been the traditional methodology for evaluations of seismic hazards for construction and operation of nuclear facilities. Siting, review, and AC for these facilities are embedded in many existing NRC documents, such as 10 CFR Part 100, Appendix A (Code of Federal Regulations, Title 10, Energy, 1998); and section 2.5.1 (*Basic Geologic and Seismic Information*); 2.5.2 (*Vibratory Ground Motion*); and section 2.5.3 (*Surface Faulting*) of the NRC Standard Review Plan (SRP) outlined in NUREG-0800 (U.S. Nuclear Regulatory Commission, 1997a). Although the deterministic approach has worked reasonably well for the past three decades they have been criticized as overly conservative. Moreover, the deterministic approach does not explicitly account for uncertainties in geological or seismological parameters. To incorporate such uncertainties, probabilistic methods have been developed to allow for proper uncertainty analyses (such as different interpretations and expert elicitations).

4.2.1 Seismic Hazard

The PSHA methodology has been identified by the NRC in 10 CFR 100.23 as an appropriate approach to address uncertainties associated with GM and fault displacement. The DOE has outlined the methodology it intends to use for a PSHA in Topical Report #1 (U.S. Department of Energy, 1997a). This approach has been accepted, in principle, by the NRC (Bell, 1996). The methodologies recommended in the *Senior Seismic Hazard Analysis Committee Report* (SSHAC) (U.S. Nuclear Regulatory Commission, 1997c) also offer acceptable approaches for evaluating the probabilistic seismic hazard at YM.

The specific RM Is based on five basic technical aspects of a PSHA: (1) seismic source characterization, (2) earthquake recurrence characteristics, (3) GM attenuation, and (4) hazard calculations and presentation. Seismic hazard is treated in postclosure PA that have a certain probability of occurrence. The probability of occurrence is derived from a geological and seismological analysis of earthquake recurrence and related factors.

4.2.1.1 Review Method for Seismic Hazard

The RM used to evaluate the preliminary Uniform AC (section 4.1) for the Seismicity subissue is focused to provide the reviewer with guidance on evaluation of the DOE treatment of seismicity as it relates to WP failure and postclosure repository performance. It also serves to highlight a path to resolution for the mechanical disruption of WP ISI. The RM addresses technical bases for adequate and conservative bounding analyses, and for the approximation of adequate and conservative parameters. Staff reviewed DOE's analyses of seismicity to determine the adequacy of DOE's conclusions, especially with regard to the DOE PSHA (U.S. Geological Survey, 1998a). For postclosure performance, the seismic hazard curve is an important input parameter for assessment of rockfall in the emplacement drifts that result from earthquake-induced ground shaking. Staff applied the following review method with five steps to determine whether the preliminary Uniform Acceptance Criteria (section 4.1) were met for this subissue. These steps are:

Step 1—Seismic Sources

Staff will ascertain that the DOE has adequately evaluated the seismic sources and potential sources of seismicity used in its analysis and will confirm that the methods used in its evaluation are appropriate and sufficient. For example, the staff will ascertain whether DOE has sufficiently addressed: (a) the geological and tectonic setting of the site and region, (b) local and regional fault (Type I faults) and areal sources, (c) earthquakes in the available historic records, (d) earthquake magnitude ranges for each source, and (e) appropriate alternatives that allow incorporation of uncertainties about geology and tectonic conditions into the overall calculation of the seismic hazard.

Step 2—Earthquake Recurrences

Staff will ascertain that the DOE has adequately evaluated the seismic activity and recurrence relationships of faults used in its analysis and will confirm that the methods used to evaluate the activity and recurrences are appropriate and sufficient. For example, staff will ascertain whether the DOE has sufficiently addressed: (a) seismic activity rate for each source (line or areal), (b) whether the seismic activity was treated as independent or as clustered events, (c) types of recurrence rate-magnitude models used, and (d) uncertainties in recurrence and recurrence models with regard to individual faults or clustered fault activity.

Step 3—Ground Motion Attenuation

Staff will ascertain that the DOE has adequately determined the GM attenuation models used in its analysis and will confirm that the methods used to evaluate the attenuation models are appropriate and sufficient. For example, staff will ascertain whether the DOE has sufficiently addressed: (a) wave propagation characteristics between the source and site, (b) if all applicable models are examined and used, (c) empirical or theoretical factors controlling the near-field GM region, (d) types of regression used in the analysis, (e) that data used in developing the attenuation models are from tectonic regimes similar to those at YM, and (d) the appropriate kappa parameter.

Step 4—Seismic Hazard Analysis

Staff will ascertain that the DOE has adequately determined the hazard calculations used in its analysis and will confirm that the methods used to perform the calculations are appropriate and sufficient. For example, the staff will ascertain whether the DOE has sufficiently addressed: (a) aleatory and epistemic uncertainties, (b) inconsistencies in the treatment of uncertainty between the experts, (c) expert elicitation process, and (d) documentation, transparency, and a technically defendable PSHA.

Step 5—Seismic Hazard Limitations and Abstraction to Performance Assessment

Staff will ascertain that the DOE has adequately addressed the limitations of applying the seismic hazard results to design and performance. For example, the staff will ascertain if the DOE has sufficiently addressed: (a) how the seismic hazard results presented in the PSHA will be applied for the postclosure period of performance and underground facility design, and (b) the sensitivity of calculated results to errors in the assumed distributions.

4.2.1.2 Technical Bases for Review Method

Geological and geophysical investigations to characterize the level of GM at YM from earthquakes have been ongoing for almost two decades. In addition, the Y M project has benefitted from several more decades of research and information from weapons testing activities at the Nevada Test Site (NTS). Much of the background information on faults, seismicity, faulting models, tectonics, and tectonic models is summarized in other sections of this report. In addition, the DOE has recently concluded a PSHA detailed expert elicitation to determine the vibratory GM and PFDHA for YM. Detailed comments on that elicitation and results from the PSHA are partially discussed in this version of this IRSR and will be completed and presented in future versions of the IRSR.

The following list highlights those data and interpretations considered by staff as most pertinent to the development and evaluation of seismicity at YM and resulting implications for repository performance. A completed evaluation of the seismicity at Y M will be in subsequent revisions of the IRSR.

Seismic Source Characterization

A seismic source is a portion of the earth's crust that has relatively uniform seismicity characteristics (including earthquake potential) and is distinct from that of its neighbors. Sources can be either fault or areal sources. Within a seismic source, the probability of earthquake occurrence and the size of the maximum magnitude are generally considered to be invariant. Characterization of the tectonic setting and identification of seismic sources are based on regional and site geological and geophysical data, historical and instrumental seismicity data, regional stress field, and geological investigations of prehistoric earthquakes (U.S. Nuclear Regulatory Commission, 1997b).

Aspects of seismic sources (Reiter, 1991) to consider in seismic hazard analysis are:

- Earthquake potential of identified geological structures
- Earthquake potential of tectonic zones (i.e., regions of uniform earthquake characteristics)
- Uncertainties associated with seismic source geometry (e.g., fault dip, width, segmentation, and depth of seismogenic crust)
- Uncertainties in recurrence and recurrence models with regard to individual faults, clustered fault activity, or regional recurrence models
- Appropriate alternatives that allow incorporation of uncertainties about the geology and tectonic conditions into the overall calculation of the seismic hazard.

Type I Faults

Faults in and around YM have been identified and investigated by (1) geologic mapping of surface exposures and underground openings (Day, et al., 1997); (2) geophysical methods, including gravity, magnetics, electro-magnetics, seismic reflection, and hypocenter mapping (Langenheim, et al., 1991; Brocher, et al., 1993, 1996, 1998; Oliver and Fox, 1993; Harmsen, 1994; Ponce and Oliver, 1995; Majer, et al., 1997; Connor, et al., 1997); and (3) borehole imaging and core logging (Carr, 1992). Insights into faults and faulting in and around YM have been gained from (1) 3D geologic framework models and balanced cross sections (Young, et al., 1992a; 1992b; Stirewalt and Henderson, 1995; Ferrill, et al., 1996b); (2) tectonic modeling (Ferrill, et al., 1996b); (3) numerical analyses of dynamic processes (Ofoegbu and Ferrill, 1998); and (4) analog modeling (Rahe, et al., 1997).

Type I faults are defined as faults or fault zones that are subject to displacement and are of sufficient length and located such that they (1) may affect repository design and/or performance of structures, systems, and components important to safety, containment, or waste isolation (sscis/wi); and/or (2) may provide significant input into models used in the design or in the assessment of sscis/wi (McConnell, et al.,1992). The concept of Type I faults in this IRSR (McConnell, et al., 1992) applies only to those faults that can directly affect the geologic repository design or performance by GM or direct fault slip during the period of performance.

The definition of Type I faults applies only to faults that are both known and mapped. Faults that are blind or buried, hypothesized in tectonic models, or whose existence is otherwise inferred from geologic, geophysical, seismological, or analog data, are not considered Type I faults because useful attributes, such as their location, extent, age of last movement, or geometry cannot be completely known. However, such faults may be considered in PSHA and PA. Type I faults are features (as in FEPs) that must be identified and investigated to determine the fault displacement hazard at the site.

There are six characteristics of faulting and seismicity used to evaluate Type I faults, following McConnell (1992) and McKague, et al. (1996). These are:

(1) Faulting Component: That region around YM in which faulting and seismicity could impact the site. Current estimates place this as a circular area with radius 100 km, centered on YM.

(2) Maximum Fault Trace Length: The maximum possible rupture length of a fault, usually the full mapped trace length. This length is used to estimate the maximum magnitude earthquake.

(3) Geologic Age of Last Movement: Faults with known or suspected movement in the last 2 Ma are considered potential Type I faults.

(4) Maximum Earthquake: The largest earthquake that a fault can potentially generate, usually based on scaling relationships that relate magnitude to the fault's rupture dimensions (i.e., length, width, area, or displacement) (Wells and Coppersmith, 1994).

(5) Closest Approach of Fault to Repository: The shortest distance from the site to the fault trace. This distance is used to determine the attenuation of the seismic energy from the earthquake as it travels to the site.

(6) Peak Acceleration: Peak ground motion that is produced at the site from earthquakes on potential Type I faults.

In 1998, DOE released the PSHA (U.S. Geological Survey, 1998), and the following is based on a review of that report. In the DOE PSHA, six expert teams consisting of three geoscientists per team developed the probabilistic seismic and faulting results. The six expert teams for seismic source and fault displacement considered two basic types of seismic sources—fault and areal. The local and regional fault sources, while not explicitly identified as either NRC Type I faults or USGS relevant or potentially relevant faults in the report, were used in the manner consistent with the definition of Type I faults (McConnell, et al., 1992). The expert teams, based on their experience and the input of experts, identified and characterized both local and regional faults. The six teams identified 30 local faults and 51 regional faults or combinations of faults (U.S. Geological Survey, 1998, table 4-2) that were used in the PSHA. The total of 81 faults exceeds the Type I faults because some of the seismic sources were formed by joining two or more individual faults together. Faults identified as seismic sources by the experts are indicated in the last column of the tables in appendix B. In that column, faults considered as seismic sources in the PSHA report (U.S. Geological Survey, 1998, table 4-2) by one or more of the expert groups are indicated by a Y; faults considered as seismic sources when combined with other faults are indicated by a C, and faults not considered as seismic sources by the expert teams are indicated by an N.

Results of the analysis of McKague, et al. (1996) reveal 78 Type I faults in the YM region (tables B-1, B-2, and B-4). U.S. Geological Survey (1996, table 11-1) tabulated 100 faults in the YM region, but these were not specifically subdivided into Type I faults. Of those faults tabulated by USGS, 69 were categorized as relevant or potentially relevant (tables B-1 and B-2). U.S. Geological Survey (1996) uses the terms relevant for faults that have documented Quaternary displacement and the earthquake generated on the fault could produce 84th percentile peak acceleration greater than or equal to 0.1 g, and potentially relevant for faults that are considered subject to displacement on the basis of potential structural association with seismicity. The staff assumes these faults to be equivalent to Type I faults. Type I faults and relevant or potentially relevant faults are compiled in tables B-1, B-2, B3, and B-4. The compilations relied on essentially the same data sources (Simonds, et al., 1995; Faulds, et al., 1994; Frizzell and Shulters, 1990; Scott and Bonk, 1984; Piety, 1996; and Nakata, et al., 1982), and studies assumed moment magnitude scales as a function of fault trace length, according to Wells and Coppersmith (1994).

Evaluation of Type I Faults

In the SDS IRSR, Revision 1, more than 115 faults within 115 km of the repository at YM were considered in evaluating their potential to affect the repository at YM by McKague, et al. (1996), Pezzopane (U.S. Geological Survey, 1996), and DOE seismic source experts (U.S. Geological Survey, 1998). In this revision, an additional check was made using the attenuation functions of Boore, et al. (1997) and or Spudich, et al. (1997) as applied to all faults in the set except those listed in table B-7. In general, the attenuation functions of Boore, et al. (1997) and or Spudich, et al. (1997) result in a lower GM than those listed in revision 1. Thus no new Type I faults have been identified and added to the original data sets used by McKague, et al. (1996) and Pezzopane (U.S. Geological Survey, 1996), (tables B-1, B-2, B-3, B-4, and B-6).

In the current version of the SDS IRSR, peak accelerations of Type I faults have been reevaluated based on the attenuation functions of Boore, et al. (1997) and Spudich, et al. (1997). Calculated values were used to subdivide tables B-1 and B-2 of Revision 1 into two groups of faults that were either equal to or exceeded the 0.1 g criteria or were less than the 0.1 g criteria, based on the results of the more recent calculations (tables B-1, B-2, B-3, and B-4). All faults in these tables (tables B-1, B-2, B-3, and B-4) meet the criteria for Type 1 faults. Table B-5 lists 33 faults classified as Type III by McKague, et al. (1996) and as not relevant or potentially relevant by Pezzopane (U.S. Geological Survey, 1996) and also have peak accelerations of < 0.10 g as determined using the attenuation functions of Boore, et al. (1997) and or Spudich, et al. (1997). In addition, nine faults, Simonds number 1 to 8, and 16 have been placed in table B-5 of this IRSR and are now considered as Type III faults. This is based on the lack of evidence for Quaternary movement (Simonds, et al., 1995; U.S. Geological Survey, 1998).

The attenuation functions of Boore, et al. (1997) and or Spudich, et al. (1997) both rely on the closest horizontal distance from the repository boundary (U.S. Geological Survey, 1996) or a point within the repository (McKague, et al., 1996) to a point on the surface that lies directly above a proposed rupture on the fault. In this analysis it was assumed that all ruptures occur from 15 km to the surface and that all faults dip at 60°. Generally, peak accelerations calculated using Spudich, et al. (1997) were less than the peak accelerations calculated using Boore, et al. (1997), and both values were less than the comparable values of those from Pezzopane (84th percentile; U.S. Geological Survey, 1996) and McKague, et al. (1996).

Table B-6 lists faults not explicitly considered by the U.S. Geological Survey (1996, 1998). However, many of these faults have been considered in various combinations or segments by the U.S. Geological Survey (1996, 1998) and they are considered Type I faults by the staff.

As shown in the tables (B-1, B-2, B-3, B-4, and B-7) within appendix B, McKague, et al. (1996), U.S. Geological Survey (1996), and the six DOE seismic source teams (U.S. Geological Survey, 1998) reviewed more than 115 faults for their capability to affect the proposed repository (e.g., appendix B; figure 4-5 and 4-6). Of these faults, 41 have now been deemed incapable of affecting repository performance (Type III fault, table B-5). Table B-1 lists 23 faults classified as Type I by McKague, et al. (1996), as relevant or potentially relevant by Pezzopane (U.S. Geological Survey, 1996), and as having peak accelerations of ≥ 0.10 g as determined using the attenuation functions of Boore, et al. (1997) and or Spudich, et al. (1997). Table B-2 lists 12 faults classified as Type I by McKague, et al. (1996), as relevant or potentially relevant by Pezzopane (U.S. Geological Survey, 1996), and as having peak accelerations of < 0.1 g as determined using the attenuation functions of Boore, et al. (1997) and or Spudich, et al. (1997). Table B-3 lists 10 faults classified as relevant or potentially relevant by Pezzopane (U.S. Geological Survey, 1996) and that have peak accelerations of ≥ 0.10 g as determined using the attenuation functions of Boore, et al. (1997) and or Spudich, et al. (1997). Table B-4 lists 22 faults classified as relevant or potentially relevant by Pezzopane (U.S. Geological Survey, 1996) and that have peak accelerations of < 0.10 g as determined using the attenuation functions of Boore, et al. (1997) and or Spudich, et al. (1997). Table B-5 lists 41 faults classified as Type III by McKague, et al. (1996), as irrelevant or potentially irrelevant by Pezzopane (U.S. Geological Survey, 1996), and that have peak accelerations of < 0.10 g as determined using the attenuation functions of Boore, et al. (1997) and or Spudich, et al. (1997). Table B-6 lists eight faults classified as Type I by McKague, et al. (1996), not specifically considered by Pezzopane (U.S. Geological Survey, 1996), and that have peak accelerations of ≥ 0.10 g as determined using the attenuation functions of Boore, et al. (1997) and or Spudich, et al. (1997). Table B-7 lists 11 faults considered by the seismic source experts, but not specifically considered in McKague, et al. (1996) or Pezzopane (U.S. Geological Survey, 1996). Most of these faults lack enough information to determine if they are Type I faults. Information on these faults has been requested from the DOE. The extent of the Carrara fault is not well known and has been identified mainly on the basis of geophysical surveys (Stamatakos, et al., 1997c, Slemmons, 1997). These faults are currently unclassified.

Of the 82 faults identified in tables B-1, B-2, B-3, B-4, and B-6, 25 faults were not considered by the experts as seismic sources. One expert team (AAR team) justified not including 10 local faults on the basis of "lack of geomorphic expression in bedrock indicating significant Quaternary activity." Another expert team (RYA team) considered the Rocket Wash-Beatty Wash fault not relevant for the same reason. No justification was given for not considering the remaining 14 faults. All of them are regional faults located more than 38 km from the repository and with peak accelerations less than 0.14 g, except for the Sundance, Yucca Wash, Pagany Wash, and Sever Wash faults, which were considered as relevant or potentially relevant faults by U.S. Geological Survey (1996) but not by McKague, et al. (1996). The Hunter Mountain fault and the Towne Pass fault, when combined with the Emigrant fault, were considered seismic sources (U.S. Geological Survey, 1998), but not Type I faults (table B-3) by McKague, et al. (1996) or relevant or potentially relevant by Pezzopane (U.S. Geological Survey, 1996).

The main differences between the NRC and USGS fault studies were interpretations of fault lengths in regions in which the mapped trace lengths are ambiguous and the choice of an appropriate attenuation function for identifying the 0.1 g criterion. A comparison of the two sets of fault data and predicted peak accelerations forms the basis for the subsequent discussion of the status of issue resolution regarding Type I faults. For simplicity, USGS relevant or potentially relevant faults are presumed to be Type I faults.

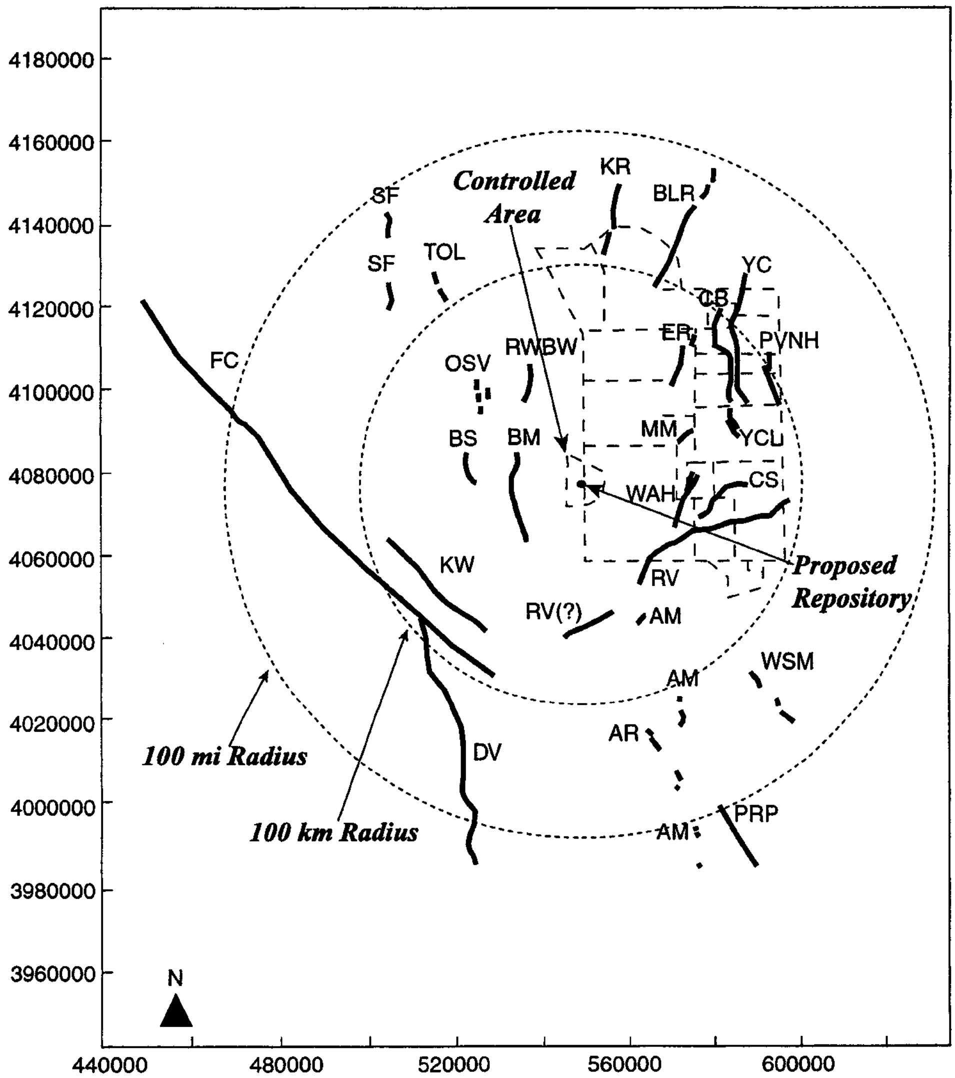

Figure 4-5. Regional map showing locations of faults beyond 10 km radius of Yucca Mountain but within 100 km radius of Yucca Mountain. Locations of faults are from Nakata, et al. (1982) Sawyer, et al. (1994); and Piety (1996). Fault names are as follows: AM–Ash Meadows, AR–Amargosa River, BLR–Belted Range, BM–Bare Mountain, BS–Beatty Scarp, CB–Carpetbag, CS–Cane Springs, DV–Death Valley, ER–Eleana Range, FC–Furnace Creek, KR–Kawich Range, KW–Keane Wonder, MM–Mine Mountain, OSV–Oasis Valley, PRP–Pahrump, PVNH–Plutonium Valley-North Halfpint Range, RV–Rock Valley, RWBW–Rocket Wash Beatty Wash, SF–Sarcobatus Flat, TOL–Tolicha Peak, WAH–Wahmonie, WSM–West Spring Mountain, YC–Yucca, and YCL–Yucca Lake. Map coordinates are Universal Transverse Mercator, Zone 11.

NOTE: The following Type I faults do not appear on either figures 4-5 or 4-6 because their locations were not available in electronic format; they will be included in revision 3: Fish Lake Valley, Drill Hole Wash, Dune Wash, East Pintwater Range, Emigrant Valley North, Grapevine, Grapevine Mountain, Hunter-Panamint Valley, South Ridge, Spotted Range, Sundance, West Pintwater, and West Specter Range.

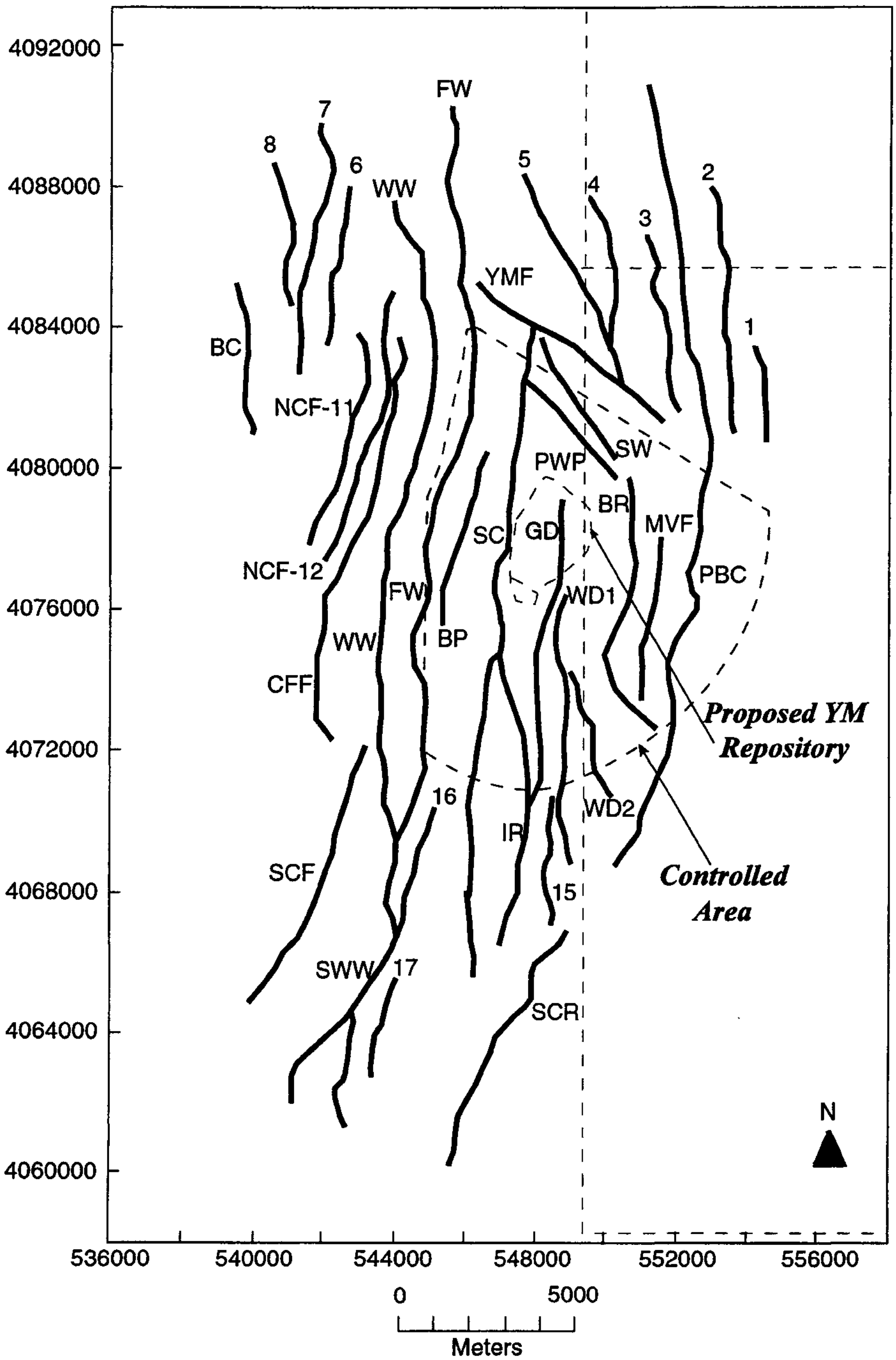

Figure 4-6. Locations of faults at or near Yucca Mountain from Simonds, et al. (1995) and Frizzell and Shulters (1990). Fault names are as follows: BC–Bonnie Claire, BP–Boomerang Point, BR–Bow Ridge, CFF–Crater Flat, FW–Fatigue Wash, GD–Ghost Dance, IR–Iron Ridge, MVF–Midway Valley, NCF–Northern Crater Flat, PBC–Paintbrush Canyon, PWF–Pagany Wash, SC–Solitario Canyon, SCF–Southern Crater Flat, SCR–Stagecoach Road, SW–Sever Wash, SWW–Southern Windy Wash, WD–West Dune, WW–Windy Wash, and YWF–Yucca Wash. Number faults are unnamed faults and refer to those described in table B-5 and McKague, et al. (1996). Map coordinates are Universal Transverse Mercator, Zone 11.

Peak accelerations calculated by McKague, et al. (1996), U.S. Geological Survey (1996), Boore, et al. (1997), and Spudich, et al. (1997), may differ by as much as several tenths of a g in the tables within appendix B. Some of this difference is caused by application of different attenuation functions and different conditions. For some faults, this difference is greater than can be accounted for by the attenuation function differences alone. In these cases, different interpretations of fault length that leads to different estimates of the maximum earthquake appears to be the source of the discrepancies. The discrepancy in length may result from obtaining the length from different technical sources (i.e., paper maps versus electronic maps), or different interpretations of how discontinuous fault traces (blind, buried, or segmented) are linked.

Fault lengths are often poorly determined, which results from variable scales of mapping, buried or otherwise obscured fault terminations or fault splays, obscured connections with other fault segments, and faults mapped by remote imaging. These factors contribute to variations in estimates of individual fault length, maximum capable earthquake, and peak acceleration at the YM site. Faults that yield peak GM values less than but near the 0.1-g minimum value (i.e., 0.09 g, or greater) should be carefully examined to ensure that alternative fault-length determinations would not lead to acceleration values above the 0.1 g threshold (McKague, et al., 1996).

McKague, et al. (1996; figure 2-1) relied on the attenuation function of Campbell (1987), because it yields the largest (most conservative) accelerations of the available published attenuation functions for the western United States, especially for near-field (within 10 km) faults. U.S. Geological Survey (1996) provided two sets of attenuation functions to determine peak horizontal acceleration. The first function derived an average acceleration value based on equal weighting of attenuation equations of Campbell (1981), Idriss (1991), Joyner and Boore (1981), and Boore, et al. (1993). The second function was the Sea96 equation based on a new formulation by Spudich, et al. (1997). The Sea96 equation yields the smallest peak accelerations for near-field earthquakes and was not used by USGS. However, they are listed in appendix B-1 through B-6. At distances greater than approximately 30 km, all the attenuation functions yield similar peak accelerations for a given moment magnitude earthquake and source-to-site distance.

McKague, et al. (1996) relied on the median value of the attenuation function of Campbell (1987). The U.S. Geological Survey (1996) used different attenuation functions, and based its results on the 84th percentile value.

Both McKague, et al. (1996) and U.S. Geological Survey (1996) conclude that the faulting component of the geologic setting has a radius of 100 km around YM (figures 4-5, 4-6). For fault displacement hazard analysis, both the staff and the U.S. Geological Survey (1996, Ch. 11) agree that the controlled area constitutes the area of concern.

Both McKague, et al. (1996) and U.S. Geological Survey (1996) used the Wells and Coppersmith (1994) equation to estimate the maximum earthquake for each fault in the faulting component and used the 0.1-g threshold GM value as suggested in NUREG-1451.
U.S. Geological Survey (1996) cites the minimum surface-rupture earthquake at Mw = 5.8 based on the Fort Sage 1950 event. That value is reasonable and technically defensible given the historic seismic record. Both U.S. Geological Survey (1996) and McKague, et al. (1996)

use the same data sources (mainly Piety, 1995) to determine the age of last motion of candidate Type I faults.

The DOE used less conservative GM attenuation functions (McKague, et al., 1996; figure 2-1); however, this difference is in part compensated for by DOE's use of the more conservative 84th percentile peak acceleration. As noted earlier, most commonly used GM functions tend to overestimate the peak acceleration. The DOE has not considered *in situ* stress in its analysis of relevant or potentially relevant faults. In McKague, et al. (1996), the Drill Hole, Pagany Wash, Sever Wash, and Yucca Wash faults were eliminated from the list of Type I faults based on their unfavorable orientation within the *in situ* stress field.

The staff currently believes the peak attenuation values used by McKague, et al. (1996) and Pezzopane, et al. (1996), are conservative values. This is supported by the conclusion reached by Abrahamson and Shedlock (1997) that commonly used attenuation relations over predict GMs from earthquakes in extensional regimes. Based on this belief, it is anticipated that no additional Type 1 faults (tables B-1, B-2, B-3, B-4, B-6, and B-7) will be identified from the existing database (i.e., Type III faults) unless new information becomes available on specific Type III faults. They should then be re-evaluated. Faults that are identified in the future or are currently poorly characterized (i.e., the Carrera Fault) should be evaluated when sufficient information becomes available.

Aspects of seismic record (e.g., Richter, 1958) to consider in seismic hazard analysis in support of RM3 and RM4, include:

- Coordinates of the epicenter
- Focus depth
- Time of event
- Highest intensity
- Magnitude (with appropriate designation of magnitude type)
- Seismic moment
- Distance to the site
- Strong motion recordings
- Co-seismic deformation (i.e., landslides, liquefaction, or fracturing)
- Surface rupture information

Earthquake Recurrence Characteristics

Earthquake recurrence relationships show the annual frequency of all earthquakes up to the maximum earthquake for each seismic source. These relationships are derived from earthquake catalog, paleoseismicity, and geological information. Typically, magnitude-recurrence models range between end-member exponential (Gutenberg and Richter, 1954) and characteristic (Schwartz and Coppersmith, 1984) models.

Aspects of earthquake recurrence (e.g., Reiter, 1991) to consider in seismic hazard analysis are:

- Activity rate (or *a* value)
- Slope of the regression (or *b* value)
- Lower bound and upper bound earthquake magnitudes
- Shape of the recurrence curve (characteristic, logarithmic, or hybrid)
- Potential for clustered activity

Ground Motion Attenuation

GM attenuation models describe the relation among earthquake magnitude, distance from source to the site, and vibratory GM at the site. According to SSHAC (U.S. Nuclear Regulatory Commission, 1997c), GM should be characterized by two basic approaches: (1) a spectrum of the natural logarithm of the GM parameter determined as a function of magnitude and distance at multiple frequencies, and (2) the standard deviation (aleatory) of the natural logarithm of the GM parameter. The standard deviation could be a function of magnitude, distance, and frequency level, as applicable. GM should be characterized for both horizontal and vertical field-free GM response spectra at the ground surface and repository depth.

Aspects of GM attenuation (Reiter, 1991) to consider in seismic hazard analysis are:

- Seismic source properties (e.g., focal mechanism, depth, directivity, or magnitude saturation effects)
- Wave propagation between source and site
- Peak GM and the response spectrum
- Empirical or theoretical factors controlling the near-field region (typically within 10 km of the site)
- Site-response models, especially surface-to-subsurface attenuation and amplification and deamplification characteristics

Hazard Calculations and Presentation

PSHA is a powerful tool for incorporating uncertainties associated with identifying and characterizing seismic sources and ground shaking. The PSHA will lead to identifying the GM hazard levels that will be used as the basis for development of seismic design basis input for YM.

Aspects of hazard calculations and presentation are:

- PSHA structure (National Research Council, 1988)
- Uncertainties, both aleatory and epistemic (SSHAC; U.S. Nuclear Regulatory Commission, 1997c)
- PSHA calculation and results (both total hazard with fractiles and [uniform hazard spectrum (UHS)] (SSHAC; U.S. Nuclear Regulatory Commission, 1997c)
- Deaggregation of results (Bernreuter, et al., 1998)

Evaluation of Department of Energy Seismic Hazard Assessment

Seismic Source Characterization

Seismic sources were characterized by the DOE in the PSHA (U.S. Geological Survey, 1998). In the PSHA, the DOE utilized six teams of experts. Each team consisted of three specialized geoscientists with expertise in either paleoseismology, Basin and Range structural geology, or Basin and Range seismology. To assess seismic sources, the teams mainly relied on USGS, DOE, and related YM studies augmented by published literature. In addition, the teams were assembled together for six workshops held between April 1995 and June 1997, at which the experts exchanged information on seismic sources and participated in additional discussions with other external experts. Details of the workshops are given in the PSHA final report (U.S. Geological Survey, 1998). Review of the elicitation methodology and related issues is treated separately under the Expert Elicitation Acceptance Criteria.

(a) Geologic and Tectonic Setting

The expert teams considered all the viable tectonic models (essentially those viable models listed in appendix C) and aspects of all the modes are incorporated into all the teams identification of seismic sources. Teams included, for example, seismogenic detachment faults as potential seismic sources (Deep Detachment Fault Tectonic Model), and hidden or buried strike slip faults with associated cross-basin faults as potential seismic sources (Amargosa Desert Fault Model). Planar block bounding faults were also incorporated into all teams' assessments. Although presented to the experts at the workshops, strain rate values derived from GPS measurements were not explicitly considered by any of the teams as a viable alternative to estimations of the seismic hazard.

(b) Fault and Areal Sources

Seismic sources for the DOE PSHA (U.S. Geological Survey, 1998) consisted of two types: fault sources and areal source zones. This follows common practice for seismic hazard assessments, especially for sites west of the Mississippi, where better exposure of bedrock and greater tectonic activity make identification of active faults more possible.

Fault sources are used in the hazard assessment to account for expected seismicity on known or suspected fault traces. Uncertainty in fault sources is accounted for by alternative interpretations of fault length, fault dip, closest approach to the site, depth within the seismogenic crust, and possible kinematic linkage with other faults. In the PSHA calculations, earthquakes are assumed to occur randomly along the fault surface, constrained by the size of the rupture area. Rupture area and rupture dimensions are specified by empirical relationships based on magnitude (e.g., Wells and Coppersmith, 1994).

Fault sources were identified by the expert teams from published USGS and DOE maps and reports (U.S. Geological Survey, 1996; Piety, 1996; Anderson, et al., 1995a,b; Simonds, et al., 1995), published scientific literature (Scott, 1990; Zhang, et al., 1990; Reheis and Dixon, 1996; Reheis and Sawyer, 1997), and CNWRA publications (Ferrill, et al., 1996b; McKague, et al., 1996). In addition, the experts benefitted from detailed discussion at several of the PSHA workshops, in which summaries of fault sources and tectonic models were presented by project and external scientific experts. The expert teams also visited many of the sources during a field trip held during PSHA workshop #3, November 18–21, 1996.

Fault sources were also identified by consideration of YM local and regional tectonics. These included sources from proposed buried or otherwise cryptic strike slip faults (Schweickert and Lahren, 1997) and seismogenic detachment faults (Wernicke, 1995). Uncertainty in the sources, both in terms of their geometric characteristics and likelihood of activity, were accounted for by the logic tree structure of the PSHA, in which various models of faulting and fault activity were weighted according to the opinions of the experts.

In sum, the expert teams considered 86 fault sources or combinations of fault sources (see table 4-2 of U.S. Geological Survey, 1998). These included 30 faults or combinations of fault sources local to YM (within YM or in the adjacent basins), 51 regional faults or combinations of faults in the YM region (generally within approximately a 100-km radius of the site), and 6 faults or combinations of fault sources inferred from the tectonic models. Included in this list are faults identified by staff's independent analysis of Type I faults (McKague, et al., 1996; also see section 4.1.1). For example, the AAR team considered 41 faults as individual fault sources (tables AAR-1, AAR-4 in U.S. Geological Survey, 1998). All are Type I faults as defined in section 4.1.1 and listed in appendix B. The AAR team also documented those Type I faults they did not consider as specific fault sources and showed how seismicity associated with these other Type I faults is accounted for by their background or areal seismic sources.

In contrast to fault sources, areal sources represent areas of distributed or background seismicity in which there is no geologic or geophysical evidence that can tie earthquakes to known faults. In this way, areal sources account for earthquakes that occur on unidentified or unidentifiable fault sources. Most commonly areal sources are developed to represent earthquakes with magnitudes that may not necessarily cause surface rupture—those earthquakes with magnitudes that produce rupture areas that are entirely contained below the surface within the seismogenic crust.

In the DOE PSHA (U.S. Geological Survey,1998), the experts relied on empirical relationships that relate the probability of surface rupture to earthquake magnitude based on empirical data from historical ruptures in the Basin and Range (e.g., Wells and Coppersmith, 1993; dePolo, 1994; U.S. Geological Survey, 1996; and figure 4-11 of U.S. Geological Survey, 1998). Given these data, there is greater than an 80-percent probability that earthquakes with magnitudes of

6.5 will rupture the surface, while there is less than a 20-percent chance that earthquakes with magnitudes of 5.5 will rupture the surface.

The boundaries of areal sources are drawn to define areas with relatively uniform seismicity and maximum magnitude, generally defined by the historic seismic record. All expert teams considered one to three areal source zones. For most teams, the source zones were used to capture background seismicity and, thus, the maximum magnitude for areal sources close to YM were less than for those further away because these teams felt the fault source characterization at YM was superior to that in the surrounding regions. Some of the expert teams also included an explicit volcanic areal source term to explicitly account for seismic activity related to volcanism.

(c) Historic Seismicity

The DOE facilitation team provided a single earthquake catalog to the expert teams. The catalog (named the Yucca Mountain Catalog) was compiled from twelve regional catalogs (listed on page G-2 of U.S. Geological Survey, 1998). The initial catalog contained 271,223 earthquakes of magnitude **M** 0.5 and larger for the period between 1868 to 1996. The catalog was truncated at August 31, 1996. This initial catalog was modified in three ways. First, all the magnitudes were converted to $\mathbf{M_w}$. Second, earthquakes from nuclear testing were removed based on compilations of all known nuclear tests. Third, foreshocks and aftershocks were removed using two standard declustering methods (Youngs, et al., 1987; Vanezianao and van Dyck, 1985). The Little Skull Mountain sequence was used to test the effectiveness of the two declustering techniques. Results show that the Vanezianao and van Dyck (1985) method was better able to isolate foreshocks and aftershocks. After modifications, the resulting catalogs contain between 26,250 (Vanezianao and Van Dyck, 1985, method) and 31,147 (Youngs, et al., 1987 method) earthquakes covering a circular area with a 300-km radius centered on YM.

(d) Maximum Magnitude

The maximum magnitude earthquake is the largest earthquake that can be produced on a fault or in an areal source regardless of its frequency of occurrence. For fault sources, the expert teams used empirical scaling relationships that relate maximum magnitude to the physical dimensions of the fault. Maximum magnitude was derived from fault length, rupture area, maximum surface displacement, and average surface displacement. In some cases, the expert teams modified their maximum magnitude estimated by considering slip rate as well as rupture dimensions following Anderson, et al. (1996). In addition, the experts considered rupture area and average slip on the fault to estimate seismic moment, which was then converted to maximum magnitude using the relationships in Hanks and Kanamori (1979). For areal sources, the experts estimated the maximum magnitude earthquake based on the largest fault in the areal source not explicitly modeled as a fault source. Alternatively, the experts relied on the empirical relationships that relate surface rupture to earthquake magnitude based on empirical data from historical ruptures in the Basin and Range (e.g., Wells and Coppersmith, 1993; dePolo, 1994; U.S. Geological Survey, 1996; and figure 4-11 of U.S. Geological Survey, 1998).

(e) Incorporation of Alternatives and Uncertainty

The elicitation used a standard logic tree approach to delineate the alternative interpretations into a coherent framework and to incorporate uncertainty. The first branch of the tree identified alternatives of faults based on different interpretations of local and regional tectonics derived from the suite of viable tectonic models. Subsequent branches evaluate alternatives in fault-specific characteristics such as fault linkage, segmentation, maximum magnitude, activity rate, and seismogenic depth (see figures 4-2 and 4-3 of U.S. Geological Survey, 1998, for example logic tree representations).

Earthquake Recurrence

The recurrence rates for the faults were estimated using either recurrence intervals or slip rates. Recurrence and slip rates were primarily derived from paleoseismic data obtained by the USGS detailed investigations of faulting in the YM region (U.S. Geological Survey, 1998). Additional constraints were derived from geologic data that estimates longer-term slip rates (e.g., Stamatakos, et al., 1997b).

For fault sources, two methods were used by the experts to estimate recurrence. The first was to estimate the frequency of the largest earthquakes on the fault and then specify the magnitude distribution function for the remaining earthquakes based on a particular recurrence model. The experts used three such recurrence models: (i) characteristic (Schwartz and Coppersmith, 1984), (ii) truncated exponential (Gutenburg and Richter, 1954), and (iii) modified truncated exponential. The second approach was to translate the slip rate into a seismic moment rate and then partition the moments into earthquakes of various magnitudes according to a magnitude distribution model (Wesnowsky, 1986).

For areal sources, the expert teams used the earthquakes in the catalog of historic earthquakes. The distribution of earthquake magnitudes in each areal source zone was interpreted following an exponential distribution (Gutenberg and Richter, 1954). Recurrence relationships for each zone were then estimated following a truncated exponential magnitude distribution in order to account for the maximum magnitude earthquake (Cornell and Van Marke, 1969).

Ground Motion Attenuation

Ideally, GMs from earthquakes in the Basin and Range Province should be used to develop attenuation relations for YM. However, strong motion data recorded from earthquakes in the Basin and Range Province were too sparse to adequately constrain an empirical attenuation model for YM. Therefore, empirical attenuation models from the western United States were used to develop an attenuation model for YM. Significant differences may exist in the seismic source, source effects (extensional versus compressional regimes and normal versus strike-slip faulting), path effects (differences in regional crustal structure), or site effects (differences in the shallow site properties) between YM and the western United States. Therefore, the GM experts needed to account for those differences when estimating the expected GM at YM. In order to find the appropriate attenuation model for YM, the facilitation team solicited GM models from the experts. Some of these models proposed by the experts are empirical regressions and some are physical models. The independent variables used in the regressions are: (a) moment magnitude, (b) distance, (c) mechanism (strike-slip or normal fault), (d) relative location of the fault, hangingwall or footwall, and (e) site conditions. Some of the GM models proposed by the experts are: empirical or hybrid empirical models (Campbell, 1997; Abrahamson and Silva,1997; Boore, et al., 1997; Spudich, et al., 1997), stochastic point and finite source simulation models (Silva, et al., 1997), semi-empirical Green's Function finite fault simulation models (Sommerville, et al., 1997), compound fractile finite fault models (Zeng, et al., 1994), and blast models (Bennett[4]).

Each expert assigned a certain weight to each of the models for evaluating horizontal and vertical estimates of spectral acceleration (SA), peak ground accelerations (PGA), and peak ground velocities (PGV). The experts provided estimates of horizontal and vertical GMs for 51 combinations of earthquake sources and station locations. In addition, the experts were asked to provide GM estimates for two special scenarios, low-angle faults and multiple-parallel faults. The suites of expert models then represented the expected epistemic uncertainty for strong GM at YM. Epistemic uncertainty results from our imperfect knowledge about earthquakes and their effects. For example, the shape of the magnitude distribution for a given seismic source is an epistemic uncertainty. This uncertainty can be reduced by collecting more data and with advancement in our knowledge. The uncertainty values associated with these GM estimates were also provided in terms of mean, μ, uncertainty on the mean value, σ_μ , and uncertainty on the standard deviation, σ_σ. There were inconsistencies in the treatment of the aleatory and epistemic uncertainties between the experts. Inconsistencies in the treatment of uncertainty and use of conversion factors were identified and corrected by the experts.

Spectral Decay (Kappa)

During the PSHA, specific issues were raised regarding (1) the definition of the shallow crustal velocity near the free surface and (2) the value of crustal kappa to be used for GM estimation at YM. These issues were raised due to the differences between the site condition at YM and those representations of the empirical strong motion database used (mainly California). There is a great difference in shear wave velocities, deep crustal damping Q(f), and shallow crustal, top 1 to 2 km, damping value (kappa) between California and YM. Kappa, defined as the spectral decay, is found to be primarily caused by subsurface geological structures near the site. It is a smaller value for hard rock sites than for soft rock sites. The value of kappa estimated by Su, et al. (1996), for the southwestern part of the NTS ranged from 0.005 to 0.024-sec. In the PSHA, a value of 0.0186 sec was used. The DOE indicated that if new studies find that the median value of kappa for material with shear wave velocity below 1,900 m/sec is different from 0.0186 sec, the median attenuation model will be adjusted. This will be addressed by DOE in Topical Report #3.

Vibratory Ground Motion Hazard Results

Median ground acceleration, aleatory uncertainty, and epistemic uncertainty for a number of earthquake magnitudes, sources-to-site distances, and different fault styles were estimated by the experts. The aleatory on random uncertainty, is a probabilistic variable that results from natural physical processes and is inherent to the unpredictable nature of future events. For

---

[4]R.J. Bennett, personal communication at Workshop on Ground Motion at Yucca Mountain, Salt Lake City, Utah, January 9–10, 1997.

example, the size, location, and time of the next earthquake and the details of the GM are examples of quantities considered aleatory. Aleatory uncertainty cannot be reduced by collecting additional data. Uncertainties in seismic source characterization and GM attenuation relations were quantified by considering inputs from six seismic source fault displacement (SSFD) expert teams and seven GM experts, respectively, and by each team and expert's own assessment of uncertainty. The moment magnitude, M_w, used in the PSHA ranged from 5.0 to 8.0 for normal and strike-slip faulting, and the distances examined were from 1 to 160 km.

The probabilistic hazard for vibratory GM was calculated for PGA, PGV, UHS, and SAs at frequencies ranging from 0.3–20 Hz. It was found that at 5–10 Hz, or high frequencies, the GMs are dominated by earthquakes of magnitude less than 6.5 and distances less than 15 Km. At lower frequencies, 1–2 Hz, the GMs are dominated by large events beyond distances of 50 km. The recurrence models contributed most to the uncertainty in the GM hazard, while geometric fault parameters were minor contributors to uncertainty. It was found that at 10 Hz, the dominant sources for seismic hazard GM are Paintbrush Canyon, Iron Ridge, and Solitario Canyon faults, and the host areal seismic source zone. For 1-Hz GM, the dominant seismic hazard comes from Death Valley-Furnace Creek faults.

The vibratory GM hazard calculations were performed for each expert proposed attenuation equation and seismic source parameters. In general, the most GM contributors to uncertainty in the hazard are σ_μ and σ_σ within expert uncertainties, rather than expert-to-expert uncertainties. The total uncertainty due to GM is larger than the uncertainty due to the seismic source-characterization. Combining the experts' hazard curves, giving each expert equal weight, a set of integrated hazard curves were produced. The integrated results, based on the six expert team inputs and seven GM expert inputs, represent the seismic hazard and its associated uncertainty at YM. The separation between the 15th- and 85th-percentile curves conveys the effects of the epistemic uncertainty on the calculated hazards. It should be noted these hazard curves were estimated at a reference rock outcrop on the surface, on a reference site at the same elevation s the repository.

Seismic Hazard Analysis

TBD FY00. Detailed description and assessment of recurrence awaits staff's independent analysis. That analysis hinges on acquisition of seismic data (initially requested from the DOE in September 1998) used to construct the DOE PSHA.

Seismic Hazard Limitations and Abstraction to Performance assessment

TBD FY00. Detailed description and assessment of recurrence awaits staff's independent analysis. That analysis hinges on acquisition of seismic data (requested from the DOE in September 1999) used to construct the DOE PSHA. In current DOE PA provided in the VA (U.S. Department of Energy, 1998b), DOE considered seismicity induced rockfall as a disruptive event. During subsequent workshops held in early 1999, DOE considered a disruptive event. Staff, in coordination with the RDTME KTI, will evaluate the abstraction of the DOE PSHA in those future PA calculations.

4.3 FRACTURING AND STRUCTURAL FRAMEWORK OF THE GEOLOGIC SETTING

Fractures, fracture zones, and fault zones provide the primary discontinuities (i.e., the structural framework) along which groundwater infiltration and percolation occurs in the UZ at YM, and along which flow occurs in the SZ beneath YM and in the surrounding area (National Research Council, 1996). Furthermore, fractures and faults represent planes of weakness along which roof failure occurs leading to degradation of underground excavations and potentially causing damage to WPs in the proposed repository. Consequently, it is important to constrain (1) distribution and characteristics of existing fracture and fault populations, (2) processes of past fracture and fault formation and reactivation, (3) processes presently affecting fracture and fault properties (e.g., *in situ* stress field), and (4) potential future generation and reactivation of fractures and faults (e.g., by faulting and other strain-release mechanisms). Furthermore, it is critical that fracture distribution and characteristics and fracture-related processes are appropriately abstracted and accounted for in models and analyses of performance affecting processes such as mechanical disruption of WPs, water WPs, spatial distribution of UZ flow, mass flux between fracture and rock matrix, and flow and retardation in the SZ (see figure 3-2). The general AC enumerated in section 4.0, and review methods enumerated in 4.3.1.1, below, ensure that an adequate geologic framework is available to the KTIs that use fracture or fault discontinuities information either implicitly or explicitly (i.e., Repository Design and Thermal-Mechanical Effects—to evaluate rock mass properties and size of rock blocks for rockfall calculations; USFIC—to evaluate water flow through fractures; Thermal Effects on Flow—to evaluate the effect of the thermal pulse on flow through fractures; IA—to evaluate magma and associated hydrothermal fluid flow through faults; Evolution of the Near-Field Environment—to evaluate seepage and mineralization in fractures; Radionuclide Transport—to evaluate radionuclide retardation in fractures; and Container Life and Source Term—to evaluate fault disruption of WPs). The staff will evaluate DOE's submittal to ensure that assumptions, quality, consistency, and consideration of uncertainty are adequately addressed. The fracture framework of YM is treated in postclosure PAs as features (as in FEPs) that are abstracted to suit the requirements and limitations of various process models that need to account for fracture parameters.

Observations and tests at the repository level of the ESF show that the site is highly fractured. Pneumatic testing above the PTn indicates that fractures are open and connected from the surface to depth. Elevated ^{36}Cl data, resulting primarily from nuclear testing in the Pacific in the 1950's, indicate that some fractures conduct surface water from the ground surface to repository depths over a period of 50 yr or less. Fracture flow is recognized by the NRC and the DOE as an operative process at YM. Given that fractures can conduct water, vapor, heat, and perhaps magma, it is necessary to understand the fracture systematics and characteristics. Fractures or their effects need to be abstracted into the following four ISIs: (1) mechanical disruption of WP (seismicity, faulting, rockfall, and dike intrusion), (2) spatial and temporal distribution of flow, (3) fracture versus matrix flow, and (4) flow rate in production zones—when structurally controlled (appendix A). This information needs to be considered because fractures are likely to be loci of rock failure (e.g., rockfall) and be pathways or barriers (low-permeability zones) to flow of fluids and heat.

Depending on the geometric characteristics of individual fractures (e.g., size, aperture, and roughness) and fracture populations (e.g., population distributions and interconnectedness), extent and type of fracture filling, and associated deformation and alteration along fracture or fault zones, fractures and faults may be either pathways or directionally to dependent barriers with respect to flow. Similarly, the role of fractures and faults in repository stability is dependent on the fracture characteristics. Documentation of fracture patterns and characteristics and analysis of potential future changes to fractures are important to assessment of flow- and stability-related performance parameters at YM.

4.3.1 Viable Fracture Models

4.3.1.1 Review Method for Fracture Framework

The review method (RM) used to evaluate the preliminary Uniform Acceptance Criteria (section 4.1) for the fracturing and structural framework subissue is focused to provide a path to resolution. The review method addresses performance-related issues or items that serve as technical bases for adequate and conservative bounding analyses, and as technical bases for the approximation of adequate and conservative parameter distributions in SDS and related KTI's (c.f. U.S. Nuclear Regulatory Commission, 1998a, 1998b, 1999b, 1999c, 1999d, 1999e, 1999f, 1999g). Performance related issues may use fracture or fault information either implicitly (i.e., in the abstract, e.g., planar distribution of permeability contrast in dual continuum models) or explicitly (e.g., fracture spacing in rockfall models). Staff provide or evaluate technical bases for bounding analyses and parameter distributions of fractures for SDS and related KTIs including but not limited to:

Repository Design and Thermal-Mechanical Effects: characterization of rock mass mechanical properties including spatial differences in intact rock properties and differences between lithologic and stratigraphic units; changes in the frequency, surface characteristics, and continuity of fractures; distribution of rock fall block size; variations of mechanical properties with time as a result of degradation of rock mass, including increased and progressive fracturing, and alteration of fracture wall rock and surfaces (U.S. Nuclear Regulatory Commission, 1999c);

Unsaturated and Saturated Flow Under Isothermal Conditions: spatial, lithologic and stratal variations in rock mass qualities—including present state and future modification of fracture coatings, fracture geometry, fracture surface characteristics, fracture size distribution, fracture connectivity, fracture intersections, fracture frequency, and degree of fracture and rock mass heterogeneity (U.S. Nuclear Regulatory Commission, 1999b);

Evolution of the Near-Field Environment: spatial and temporal variations in fracture coatings, fracture connectivity, fracture aperture, fracture density, fracture surface characteristics and fracture size distribution (U.S. Nuclear Regulatory Commission, 1999e);

Thermal Effects on Flow: spatial and temporal variations in heat flow and in seepage and flow related to fracture characteristics (U.S. Nuclear Regulatory Commission, 1999g);

Radionuclide Transport: spatial and temporal variations in heat flow and in seepage and flow related to fracture characteristics (U.S. Nuclear Regulatory Commission, 1999f).

In addition to the above KTIs, the SDS fracture and structural framework subissue provides technical bases for bounding analyses and parameter distributions ISIs (figure 3-2). NRC staff reviewed DOE's analyses of fractures to determine the adequacy of DOE's conclusions. Staff applied the following review method with five steps to determine whether the preliminary Uniform AC (section 4.1) were met for the fracture framework:

Step 1—Characterization of Fractures

Staff will independently evaluate the adequacy of DOE's distribution and geometric (e.g., orientations, spacing, clustering, abutting relationships, interconnectedness, apertures, and lengths) and mechanical characteristics of fractures. For example, a comprehensive unit-by-unit description of fractures that captures lateral and vertical variability of fracture development and interconnectivity throughout the Tertiary volcanic rock sequence and pre-Tertiary rock sequence at YM should be estimated or bounded to reasonably assess aspects of fractures and faults that affect repository performance.

Step 2—Origins of Fractures

Staff will independently evaluate the adequacy of DOE's determination of the origins of fractures. For example, an adequate explanation of the mechanisms for fracture generation that include development of cooling joints, tectonic joints, and unloading joints that is consistent with evolution of the applicable regional and/or local stress field, and detailed to the extent necessary, should be provided as the necessary basis for interpolation between and extrapolation beyond localized fracture and fault data sets to constrain process level models for assessments of repository performance.

Step 3—Past Modification of Fractures

Staff will independently evaluate the adequacy of DOE's constraints on subsequent modifications of fractures in the SZ and UZ by dissolution, precipitation, wall rock alteration and deformation, and other fracture-filling processes (e.g., deposition of water-entrained particles). For example, reduction of rock-mass strength and stiffness due to wall rock alteration (perhaps enhanced by extended exposure to heat and moisture), characteristics of fracture-filling materials that would affect the sorption of water into the matrix from the fracture (e.g., armoring of wall rock surfaces by fracture coating), role of fractures as conduits for flow, and precipitation of fine-grained calcite and silica along fractures that may enhance hydraulic conductivity in the UZ (at low flow rates) were estimated or bounded to reasonably assess aspects of fractures and faults that affect repository performance (see ENFE, RDTME, and RT IRSRs).

Step 4—Current and Future Modification of Fractures

Staff will independently evaluate the adequacy of DOE's definition of potential current and future tectonically and thermally controlled alteration of fracture characteristics during the repository performance period and their accounting in process-level models. For example, evaluations of structural and tectonic models for contemporary, or future changes to, fracture characteristics (e.g., increases and decreases in fracture apertures) caused by *in situ* stress, contemporary strain accumulation, seismic and aseismic deformation events, or differential thermal expansion and contraction must be documented and propagated through flow and transport, and total system models, to the extent necessary to assess aspects of fractures and faults that affect repository performance (see RDTME KTI). Similarly, long term effects and chemical alteration of fracture-wall rock, as a result of extended exposure to heat and moisture, or rock mass strength and stiffness should be considered for their potential effects on performance (see RDTME IRSR for further discussion).

Step 5—Abstraction of Fracture Data and Models

Staff will independently evaluate the adequacy of DOE's abstraction and consideration of fracture data and models of origin and their past, present, and future modifications in process-level models (figure 3-2). In evaluating DOE's abstractions, particular emphasis will be placed on continuity of consideration of fracture data and models across issues, faithfulness of abstraction to data and models, and transparency of abstractions.

4.3.1.2 Technical Basis for Review Method and Acceptance Criteria

Fracturing at YM has been the subject of numerous focused investigations. Key elements of fracture characterizations are listed below with associated topical references to highlight selected data and interpretations considered by staff as most pertinent to the evaluation of fracturing processes at YM and resulting implications for repository performance. Many of these studies have recently been integrated and summarized in the DOE Yucca Mountain Site Description (U.S. Department of Energy, 1998c).

Regional and Local Stratigraphic Elements

Stratigraphic elements to consider in fracture models are:

- Age of host geologic units, especially with respect to timing of fracture formation events (Sawyer, et al., 1994; Buesch, et al., 1996; Day, et al., 1997)

- Host rock types (igneous rocks, lithified sedimentary strata, and unlithified sediments) in the SZ and UZ at YM, including lateral and vertical lithologic variations, such as degree of welding, lythophysal development, alteration, and pumice content of tuff (Sweetkind, et al., 1997a,b) that could potentially affect fracturing.

- Host rock types in the Proterozoic and Paleozoic units of the subregional SZ, with particular emphasis on solubility features of Paleozoic carbonate units potentially related to karstic flow systems.

Regional, Subregional, and Local Structural and Tectonic Elements

Regional and subregional structural and tectonic elements to consider in fracture models are:

- Evolution of regional stress field (Zoback, et al., 1981; Minor, 1995; Minor, et al., 1997; Ferrill, et al., 1996b; Morris, et al., 1996)

- Contemporary stress field (Stock, et al., 1985, 1986; Stock and Healy, 1988; Zoback, 1992; Zoback, et al., 1992; Wittmeyer and Ferrill, 1994; Wittmeyer, et al., 1994; Barton, et al., 1995; Ferrill, et al., 1994, 1995a, 1996b; Morris, et al., 1996; also cf. Engelder, 1993; Wesnousky and Jones, 1994)

- Geologic maps (Swadley and Parrish, 1988; Frizzell and Shulters, 1990; Scott and Bonk, 1984; Faulds, et al., 1994; Day, et al., 1997; Scott, 1990; Piety, 1996; Simonds, et al., 1995)

- Structural cross sections (Scott and Bonk, 1984; Scott, 1990; Young, et al., 1992a, b, 1993; Ferrill, et al., 1996b; Ofoegbu and Ferrill, 1995, 1996, 1998; Day, et al., 1997)

- Structural and tectonic setting including known and interpreted regional and subregional scale structural features such as faults and folds, with emphasis on structural features (both emergent and buried) in Crater Flat (including the BM fault), YM, Jackass Flat, and Amargosa Valley (Snyder and Carr, 1982; Swadley, et al., 1984; Reheis, 1988; Scott, 1990; Young, et al., 1992b; Ferrill, et al., 1995b, 1996 a,b,c, 1997b, 1999a,b; Menges, et al., 1995; Stamatakos, et al., 1997b; Ofoegbu and Ferrill, 1998; Stamatakos, et al., 1998)

- Geophysical data to constrain fault-related deformation (Brocher, et al., 1998; Majer, et al., 1997)

- Geodetic strain measurements (Gilmore, 1992; Savage, et al., 1994; Ferrill, et al., 1996b; Bennett, et al., 1997a; Wernicke, et al., 1998)

- Long-term strain and deformation estimates, including geologically derived strain and fault displacement estimates and paleoseismic (trenching) studies (Ferrill, et al., 1996a,b; 1997; Stamatakos, et al., 1997b)

- Local stress field including lithostatic, tectonic, topographic, and excavation-related stresses and fluid pressure and effects on permeability (Wittmeyer and Ferrill, 1994; Wittmeyer, et al., 1994; Barton, et al., 1995; Morris, et al., 1996; Finkbeiner, et al., 1997; Ferrill, et al., 1999b)

- Fracture and fault characteristics at YM, resulting from surface studies such as pavement mapping, outcrop investigations, subsurface studies such as borehole analyses, ESF mapping, and scanline studies (Barton and Hsieh, 1989; Carr, 1992; Stuckless, et al., 1992; Barton, et al., 1993; Carlos, et al., 1993; Lin, et al., 1993; Barton, et al., 1995; Chekuri, et al., 1995; Throckmorton and Verbeek, 1995; Sweetkind, et al., 1995a,b, 1996, 1997a, b; Sweetkind and Williams-Stroud, 1995a,b, 1996; Paces, et al., 1996; Piety, 1996; Potter, et al., 1996; Anna, 1997; Anna and Wallman, 1997; U.S. Department of Energy, 1998c)

- 3D geometry of YM faults and fault blocks, intersection relationships of faults, and patterns of fault displacements (e.g., vertical and lateral gradients) (Scott, 1990; Stamatakos and Ferrill, in press; also Gay and Ortlepp, 1979; Allan, 1989; Higgs, et al., 1991; Peacock and Sanderson, 1991, 1994; Scholz, et al., 1993;

Dawers and Anders, 1995; Willemse, et al., 1996; Zhang and Sanderson, 1996; Davies, et al., 1997; Ferrill and Morris, 1997; Willemse, 1997; Yielding, et al., 1997; Alexander and Handschy, 1998; Ferrill, et al., in review, 1998, 1999a,b; Morris and Ferrill, 1999)

- Partitioning of regional and subregional strain (Ferrill and Dunne, 1989; Dunne and Ferrill, 1995) among mechanisms such as seismic and aseismic slip on large faults (Pezzopane, 1995; Ferrill, et al., 1996a, 1999a; Stamatakos, et al., 1997a; Ofoegbu and Ferrill, 1998), dilation and slip on fractures Ferrill, et al., 1999b), small faults (Lienkaemper, et al., 1987), bedding-parallel foliations and layering (Morris, et al., 1996; Ferrill and Morris, 1997; Ferrill, et al., 1998), elastic deformation, and dike intrusion (Wernicke, et al., 1998; Connor, et al., 1999)

- Hydrologic features associated with structural features such as faults or fracture zones (Hill, et al., 1995; also Mozley and Goodwin, 1995; Fridrich, et al., 1994; Bredehoeft, 1997; Ferrill, et al., 1999b)

Topographic Elements

Local topographic elements to consider in fracture models are:

- Morphology of topographic surface (Henderson, et al., 1996)

- Geometric relationship of topographic surface with respect to layering, foliations, and structural features (important for surficial and mass-wasting processes).

- Depth

Hydrologic, Geochemical, and Pneumatic Elements

Hydrologic, geochemical, and pneumatic elements to consider in fracture models are:

- Observations, measurements, and models of infiltration and subsurface flow processes (Montazer and Wilson, 1984; Barton, et al., 1993; Flint and Flint, 1995; Flint, et al., 1996; Stothoff, et al., 1997; also Ritzi and Andolsek, 1992; Mayer and Sharp, 1998; Ferrill, et al., 1999b)

- ^{36}Cl measurements in ESF (Levy, et al., 1997)

- Air and seepage permeability measurements (Le Cain, 1997; Wang, et al., 1997, 1998)

- Water table elevation data and their relationship to fracture systems (Czarnecki, et al., 1997; d'Agnese, et al., 1997)

- Saturated-zone tracer test and pump test results (Geldon, et al., 1997; Ferrill, et al., 1999; Winterle, 1999)

Summary of Yucca Mountain Fractures

Fractures are surfaces along which rocks or minerals have broken and lost cohesion (Twiss and Moores, 1992). Extension fractures (Mode I fractures) are characterized by motion perpendicular to the fracture walls. Shear fractures (Mode II and III fractures) are characterized by motion parallel to the fracture surface. Mode II shear fractures are distinguished by motion perpendicular to the edge of the fracture, whereas, sliding on Mode III shear fractures is parallel to the edge of the fracture. Fractures that display very small displacement normal to their surfaces and little or no displacement parallel to their surfaces are called joints. Joints may originate in any of the above fracture modes. Fractures that have opened perpendicular to the fracture walls and that are filled with a mineral are termed filled (or partially filled) fractures or veins.

A fault is a surface or thin tabular zone along which opposing sides have moved in a direction parallel to the surface or zone, across which, the displacement parallel to the zone is appreciably greater than the thickness of the zone, and in which, the deformation is greater than outside the zone (Twiss and Moores, 1992; Groshong, 1988). Fault zones commonly consist of a fault core within which most of the displacement is accommodated and a fault damage zone that consists of a network of subsidiary structures that bound the fault core (Caine, et al., 1996). In porous rocks, fault cores commonly have lower permeability than the protolith because of grain size reduction and mineral precipitation. Fault damage zones commonly have enhanced permeability because of fracturing and faulting. Fault core and fault damage zone development is variable from fault to fault and along an individual fault (Caine, et al., 1996).

Joints in the central repository block at YM may be divided by age and genesis into three groups: (1) oldest cooling joints, (2) tectonic joints of intermediate age, and (3) youngest unloading joints (Barton and Larsen, 1985; Barton and Hsieh, 1989; Barton, et al., 1993; Sweetkind, et al., 1995a, b; Throckmorton and Verbeek, 1995; Sweetkind and Williams-Stroud, 1996). Eight joint sets have been identified between these origins and ages, but no analyzed exposure contains all eight sets. Cooling joints are distinguishable because they: (1) locally have degassing-related tubular structures (Barton, et al., 1984), (2) do not cut lithophysae, (3) have a smooth planar appearance, (4) have surface areas in excess of 100 m^2, and (5) predate other joints abut (determined based on abutting relationships). Tectonic joints are distinguishable from cooling joints because they: (1) lack tubular structures, (2) cut lithophysae, (3) are not normally as smooth, (4) are commonly smaller, and (5) in many cases, abut against cooling joints. Some tectonic joints, however, cut across cooling joints, which suggests that either the cooling joints were minerals filled at the time of tectonic joint propagation, or that the crossing tectonic joints originated as shear fractures. Thus, some cooling joints were not voids that blocked propagation of tectonic joints. Finally, unloading joints are: (1) subhorizontal, (2) near surface, (3) rough and curviplanar, and (4) generally terminate against cooling and tectonic joints.

Cooling joints form during thermoelastic contraction resulting from heat loss after deposition of the welded tuffs. During heat loss in the thick cooling units, isotherms are not arranged in a blanket-like manner parallel to the unit boundaries. Instead, some fluid circulation occurs, creating thermal plumes and sinks that would have locally affected joint intensity and orientation. Typically, igneous cooling joints form polygonal patterns in situations where the minimum and maximum horizontal stresses are near equal, and the rocks are not free to expand laterally, which is the fixed-grip situation (Engelder and Fischer, 1996). Yet, the cooling joints in the welded tuffs of the Paintbrush Group are orthogonal (Sweetkind and Williams-Stroud, 1996) with two joint sets subnormal to layering and one parallel to layering. This deviation from typical geometry may be controlled by lateral thickness variations, paleotopography, differential compaction, tectonic stresses, and horizontal stresses that were significantly anisotropic. The setting was not fixed-grip but rather one of regional east-west extension during the Miocene (Zoback, et al., 1981; Scott, 1990; Wernicke, 1992; Ferrill, et al., 1996b; Morris, et al., 1996; Day, et al., 1997). Thus, cooling joints at YM formed in a local stress field that was probably produced by a combination of sources, including thermoelastic cooling stresses, topographic stresses, lateral thickness variations, differential compaction, remote regional stress field, and stress perturbations around active faults (Engelder, 1993).

Tectonic joint development did not necessarily postdate cessation of cooling joint formation by an extended period because the oldest tectonic joints (T1, Sweetkind and Williams-Stroud, 1995) strike north-south, are subnormal to layers, and are attributed to the east-west horizontal extension during the Miocene. The next youngest joint set, northwest-trending T2 joints, would appear to require a regional stress field where minimum principal stress trended northeast-southwest. This stress-field geometry is undocumented by other geological features, and the existence of this set is not strongly supported (Sweetkind and Williams-Stroud, 1995a). T3 joints strike northeast-southwest and are related to the recent regional stress field where the minimum principal stress trends northwest (Sweetkind, et al., 1995b). The youngest tectonic joints are east-west trending T4 joints, which have a problematic tectonic origin as no regional stress field has been identified to account for north-south extension. As a result, Throckmorton and Verbeek (1995) and Sweetkind and Williams-Stroud (1995b) attributed fractures of this set to an unspecified surficial unloading event. A possible tectonic rather than unloading origin for some T4 fractures would be as secondary structures accommodating north-south extension in the regions between two overlapping normal faults that strike north-south (Trudgill and Cartwright, 1994; Peacock and Sanderson, 1994; Ferrill, et al., 1999, in press). As previously described, late subhorizontal joints with significant surface roughness and curviplanar form are attributed to erosional unloading (Sweetkind and Williams-Stroud, 1995).

<u>Nonwelded Topopah Spring Tuff</u>

Overall fracture intensity of the Topopah Spring non welded or tuff (PTn) is lower than in the overlying and underlying welded tuffs of the Tiva Canyon and Topopah Spring Tuffs, respectively, and fractures are poorly connected within and between layers of the PTn (Sweetkind, et al., 1996, 1997a,b). Extension fractures in the PTn typically terminate at welding or lithologic breaks. Faults, which typically originate as shear fractures capable of fracturing across discontinuities, are considered to be structural pathways through the PTn. The exposures of the PTn in the ESF have lower fracture densities than those observed on the surface (Rousseau, et al., 1996).

Clustering of Fractures at Yucca Mountain

One important morphological aspect of the joint sets, which was first noted during pavement studies by Barton, et al. (1993), is that joints do not have uniform spacing (figure 4-7). Instead, some joints are closely spaced in swarms or clusters. The clusters are separated by large

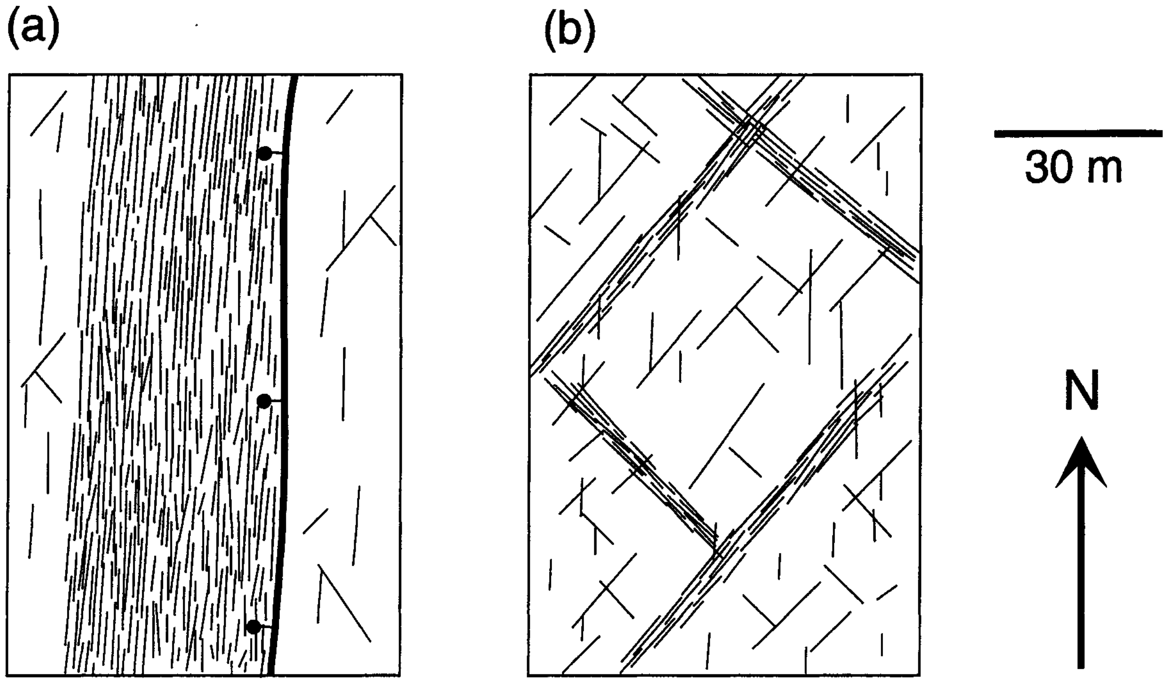

Figure 4-7. Schematic illustration of (a) fault related joint swarms and (b) cooling joint swarms at Yucca Mountain. Solid lines are fracture traces, a bold line is a fault with blackened circle on hangingwall. Both (a) and (b) are plan views.

distances in excess of 10 m, where joint spacing is in excess of 1 m. Development of joint clusters clearly demonstrates that deformation in the rock was heterogeneously distributed in the rock during fracture formation. One type of cluster geometry is best exemplified by the joints in the hangingwall of the Ghost Dance fault (Sweetkind and Williams-Stroud, 1995a). Surface mapping around the north-south striking Ghost Dance fault has identified a 50-m-wide zone of highly fractured rock in the hangingwall of the fault (Sweetkind and Williams-Stroud, 1995). North-south striking joints and north northwest-south southeast striking joints are intensely developed with spacings of a few centimeters at distances up to 50 m from the main fault trace, which also strikes north-south. The deformation concentrator here appears to be partitioning of a small portion of the east-west regional extension into hangingwall deformation by joint formation, perhaps, in a dilational quadrant during fault displacement. The width of hangingwall fault-damage zones is smaller in the ESF than at the surface. Fault footwalls typically show little or no increase in fracturing near faults (Sweetkind, et al., 1997a,b).

Another type of cluster geometry is closely spaced cooling joints (Barton, et al., 1993). Detailed mapping of large joints (lengths >2m) in the upper lithophysal unit of the Tiva Canyon Tuff on Live Yucca Ridge shows that cooling joints tend to be clustered into swarms that trend northeast and northwest (figure 4-8). Swarm spacings are on the order of 30 to 100 m. Cooling joint swarms consist of extensive planar smooth fractures occurring in sets of three to eight fractures, with joint spacings of about 25 cm and trace lengths typically 10 m. Individual cooling joint trace lengths exceed 25 m in some cases. Swarms span the entire thickness of the upper lithophysal unit of the Tiva Canyon Tuff, and have observed lengths that exceed 100 m. True lateral extents of swarms remain unconstrained. Why cooling joints would be (i) heterogeneously distributed in space, and (ii) form orthogonal sets rather than columnar arrays is not well understood but may be a function of thermal gradients and topographic and fault related effects on the local stress field during cooling.

The presence of clusters may indicate that the majority of cooling joints were mineralized early (e.g., by vapor phase minerals). Otherwise, these large fractures would be expected to generate significant stress shadows up to meters away. These shadows would prevent nearby initiation of new joints, so joint spacings should be on the order of meters and not tens of centimeters. The spacings at a scale of tens of centimeters would either be achieved by mineralizing the joints, preventing them from acting as voids with associated stress shadows, or by increasing the driving stress for joint formation due to increased regional extension.

Sampling biases

Characterization of fracture networks at YM is impaired by several important sampling biases that are common to fracture analyses. If left uncorrected, these sampling biases lead to underrepresentation of fracture intensity, porosity, permeability, and connectivity.

First, the lengths of the longest fractures in a population are often unconstrained because the ends of the fracture are obscured (blind). This bias can lead to underestimation of fracture connectivity.

Second, the orientation of a one-dimensional sampling line [e.g., borehole or detailed line survey (DLS) scanline] or 2D sampling surface (e.g., pavement, roadcut) inherently biases sampling against discontinuities parallel to the sampling line or surface, and in favor of

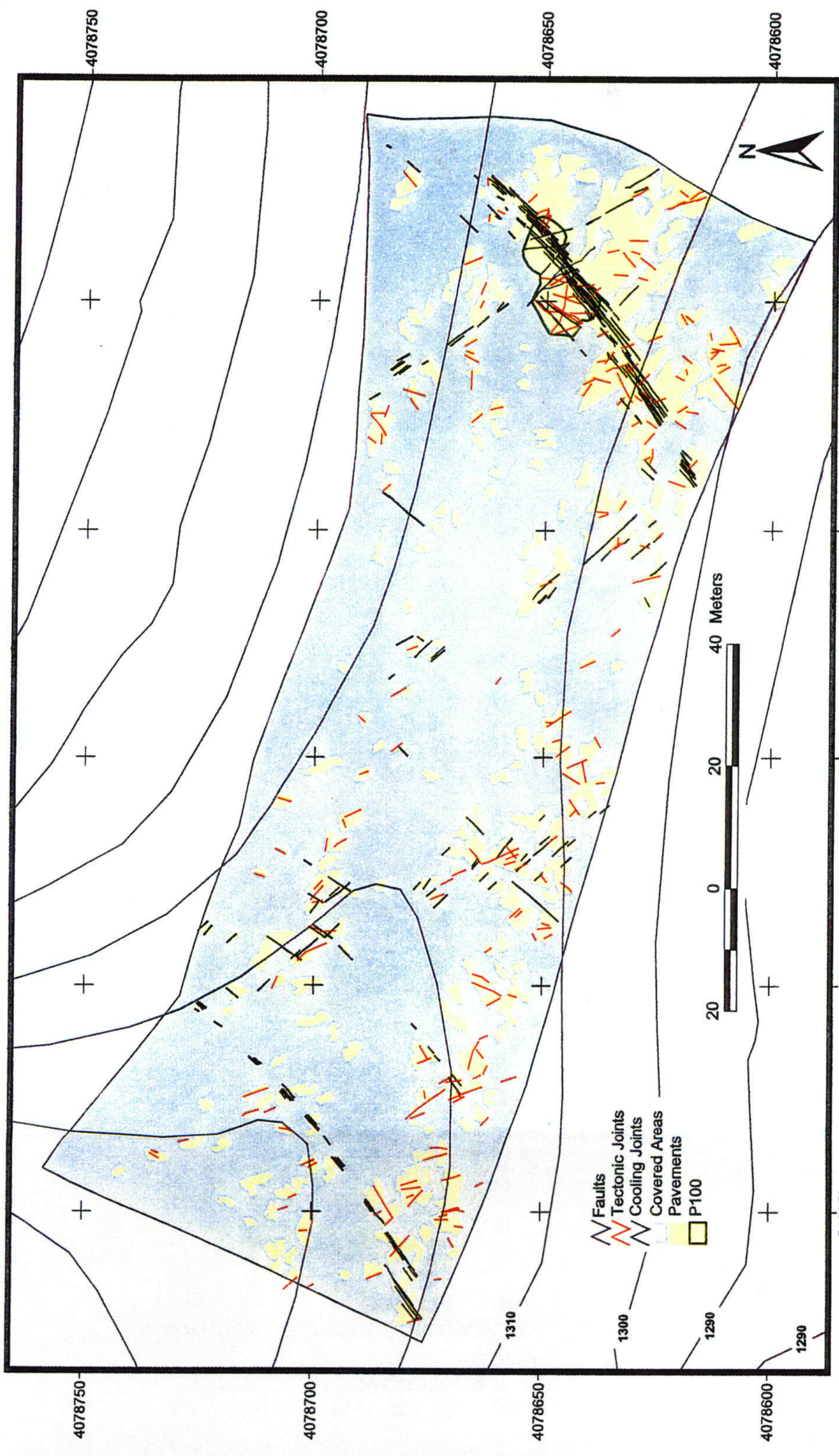

Figure 4-8a. (a) Map of cooling joints and tectonic joints and faults in the Upper Lithophysal Unit of the Tiva Canyon Tuff on Live Yucca Ridge, Yucca Mountain, Nevada. Contour interval is 10 m. Map projection is Universal Transverse Mercator zone 11, reference datum is NAD83.

(b) Cooling Joints

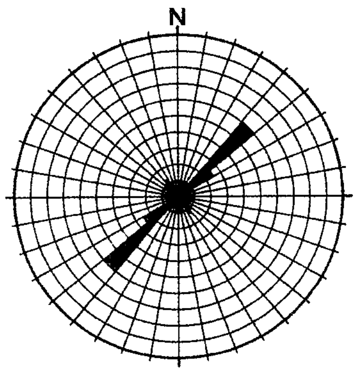

Length Weighted
N = 1069m (cumulative fracture length)
n = 272 (number of fractures)
Plot Radius = 40%

(c) Tectonic Joints and Faults

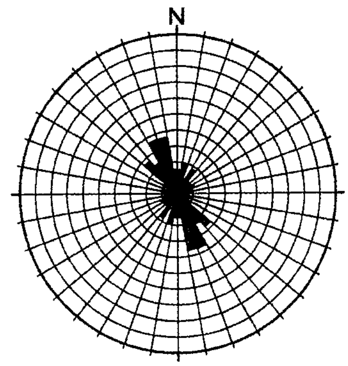

Length Weighted
N = 737m (cumulative fracture length)
n = 214 (number of fractures)
Plot Radius = 20%

(d) All measured joints and faults

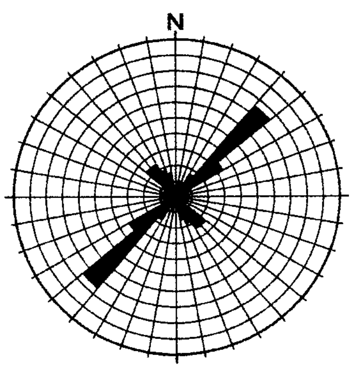

Length Weighted
N = 1806m (cumulative fracture length)
n = 486 (number of fractures)
Plot Radius = 20%

Figure 4-8b–d. (b)–(d) Rose diagrams of fractures shown in (a). n = number of fractures, N = cumulative fracture length in meters.

sampling discontinuities at a high angle to the sampling line or surface. Mathematical corrections (Terzaghi, 1965) can partially compensate for this sampling bias.

Third, because measuring every fracture from microscale to megascale is impractical or impossible for large sample areas, fracture studies usually have a size (e.g., length) cutoff. Fractures smaller than a given dimension are not counted. Consequently, small fractures are underrepresented in fracture characterization. Exclusion of small fractures could lead to an underestimation of hydrologic properties such as porosity, permeability, and fracture connectivity in these units. Elimination of fractures less than 1 m also may modify fracture intensity interpretations near faults such as for the Ghost Dance fault in the ESF, where the 1-m cutoff for trace length leads to extremely variable fracture intensity estimates over a wide zone (Sweetkind, et al., 1997a,b).

We use analyses of fractures in the upper lithophysal unit of the Tiva Canyon Tuff on Live Yucca Ridge to illustrate the importance of sampling location and fracture trace length and directional sampling bias (figures 4-8 and 4-9). Analyses of ESF and Enhanced Characterization of Repository Block (ECRB) data illustrate correction for directional sampling biases (figure 4-10).

<u>Location Bias</u> – A strong bimodal distribution of fractures is apparent on Live Yucca Ridge (figure 4-8a and 4-8d). This bimodel distribution is not well represented in P100 (figure 4-9a and 4-9b). Although a subset of the Live Yucca Ridge map area (figure 4-8a), P100, samples an area that is too small to be representative of fracturing at Live Yucca Ridge as a whole.

<u>Trace Length Bias</u> – Rose diagrams are not typically weighted by fracture length; they treat all fractures as equally important. Visual inspection of P100 (figure 4-9a) gives a clear impression of dominant northeast-southwest fractures that are only partially captured by the rose diagram in figure 4-9b. Plotting a length-weighted rose diagram (figure 4-9c) emphasizes the importance of the northeast-southwest fractures. When considering vertical percolation pathways, and potential rockfall into a tunnel, for example, fracture size (in this case length) is an important parameter.

<u>Directional Sampling Bias</u> – A common approach to correcting for directional sampling bias is the Terzaghi (1965) method, which applies a correction for the angle between the scanline and the pole to each sampled fracture. The frequency of each fracture is given by a Terzaghi factor:

$$T_f = \frac{1}{\cos\theta}$$

where θ is the angle between the normal to the fracture and the scanline. In this example, the Terzaghi correction was truncated for $T_f > 4$ (i.e., for $\theta \geq 75°$, fractures are assigned a frequency of 4). This correction accounts, in part, for underrepresented fractures that intersect the scanline at low acute angles.

In addition to sampling biases, fracture characterization based on existing studies is impaired because fracture data were collected from different sources including boreholes, pavements, and the ESF, and different information was collected from each of the three sets of studies.

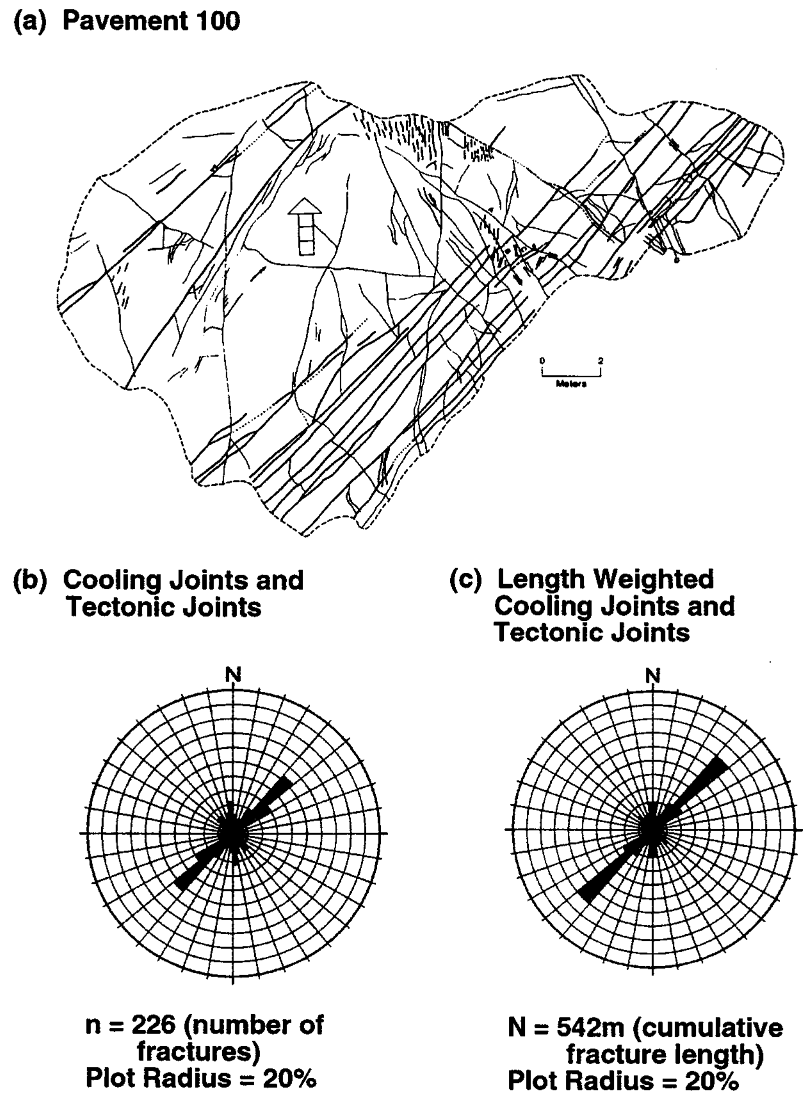

Figure 4-9. (a) Map of pavement 100 on Live Yucca Ridge, after Barton, et al. (1993). (b) Rose diagram of fractures in pavement 100. (c) Length-weighted rose diagram of fractures in pavement 100.

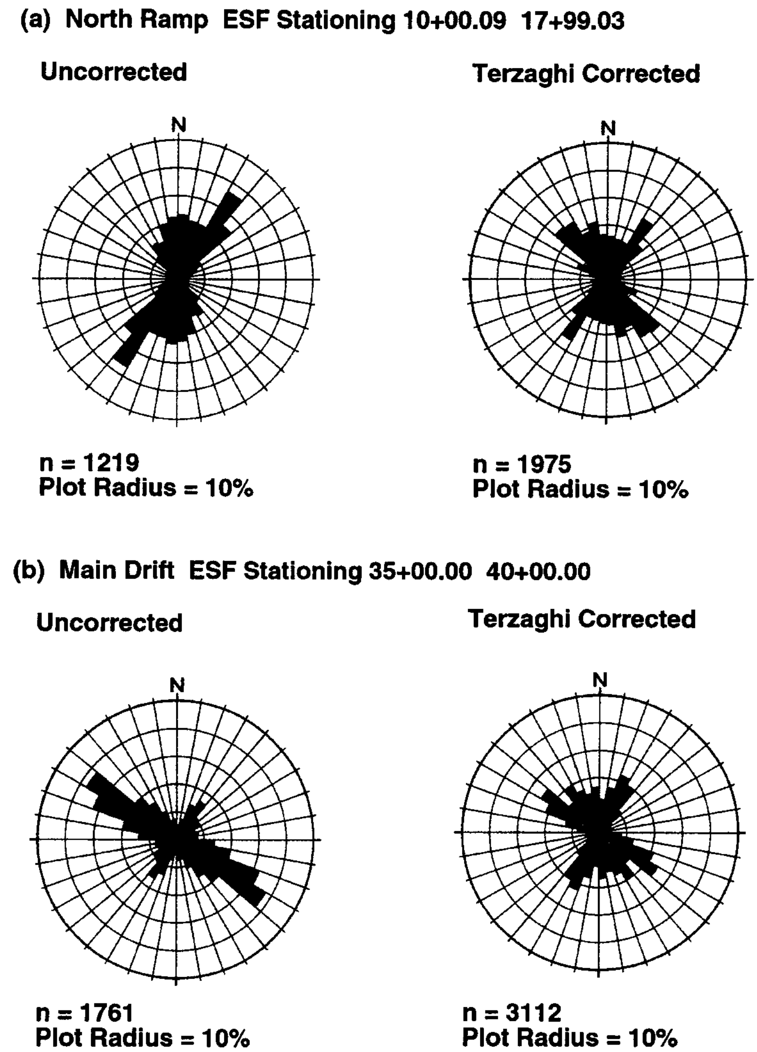

Figure 4-10a–b. Examples of Terzaghi (1965) correction of detailed line survey data from the Exploratory Studies Facility (ESF) at Yucca Mountain. Raw data from Exploratory Studies Facility detailed line survey data were collected by the Bureau of Reclamation and U.S. Geological Survey (ESF data transmitted from DOE to the CNWRA, August 1998, DOE DTN numbers GS960708314224.008, .101, 011, .014, .003, .008, .010,.012, .020, .021, .022, .023, .024, .025, .026, and .028; TDIF numbers 305556, 305554, 305624, 306645, 306017, 306284, 306298, 306299, 306509, 306510, 306511, 306512, 306513, 306514, 306515, 306517.). The files used in (a), (b), and (c) represent the midpoint of the North Ramp, Main Drift, and South Ramp of the ESF, respectively. Rose diagrams were constructed using StereoNet, Ver. 3.0 for Windows software. The raw data were Terzaghi corrected to compensate for directional sampling bias. (a) The North Ramp between Sta. 10+00.09 and 17+99.03 traversed the Tpp, Tpbt2, Tptrv, Tptrn, Tptrl units into the Tptpul unit. (b) The Main Drift from Sta. 35+00.00 to 40+00.00 is entirely in the Tptpul.

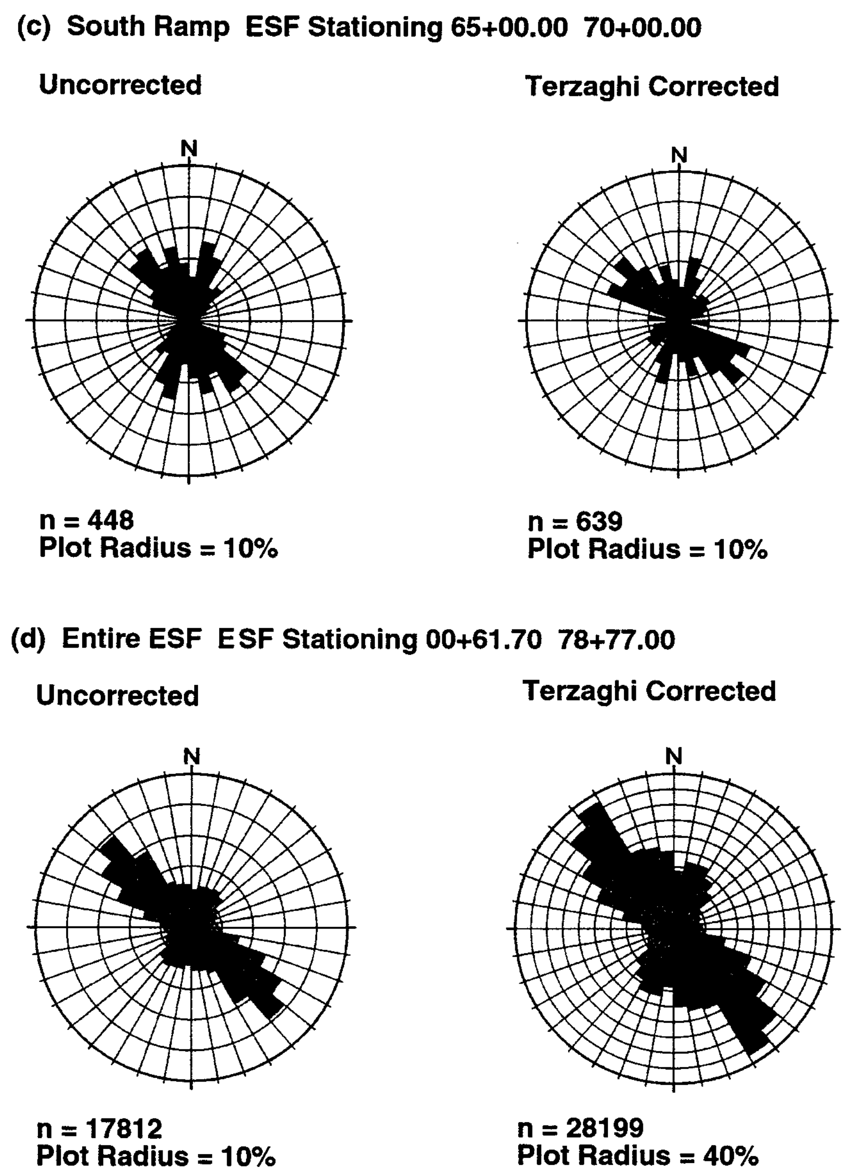

Figure 4-10c–d. (c) The middle section of the South Ramp encounters Tptrl, Tptrn, Tptrv, Tpbt2, Tpcpv, Tpcpln, and Tptpul units from Sta. 65+00.00 to 70+00.00. (d) Terzaghi correction of detailed line survey data from the entire ESF at Yucca Mountain. Note that the rose diagrams of uncorrected and Terzaghi corrected fracture orientations for the entire ESF are similar, due to the combination of data from nearly orthogonal scanlines (approximately east-west ramps and north-south main drift). Combination of all of the detailed line survey data, however, suppresses important local variability related to lithology and structural position.

The only observations consistent to all data sets are orientation and lithology (Sweetkind and Williams-Stroud, 1996).

Local controls on fracturing and small scale faulting

YM consists of a thick accumulation of volcanic tuff deposited on an irregular surface of eroded and deformed Paleozoic and Precambrian basement composed of highly faulted and folded sedimentary and metasedimentary rocks. These tuffs were erupted from a series of Middle to Late Miocene (15 to 9 Ma) calderas that collectively form what has been defined as the southwestern Nevada volcanic field (see Sawyer, et al., 1994, for the most recent regional stratigraphy of the Miocene volcanic rocks in the YM region). Rocks of the Paintbrush Group, principally ash flows of the Topopah Spring Tuff (12.8 Ma) and Tiva Canyon Tuff (12.7 Ma) make up the main surface exposures of YM. The Paintbrush Group Tuffs rest on a sequence of older tuffs, including the Prow Pass and Bullfrog members of the Crater Flat Group. Younger tuffs related to the Timber Mountain Group are locally exposed at YM in topographic lows between large block-bounding faults. This observation, along with evidence for growth faults in the Paintbrush rocks in Solitario Canyon (Carr, 1990; Day, et al., 1997), suggests that faulting and tuff deposition were synchronous at YM.

The majority of faults at YM are either north-trending normal faults or northwest-trending dextral strike-slip faults. The larger faults in these two orientations bound the fault blocks that underlie the study area. These two sets of faults are interpreted to be coeval, based on mutual terminations and secondary structures between them such as pull-apart basins (Day, et al., 1997). Some northwest-trending faults are dominantly normal faults, accommodating extension in relay ramps between overlapping normal faults (Ferrill, et al., 1999a). Only four reverse faults with north-south or northeast-southwest strikes have been identified, but they are potentially key features for constraining the kinematic history of the region (Day, et al., 1997). Based on ^{36}Cl data from the ESF, one of these, the Diabolus Ridge fault, has been interpreted to be an important infiltration pathway (Levy, et al., 1997). Much of the detailed fieldwork to study faults in the central block focused on the Ghost Dance and Sundance faults, which are close to the subsurface trace of the ESF (Spengler, et al., 1994; Potter, et al., 1996).

YM itself consists of a sequence of north to north-northeast-trending fault-bounded ridges crossed by occasional northwest-trending dextral strike-slip faults. Faults dip almost uniformly to the west and separate blocks of gentle to moderate east-dipping tuff strata. From north to south, both fault displacement and stratal tilt increases, indicating progressively greater extension of the Crater Flat basin southward. This pattern is most profound on the west flank of YM, which is defined by a series of left-stepping and north-trending en echelon faults. The southward increase in fault offset is coupled with greater block rotation, both horizontal and vertical (Scott, 1990). Work by the USGS (Hudson, et al., 1994; Minor, et al., 1997) suggests that this pattern of faulting, along with rotated paleomagnetic direction in the tuffs, resulted from a discrete period of extension followed by a discrete period of dextral shear, akin to an oroclinal bending model. More recent reanalysis of these data suggests an alternative explanation. The north-to-south displacement gradient and rotation of fault blocks is simply a result of increased rollover deformation in the hangingwall above a listric BM fault (Stamatakos and Ferrill, 1998).

En echelon faulting defines the western edge of Yucca Crest and the fault line escarpment that follows the west-dipping Solitario Canyon, Iron Ridge, and Stagecoach Road faults (Simonds, et al., 1995). The geometry of faults and ridges defines a scallop trend, composed of linear north-trending fault segments connected by discrete curvilinear northwest-trending fault segments. For example, the ends of the north-trending curvilinear Iron Ridge fault bends to the northwest near its overlap with both the Stagecoach Road and Solitario Canyon faults. YM also contains numerous swarms of small northwest-trending faults that connect the large north-trending faults. One example is at West Ridge, which is cut by numerous small faults that connect segments of the Windy Wash and Fatigue Wash faults. This geometry strongly suggests that the entire YM fault system is an en echelon branching fault system (Ferrill, et al., 1999, in press), in which faulting on the large block-bounding fault triggers relatively widespread, but predictable, secondary faulting on connecting and linking faults. Linkage of the en echelon system is either by lateral propagation of curved fault tips or formation of connecting faults that breach the relay ramps (figure 4-11; Ferrill, et al., 1999a, in press; Peacock and Sanderson, 1994; Trudgill and Cartwright, 1994). The western YM fault system contains examples of both linking mechanisms (figures 4-11, 4-12, and 4-13). More importantly, from this interpretation of en echelon faulting, it follows that locally developed faults and fractures were produced by local variations of the stress field, rather than dramatic swings of the regional extension direction (Throckmorton and Verbeek, 1995). Recent numerical modeling of stresses related to displacement on overlapping normal faults show that local perturbations of the stress field in the fault overlap zone are likely to lead to the development of faults and fractures in orientations oblique to the regional trend (Crider and Pollard, 1998).

This model for the evaluation of an en echelon fault system has several potentially important implications for groundwater flow. Unfaulted relay ramps may provide important aquifer connectivity across faults (figure 4-11d). Faulted relay ramps may provide local fault-controlled traps for perching of groundwater. Localized fracting in relay ramps may locally enhance hydraulic conductivity (figure 4-11d).

Fracture and Fault Controls on Saturated Zone Permeability

A primary control on the permeability architecture of stratified rocks is the difference in permeability of sequential rock layers. If the stratigraphic sequence is undeformed, the anisotropy vertical heterogeneity and will dominate the permeability architecture. In faulted aquifers, however, such as those at YM, geologic structures (fault zones and fractures) exert four additional controls on subregional to regional and flow: (i) fault offsets alter the overall geometry of the aquifers and control aquifer communication between fault blocks (Allan, 1989), (ii) fault zones commonly form relatively impermeable barriers to cross-fault flow and permeable pathways for along-fault flow (Caine, et al., 1996), (iii) relatively small fracture and fault zones lead to permeability anisotropy in fault blocks, and (iv) fracture and fault zone conductivity and anisotropy may be influenced by the *in situ* stress field (Barton, et al., 1995; Finkbeiner, et al., 1997; Ferrill, et al., 1995; Ferrill, et al., 1999b).

Fractures, including faults, impart a permeability characteristic to the rocks that may be measured at various scales. Fault zones commonly consist of a fault core, within which most of the displacement is accommodated, and a fault damage zone that consists of a network of subsidiary structures that bound the fault core (Caine, et al., 1996). Fault cores commonly have lower permeability than the protolith, because of grain size reduction and mineral precipitation. Fault damage zones commonly have enhanced permeability because of fracturing and faulting.

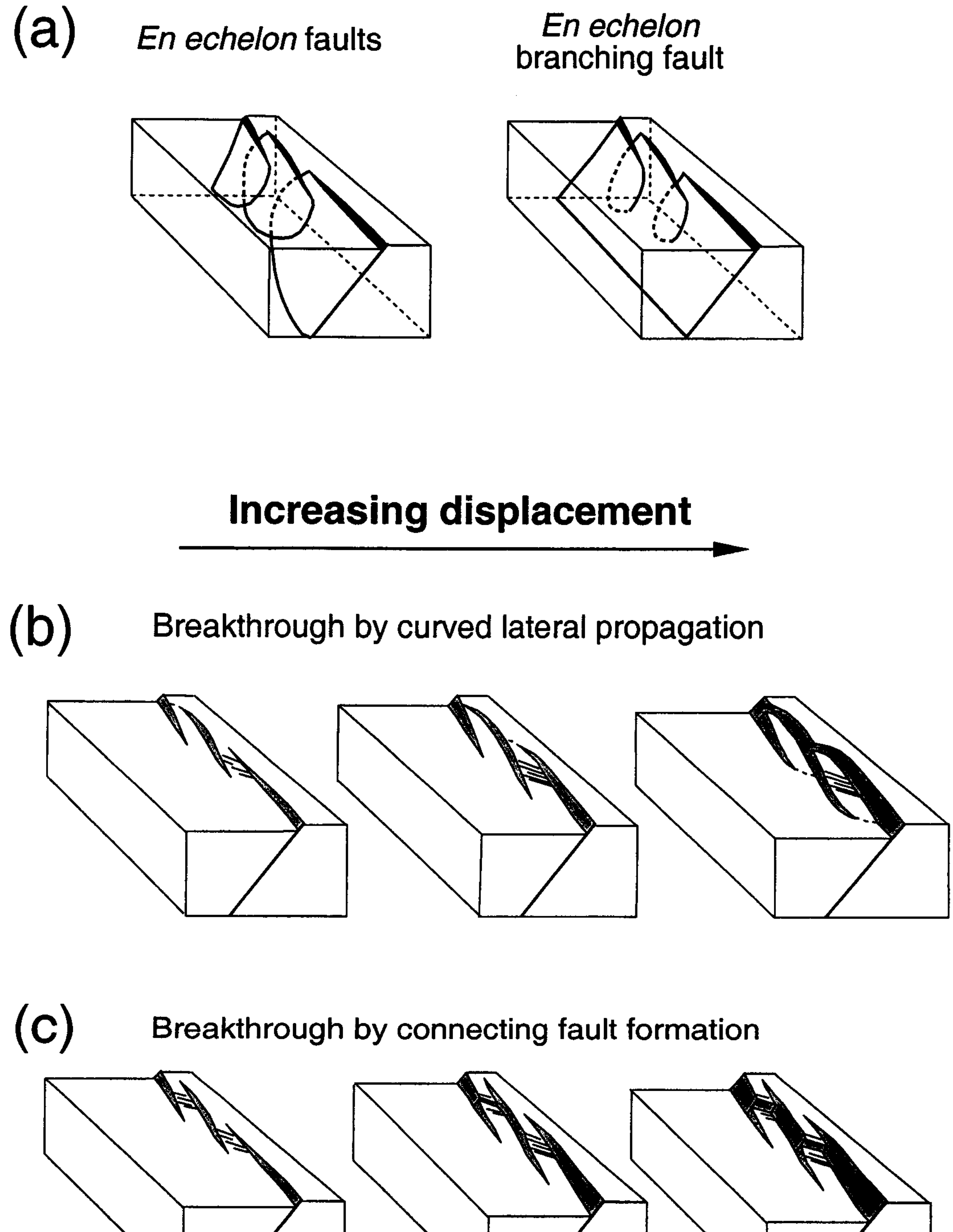

Figure 4-11. Block diagrams illustrating (a) topology of en echelon fault system and en echelon branching fault, (b) sequence of evolution of en echelon normal fault array or en echelon branching normal fault involving linkage and breakthrough by lateral propagation of curved fault tips, and (c) sequence of evolution of en echelon normal fault array of en echelon branching fault system involving linkage and breakthrough by connecting fault formation.

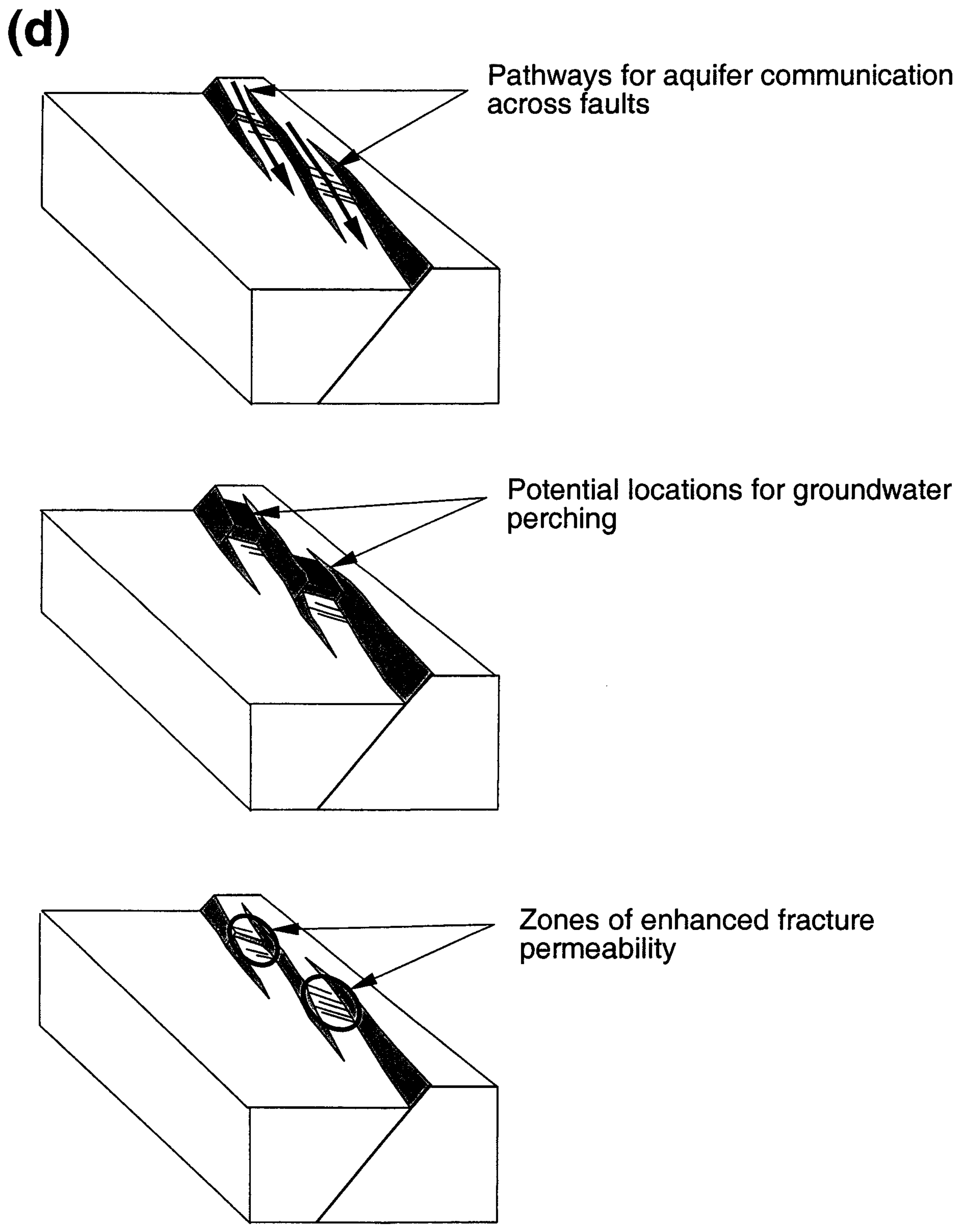

Figure 4-11d. (d) Block diagrams illustrating aspects of fault interaction and fault-break geometry important for groundwater flow and perching.

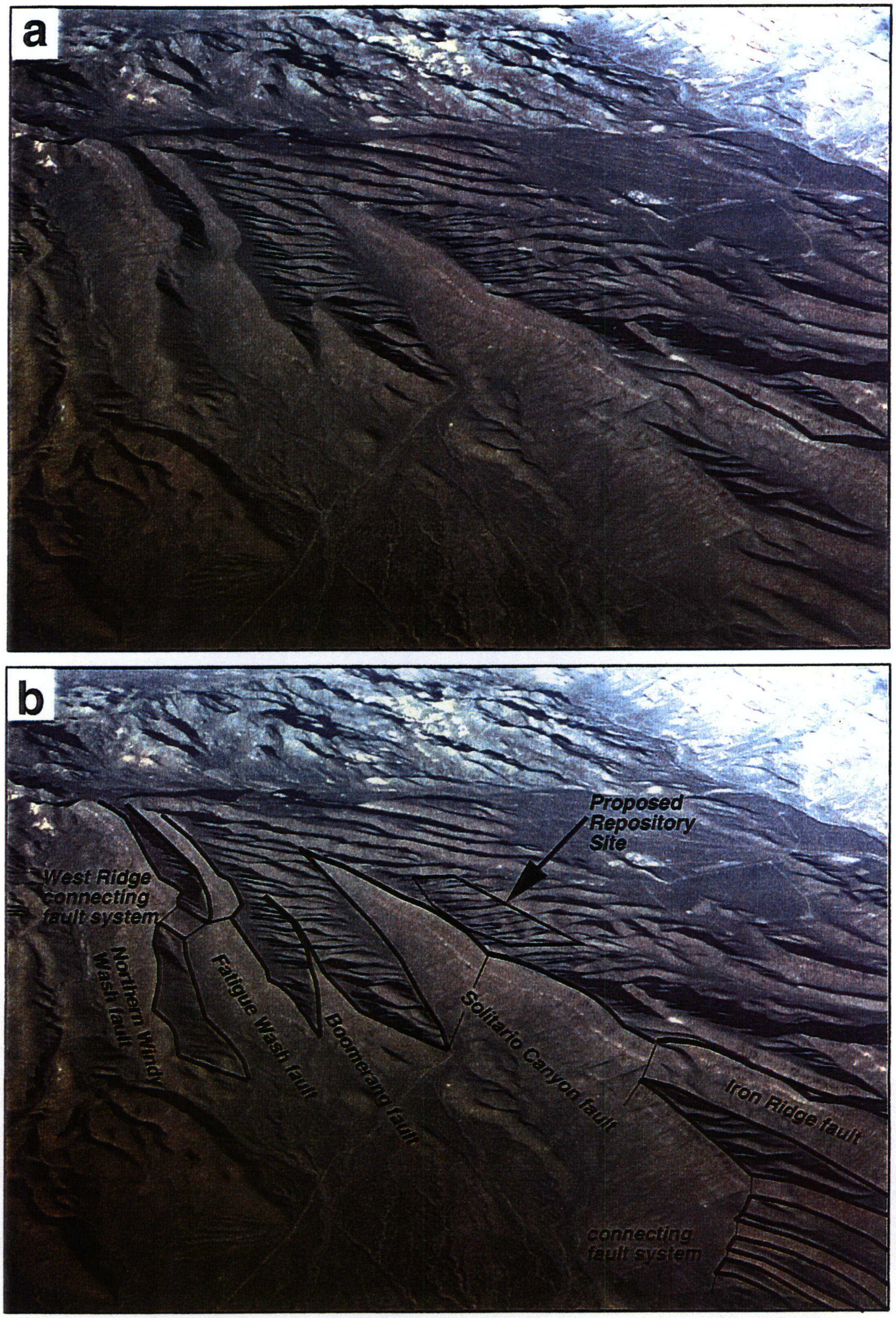

Figure 4-12. An en echelon fault system bounds the western side of Yucca Mountain. (a) Unannotated and (b) annotated aerial photographs (looking northeast) of Yucca Mountain, Nevada, illustrate the Solitario Canyon-Iron Ridge fault system and the overall en echelon geometry of the western Yucca Mountain fault system. Width of the field of view is approximately 15 km.

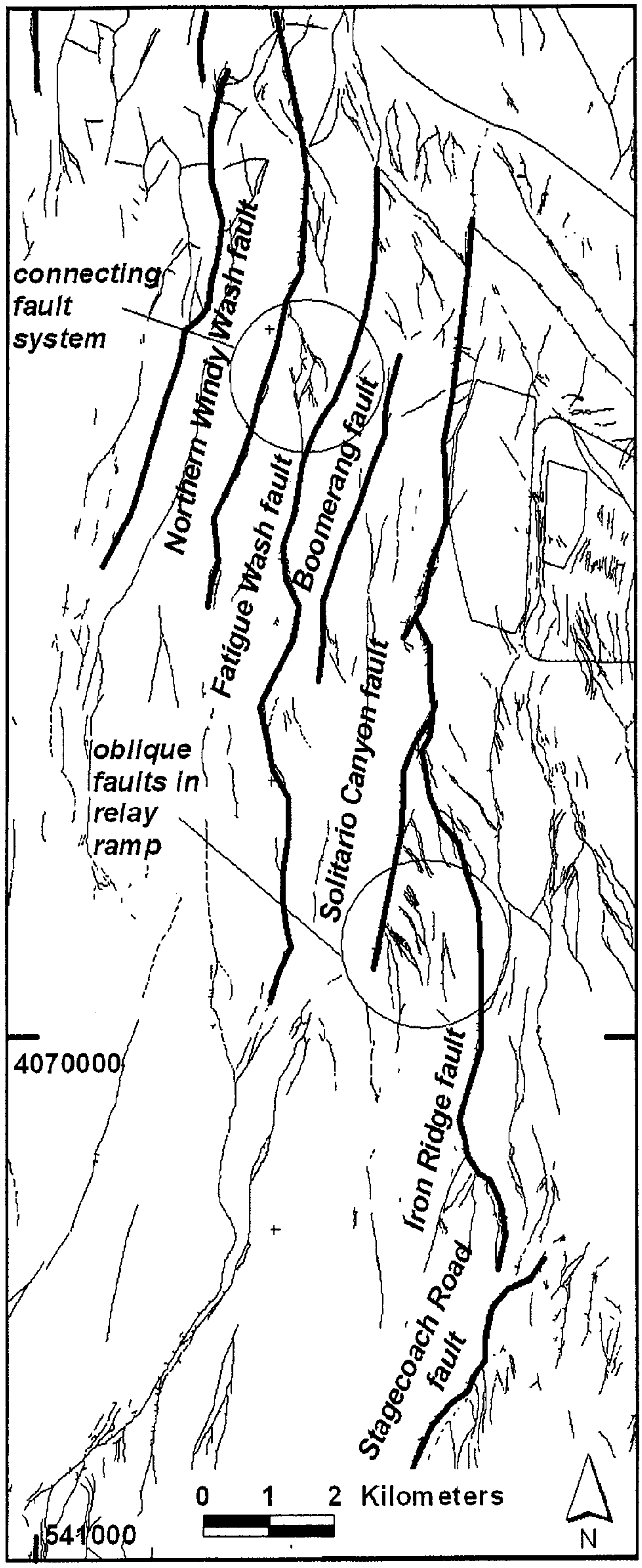

Figure 4-13. Map of western Yucca Mountain fault system (after Simonds, et al., 1995) illustrates arrangement and connection of major normal faults (bold lines)

Fault core and fault damage zone development is variable from fault to fault and along an individual fault (Caine, et al., 1996).

Fault zone architecture and related permeability structures may strongly control fluid flow into and out of the repository (Caine, et al., 1996). In many rock types, fault zones exhibiting grain-size reduction, and mineral precipitation generally contain core gouge zones with lower permeability and porosity than the adjacent protolith (Goddard and Evans, 1995; Caine, et al., 1996). These faults would form barriers to flow. In contrast, faults with coarse-grained breccias and wide fault damage zones containing numerous subsidiary structures that bound the fault core gouge may have greater permeability and porosity than the protolith, thereby enhancing fluid flow (Chester and Logan, 1986). These faults would act as conduits to fluid flow. Because faults commonly contain a less permeable core and a more permeable fault damage zone (Caine, et al., 1996), they have enhanced permeability parallel to the fault, but reduced permeability perpendicular to the fault. In the case of faults in welded tuff in the UZ at YM, fault cores probably have greater permeability than the protolith, but lower permeability than fault damage zones. Relatively fine-grained fault core material may be particularly important for water movement under low flux conditions, due to capillary forces.

Analysis of layer juxtaposition across faults and identification of fluid flow barriers and pathways is now routine practice in the oil industry (Allan, 1989). These analyses are key elements to assessing probability of fault-related trapping of hydrocarbons. Recently, fault zone deformation has been the subject of intensive investigation, with particular emphasis on fault zone permeability in sand and shale sequences, and implications for hydrocarbon migration and trapping (Knipe, 1997; Yielding, et al., 1997, 1999; Alexander and Handschey, 1998). Consideration of aquifer and aquitard juxtaposition, fault zone deformation mechanisms in YM tuff aquifers, and the resulting influences on groundwater flow will be key elements for understanding groundwater flow and contaminant transport at YM.

The importance of fracture network characteristics differ considerably according to the flow regime under consideration. For example, narrow fracture apertures, and fine-grained fracture fillings comprise the percolation pathway under low UZ flow conditions. In contrast, large fracture apertures are important percolation pathways under high UZ flow conditions, such as caused by large precipitation events. Characteristics such as aperture distribution, including variation along fractures, and fracture intensity are also important in the percolation and near-drift UZ environments. Groundwater movement in the UZ may be relatively less sensitive to differences in fracture strike, due to the dominantly vertical gravity-driver flow in the UZ. In contrast, fracture strike is of relatively major importance for groundwater flow in the SZ, due to the dominantly lateral flow below the water table. Hydraulic properties and flow rates in the SZ are more directly dependent on fracture apertures than in the UZ.

Although many SZ flow modeling efforts have assumed homogeneous and isotropic permeability properties for aquifer strata, a mounting body of evidence indicates that aquifer permeability is strongly controlled by fault zones and fractures. Tectonic and structural features, such as fractures and fault zones, exert a principal control on permeability, and therefor groundwater flow. These effects occur over a large range of scale of observation from tens of square meters to thousands of square kilometers:

- At the regional scale (thousands of sq km), groundwater flow in the YM region flows from an area of recharge in higher altitude areas north of YM, to lower elevation areas of discharge in Amargosa Valley and ultimately the Death Valley pull-apart basin.

- At the subregional scale (tens to hundreds of square kilometers), large faults control the overall structural framework of YM and produce offset and tilting of aquifer strata and juxtapose different aquifers, allowing fluid communication between aquifers. In some cases, faults provide preferred pathways for groundwater flow. Furthermore, within strata in the YM area, fault zones and fractures produce the primary aquifer permeability. Fault and fracture permeability at the subregional scale can be addressed by dividing the subregion into domains represented by different permeability/conductivity tensors; some domains may represent specific fault zones.

- At the local scale (hundreds of square meters up to several square kilometers), individual faults and fracture swarms may dominate permeability or be fast flow paths, and intervening blocks of less fractured rock can be approximated by separate permeability tensors.

Influence of Stress on Permeability

Anisotropic permeability in fractured aquifers arises from the abundance and distribution of faults and fractures and permeability of associated damage zones (e.g., breccia). Although it is known that faulted and fractured aquifers commonly have anisotropic transmissivity (National Research Council, 1996), maps depicting regional-scale groundwater flow usually assume flow parallel to the gradient of the potentiometric surface. This is true only if the transmissive properties of the aquifer are isotropic or if the major or minor semi-axis of the transmissivity tensor is everywhere parallel to the potentiometric gradient.

Recent studies, including one example from YM, have shown that faults favorably oriented for slip in the current stress field tend to be the most active groundwater flow pathways (Barton, et al., 1995; Finkbeiner, et al., 1997). This observation has been explained by increased small-scale fracturing and faulting in the vicinity of faults on the verge of shear failure (Barton, et al., 1995). The ability to recognize such faults allows us to identify the loci of increased fracturing.

A secondary, but measurable, influence on permeability is the effect of contemporary stress on reducing apertures of existing faults and fractures (Carlsson and Olsson, 1979; Barton, et al., 1995; Finkbeiner, et al., 1997). Faults and fractures perpendicular to the maximum principal stress are preferentially closed, thereby reducing permeability perpendicular to the maximum principal stress. Permeability perpendicular to the minimum principal compressive stress direction is relatively enhanced because lower resolved normal stress results in less fracture aperture reduction (e.g., Carlsson and Olsson, 1979).

Slip Tendency and Dilation Tendency

Stress analysis involves calculating resolved stresses on fault and fracture surfaces in order to analyze likelihood for slip or dilation in crustal stress fields.

Slip tendency analyses are applicable to planar discontinuities like faults, extension fractures, or layering (Morris, et al., 1996; Ferrill, et al., 1998a). For faults and fractures, slip is likely to occur on a surface when the resolved shear stress, τ, on that surface equals or exceeds the frictional resistance to sliding. Frictional resistance is proportional to normal stress, σ_n, acting across that surface (Jaeger and Cook, 1979). The slip tendency, T_s, of a surface is the ratio of shear stress to normal stress acting on that surface (Morris, et al., 1996).

$$T_s = \tau / \sigma_n$$

As such, T_s depends solely on the stress field (stress tensor), and surface orientation. Whether or not a surface slips depends on its cohesive strength, if any, and the coefficient of static friction, μ. The coefficient of static friction, μ, is the value of T_s that causes slip on a cohesionless surface and is often referred to as the fault strength in earthquake focal mechanism analysis (Harmsen, 1994). Under most crustal conditions, faults with $T_s = 0.6$ are ideally oriented for slip (Byerlee, 1978). Slip-tendency analysis provides a way to assess which faults are near the ideal orientation for slip and which are the most likely to be associated with zones of increased fracture density and enhanced fracture permeability.

Dilation of fractures is largely controlled by the resolved normal stress, which is a function of lithostatic and tectonic stresses and fluid pressure. The normal stress that a fracture feels depends on the magnitude and direction of the principal stresses relative to the fracture plane. The ability of a fracture to dilate and transmit fluid is directly related to its aperture, which in turn is a function of the effective normal stress acting upon it. The magnitude of the normal stress can be computed for surfaces of all orientations within a known or hypothesized stress field. This normal stress can be normalized by comparison with differential stress. The resulting dilation tendency (T_d) for a surface is then defined as

$$T_d = (\sigma_1 - \sigma_n) / (\sigma_1 - \sigma_3)$$

where σ_1 is the maximum principal compressive stress, and σ_3 is the minimum principal compressive stress.

Bulk Transmissivity Anisotropy

A population of steep, aligned, relatively permeable faults and fractures cutting a less permeable rock mass will tend to orient the maximum directional transmissivity parallel to the structural grain. In the case of unequal horizontal stresses acting on a population of steep faults and fractures, those with strikes *parallel* to the maximum horizontal compressive stress tend to open. Those with strikes *perpendicular* to the maximum horizontal stress tend to close. Similarly, some faults in an anisotropic stress field will be more ideally oriented for slip and others for locking. Thus, even if fault and fracture orientation distribution is isotropic, transmissivity in the maximum horizontal stress direction can be enhanced, producing transmissivity anisotropy.

Because fault and fracture populations commonly exhibit preferred orientations and *in situ* horizontal stresses are commonly unequal, both are likely to occur together in nature and lead to anisotropic transmissivity. For example, in cases where σ_3 is horizontal, vertical faults and fractures perpendicular to σ_3 have the highest dilation tendency and are likely to be more conductive than those in other orientations (figure 4-14a). Faults and shear fractures are sensitive to the σ_1 direction and commonly form two conjugate sets intersecting at an acute angle (~60°) centered on σ_1 (figures 4-14b and 4-14c). In normal fault regimes where σ_1 is vertical, two sets of opposite-dipping conjugate normal faults commonly develop (figure 4-14b). In strike-slip fault regimes where σ_1 is horizontal, two sets of vertical conjugate strike-slip faults commonly develop (figure 4-14c). In areas where σ_3 is horizontal, fault and fracture preferred orientations, and slip tendency and dilation tendency, all promote development of a net bulk transmissivity anisotropy with a maximum horizontal transmissivity perpendicular to σ_3 (figure 4-14d). The interaction of aquifer transmissivity with faults and fractures can be field tested by aquifer pumping tests. The results can be used to determine the full transmissivity tensor and to compare the orientation of the principal components of this tensor with the maximum and minimum *in situ* horizontal stress orientations and the distribution of faults and fractures.

Prediction of Anisotropic Transmissivity at Yucca Mountain

The pattern of faults and fractures in the YM region (figure 4-15) resulted from deformation in a regional stress field that evolved from east-west extension before 10 Ma to west-northwest to east-southeast extension after 10 Ma (Zoback, et al., 1981), and from thermoelastic contraction during cooling of the ash-flow tuffs (Sweetkind and Williams-Stroud, 1996). The result is a dominant population of north-south to northeast-southwest trending normal faults, a subordinate population of northwest-southeast trending strike-slip faults, and a group of minor connecting faults and curved fault tips (Day, et al., 1998; Ferrill, et al., 1999, in press). Fault growth by connection of overlapping fault segments produced irregular fault traces with cusps at fault intersections. Although faults at YM are related to several deformational episodes, some faults are unlikely to slip because of unfavorable orientations relative to the contemporary stress state.

YM lies within the western Basin and Range in a region characterized by both normal and strike-slip earthquakes. The regional occurrence of both normal and strike-slip earthquakes indicates that the maximum (σ_1) and intermediate (σ_2) principal compressive stresses have similar magnitudes (Zoback, 1992; Zoback, et al., 1992). The least principal compressive stress (σ_3) is approximately horizontal and trends west-northwest to east-southeast. Therefore, σ_3 is the odd axis of Krantz (1988) and has the most direct control on the pattern of fault-slip tendency. Stock, et al. (1985) estimate the following effective principal stresses (corrected for fluid pressure) at a depth of 1 km: σ_1 = vertical = 21 MPa, σ_2 = N25°–30°E = 17 MPa, and σ_3 = N60°–65°W = 11 MPa for the region.

Slip-Tendency Analysis of Yucca Mountain Faults

Slip-tendency analysis of YM faults was performed using the relative stress values of Stock, et al. (1985) given above, a 3D fault model for western YM and the faults mapped by Simonds, et al. (1995; figure 4-16a). Maximum slip tendencies are experienced by faults that strike parallel to the north-northeast-trending maximum horizontal stress (025°–030°; 028° in figure 4-16a) and dip 55°. Slip tendencies are also near maximum (>0.3) for moderately to steeply dipping (40–65°), north-south to northeast-southwest (000-055) striking faults. Faults at

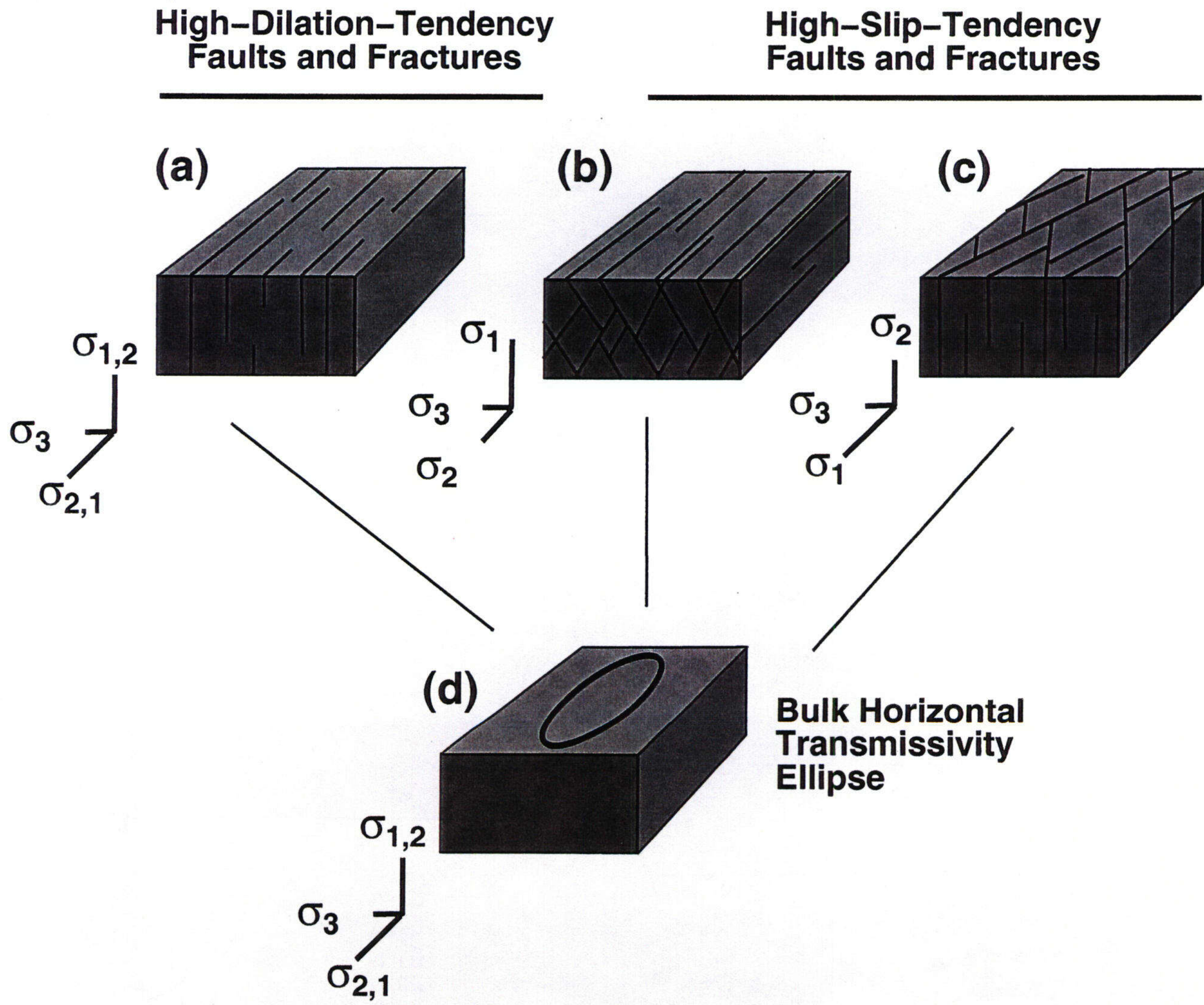

Figure 4-14. Conceptual illustration of effects of faults with high slip tendency or high dilation tendency on development of anisotropic permeability in areas, like the Yucca Mountain (Nevada) region, where the minimum principal compressive stress (σ_3) is horizontal

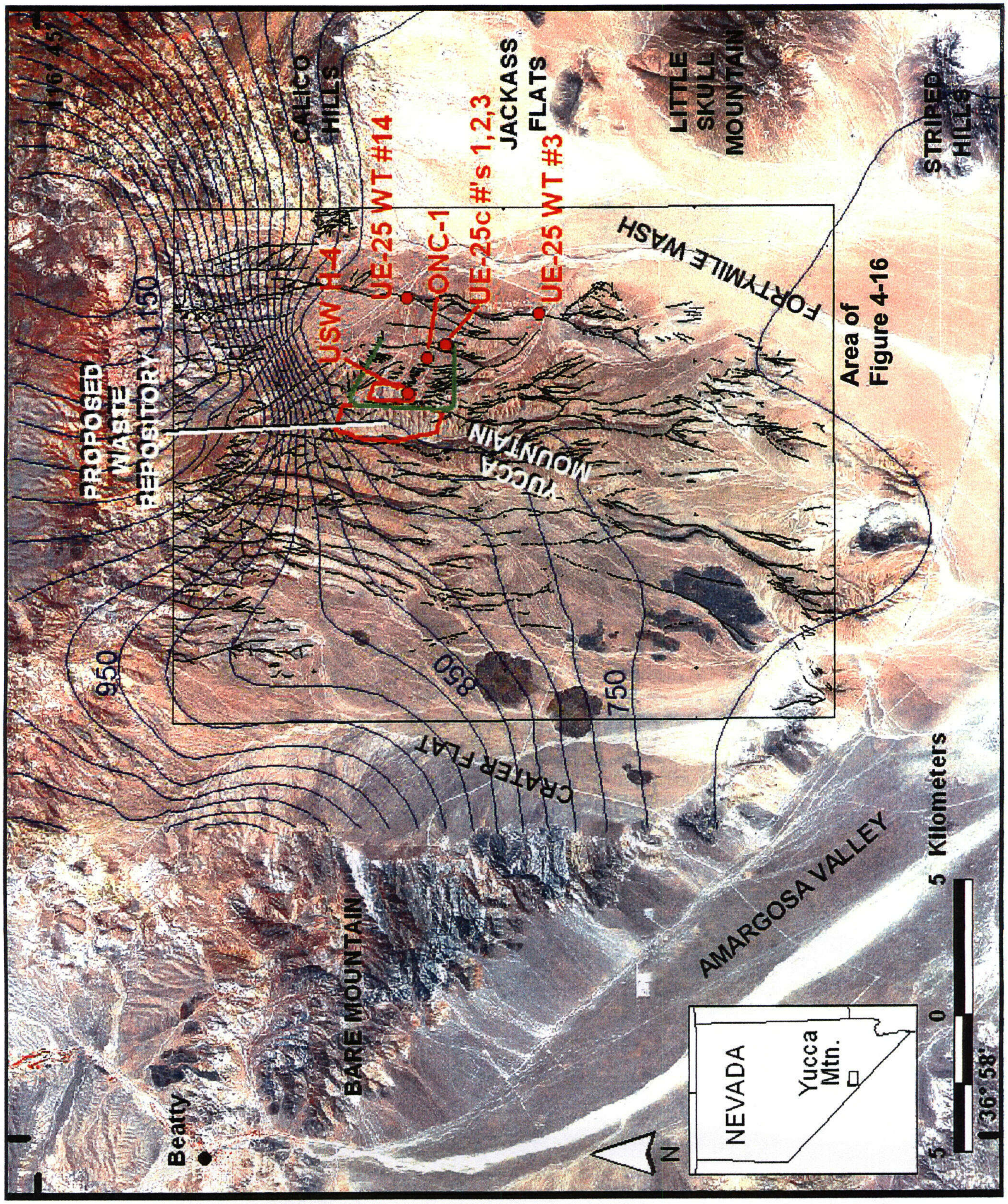

Figure 4-15. Thematic mapper scene with potential repository location, wells (red dots), faults (irregular black lines), and water table contours (blue lines). Water table contours are from Czarnecki, et al. (1997). Green lines show the path of the Exploratory Studies Facility.

1-km depth have moderate slip tendencies relative to typical failure conditions. In contrast, at depths of earthquake rupture initiation (e.g., 5–15 km), stresses resolved on similarly oriented faults produce near-failure slip tendencies (Morris, et al., 1996). As described by Harmsen (1994), the pattern of slipped faults in the Little Skull Mountain (figure 4-15) earthquake sequence is dominated by dipslip on southeast dipping normal faults and right-lateral strike-slip on vertical north-south trending faults. This is the pattern predicted by slip-tendency analysis of the YM stress field, and it supports simultaneous activity of strike-slip and normal faults in this area (Morris, et al., 1996).

Examination of Simonds, et al. (1995) reveals that nearly all faults with known or suspected late Quaternary displacement are in orientations of high-slip tendency (figure 4-16a). Some noteworthy examples are the Northern and Southern Windy Wash, Fatigue Wash, Solitario Canyon, Iron Ridge, and Stagecoach Road faults (figure 4-16a). In contrast, the northwest-southeast trending Pagany Wash, Sever Wash, and Yucca Wash faults are in low slip-tendency orientations (figure 4-16a) and lack evidence of late Quaternary slip (Simonds, et al., 1995).

Dilation-Tendency Analysis of Yucca Mountain Faults

Dilation-tendency analysis of faults and associated fractures at YM (e.g., figure 4-16b) was performed assuming the same relative stresses and mapped faults used for slip-tendency analysis. The results show that maximum dilation tendencies are experienced by vertical faults and fractures that strike parallel to the maximum horizontal stress (025°–030°; 028° in figure 4-16). Faults trending 028° ± 35° and dipping 65° to 90° have dilation tendencies of 0.8 or greater in the present stress field. Dilation-tendency analysis of faults at YM illustrates an abundance of steeply dipping north-northeast trending faults that have high-dilation tendency.

Summary

Faults with favorable orientations for slip or dilation present potential flow pathways for the SZ. Although only large map-scale faults were explicitly considered in the analysis described previously, the processes that alter permeability of large faults and fracture systems also apply to abundant smaller-scale fractures and faults like those seen in outcrops, boreholes, and the ESF (Sweetkind and Williams-Stroud, 1996), resulting in an effective hydraulic continuum at the site scale. The dominant trend of faults at YM is approximately north-south (005°; see rose diagrams in figure 4-16). The dominant fault population strike, maximum slip tendencies, and maximum dilation tendencies indicate the possibility of anisotropic transmissivity, with the direction of maximum transmissivity in the azimuth range between 005 (based on dominant fault trend) and 030 (based on slip- and dilation-tendency constraints). The presence of anisotropic transmissivity is supported by long-term pumping test data from the C-wells. The anisotropic transmissivity estimated at YM has a maximum principal direction of approximately 030, consistent with the hypothesis that anisotropy is controlled by faults and fractures in the present-day *in situ* stress field. Such aquifer anisotropy has the potential to alter groundwater flow paths to more southward directions. Modeled flow directions are sensitive to the degree of anisotropy, and the direction of maximum principal transmissivity.

Evaluation of Viable Fracture Models

TBD in 1999–2000.

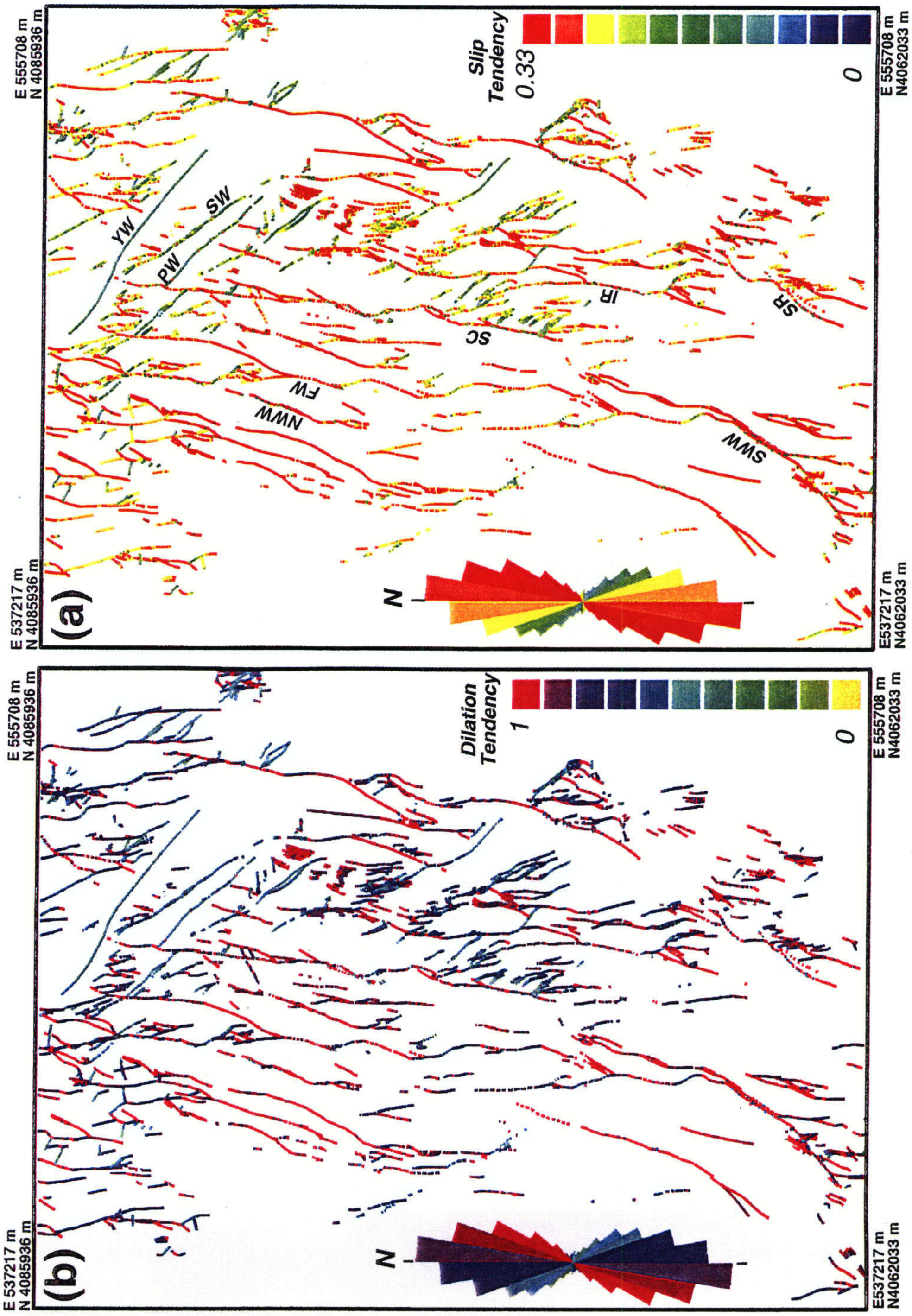

Figure 4-16. (a) Slip tendency map of Yucca Mountain faults by Simonds, et al. (1995). Inset rose diagram shows cumulative fault length in 10-degree strike azimuth bins. Map and rose diagram are colored according to slip tendency as shown by color bar. Area as shown in figure 4-9. Named faults discussed in text are labeled on map according to the following abbreviations: NWW = Northern Windy Wash, SWW = Southern Windy Wash, FW = Fatigue Wash, SC = Solitario Canyon, IR = Iron Ridge, SR = Stagecoach Road, PW = Pagany Wash, SW = Sever Wash, and YW = Yucca Wash. (b) Dilation tendency map of Yucca Mountain faults. Map and rose diagram are colored according to dilation tendency as shown by color bar.

4.4 TECTONIC FRAMEWORK OF THE GEOLOGIC SETTING

4.4.1 Viable Tectonic Models and Crustal Conditions

The RM used to evaluate the preliminary Uniform AC (section 4.1) for the Tectonic Framework subissue is focused to provide the reviewer with guidance on evaluation of DOE tectonics. It also serves to highlight a path to resolution for other subissues and ISIs. The RM addresses technical bases for adequate and conservative bounding analyses, and for the approximation of adequate and conservative parameter distributions in SDS and related KTI's (c.f. U.S. Nuclear Regulatory Commission, 1998a, 1998b, 1999a, 1999b, 1999c, 1999d, 1999e, 1999f, 1999g). Performance related issues may use the tectonic framework technical bases either implicitly or explicitly. The tectonic framework subissue provides viable tectonic models for the geologic setting, technical bases for bounding analyses and parameter distributions for SDS subissues, and related KTIs including but not limited to:

Repository Design and Thermal-Mechanical Effects: tectonically induced spatial and temporal changes in the frequency, recurrence interval, zone width, orientation, damage zone characteristics, and continuity of faults, and; tectonically induced increased and progressive fracturing (U.S. Nuclear Regulatory Commission, 1999c);

Saturated and Unsaturated Flow Under Isothermal Conditions: fault spatial distributions, fault geometries, fault connectivity, fault orientation, fault zone physical properties (including width, associated fracture zones, fault rock and fault rock alteration); potential for tectonically induced alteration of fractures and fault zones; spatial variations in fracture and fault properties related to structural context; stratal variation in fault zone properties; structural control of rock layer orientation and continuity, and; in heterogeneities related to faulting (U.S. Nuclear Regulatory Commission, 1999b);

Evolution of the Near-Field Environment: tectonically induced spatial and temporal variations in fault and fracture connectivity, fracture aperture, fracture density, fracture surface characteristics and fracture size distribution (U.S. Nuclear Regulatory Commission, 1999e);

Thermal Effects on Flow: tectonically induced spatial and temporal variations in heat flow related and in seepage and flow related fracture and fault characteristics, including connectivity, density, and fracture aperture and size (U.S. Nuclear Regulatory Commission, 1999g);

Radionuclide Transport: spatial and temporal variations in radionuclide movement related fracture and fault characteristics, including geometry, connectivity, density, aperture, and size distribution (U.S. Nuclear Regulatory Commission, 1999f);

Igneous Activity: Probability related tectonic framework characteristics - including consistency with viable tectonic models, structural control of magma ascent, crustal conditions controlling magma generation, and; consequences related to tectonic framework characteristics, including associated seismicity (U.S. Nuclear Regulatory Commission, 1999a).

In addition to the above KTIs, the SDS Tectonic Framework subissue provides technical bases for bounding analyses and parameter distributions for Integrated Subissues (figure 3-2). NRC staff reviewed DOE's analyses of tectonics to determine the conservatism of DOE's conclusions. In doing so Staff applied the following review method, with four steps, to determine whether the preliminary Uniform AC (section 4.1) were met for the Tectonic Framework:

Step 1—Viable Tectonic Models

Staff will ascertain that the DOE has adequately evaluated all viable tectonic models proposed for the YMR. For example, the DOE should have examined a comprehensive range of models. The development of these models should include (1) a reasonable explanation of the technical bases for selection of viable tectonic models, (2) purposes of each model, and (3) demonstrations that each model is internally consistent with the appropriate structural style and deformation mode and compatible with the tectonic framework of the southern Cordillera and Basin and Range province.

Step 2—Geological and Geophysical Data

Staff will ascertain that DOE has considered existing geological, geophysical, seismological and geodetic data for the YMR. For example, the DOE should establish appropriate data, [including but not restricted to: (1) geological—structural, geothermal, geochronological; (2) geophysical—gravity, magnetics, paleomagnetics, seismic refraction/reflection, teleseismic; (3) seismological—historical seismicity, crustal condition, paleoseismicity; and (4) geodetic—GPS, trilateration survey, level line survey] and describe in detail sufficient data inconsistencies.

Step 3—Characterization of Tectonic Models

Staff will ascertain that the DOE has characterized, both qualitatively and where possible quantitatively, the viable tectonic models and related crustal conditions that are used as bases for other process models and abstractions. For example, the data and interpretations, including (but not restricted to) geologic maps, block diagrams, and restorable cross sections should be used appropriately in abstractions. Reasonable interpretations of geologic, geophysic, geometric, kinematic, and mechanical relationships should be adequately applied to constrain and evaluate key uncertainties.

Step 4—Abstraction of Tectonic Models

Staff will ascertain that the DOE has applied the abstraction of viable tectonic models across all affected subissues in a reasonable and consistent manner. For example, staff should ascertain that abstractions and implementations of viable tectonic models and related crustal conditions depict all critical model elements, and whether the depictions and incorporations (1) are consistent with intended use; (2) are consistent across issues, including probability estimations and consequence analyses; (3) are clearly presented. This includes application of site specific data to development of site scale models such as the DOE GFM models.

4.4.1.2 Technical Bases for Review Method

Geological and geophysical investigations to characterize the YM site have been ongoing for two decades. In addition, the region has been the subject of detailed geological and geophysical investigations related to: (1) weapons testing activities at the NTS; (2) academic research in the Basin and Range; and (3) mineral and petroleum exploration. All of these efforts have provided the DOE (and subcontractors) and the NRC (and subcontractors) with a plethora of geological and geophysical data and interpretations.

The list following highlights those data and interpretations considered by staff as most pertinent to the development and evaluation of viable tectonic models.

Regional and Local Stratigraphic Elements

Regional and local stratigraphic elements to consider in tectonic models are

- Archean and Proterozoic rocks (table E-1) that make up the basement in the YM region (Bowring and Karlstrom, 1990).
- Neoproterozoic, Paleozoic, and Mesozoic rocks (table E-1) that constitute the bulk of the seismogenic crust in the YM region (Cornwall and Kleinhample, 1961, 1964; Stewart, 1970; Cornwall, 1972; Monsen, 1983; Poole, et al., 1992, and references therein; Stevens, et al., 1991; Trexler, et al., 1996).
- Cenozoic sedimentary and igneous rocks that underlie most of the Quaternary basins (table E-1) and make up YM itself (Ransome, et al., 1910; Byers, et al., 1976; Christiansen, et al., 1977; Vaniman and Crowe, 1981; Swadely, et al., 1984; Carr, et al., 1986a; Bradshaw and Smith, 1994; Sawyer, et al., 1994; Connor and Hill, 1995; Crowe, et al., 1995; Buesch, et al., 1996; Fleck, et al., 1996; Hill and Connor, 1996; U.S. Nuclear Regulatory Commission, 1999a).

Regional and Local Tectonic Elements

Regional and local tectonic elements to consider in tectonic models are

- Paleozoic and Mesozoic tectonic features including the Mississippian Antler (Nilsen and Stewart, 1980; Burchfiel and Davis, 1972; Oldow, 1984), Permian Last Chance (Snow, 1992a), Permian Sonoma (Gabrielse, et al., 1983), and Mesozoic Sevier (Armstrong, 1968; Camilleri and Chamberlain, 1997) orogenies.
- Oligocene and older (table E-2) extensional features (Wernicke, et al., 1987; Hodges and Walker, 1992; Axen, et al., 1993) including those presently exposed along the southwestern flank of BM (Ferrill, et al., in review, 1998a; Stamatakos and Ferrill, 1996a).
- Neogene (table E-2) tectonic features including: (1) plate motions (Atwater, 1970; Dokka and Travis, 1990; Bohannon and Parsons, 1995; Dickenson, 1996); (2) Walker Lane seismotectonics (Stewart, 1988; Hardyman and Oldow, 1991; Oldow, et al., 1994);

(3) Basin and Range detachment faulting (Anderson, 1971; Wright and Troxel, 1973; Stewart, 1978; Wernicke, 1981; Burchfiel, et al., 1982, 1987; Hamilton, 1987; Wernicke, et al., 1988; Maldonado, 1990); and (4) Basin and Range core complexes (Davis and Coney, 1979).

Geometric Elements

Geometric elements to consider in tectonic models are

- Seismic reflection data (Majer, et al., 1997; Brocher, et al., 1993, 1996, 1998; Young, et al., 1992a)
- Gravity and aeromagnetic data (Snyder and Carr, 1982; Kane and Bracken, 1983; Langenheim, et al., 1991, 1993; Ponce, et al., 1992; Oliver and Fox, 1993; Langenheim and Ponce, 1995; Ponce and Oliver, 1995; Brocher, et al., 1996,1998)
- Ground magnetic data (Brocher, et al., 1996; Connor, et al., 1997; Stamatakos, et al., 1997a)
- Geologic maps (Cornwall and Kleinhample, 1961; Nakata, et al., 1982; Scott and Bonk, 1984; Swadely and Parrish, 1988; Frizzel and Shulters, 1990; Maldonado, 1990; Monsen, et al., 1992; Faulds, et al., 1994; Simonds, et al., 1995; Day, et al., 1998)
- Borehole data (Carr and Parrish, 1985; Carr, et al., 1986b, 1995)
- Structural cross sections (Scott and Bonk, 1984; Scott, 1990; Young, et al., 1992b; Ferrill, et al., 1996b; Fridrich, in press)

Kinematic Elements

Kinematic elements to consider in tectonic models are

- Vertical-axis rotation markers from paleomagnetism (Gillett and Van Alstine, 1982; Nelson and Jones, 1987; Rosenbaum, et al., 1991; Hudson, 1992; Gillett and Geissman 1993; Holm, et al., 1993; Snow, et al., 1993; Zhang, et al., 1993; Hudson, et al., 1994, 1996; Sonder, et al., 1994; Ferrill, et al., 1995; Stamatakos and Ferrill, 1996, 1998; Fridrich, et al., in press; Stamatakos, et al., 1998) and sedimentological markers (Snow and Prave, 1994)
- Exhumation and horizontal-axis tilting from radiogenic thermochronology studies (Noble, et al., 1989,1991; Maldonado, 1990; Monsen, et al., 1992; Hoisch and Simpson, 1993; Sawyer, et al., 1994; Ferrill, et al., 1996b; Weiss, 1996; Hoisch, et al., 1997, Ferrill, et al., in review), calcite-twin deformation studies (Ferrill, et al., in review; Stamatakos and Ferrill, 1996), conodont color alteration indices (Grow, et al., 1994), and paleomagnetic data (Stamatakos and Ferrill, 1996, 1998; Stamatakos, et al., 1998)
- 3D motions from regional reconstructions based on palinspastic markers (Prave and Wright, 1986; Snow and Wernicke, 1989; Carr, 1990; Stevens, et al., 1991; Caskey and

Schweickert, 1992; Snow 1992a,b; Axen, et al., 1993; Snow, 1994; Serpa and Pavlis, 1996; Schweickert and Lahren, 1997).

- Fault displacement analyses (Wesnousky and Jones, 1994; Minor, 1995; Ofoegbu and Ferrill, 1995, 1998; Bruhn and Schultz, 1996; Ferrill, et al., 1996a, 1997b, 1999a; Piety, 1996; Stamatakos, et al., 1997b; Marrett, et al., 1998).

- Remote sensing, geodetic, and GPS results (Gilmore, 1992; Savage, et al. 1994,1998; Ferrill, et al., 1996b; Bennett, et al., 1997 ; Savage, 1998; Savage, et al., 1998; Wernicke, et al., 1998; Pezzopane, 1999).

- Stress analyses (Stock, et al., 1985, 1986; Stock and Healy, 1988; Zoback, 1992; Zoback, et al., 1992; Barton, et al., 1995; Bellier and Zoback, 1995; Morris, et al., 1996; Ferrill, et al., 1999b) or seismic moment analysis (Smith, et al., 1989; King, et al., 1994).

- Partitioning of strain (Lienkaemper, et al., 1987; Ferrill and Dunne, 1989; Dunne and Ferrill, 1995; Pezzopane, 1995; Ferrill, et al., 1996c, 1998; Morris, et al., 1996; Ferrill and Morris, 1997; Stamatakos, et al., 1997a; Ofoegbu and Ferrill, 1998; Marrett, et al., 1998; Wernicke, et al., 1998; Pezzopane, 1999a, b; Savage, et al., 1998)

Paleoseismic and Historical Seismic Elements

Paleoseismic and historical seismic elements to consider in tectonic models are

- Historic seismicity in the YM region, including the Little Skull Mountain earthquake (Arabasz and Julander, 1986; Harmsen, 1991; Rogers, et al., 1991; Smith and Arabasz, 1991; Harmsen and Bufe, 1992; Harmsen, 1993, 1994; Stover and Coffman, 1993; Meremonte, et al., 1995).

- Paleoseismic data from trenching studies along fault scarps and aerial photography analyses of surface deformation studies (Reheis, 1988, 1994; Anderson and Klinger, 1994; Menges, et al., 1995; Pezzopane, 1995; U.S. Geological Survey, 1996), including triggered and clustered seismicity (Anderson, et al., 1994; Bodin and Gomberg, 1994).

Viable Tectonic Models

Review of the geologic literature by staff suggests that tectonic interpretations of the Y M region can be organized into 11 tectonic models. Staff from the NRC, the CNWRA, the DOE, the USGS, and the State of Nevada met in San Antonio on May 7–8, 1996, for an Appendix Seven meeting to discuss conceptual tectonic models. In this meeting, the 11 tectonic models proposed for the YM region were reviewed in the context of the most recent geological and geophysical data.

From discussions in the meetings, it was clear that 5 out of the 11 tectonic models were presently supported by the existing data (appendix C-1). Although new data may promote one of the other six models currently considered not viable (appendix C-2), the five models listed in appendix C-1 form the bases for issue resolution at this time. In addition, there was no general consensus on which models are truly independent and which models may function as subsets of others. In a broader sense, these five models can be considered in two general categories of deformation. The first three are dominantly related to extensional deformation, and the latter five are dominantly related to strike-slip deformation. Moreover, the five models are not mutually exclusive. Locally, extensional-dominated deformation (within Crater Flat, for example) can exist within a larger region of trans-tensional deformation related to a pull-apart basin. The implications of the five viable models to repository performance subissues are summarized in appendix C-3.

All five viable tectonic models should be used to bound the impact of faulting, fracturing, and seismicity on repository performance. Staff considers the treatment and inclusion of viable tectonic models in DOE's PSHA expert elicitation process to be adequate. SDS-related issues should consider at least the full suite of viable tectonic models as supported by existing data, as are incorporated in DOE's PSHA expert elicitation. Staff do not consider the treatment of regional tectonic models in DOE's YM Site Description (U.S. Geological Survey, 1998) to be complete or adequate.

U.S. Geological Survey (1998) and O'Leary (U.S. Geological Survey, 1996) proposed a reclassification of the 11 tectonic models and suggested that the elastic-viscous model was the preferred or favored model. U.S. Geological Survey (1998) and O'Leary (U.S. Geological Survey, 1996) organized tectonic models into three generic classes, based on what O'Leary termed bulk mechanical behavior (U.S. Geological Survey, 1996, p. 8–51). These classes were simple, pure, and lateral shear. By simple shear, U.S. Geological Survey (1998) and O'Leary (U.S. Geological Survey, 1996) actually refer to models that evoke some form of detachment faulting, that is the deep, intermediate, and shallow detachment models described in Appendices C-1 and C-2. By pure shear, U.S. Geological Survey (1998) and O'Leary (U.S. Geological Survey, 1996) refer to models that evoke horsts and graben fault block models like the planar fault block and domino fault block models (Stewart, 1978; Fridrich, in press). By lateral shear, U.S. Geological Survey (1998) and O'Leary (U.S. Geological Survey, 1996) refer to strike-slip-dominated models like the Amargosa shear model of Schweickert and Lahren (1997). The caldera model of Carr (1982, 1984, 1988, 1990), and Carr, et al. (1986a) was considered as a fourth unique model. The synclinorium model of Robinson (1985) was not discussed in U.S. Geological Survey (1996).

In summary, U.S. Geological Survey (1998) presents a favored model of planar, steeply-dipping faults. Fault blocks are considered to deform internally, and voids between fault blocks are allowed to be filled by a ductile (fluid) middle crust. The model is based on the boundary element modeling of Janssen (1995). In the model, the seismogenic crust is treated as a quasi-elastic layer resting on a viscous middle and lower crust. According to U.S. Geological Survey (1998), the model addresses the following important geological and geophysical considerations:

- Faulting and basaltic volcanism are episodic and coupled.
- The Crater Flat domain is essentially a half-graben with YM faults antithetic to the master BM fault.
- The vertical-axis rotations from strike-slip faulting are a secondary phenomena, related to a discrete period of oroclinal bending.

- Faults are planar to the base of the seismogenic crust and dip between 30° and 60°. They are essentially linear cracks in which displacements are treated as stress perturbations.

- Stress conditions at the base of the crust control distribution of basaltic volcanism.

- Faulted blocks are in isostatic equilibrium.

- Elastic behavior of the crust (brittle and ductile) during an earthquake with relaxation creep in lower crust between earthquakes.

- Rollover into faults in Crater Flat, especially the B M fault, is not a result of fault geometry but of elastic flexure of the hangingwall.

Role of Tectonic Models in Assessment of Data

Interpretations from the suite of viable tectonic models form the basis for investigators to assess the significant data, such as trenching results in the large context of the site's faulting and seismic hazards. For example, trenching data alone provides useful information on age and amount of net separation of once contiguous horizons or other markers across a fault zone, but rarely provides enough information on actual fault displacement or fault zone kinematics. Additional information, including constraints from viable tectonic models, is needed to obtain a full picture of faulting and seismicity history. Constraints drawn from viable tectonic models help researchers assess other important considerations, including completeness and relative importance of the data to other measures of faulting and seismicity such as GPS strain rate measurements or the historic seismic record, development and importance of fractures, and development of site models such as the GFM models.

To highlight these points consider the following two examples:

- One of the five viable tectonic models proposed for the region is the Amargosa Desert fault of Schweickert and Lahren (1998). This model predicts cryptic strike-slip faulting under the proposed repository. This component of faulting, if it exists, would be poorly represented or completely overlooked by the trenching data results. Trenching techniques are, by themselves, limited to quantifying conspicuous expressions of mainly vertical fault displacement at the surface. Strike-slip faulting is difficult to quantify by trenching, especially if it is distributed, because the motion is horizontal and often results in subtle surface deformation. Even in cases where strike slip faults are located and trenched, palinspastic markers are not available in the trench walls to allow investigators to gauge actual fault displacement. Other features, including offset stream channels, fold axes, or stratigraphic pinch-outs are necessary to fully describe such fault motion. Naturally, trenching techniques would be of no use in quantifying fault slip on a buried or cryptic strike-slip fault of the type proposed by Schweickert and Lahren (1998). The experts on the DOE PSHA (U.S. Geological Survey, 1998) included possible seismic sources based on the viable tectonics models, in addition to those quantified by the trenching data. The resulting seismic hazard curve for YM forecasts a greater seismic hazard than one would predict if it the trenching data were used in isolation from all other geologic observations.

- Recent controversy regarding GPS strain-rate measurements (c.f., Wernicke, et al., 1998; Savage, et al., 1998) also raised concerns regarding the applicability of the paleoseismic data to the generation of a reliable seismic hazard assessment. As discussed in this section of this report, recent confirmatory analyses by the CNWRA and the USGS specifically designed to test the Wernicke, et al. (1998) results shows that the GPS readings are anomalous and not representative of actual crustal strain conditions that would lead to enhanced seismic activity at YM (e.g., Marrett, et al., 1998; Pezzopane[5]. A critical part of those confirmatory analyses was the application of a tectonic models to test the GPS strain rate results.

Evaluation of Viable Tectonic Models

The following addresses the U.S. Geological Survey's (1998) favored model.

U.S. Geological Survey (1998), following U.S. Geological Survey (1996) and Fridrich, et al. (1999), further subdivides the Crater Flat domain by a subdomain boundary simply referred to as the hinge line (see figure 8.6 in U.S. Geological Survey, 1996 and figure 3.3-1 in U.S. Geological Survey, 1998). The hinge line is defined as both a conceptual and physical feature. It apparently follows a subtle, but sudden, decline in average elevation of YM blocks—lower to the southeast (Fridrich, et al., in press)—along a series of ridge terminations, aligned fault splays, Z-shaped bends in the ridge crests, and several small-magnitude aeromagnetic anomalies (U.S. Geological Survey, 1996). Northeast of the line, fault blocks with relatively high relief are juxtaposed across steeply dipping faults with relatively small displacements. Southwest of the hinge line, fault blocks are more strongly tilted and juxtaposed across faults with shallower dips and greater displacement (Scott and Bonk, 1984; Scott, 1990; Day, et al., 1997).

U.S. Geological Survey (1998), Fridrich, et al. (1999), and U.S. Geological Survey (1996) consider the amount of clockwise vertical-axis rotations indicated by anomalous paleomagnetic declinations in the tuffs (Rosenbaum, et al., 1991; Hudson, et al., 1994) to be the most important indicator of the hinge line. Northeast of the line, clockwise vertical-axis rotations are limited to 20° or less. Southwest of the hinge line, vertical-axis rotations range between 20° and 45°. The vertical axis rotations are interpreted in terms of a discrete period of dextral, strike-slip strain following within about 1 my of the major pulse of Crater Flat extension (Hudson, et al., 1996) or the result of concentrated strain along bending beams due to differential extension of southern YM (U.S. Geological Survey, 1996). Along with spatial and temporal variations in the amount of extension on faults, the significance of the paleomagnetic data is that the main locus of deformation in the Crater Flat domain has migrated to the southwest with time. The implication is that the hinge line effectively isolates YM in the northeast subdomain from active deformation in the southwest subdomain, thereby reducing the risk of future seismicity and volcanism at YM.

Several aspects of the hinge-line argument are inconsistent with the available geological and geophysical data. First, structural and gravity data define a diffuse eastern margin of the Crater Flat half graben well east of the ridges that comprise YM proper (Ferrill, et al., 1996b; Connor, et al., 1996). Within this half-graben, YM appears, in plan view, as bow-shaped, convex toward

[5]Private communication, Appendix Seven Meeting March 2–3, 1999.

the east. Similar to many curvilinear structural features worldwide, curvature alone is not indicative of horizontal bending of a previously more linear feature (e.g., Stamatakos and Hirt, 1994), as supposed by the U.S. Geological Survey (1996) explanation. Numerous curved structural features are primary and simply reflect the interplay between local variations of the imposed deformation and lateral variations in crustal anisotropy (e.g., Marshak, 1988; Ferrill and Groshong, 1993).

Second, the interpretation that all faults change strike northwest and southwest of the hinge line is misleading. In northern Crater Flat, the northeast trending faults are an extension of the radial pattern of faulting in the region immediately surrounding the Miocene Timber Mountain caldera. In southern YM, there are some northeast trending faults, but many faults also have north-south strikes, contrary to the USGS interpreted fault map (compare figure 3 and figure 9; Fridrich, et al., in press).

Third, the interpretation that anomalous paleomagnetic declinations necessarily signify vertical axis rotations related to oroclinal bending is overly simplistic (e.g., Gray and Stamatakos, 1998). The rigorous test of vertical-axis rotations resulting from oroclinal bending was defined in Schwartz and Van der Voo (1984). The test plots paleomagnetic declinations as a function of the orientation of structural trends. The assumption in an oroclinal bending model is that both prebending structures (in this case, normal faults) and corresponding paleomagnetic vectors will correlate if both were passively reoriented by vertical-axis rotations. A significant correlation between declination and strike with a slope of one implies bending of an originally linear feature (e.g., Van der Voo, et al., 1997). Significant correlations between declination and strike with a slope of less than one implies bending of an originally curved feature (e.g., Eldredge, et al., 1985).

Plots of the paleomagnetic declination versus strike of structural trends in Crater Flat and at YM based on available data do not support a simple orocline (vertical-axis rotation) model (figure 2b, Stamatakos and Ferrill, 1998), especially when compared to regions in which oroclinal bending is well established (cf. figure 8 in Van der Voo, et al., 1997). The analysis of Stamatakos and Ferrill (1998) shows that the distribution of magnetic declinations recorded in the Tiva Canyon Tuff (Rosenbaum, et al., 1991) at Crater Flat and YM is independent of structural trend.

An alternative explanation of the rotated paleomagnetic directions is that they resulted from differential displacement on listric normal faults (figure 3a, Stamatakos and Ferrill, 1998). In this geometry, hangingwalls rotate about a steeply inclined axis as displacement proceeds (figure 3b, Stamatakos and Ferrill, 1998). Faults that are incorporated into the hangingwalls of other faults may also rotate. Faults that form the ultimate footwall (not incorporated into a hangingwall of another fault) or faults that form after an initial period of extension may not necessarily be rotated (figure 4c, Stamatakos and Ferrill, 1998). This situation appears to mimic that at southern YM [compare Stamatakos and Ferrill (1998), figure 4c with figures 1 and 2]. In this interpretation, the increase in the amount of clockwise rotations indicated by the paleomagnetic declinations in southwestern Crater Flat result from lateral southward increases in displacement on Crater Flat faults, like the Solitario Canyon Fault (e.g., Scott, 1990). Moreover, this interpretation is entirely consistent with the observation that the greatest amount of extension is in the southern part of Crater Flat (e.g., Scott, 1990; Ferrill, et al., 1996a; Stamatakos, et al., 1997b; Fridrich, 1998).

Planar versus Listric Fault Geometries

The first-order structure of the Crater Flat-B M region is the pronounced rollover of the Miocene tuffs into the BM fault (Young, et al., 1992b; Ferrill, et al., 1996b). This rollover defines the shape of the Crater Flat half-graben, in which the deepest portion of the Crater Flat basin is adjacent to the BM fault (e.g., Snyder and Carr, 1982; Ferrill, et al., 1996b). Rollover has long been recognized as the result of hangingwall deformation above a curved or listric fault (Groshong, 1990). The exact geometry of rollover and fault shape depends on the nature of deformation in the hangingwall (Dula, 1990), on the assumption that faulting is restorable because hangingwall volume is preserved during deformation.

The alternative proposed by O'Leary (U.S. Geological Survey, 1996) supposes that elastic flexure of the hangingwall causes the rollover geometry. The model does not consider surface geometry as a constraint to deformation kinematics. The ductile middle crust is allowed to fill voids in the subsurface where gaps open between fault blocks. Fault blocks can deform internally if space problems at the surface exist where fault blocks of different dip overlap. The potential mechanisms for internal block deformation, including increased fracturing, are not discussed. According to O'Leary (in U.S. Geological Survey, 1996) and U.S. Geological Survey (1998), the model accounts for the observation that few, if any, historic earthquakes ruptured shallow-angle (detachment) normal faults, including the 1992 Little Skull Mountain earthquake, which appeared to have ruptured a steeply dipping fault near the base of the seismogenic crust.

The Role of Faults in the Distribution of Dikes and Volcanoes

Normal faults exert two primary controls on basaltic magmatism in the Basin and Range province. First, they provide the mechanism for crustal extension, producing isothermal decompression-induced partial melting in the mantle. Second, they provide pathways for magma ascent to the surface. The structural pathways for ascent of basaltic magma are of two types (i) new dike fractures that propagate upwards uninfluenced by pre-existing structure, and (ii) dikes that are partially controlled by pre-existing fractures or faults that behave as barriers or pathways for magma ascent. Low recurrence rate basaltic volcanic activity in the Basin and Range Province occurs where magmas are generated by decompression of fertile [(i.e., lithophile enriched) lithospheric] mantle during crustal extension (e.g., McKenzie and Bickle, 1988; Rogers, et al., 1995). Ascent of this magma through the crust is enhanced by crustal structures produced by extension. This correlation between basaltic volcanism and structure occurs across a range of scales, from the superposition of individual faults and vents to the occurrence of entire volcanic fields at the margins of extensional basins (Parsons and Thompson, 1991; Conway, et al., 1997). Capture of ascending basaltic dikes by faults is important for volcanic risk assessments because of the potential for lateral diversion of basalt, thereby producing intrusion or volcanic eruptions laterally offset from the location of magma generation (Connor, et al., 1996). Conceivably, this lateral diversion could have beneficial or adverse consequences for a specific site by diverting magma away from or toward the site.

There are several possible modes of interaction between a vertically propagating dike (figure 4-17a) and a pre-existing planar weakness such as a fault or fracture zone (Ferrill, et al., 1997a). The dike may (i) propagate vertically across the fault plane (figure 4-17b); (ii) intrude the fault plane and use it as a conduit (figure 4-17c); (iii) use the fault as a pathway for some distance then break out up-dip, to propagate vertically toward the surface (figure 4-17d);

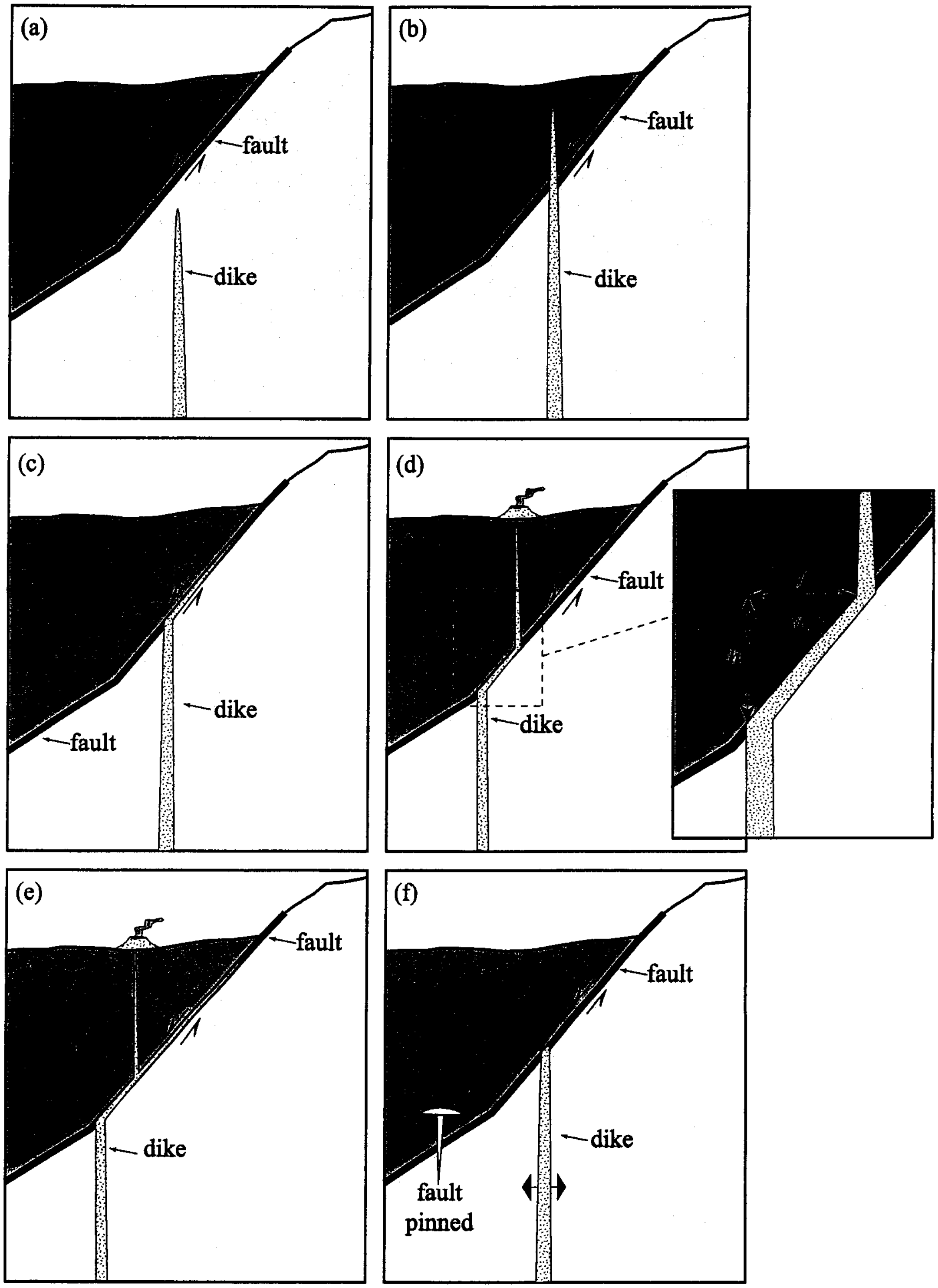

Figure 4-17. Schematic models of fault-dike interaction in profile. Ascending magma is represented by gray pattern and faults are illustrated by thick black lines. Lateral diversion distance (*d*) is defined as a function of the vertical distance of dike capture by a fault (*h*), and the dip of the fault (*α*).

(iv) intersect a fault with the fault capturing part of the dike while a portion of the dike material breaks out vertically toward the surface (figure 4-17e); or (v) terminate beneath the fault, accommodating horizontal extension by dike widening beneath the fault and fault slip above the top of the dike (figure 4-17f).

The potential for lateral diversion of magma is particularly important to the performance of the proposed high-level radioactive waste repository at YM, Nevada, which lies within or along the edge of the active Crater Flat volcanic field, a low-volume basaltic volcanic field (e.g., Connor and Hill, 1995). The proposed repository site is 10–15 km northeast of the center of recurrence for volcanism in the Crater Flat volcanic field. The proposed repository site, however, is within a system of west-dipping normal faults, which might be capable of channeling magma laterally away from the area of highest recurrence rates in Crater Flat volcanic field, including towards the repository site.

<u>Theoretical analysis</u>. The lateral distance of magma diversion (d) once capture has occurred is a function of the dip (α) of the fault and the vertical distance of magma channeling along the fault (h) (see figure 4-17d) is

$$d = h \,/\, (\tan \alpha) \qquad \textbf{(1-1)}$$

For a dike captured by a fault, lateral diversion increases with decreasing fault dip and increasing vertical distance of magma channeling. However, the likelihood of magma channeling along a fault decreases with decreasing fault dip.

Although gently dipping faults are not as capable of capturing dikes as steeply dipping faults, analytical models indicate that at shallow depths (e.g., <0.1 to 1 km), moderate to low angle faults may be able to capture dikes. The depth of crossover between vertical dike propagation and dike capture depends on the strength of the host rock, with increasing rock tensile strength favoring dike capture by faults versus vertical dike propagation (McDuffie, et al., 1994; Connor, et al., 1993, 1994; Ferrill, et al., 1997a). Numerical modeling generally supports results of analytical modeling, however, intermediate cases were produced numerically in which the dike both intruded the 50–70° fault, and continued to propagate vertically.

Total lateral diversion of a dike captured initially by a high-angle fault and then recaptured by a low-angle fault should be no more than 3–5 km. Lateral diversion by a 60–65°-dipping fault (e.g., Solitario Canyon fault) through 12 km of brittle crust would not exceed 6–7 km.

Fractures within the earth's crust react to the *in situ* stress state. For example, fractures that are subparallel to the plane that contains the maximum (s_1) and intermediate (s_2) principal compressive stresses and sub-perpendicular to the minimum principal compressive stress (s_3) experience less normal stress than fractures with other orientations, and are therefore more easily opened or dilated by fluid (water, hydrocarbon, or magma) pressure. Dilation tendency analysis is a technique for evaluating the potential for dilation of any mapped fracture or fault within a 3D space. YM region faults that experience high dilation tendency in the current stress field include the Solitario Canyon, the Ghost Dance, and the Bow Ridge faults (Ferrill, et al., 1999b). Faults that experience high dilation tendency should be considered as more likely to act as magma conduits than faults with other orientations.

Geological Observations in the Yucca Mountain Region. Observations in the YM region indicate there is a strong correlation at the local scale between geologic structures and basaltic volcanism. These observations include the development of volcanic vent alignments (Smith, et al., 1990; Connor, et al., 1997) and occurrence of cinder cones along faults (Connor, et al., 1997). Faults and related structures likely influence magma ascent, at least on local scales, in the YM region, and this influence should be considered in volcanic hazard analyses of the proposed repository.

The strongest evidence supporting fault-channeling of dikes is the occurrence of basaltic dikes in fault zones within Miocene tuffs at YM and in the nearby Bullfrog Hills. An approximately 11 Ma basalt dike in the Solitario Canyon fault (Crowe, et al., 1983; Smith, et al., 1997) extends along a ~1-km segment of the fault near the northwestern edge of the proposed repository block. The fault at the surface trends north 10 east and dips 60–65° west along this part of the fault (Simonds, et al., 1995). The stress field at the time of intrusion was likely dominated by the least principal compressive stress (σ_3) oriented approximately east-west (Zoback, et al., 1981). The strike trend of the fault is nearly optimal for intrusion during east-west extension. At the time of dike intrusion, however, the fault may have been steeper than its present dip. Layering in the tuffs presently dips 10–12° east (Simonds, et al., 1995). If this tilt was produced in association with concomitant tilting of the fault, the original (restored) dip may have been as steep as 70–77° W. Brecciation at the Solitario Canyon dike at Little Prow indicates fault slip after dike intrusion, consistent with at least a small component of fault activity after intrusion. Similarly, basaltic dikes in the Bullfrog Hills primarily intruded along pre-existing planes of weakness such as normal faults and layering (Maldonado and Hausback, 1990).

The occurrence of volcanoes along mapped surface traces of faults and linear alignments of volcanoes near YM also is consistent with an interpretation that faults may provide preferential pathways for magma ascent. Two alignments of basaltic volcanoes parallel the north-south and northeast-southwest trends of many active normal faults in the YM region. The 11.2-km-long Crater Flat alignment consists of four Quaternary volcanic centers (Stamatakos, et al., 1997b). The 4.5-km-long Amargosa alignment consists of three magnetic anomalies interpreted to be three basaltic volcanoes buried by alluvium (Connor, et al., 1997).

Ground magnetic data collected from the northernmost volcano in the Crater Flat alignment (Northern Cone) indicate a strong north-south structural grain beneath the Crater Flat alluvium (Connor, et al., 1997). The 0.1-Ma Lathrop Wells volcano in southern YM occurs along or near the projected intersection of three normal faults. Both these observations strongly suggest structural control of magma ascent either directly along faults or as vertical breakout from faults at depth.

Summary—The Role of Faults in the Distribution of Dikes and Volcanoes. Analyses of fault-magma interactions based on theoretical and analog modeling results, *in situ* stress, 3D geometric constraints, and geological considerations (summarized by Ferrill, et al., 1997) suggest the following conclusions: (1) The distance of lateral diversion of dikes by magma channeling along nonvertical faults depends on the dip of the fault and depth range of magma channeling along the fault. (2) Analytical models indicate that even moderate to low angle faults may be able to capture dikes within 1-km of the earth's surface, and stronger rocks favor dike capture over vertical dike propagation. (3) The transition from capture to continued vertical propagation is not sharp and intermediate cases comparable with figure 4-17e can occur in the fault-dip range of 50–70°. (4) Dilation-tendency analysis of YM faults indicates that several faults in and around the proposed repository block are in high-dilation-tendency orientations. (5) Geological observations indicate that there has been significant structural control of magma ascent in the YM region within the last 13 Ma.

Crustal Conditions and Tectonic Strain

Crustal conditions characterize past, current, and predicted future stress and strain states and strain rates at the YM site and tectonic environs. Crustal conditions are critical to tectonic model development, fault slip, seismic motion, and development and reorientation of fractures. Technical bases are primarily derived from consideration of the application of crustal conditions as tools to evaluate seismic sources, faulting probability, structural control of groundwater flow, long-term evolution of natural and engineered barriers, and related SDS issues.

Geologic stress components applicable to resolution of the SDS KTI are lithostatic, hydrostatic, thermal, and seismotectonic stress. The present and predicted future states, including occurrence, distribution, and mechanisms of strain accommodation and how these strains affect the YM site and tectonic environs, form the primary bases for review methods and acceptance criteria for crustal conditions.

Stress states in rock may be: (1) measured directly from fluid pressure, overcoring, borehole strain meters, hydro/gas-fracturing in well bores; (2) indirectly inferred from strain measurements, faults, fractures, overburden, dike orientations, earthquake focal mechanisms; or (3) abstracted from numerical and physical analog models. Stress states determined from local *in situ* strain or stress measurements yield local values that are extrapolated over large volumes and may not reflect stress states at the larger scale. For example, upward scaling of locally determined stress and strain values may be affected by topography (Jaeger and Cook, 1979; Stock, et al., 1985; Stock and Healy, 1988), changes in lithology (Engelder, 1993; Crider and Pollard, 1998) or mechanical interactions between structures (Dupin, et al., 1993). As a result, regional stress fields determined from direct and indirect local strain or stress measurements require sampling in multiple and spatially distributed locations (Bellier and Zoback, 1995; Minor, 1995; Minor, et al., 1997).

Strain release in the upper crust may be local or regional in scale and induce a combination of seismic, microseismic, or aseismic responses. Seismic response results from significant displacement or rupture along discrete fault surfaces or fault zones and may result in regional or local uplift or subsidence or both, with present or subsequent effects upon groundwater levels. Displacement along faults may introduce fast communication pathways between previously discrete fluid reservoirs or conduits or create or sever conduits between fluid systems or aquifers (Allan, 1989). Microseismic response may result from microcracking, formation or growth of fractures or joints, or slip on small-scale faults. The introduction of new fractures or fracture sets may provide new fluid pathways that accelerate, retard, or redirect fluid flow (Finkbeiner, et al., 1997). Aseismic responses include positive or negative dilation of existing fractures or both, depending upon fracture orientations relative to the stress field (Engelder, 1993). Preferential fracture dilation results in anisotropic changes in porosity and permeability (Ferrill, et al., 1999a). In every case, introducing fractures and faults reduces, to some degree, the bulk strength of coherent rock (Hoek and Brown, 1980).

Geologic strain rates and related seismic hazard risk analyses are commonly determined by comparing the length of palinspastically restored or retro-deformed cross-sections with the present-day length along the same line of section, given the longevity of the regional deformation. One of the basic assumptions in this method, when applied to rocks deformed in the uppermost crust, is that all strain is accommodated by cross-section scale faulting.

Estimates of regional extension based upon cross-section construction and restoration are minimum estimates of strain and do not account for the nonseismogenic strains accommodated by fractures, joints, small-scale faults, and microscale deformation (Wu, 1993; Dunne and Ferrill, 1995). Considering the contribution of fractures, small faults, dikes, and pressure solution features, it seems improbable that the total strain of the YM region is accommodated by seismogenic rupture on fault surfaces.

Strain rates are inherently sensitive to errors in estimation and timing of cumulative slip on faults. Estimates of slip on individual faults or fault systems as determined from neo-tectonic features, including techniques such as trenching, stream offset mapping, and alluvial fan mapping, are considered minimum values (Reheis, 1988; Klinger and Anderson, 1994; Ferrill, et al., 1996a; 1997b). Fault restoration models assume that deformation or slip rates are constant throughout the life of the developing structure. This assumption effectively smooths or averages crustal deformation to a constant or fixed strain rate and cannot account for the likely episodic nature of many crustal scale deformation events. An average rate will neither distinguish nor accurately model areas where quiescence is interspersed with periods of strain rates that are relatively high when compared to the averaged or smoothed strain rate. For the same reasons, GPS and other geodetic measurements of extension rates, gathered over the span of a few years or tens of years, represent only a small fraction of the life of crustal-scale structures and may not accurately reflect longer term rates of strain. Recent GPS and geodetic results from several locations, including the YM site, indicate possible anomalously high rates of strain (Wernicke, et al., 1998; Martinez, et al., 1998; U.S. Geological Survey, 1998) with varying degrees of confidence (Gilmore, 1992; Savage, et al., 1994).

Geodetic leveling surveys beginning in 1907 (Gilmore, 1992) indicate subsidence in at least southern Crater Flat, across the eastward dipping, normal-slip BM fault zone. East of the BM fault, survey results indicate a 20–100-mm drop in elevation over a period of 69 yr (Gilmore, 1992), corresponding to throw rates well in excess of those measured from paleoseismic data (e.g., Anderson and Klinger, 1994). Slip rates on the BM fault zone appear to increase southward concomitant with an increase in fault dip (Monsen, et al., 1992; Ferrill, et al., 1996a; Stamatakos, et al., 1997a). The change in slip rate and subsequent southward-increasing subsidence of Crater Flat is supported by studies of alluvial fan deposits along the eastern flank of B M (Ferrill, et al., 1996a). Although the level-line results of Gilmore (1992) are not reflected in later surveys along a different line (U.S. Geological Survey, 1996), the earlier level-line surveys present additional uncertainty about the nature and rate of displacement on the BM fault.

Although the U.S. Geological Survey (1996) reports no changes in elevation due to displacement on the BM fault zone, its level-line survey does not cross the southern portion of the BM fault zone. Instead, the survey deviates northward on the east side of the B M fault (benchmark S16, figure 6-1) to cross Crater Flat to the northeast. The U.S. Geological Survey (1996) does report negative height changes in the 1980–1984 survey with respect to the 1915 survey (Gilmore, 1992). Considering the brief (4-yr) time span of the level-line surveys

(U.S. Geological Survey, 1996) and the deviation from the level line of the 1915 survey, sufficient evidence does not exist to negate the possibility of height change across the southern portion of the BM fault.

Large slip rates exist within 50–100 km to the west and southwest of the YM site. GPS surveys indicate high slip rates on the Death Valley fault and Hunter Mountain fault systems within the Death Valley Shear Zone southwest of YM (Bennet, et al., 1997a). Rates on the Death Valley fault alone are 3–5 mm/yr. If these rates persist or increase over time, the potential exists for multiple M_w 6.5–7.5 seismic events in the next 10,000 yr (Bennet, et al., 1997). Seismic activity to the east of the YM site at Little Skull Mountain resulted in measurable changes in elevation related to the 1992 Little Skull Mountain earthquake (M5.4) (Savage, et al., 1994; U.S. Geological Survey, 1996).

Wernicke, et al. (1998) propose crustal scale strain rates across YM that greatly exceed those inferred from the geologic record (Ferrill, et al., 1996a, 1997b; Connor, et al., 1998; Marrett, et al., 1998). These results are important because they provide alternative estimates to significant SDS and IA performance parameters including: (1) the frequency and magnitudes of earthquakes, (2) recurrence rates of faulting, and (3) probability of volcanism. Results from Wernicke, et al., (1998) suggest contemporary strain rates of 2 mm/yr across YM and Crater Flat, more than ten times the strain rate estimated from the geological record of faulting. Wernicke, et al. (1998) interpreted these anomalous rates to suggest an order of magnitude increase in seismic (including faulting) and volcanic hazards over the next 10 ka.

Savage, et al. (1998a,b; 1994) evaluated crustal-scale strain rates using a geodetic strain network. The Savage, et al. (1998b) survey consisted of a 13-station, 50-km aperture array, centered on YM, that encompassed the GPS baseline survey of Wernicke, et al. (1998). Savage, et al. (1998b) surveyed the trilateration network in 1983, 1984, 1993, and 1998. Years 1983 and 1984 were completed with an electro-optical distance-measuring geodolite. The 1993 occupation was completed with GPS, and 14 lines were verified with geodolite (Savage, et al., 1994). Year 1998 was completed with GPS (Savage, et al., 1998a). The Wernicke, et al. (1998) GPS survey consisted of five geodetic markers arrayed along a 14-km baseline from BM to Jackass Flats. The ground-surface (rock) mounted stations were occupied annually from 1991 to 1997. The Little Skull Mountain earthquake (June 29, 1992, $M = 5.4$) occurred within the time-span of both surveys. The epicenter of the Little Skull Mountain earthquake was located approximately 8-km southeast of the easternmost station of the Wernicke, et al. (1998) baseline survey, and was encompassed by the trilateration network of Savage, et al. (1998; Savage, et al., 1994). Coseismic offsets related to the Little Skull Mountain earthquake were calculated and removed from the results of Savage, et al. (1998). Wernicke, et al. (1998) quantified coseismic offset, but did not use the quantified values to correct the survey results (Savage, 1998a).

Wernicke, et al. (1998) reported strain rates of 50 ± 9 nanostrain/yr along the N65° W oriented baseline. Results from the Wernicke, et al. (1998) survey are not supported by the trilateration network of Savage, et al. (1998a,b, 1994). Strain rates from trilateration surveys are reported in two dimensions. Savage, et al. (1998a,b) report a N65° W oriented strain rate of 5 ± 12 nanostrain/yr. The results from Savage, et al. (1998a,b) are an order of magnitude less than the rate reported by Wernicke, et al. (1998), and compare favorably with the rates inferred from the geologic record.

Pezzopane[6] used satellite radar interferometry to evaluate surface displacement related to the Little Skull Mountain earthquake. Preliminary results indicate as much as 25 ± 5 mm of subsidence related to the seismic event, with the area of subsidence including the upland region of Little Skull Mountain. Modeling of displacement contours indicates predominately normal dip-slip on a northeast striking, steeply southeast-dipping planar fault. This places the structurally high Little Skull Mountain on the hangingwall of a normal fault. Based upon the relationship of Little Skull Mountain to the interpreted fault orientation and displacement, Pezzopane, et al. (1999) interpret the fault as a tectonically minor component of the regional setting, related possibly to gravitational collapse of the Little Skull Mountain block. If correct, the interpretation of Pezzopane, et al. (1999) implies that either (1) the Little Skull Mountain earthquake is not related to an anomalous increase in strain rate as proposed by Wernicke, et al. (1998), or (2) the interpreted anomalous increase in strain rate is incorrect.

Wernicke, et al. (1998) imply that the tenfold increase in strain rate determined from the GPS baseline survey results in a tenfold increase in hazard at YM. However, assessing an increase in hazard proportional to the increase in strain rate requires a series of suppositions that, at present, are not supported by the structural setting at YM or by conflicting assessments of crustal conditions (Pezzopane, et al., 1999; Savage, et al., 1998) or are not addressed in the current tectonic models (Savage, et al., 1998).

Suppositions that must be evaluated before seismic and volcanic hazards and hydrogeologic effects can be considered using GPS-determined strain rates are:

(1) That high strain rates must persist on time scales (10^3–10^4 yr) of duration sufficient to affect hazard estimates compared to estimates derived from the geologic record (10^5–10^6 yr)

(2) That episodic strain accumulations must directly correlate with episodic volcanic eruptions or increased seismicity

(3) The degree to which strain is partitioned between seismic, microseismic, and aseismic responses

(4) The effects of partitioned strain upon groundwater flow.

If the YM region is experiencing an episode of anomalous strain, it is difficult to assess or predict the future duration. If crustal strain is episodic, with bursts of rapid strain accumulation and release covering 10^3 to 10^4 yr between much longer periods of quiescence, average recurrence rates derived from the geologic record may not afford a reasonable measure of hazard over the next 10^3 to 10^4 yr.

It is unclear that episodic strain accumulations at YM directly correlate with episodic volcanic eruptions or increased seismicity. Wernicke, et al. (1998) suggest that anomalously high strain rates have been occurring in the YM region for the last 100 to 150 ka. However, this periodicity of strain has not resulted in a one order of magnitude increase in recurrence rate of volcanism or faulting. Clustered activity like the alignment of Quaternary volcanic cones in Crater Flat or

[6]Private communication, Appendix Seven Meeting, March 2–3, 1999.

the apparent clustered faulting at YM at 70 ka (figure 1 in Savage, et al., 1998) are representative of the periodicity of crustal strain accumulation and release. The paucity of neotectonic features at YM indicates that the postulated high-strain episode is, at the scale of geologic time, newly begun. The relatively short time span of the geodetic/GPS/level-line surveys as conducted thus far is not sufficient to define such an episode. Continuation of the geodetic/GPS surveys should increase the degree of confidence in strain-rate assessment.

Crustal strain can be accommodated by seismic, microseismic, and aseismic processes. The current strain rates observed by Wernicke, et al. (1998), although high for geologically determined rates for the Basin and Range, may not be anomalous. Rather, the apparently high strain rate may be instead an average rate for the Quaternary across the YM region. In this case, total strain is partitioned between geological processes that contribute to hazard estimates (earthquakes and volcanoes) and those that do not (small faults, fractures, and other aseismic or microseismic deformation). Using fracture data from the ESF, regional fault observations, and a regional seismic catalogue to quantify extension rate, Marrett, et al. (1998) estimated extension rates for a variety of time and length scales. The estimates are in reasonable agreement, and range from 5 to 20 nanostrain/yr, 2.5 to 10 times smaller than that predicted by the GPS measurements of Wernicke, et al. (1998), but 5 to 20 times greater than that predicted by the paleoseismic record (Marrett, et al., 1998).

Geologic Framework Model Version 3.1 (GFM3.1)

DOE's GFM3.1 is an update of GFM3.0. The GFM3.1 is DOE's stratigraphic and fault framework component of DOE's Integrated Site Model 3.0 (ISM3.0) shared by the following users: (1) unsaturated flow and transport; (2) SZ flow and transport; (3) near-field environment models; (4) repository design; (5) mineralogy; and (6) PA (M. Tynan[7]). The SZ, Repository Design, and PA groups will be relying on the stratigraphic and fault depictions for their assessments. The staff has reviewed GFM3.1 for the purposes of evaluating its various uses by the DOE are and considering using it to enhance the staff's 3D-modeling capability.

The staffs at CNWRA and NRC headquarters, in coordination, conducted tests and evaluations of GFM3.1. Briefly, the staffs reviewed GFM3.1 with the following objectives : (1) To determine the main differences between GFM3.1 and GFM3.0 and the rationales for the revision. (2) To test and evaluate GFM3.1 for DOE's purposes of representing site stratigraphy and faults as a framework for its Integrated Site Model 3.0 (ISM3.0). (3) To evaluate GFM3.1 as a necessary step toward the evaluation of the adequacy of DOE's ISM3.0. (4) To consider replacing the NRC's EV GFM with an adapted version of GFM3.1. Overall, the staff found GFM3.1 adequate for the purposes of: (1) depicting faults , fault blocks, stratigraphic horizons and the topographic surface at the scale of the repository site vicinity, and (2) providing a geologic framework for displaying and assessing the parameter distributions of other site characteristics. The testing and assessment procedures, results, and selected observations and limitations are presented in appendix E.

As a result of the staff's favorable review of GFM3.1 and with consideration of the time and resources needed to develop a tool similar to GFM3.1, the staff will adopt and adapt GFM3.1

---

[7]M. Tynan, personal communication, 3D Modeling, Geologic Framework Model, DOE/NRC Quarterly Meeting, June 3–4, 1998.

and updates, as needed, for the purposes of independent evaluation and analyses of the YM site.

Although GFM3.1 is the most detailed representation of the geologic framework of YM, it has apparently not been utilized in the development and testing of tectonic models of the YM area. Incorporation of the GFM3.1 into viable tectonic models will increase the level of confidence in DOE's ISM3.0, and in the models abstracted and extracted from ISM3.0.

5.0 STATUS OF SUBISSUE RESOLUTION

The SDS issue is open because the ancillary four subissues are still under investigation. When the four subissues are adequately addressed by the DOE, the SDS KTI will be resolved. In reviewing the current status of issue resolution, staff apply the subissue RMS to the pertinent ACs to determine the adequacy and acceptability of DOE's conclusions. The following sections provide details regarding the related subissues, including their status ,justification for status, and, if open, the path to resolution of the subissues. Staff define resolved and open as follows:

Resolved Issue or Subissue or Item

During the pre-licensing phase only , NRC staff consider an issue, or subissue or item resolved because staff have no further questions or comments at a particular time. Such resolution at the staff level would not preclude the issue, subissue, or item from being considered during licensing proceedings. There may be cases where resolution at the staff level is limited to documentation of a common understanding, regardless of differences in NRC and DOE points of view. Pertinent additional information could raise new questions or comments regarding a previously resolved issue, subissue, or item.

Open issue, subissue, or item.

During the pre-licensing phase only, NRC considers an issue, subissue, or item open (not resolved) because staff have further questions or comments on the issue, subissue, or item.

Open and resolved subissues and items are summarized in table 5-1 and discussed in detail in the following sections.

Table 5-1. Status of Subissue Resolution

Subissue	Resolved	Open	Comment
Faulting:	**resolved**		
AC 1	resolved		Nature of faulting is adequately evaluated
AC 2	resolved		Adequate fault data is available
AC 3	resolved		Probability of faulting is adequately described
AC 4	resolved		Alternative models have been considered
AC 5	resolved		Results are adequate. No questions based upon independent PA (section 3.3.1.1).
Seismicity:		**open**	
AC 1	resolved		Source characterization is adequate

Table 5-1. Status of Subissue Resolution (cont'd)

Subissue	Resolved	Open	Comment
AC 2		open	Will be reviewed pending receipt of seismic data.
AC 3		open	Will be reviewed pending receipt of seismic data.
AC 4		open	Will be reviewed pending receipt of seismic data.
AC 5		open	Will be reviewed pending future iterations of DOE PA
Fracture Framework:		**open**	
AC 1		open	Fracture characterization is inadequate
AC 2		open	Fracture data inadequate
AC 3		open	Abstractions are not defendable
AC 4		open	Insufficient consideration of alternative model approaches in abstractions
AC 5		open	Abstractions not adequately verified
Tectonic Framework:		**open**	
AC 1	resolved		Based upon review of PSHA, staff have no further questions at this time.
AC 2	resolved		Based upon review of PSHA, staff have no further questions at this time.
AC 3	resolved		Based upon review of PSHA, staff have no further questions at this time. Staff anticipate that DOE will incorporate results from continuing characterization of crustal conditions, and staff will review crustal conditions at that time.
AC 4	resolved		Based upon review of PSHA, staff have no further questions at this time.
AC 5		open	It is anticipated that AC5 will be resolved when staff review abstractions to all related subissues.

5.1 FAULTING

The goal of the faulting analyses performed by DOE was to locate and characterize the properties of faults that may be significant to repository design and repository performance. Faults (and fractures, discussed subsequently) constitute the principal structural weaknesses of the repository block, and the preferred pathways for heat and fluids through the NBSs and EBSs. With respect to design, DOE sought faults that might be seismogenic or able to intersect WPs, in order to ascertain the faulting and seismic hazards. DOE intends to place its WPs in positions that are setback from known faults. This consideration has already greatly influenced the repository boundary and layout plan for WPs.

5.1.1 Analysis of Subissue Resolution

For resolution of the faulting subissue the staff have to insure that the ACs have been met. The staff evaluated the DOE PSHA (U.S. Geological Survey, 1998) considering the ACs and RM discussed in section 4. At present, staff have no further questions regarding faulting and staff considers this subissue resolved. Staff will continue to monitor DOE's program and will re-evaluate the subissue as new information, such as Topical Report #3, become available. However, the effects of faulting on fluid, heat and magma flow is considered in other KTI IRSRs. Applying the faulting subissue review methods to the preliminary uniform ACs (section 4.1), staff conclude that the faulting subissue is resolved.

Based on staff's independent analysis of faulting (section 3.3.1.1), staff conclude that DOE's assessment of fault displacement hazard is adequate. Staff, however, continue to assess DOE's results on this topic because they will also relate to preclosure issues and indirect analysis of other DOE proposed FEPs.

Step 1—Nature of Faulting at YM

> Independently evaluate the adequacy of DOE's determination of the nature and amount of faulting and the appropriate faulting hazard sources within the repository block (style, recent and Quaternary activity, type) from the range of possible interpretations.

Staff conclude that DOE has adequately evaluated the nature and amount of faulting and the appropriate faulting hazard sources within the repository block, both principal and secondary from the range of possible interpretations. Given present knowledge, staff concludes that DOE's interpretations of faulting from surficial and underground mapping as presented in the DOE PSHA (U.S. Geological Survey, 1998) are geologically consistent and reasonable, and that they are compatible within the range of viable interpretations of YM tectonics. The experts adequately noted faults as primary or secondary as these classifications pertain to the PFDHA. Faulting characteristics identified subsequently or for which new data are developed should be evaluated or re-evaluated, respectively.

Step 2—Consistency of Faulting Models

> Independently evaluate the consistency of DOE's determination of models of faulting from fault geometry, kinematics, and mechanical behavior with existing geological and geophysical results, stress and strain considerations, and viable tectonic models.

Staff conclude that DOE has adequately determined fault geometry applicable to development of the PFDHA. However, methodologies (displacement and earthquake approaches) to assess fault kinematics and dynamics as they relate to primary and secondary faulting are too new to have gained general acceptance for the staff to accept a priori. Nevertheless, staff have determined that the faulting hazard results in the DOE PSHA (U.S. Geological Survey, 1998) are bounded by staff's independent analysis of faulting (section 3.3.1.1). Analyses by staff, show that faulting-induce failure of WPs is not significant to repository performance. The staff recommends that DOE publish the displacement and earthquake methods in the peer reviewed literature so they can be reviewed by the scientific community at large.

Step 3—Faulting Recurrence

> Independently evaluate the adequacy of DOE's estimates of fault slip-rate, recurrence, and recurrence relationships for faulting derived from paleoseismic, or historical earthquake data and ensure it is consistent with fault slip-rate, recurrence, and recurrence models used to evaluate seismicity.

As in Step 2, staff conclude that the displacement and earthquake methodologies developed by the PSHA expert teams is too new to have gained a priori acceptance. Nevertheless, staff have determined that the faulting hazard results in the DOE PSHA (U.S. Geological Survey, 1998) are bounded by staff's independent analysis of faulting (section 3.3.1.1). Those analyses showed that faulting-induce failure of WPs is not significant to repository performance.

Based on the conclusions in section 3.3.1.1 above, the staff also accepts DOE's Hypothesis No. 16, "The amount of movement of faults through the repository horizon will be too small to bring waste to the surface, and too small and infrequent to significantly impact containment during the next few thousand years" (U.S. Department of Energy, 1998, p. 15). Faulting through the repository horizon will not likely have single or cumulative displacements sufficient to cause exhumation of a WP during the performance period. The staff recommends, however, that DOE publish the displacement and earthquake methods in the peer reviewed literature so that they can be reviewed by the scientific community at large. Although staff can not accept a priori DOE's earthquake and displacement methodologies, staff conclude that the results from faulting analyses performed by DOE are adequate. Staff have no further questions at this time, and conclude that the faulting subissue is resolved.

5.1.2 Site Characterization Analysis (SCA) Items

All comments on faulting items are resolved (see appendix D for resolution).

5.2 SEISMICITY

The goal of the seismic hazard analysis performed by DOE was to define the earthquake hazard at YM (i.e., to establish the frequency and spectra of anticipated GMs at YM for the next 10,000 yr). The principal application of the seismic hazard curve for postclosure assessments are as an input parameter to PA calculations, both as a base case condition and disruptive event, and as a parameter to evaluate FEPs. Assessment of the DOE PSHA for preclosure issue will be evaluated by the NRC in separate documents after receiving Topical Report#3.

5.2.1 Analysis of Subissue Resolution

For resolution of the seismicity subissue the staff has to insure that the ACs have been met. The staff evaluated the PSHA results submitted by DOE (U.S. Geological Survey, 1998) considering the applicable ACs and RM discussed in section 4.

Step 1—Seismic Sources

> Independently evaluate the adequacy of DOE's determination of seismic sources used to describe the potential sources of seismicity that will affect calculation of the peak and spectral GMs for the lifetime of the repository.

The staff conclude that the seismic sources identified by the experts in the PSHA (U.S. Geological Survey, 1998) adequately describe the potential sources of seismicity that will contribute to the calculation of the peak and spectral GMs at YM. The numbers and types of faults that may contribute to the hazard at the site were agreed upon between the staff and DOE.

For example, staff agree that Type I faults have been identified. DOE (U.S. Geological Survey, 1996) uses the terms relevant and potentially relevant in describing faults. Relevant faults are defined as those having documented Quaternary displacement and the capability of the maximum magnitude earthquake on the fault to produce 84th percentile peak acceleration greater than or equal to 0.1 g at the repository site. Potentially relevant faults are considered subject to displacement on the basis of potential structural association with seismicity.

In Revision 1, 13 specific faults listed in appendix B-4, described by DOE (Simonds, et al., 1995) were considered Type I faults by NRC (McKague, et al., 1996), but were not specifically considered by DOE (U.S. Geological Survey, 1996). Eight of these faults showed no evidence of Quaternary movement and have been moved to table B-5, i.e., Type III faults. The remaining faults or combinations of them have been considered to be of significance to design or performance by DOE experts (U.S. Geological Survey, 1998). At this time, staff is satisfied that all known candidate Type I faults in the YM region have been adequately evaluated. Staff have found that differences between DOE and NRC classifications of particular faults are rooted in just a few parameters. The parameters are: (1) fault trace length, (2) attenuation function, and (3) selection of median or 84th percentile for identification of 0.1 g criterion. These differences lead to only minor differences in predicted GMs (< 0.1 g) and are not considered significant overall repository performance. In reaching its conclusions regarding faulting, staff applied the following RMs.

The earthquake historical data and paleoseismicity were defined at the site and region, about 30,000 earthquakes from historical earthquake catalogues were used by the experts in the PSHA. The earthquake magnitudes used in the analysis ranged from 5.0-8.0. The maximum magnitude for the fault sources was estimated based on the rupture dimensions of the source and use relationships between and rupture dimensions. The empirical relationships between magnitude versus rupture length, rupture area, maximum surface displacement (e.g., Wells and Coppersmith, 1994) were adequately used to estimate maximum magnitude. Estimates of the rupture area and average slip on the fault were also be used by the experts to calculate the maximum event magnitude (Anderson, et al., 1996). For area sources, the maximum magnitude earthquake was based on the maximum earthquake to occur within the area. The magnitude ranges used by the experts were based on moment magnitude M_w. The seismic source expert teams addressed the uncertainties in estimating the maximum magnitude for fault sources due to: (1) whether using fault length or maximum fault displacement, (2) the use of different empirical relations to estimate the magnitude, (3) uncertainty in measuring the dimension of the rupture on the fault, and (4) uncertainty in measuring the slip rate.

Step 2—Earthquakes Recurrences

> Independently evaluate the adequacy of DOE's descriptions of seismic activity and recurrence relationships of faults and tectonic sources used to determine GM at YM.

The staff concludes that the six seismic source expert teams addressed the seismic activities for each source whether it is a fault or an areal source. To assess the seismic hazard from earthquakes, estimates of earthquake recurrence were required. Fore shocks, aftershocks, and test-site earthquakes (dependent events) were identified by the experts and removed from the catalog. The earthquake data was declustered using Youngs, et al. (1987) or Van Dyck (1985) procedure. Using Youngs' approach 26250 earthquakes (within 300 Km radius of YM) remained in the catalog, while 31,147 earthquakes remained using Van Dyck's procedure. In certain instances some of the experts considered the seismicity rate within an areal source may vary per unit area. The expert teams considered several types of recurrence relations such as: A characteristic, truncated exponential, modified truncated exponential, and maximum moment models. For fault sources, the expert teams used two approaches to estimate the earthquake recurrences. First by estimating the number of ruptures on the fault either by dating of paleoearthquakes or by dividing the total slip on the fault by the average slip per event. The second approach is to translate the fault slip into seismic moment rate and then partition the moment into earthquakes of various magnitudes or recurrence models.

Detailed assessment of recurrence awaits staff's independent analysis. That analysis hinges on acquisition of seismic data (requested from DOE in September 1999) and not yet received by NRC.

Path to Resolution

NRC will acquire seismic data from DOE and perform independent assessment to analyze DOE results.

Step 3—Ground Motion Attenuation

> Independently evaluate the adequacy of DOE's determination of GM attenuation used to estimate vibratory GMs at the site.

In the DOE PSHA (U.S. Geological Survey, 1998), the facilitation team and the seven GM experts examined several cross sections and well logs to identify shear velocities at the site. There was a large variation in shear velocity within the YM region. The experts recommended that site-specific shear velocities will be needed for addressing the geotechnical properties and design issues at the surface handling facility. Several GM models were utilized by the experts to estimate the PGA, peak ground velocity, and SA. The GM models the experts used ranged from, the empirical or hybrid empirical models, stochastic point and finite source simulation model, semi-empirical Green's Function finite fault simulation model, compound fractile finite fault model, and blast model. The aleatory and epistemic uncertainties associated with the GM estimates were provided. The staff considers the spectral decay parameter, kappa, was not finalized in the PSHA. A workshop was held on March 2–3, 1999, to discuss this issue but a final decision about what is the appropriate value of Kappa to be used has not been reached yet. DOE indicated that this issue will be discussed in Topical Report #3. The staff considers this subissue open at this time and will readdress it in IRSR Revision 3 after reviewing Topical Report #3.

In addition, detailed description and assessment of GM attenuation awaits staff's independent analysis. That analysis hinges on acquisition of DOE PSHA data (requested from DOE in September, 1999) and not yet received by NRC.

Path to Resolution

NRC will acquire seismic data from DOE and perform independent assessment to analyze DOE results and staff review of Topical Report #3.

Step 4—Seismic Hazard Analysis

Independently evaluate the adequacy of DOE's hazard calculations.

The staff considers DOE's probabilistic seismic calculations and hazard curves represent the probability of accedence at different levels of accelerations for a free-field reference rock outcrop at 300 m depths at YM. DOE presented the PSHA results, associated uncertainty, and the weight estimates provided by the GM experts. The GMs were computed for a rock outcrop condition with shear velocity of 1,900 m/sec. The GM estimates for the reference rock outcrop will need to be modified to account for the shallow material at the surface. The GM input for seismic design of the repository will be finalized by DOE in a technical report (Topical Report #3) titled "Seismic Design Basis Input for a High-Level Radioactive Waste Repository at YM." Before finalizing Topical Report #3 DOE is planning to:

1 Acquire site-specific soil and rock properties as part of foundation studies for the Waste Handling Facilities.

2 Determine site-specific values for near surface attenuation of GM (Kappa).

3 Continue monitor earthquakes at the surface and in boreholes, to better define the attenuation and its variability at YM.

DOE's probabilistic approach to seismic hazard analysis (U.S. Department of Energy, 1997) was accepted in principle by NRC staff (Bell, 1996) for the evaluation of the seismic hazard and fault displacement hazard at YM (see DOE's Topical Report #1). DOE decided, and the staff accepted, that the seismic hazard component of the "Seismicity" subissue will be addressed through the issuance of three Topical Reports (U.S. Department of Energy, 1997, "Methodology to Assess Fault Displacement and Vibratory Ground Motion Hazards at YM)."

The staff has conducted an acceptance review of Topical Report #1 in accordance with NRC's Division of High-Level Waste Management Review Plan, dated February 1994. In a letter dated September 7, 1994, the staff provided its comments on Topical Report #1. On January 29, 1996, DOE provided responses to the staff comments. In a letter dated July 25, 1996 (Bell, 1996), the staff informed DOE that sufficient information had been provided to close all open issues related to Topical Report #1. Because Topical Report #1 is limited to describing the seismological assessment methodology, and Topical Report #2 (U.S. Department of Energy, 1997b), which also had been accepted by the staff, addressed "Preclosure Seismic Design Methodology for Geologic Repository at Yucca Mountain," the staff decided to issue a Preliminary Evaluation Report after receiving Topical Report #3, which will document the results of both PSHA and seismic design values needed for the design of the facilities.

Path to Resolution

NRC will acquire DOE's seismic data and perform independent assessment to analyze DOE results. In addition to these plans, DOE should consider:

> Describing the method to be used to transfer the results for a hard rock outcrop at 300-m depths in the current analysis to the surface to account for soil amplification, i.e., how the mean rock hazard curves will be translated to mean soil hazard curves. In doing that, DOE should address how uncertainties in rock hazard curves will be translated into uncertainties in soil hazard curves considering the uncertainties in soil dynamic properties (e.g. shear wave velocity, stiffness, and damping characteristics).
>
> Addressing if the mode of the joint distribution M, R, and ε conditional on $S_a > x$ would differ from the following joint distribution M, ln R, and ε.
>
> Addressing the potential hazard that GM directivity effect may have on structure located close to a causative fault.
>
> Providing the binning selection criteria applied in choosing the bin size in the analysis, and how the final results will be affected if different bin sizes are used (e.g., uniform or nonuniform, large, or small).
>
> Elaborating on the inconsistencies in the treatment of uncertainty between the experts and how much the lack of knowledge about the parameter σ_σ contributed to the final hazard results.
>
> Addressing how the results from the PSHA analysis will be used to assess the performance of the repository for the post closure period of performance (10,000 yr).

Step 5—Seismic Hazard Limitations and Abstraction to Performance Assessment

> Independently evaluate the adequacy of considering limitations and uncertainty in applying the seismic hazard results to design and PA evaluation.

Direct and indirect effects of seismic disturbances such as rockfall, ground vibrations, alteration of flow paths or changes in the water table elevation could have significant effects on the repository performance. Water-table rise has been shown to be a transitory and of limited extent (Carrigan, et al., 1991; Gauthier, et al., 1995; Arnold, 1996). Rockfall is expected to be the primary source of disturbances. The sizes of rocks that could fall depend on the number of fractures present, the competency of the rock, state of stress, and magnitude and duration of

GM (Sharma, et al., 1991; Kaiser, et al., 1992; Hsiung, et al, 1992). It is expected that the most likely blocks to fall are from those areas of high thermal loads. DOE based their rockfall analysis on Kaiser, et al. (1992) empirical relationship for rockfall caused by shaking. DOE found that about 27 percent of the rock masses that could fall have a weight of 50 Kg, 24 percent are less than 350 Kg, and 1 percent are larger than 2,500 Kg. Based on this finding, DOE indicated that the contribution of the seismic disturbance to the dose release is insignificant. A detailed review of effects of rockfall on a WP is provided in Chapter 3 of the Repository Design and Thermal Mechanical Effect KTI, Revision 2.

Path to Resolution

Currently, the staff requested seismic data used by DOE and its contractors to generate the PSHA results. The intent of this request is, for the staff and its contractor, to perform independent analysis and perform sensitivity analysis and compare our results with those generated by DOE. The staff independent analysis will be discussed in IRSR, SDS, Revision 3.0. In addition, staff provided informal feedback to DOE regarding application of the seismic hazard results. In the DOE VA (U.S. Department of Energy, 1998b), seismicity was treated as a disruptive scenario. In plans to update their PA, DOE is now considering including seismicity as a base case phenomena. Staff will evaluate the application of the DOE PSHA results to future iterations of repository PA as they become available.

5.2.2 Site Characterization Analysis (SCA) Items

All SCA items on seismicity are resolved. NRC staff has resolved Comments 66 and 67 in the area of seismic motion. Comment 66 dealt with the 10,000-yr, cumulative-slip earthquakes, and Comment 67 dealt with a magnitude 5.5 cutoff (see appendix D for resolution rationale).

5.3 FRACTURING AND STRUCTURAL FRAMEWORK OF THE GEOLOGIC SETTING

The goal of DOE's characterization of fractures at YM has been to provide a technical basis for process models, repository design, and related issues. Fracture data have been collected from surface exposures at YM and the surrounding region, from boreholes, and from the ESF and ECRB.

5.3.1 Analysis of Subissue Resolution

For resolution of the fracturing subissue, the staff has to ensure that the ACs have been met. The resolution of this subissue depends not only on geological characterizations of fractures, and development of geological models of fracture development and modification, but also on adequate abstraction of fractures and fracture models in the seven dependent ISI's (see figure 3-2) that implicitly or explicitly incorporate fracture information. The discussions below summarize results to date of staff review according to the RM described in section 4.3.1.1. Review to date has yielded inadequacies in DOE analyses.

Step 1—Characterization of Fractures

> Independently evaluate the adequacy of DOE's distribution and geometric (e.g., orientations, spacing, clustering, abutting relationships, interconnectedness, apertures, lengths, roughness) and mechanical characteristics of fractures.

Staff review of fracture data and fracture data summaries have yielded the following inadequacies in fracture characterization and summarization to date: (i) directional sampling biases not corrected, (ii) truncation biases not corrected, (iii) censorship bias not corrected, (iv) role of lithology overemphasized, (v) fracture aperture distribution underconstrained, (vi) fracture connectivity across stratal boundaries underconstrained, (vii) fracture characterization in key units in UZ inadequate (e.g. Calico Hills formation), (vii) spatial heterogeneity in fracture distribution underconstrained, (ix) abundance of subhorizontal fracture underconstrained, (x) downwardly-convergent fracture networks (flow paths) unconstrained, and (xi) role of mining-induced alteration of fractures underconstrained. The following discussions summarize these findings in additional detail.

Directional sampling biases not corrected

Raw orientation data from the ESF were used to develop permeability tensors for the UZ site scale model of YM (chapter 7 of Bodvarsson, et al., 1997). DLS data from the ESF have an inherent sampling bias from preferentially unsampling fractures that are more perpendicular rather than parallel to the survey line. The sampling bias may be corrected by using the Terzaghi correction, which will also affect fracture spacing values. This problem may partially be eliminated by comparing DLS results from the ESF and ECRB for the same stratigraphic units, because the two tunnels are not parallel, or by comparing data from nearly orthogonal scanlines from the ESF and alcoves. Caution may be needed in this comparison if the fracture pattern in a stratigraphic unit is not spatially homogeneous on the scale of analysis.

Truncation biases not corrected

Existing data sets in their present forms do not allow the necessary incorporation of trace length into fracture network characterization. Fracture size is particularly important for groundwater flow considerations because large fractures are often found to be primary conduits for flow. Tunnels and small diameter boreholes are inadequate for determining trace lengths, especially for fractures that are long with respect to the sample area or tunnel/borehole diameter. One of the most useful components of surface data sets, however, is for trace length determination. Many cleared pavements (Barton, et al., 1993; Sweetkind, et al., 1995a), however, expose areas that are too small because the longer fractures extend beyond the pavement boundaries, preventing length determination. Full periphery maps for the ESF partially illustrate trace lengths, but they too are incomplete representations of particularly the larger fractures because of blind terminations.

Censorship bias not corrected

During fracture data collection, it is typical to set a size threshold; fractures below the size (usually length) threshold are not measured. This has been the case for data collection in the ESF and ECRB. Small (below threshold size) fractures, however, can be very important for fracture-flow considerations (total fracture permeability, fracture network connectivity) and rockfall (block boundaries) issues (see additional discussion under RM 5 below).

Role of lithology overemphasized

Existing characterizations of the fracture network in YM tend to focus on establishing descriptions for each individual lithological unit (e.g., Sweetkind and Williams-Stroud, 1996;

chapter 7 of Bodvarsson, et al., 1997; Beason[8]; U.S. Department of Energy, 1998b). Certainly, welded tuffs fracture in a manner distinct from unwelded tuffs and the abundance of lithophysae is an important factor for joint morphology. However, several nonlithological parameters are important: (a) The timing of joint formation (cooling versus tectonic) controls the size and spacing of the fractures. (b) The regional stress field at the time of joint formation would control joint orientation, and hence, the magnitude of regional extension would control joint abundance. (c) The presence and possible active displacement of the north-south trending faults could perturb and locally intensify the local stress field producing joint networks that would not be predicted from the regional stress field. Failure to consider these factors has lead to an inability to predict key aspects of the joint network such as abundant northeast-trending cooling joints in the Tiva Canyon Tuff, abundant northwest-trending cooling joints in the Tiva Canyon Tuff, and the unexpected west-northwest-trending abundant fractures in the Topopah Spring Tuff along much of the main drift of the ESF. Given that the repository will be sited in rocks that will not be sampled directly for fracture networks until repository construction, it is critically important to be able to predict the most likely fracture trends and abundances before construction. Thus, a better understanding of these nonlithologically-derived fracture network characteristics is needed.

Fracture aperture distribution underconstrained

Although single aperture measurements are available for fractures in ESF fracture data sets, aperture distribution and variations along fractures remain unconstrained. Aperture distribution along fractures is a key consideration in modeling of the flow along fractures in the UZ, and largely determines the type of flow in fractures: sheet or rivulet surface flow on a single fracture wall, flow induced by local filling of the fracture gap by capillary forces, and locally saturated flow down the fracture. Detailed characterization of fracture aperture distribution for different types of fractures (cooling joints, tectonic joints, and unloading joints) is needed to constrain models of UZ fracture flow at YM.

Fracture connectivity across stratal boundaries underconstrained

Vertical connectivity of fractures is a key issue for meteoric infiltration, percolation into the repository, and for escape of heated fluids from the repository, particularly across lithological boundaries. This issue has been investigated explicitly for the role of faults as fracture pathways through the nonwelded tuffs in the interpretation of the causes for ^{36}Cl anomalies (Levy, et al., 1997). However, illustrations and analyses of fractures in the welded tuffs do not adequately define the interconnections of fractures at thermomechanical layer boundaries, and within hydrostratigraphic layers and across hydrostratigraphic layer boundaries. Unlike the abrupt stratal boundaries that terminate fractures at layer boundaries in sandstone and shale multilayers, the relatively gradational boundaries between layers in the Tiva Canyon and Topopah Spring Tuffs probably lead to greater vertical interconnection. Although vertical connectivity must exist for the fracture network to act as a flow network, several questions remain. Is the connectivity restricted to faults? Is it dependent on the presence of abundant early large cooling joints that cross lithological unit boundaries? Is it enhanced by fracture reactivation? Locations for examining vertical connectivity across unit boundaries need to be identified and examined. The most promising examples may well be in the ESF where

[8]Personal communication, Appendix Seven Meeting, March 2–3, 1999.

re-examination of full-periphery maps may provide a sufficient basis for addressing this issue. Surface exposure of lithologies is very dependent on lithology, slope orientation, soil development and fracture abundance, so surface sites for examining vertical connectivity may be less available for systematic sampling.

Fracture characterization in key units in unsaturated zone inadequate

Although current plans call for the bulk of the proposed repository to be constructed in the lower lithophysal zone (Tptpll) of the crystal poor Topopah Spring Tuff, there are very limited data to constrain orientations and intensity of fracturing in this unit within the repository block. Characterization activities have concentrated on the overlying middle nonlithophysal zone (Tptpmn) and younger units, based on earlier plans to site the repository within the Tptpmn. This issue is particularly important for the RDTME KTI, and is discussed in the RDTME IRSR (Revision 2).

Data available to constrain the fracture network in strata below the Topopah Spring Tuff (most importantly, the Calico Hills Formation) are few (U.S. Department of Energy, 1998b) and of limited utility due to directional sampling biases (due to inability of vertical borehole to adequately sample vertical fractures). This lack of data produces first order uncertainty in UZ flow path and transport modeling.

Spatial heterogeneity in fracture distribution underconstrained

Much of the network characterization and application of the network to KTI's and subissues tends to amalgamate large data sets from large areas, and tend to assume spatial homogeneity. However, existing work indicates (Barton, et al., 1993; Sweetkind and Williams-Stroud, 1996) that the fracture network has significant spatial heterogeneities. The two most prominent cases are increased joint intensities near normal faults and cooling joint swarms. Although cooling joint swarms were identified by earlier workers in at least the Tiva Canyon Tuff (Barton, et al., 1993), the current visualization of the fracture network in this unit (D.S. Sweetkind[9]; U.S. Department of Energy, 1998b) does not incorporate this strongly anisotropic and heterogeneous aspect of the network. In particular, the actual dimensions (>100 m length, cutting entire thickness of thermomechanical unit) has been under recognized. Fracture swarms are likely to be loci of increased infiltration where exposed at the surface, and may be under characterized fast paths for groundwater flow at YM.

Abundance of subhorizontal fractures underconstrained

Subhorizontal fractures are a key element in the fracture network for facilitating block formation and detachment above WPs and as possible patterns for lateral flow in UZ (e.g., for lateral eastward movement of water from Solitario Canyon). Therefore, explicit treatment of their abundance, size and distribution is necessary to accurately estimating the risk from block fall and lateral UZ flow. The ESF, ECRB and alcoves provide the best available data set for examining these fractures despite the fact that the subhorizontal attitude of the tunnels creates a bias against sampling these fractures. Re-examination of the DLS and full-periphery maps should provide a basis for constructing a systematic description of these fractures, which would

---

[9]D.S. Sweetkind, Appendix Seven Meeting, March 2–3, 1999.

be particularly important for the crystal-poor middle nonlithophysal and lower lithophysal unit of the Topopah Spring Tuff.

Downwardly-convergent connected fracture networks (flow paths) unconstrained

Although recent identification of ^{36}Cl anomalies in the ESF have indicated the occurrence of spatially heterogeneous groundwater flow in the UZ, the fracture network characteristics that lead to heterogeneous groundwater flow in the UZ remain unconstrained. For example, direct association of some ^{36}Cl anomalies with faults has indicated that faults are fast paths for an underdetermined portion of UZ percolation. The mechanism of water collection by the faults, however, remains unknown. Do faults only collect water from directly connected steeply dipping fractures that reach the surface, or does significant lateral flow occur within interconnected "stratal-bound" fracture networks? Other ^{36}Cl anomalies were not directly associated with faults, which raises the questions about what aspect of the fracture network produced localized heterogeneous fracture flow, and the drainage area and water flux that produced these anomalies.

Role of mining-induced alteration of fractures underconstrained

Although the occurrence of mining induced fracturing is to be expected, the separation of man-induced fractures from natural fractures is critical for correcting fracture data sets for use in larger-scale groundwater flow analyses. Likewise, the ability to predict mining induced fracturing in drifts will be critical for analyses of rockfall and drift seepage.

Path to Resolution

Technical bases must be clearly presented where DOE contends that fracture distribution, and geometric and mechanical character are not significant to performance. Where fracture distribution and geometric and mechanical character are significant to performance, data must be sufficient to provide technical bases for adequate and conservative bounding analyses, and for the approximation of adequate and conservative parameter distributions in PA. Inadequacies in fracture characterization can be resolved by DOE through detailed analysis of currently available data and additional data collection. Recent data collection by DOE investigators from the surface, ESF, and ECRB have considerably improved understanding of the YM fracture network. Staff view the data collection and analysis activities necessary to resolve the inadequacies discussed above as a logical continuation of site characterization. Future characterization activities should be focused on providing detailed constraints for process models, with specific attention paid to the characterization discussion provided above.

Step 2—Origins of fractures

Independently evaluate the adequacy of DOE's determination of the origins of fractures.

Staff review of fracture data and fracture data summaries have yielded the following inadequacies in fracture origin description and interpretation, which lead to an insufficient basis for interpolating between and extrapolating beyond measured fracture information: (i) the origin of the intensely fractured zone encountered in ESF, (ii) the development of fracture sets in orientations inconsistent with known regional stress fields, (iii) cooling versus tectonic versus unloading origins of some joint sets. The following discussion summarizes these findings in additional detail.

Several nonlithological parameters are important in the development of fractures. Understanding the role of these parameters in fracturing at YM is critical for interpolation and extrapolation from fracture data. The timing of joint formation (cooling versus tectonic) controls the size and spacing of the fractures. The regional stress field at the time of joint formation dominantly controls joint orientation and the magnitude of regional extension controls joint abundance. The presence and possible active displacement of the north-south trending faults could perturb and locally intensify the regional stress field producing joint networks that would not be predicted from the regional stress field. Failure to consider these factors has led to an inability to predict key aspects (all of which bear directly on the calculation of the permeability tensors and likely flow behaviors in the UZ) of the joint network: (a) abundant northeast-trending cooling joints in the Tiva Canyon Tuff; (b) abundant northwest-trending cooling joints in the Tiva Canyon Tuff; and (c) the unexpected west-northwest-trending abundant fractures in the Topopah Spring Tuff along much of the main drift of the ESF. Given that the repository will be sited in part of YM that will not be directly characterized for fracture networks until repository construction, it is critically important to be able to predict the most likely fracture trends and abundances before construction. Thus, a better understanding of these nonlithological features is needed.

The accepted understanding of the regional evolution of stress fields since deposition of the Paintbrush Group Tuffs, is a change from an east-west directed minimum principal stress to a northwest-southeast directed minimum principal stress. These minimum stress orientations should produce Mode I fractures (joints) with dilating walls that trend north-south and northeast-southwest, respectively. Both such sets of tectonic joints have been identified by previous DOE investigations, and they are referred to as T1 and T3 joints, respectively. However, northwest-southeast trending T2 joints have an orientation for Mode I fractures that could not be produced by either regional stress field, yet they are certainly abundant in the Tiva Canyon strata in some areas above the proposed repository. So, the issue is determining the origin of the joints, particularly for the purpose of establishing whether they are areally abundant or just restricted to certain subregions of the repository and overlying rocks. For example, a possible origin of the joints would be formation in a perturbed stress field between two actively moving north-south trending normal faults (e.g., Solitario Canyon and Ghost Dance or Bow Ridge faults).

Path to Resolution

Technical bases must be clearly presented where DOE contends that the origin of fractures is not significant to performance. Where fracture origin is significant to performance, data must be sufficient to provide technical bases for adequate and conservative bounding analyses, and for the approximation of adequate and conservative parameter distributions in PA. Resolution of inadequacies in description and interpretation of origins of fractures can be reached through a combination of detailed analyses of existing data, analog studies, numerical modeling, and additional data collection and field checking.

Step 3—Past modifications of fractures

> Independently evaluate the adequacy of DOE's constraints on subsequent modifications of fractures by dissolution, precipitation, fault rock and wall rock deformation, and other fracture filling processes (e.g., deposition of water-entrained particles).

Staff review of descriptions of past modifications of fractures have yielded concerns regarding lack of information regarding fault zone deformation and resulting permeabilities in UZ and SZ due to past fault rupture, fault core development, and related fracturing in fault damage zones. The resulting fault zone permeabilities are extremely poorly constrained, yet faults are considered to be potentially important pathways for groundwater flow. Considerable uncertainty remains regarding timing and conditions (especially temperature) of past fluid movement along YM faults. Some evidence exists supporting relatively hot fluid movement along faults. Constraint on the timing of interpreted movement of relatively hot fluid along faults is of particular importance for assessment of repository performance.

Path to Resolution

Technical bases must be clearly presented where DOE contends that descriptions of and constraints on past modifications of fractures are not significant to performance. Where descriptions of and constraints on past modifications of fractures are significant to performance, data must be sufficient to provide technical bases for adequate and conservative bounding analyses, and for the approximation of adequate and conservative parameter distributions in PA. Inadequacies in description of and constraints on past modifications of fractures can be resolved through detailed analysis of limited data currently available, and by collection of additional data from YM and/or analog sites.

Step 4—Current and future modifications of fractures

> Independently evaluate the adequacy of DOE's definition of current and future tectonically and thermally controlled alteration of fracture characteristics during the repository performance period and their accounting in process level models.

Staff review of analyses of current and future modifications of fractures have yielded the following inadequacies to date: (i) influences of local and regional stress fields on fracture and fault permeabilities underconstrained, (ii) influences of future deformation on fault zone and fracture permeability underconstrained, (iii) thermal effects on fractures underconstrained, (iv) effects of mining on fracture system underconstrained.

Staff expect significant alteration to the YM fracture network due to ongoing influences of tectonic factors (local and regional stress field and deformation), thermal loading and underground excavation at the site. For example, staff consider it likely that an earthquake on the BM fault would trigger secondary surface deformation (faulting and extension fracturing) in the uppermost strata at YM. Formation of new fractures and dilation of existing fractures would at least locally increase fracture network permeability. Although probability of slip on the BM fault (and other YM area faults) has been considered in the PSHA for YM, the consequences of such future deformation on the fracture network permeability have not been considered in assessments of repository performance. Similarly, ongoing effects and changes in the YM stress field (e.g., local stress field perturbation caused by slip on one of the YM faults) have not been considered in PAs. Although currently under investigation, influences of thermal loading and mining on the fracture network remain underconstrained.

Path to Resolution

Technical bases must be clearly presented where DOE contends that descriptions of and constraints on current and future modifications of fractures are not significant to performance. Where descriptions of and constraints on present and future modifications of fractures are significant to performance, data must be sufficient to provide technical bases for adequate and conservative bounding analyses, and for the approximation of adequate and conservative parameter distributions in PA. Inadequacies in description of and constraints on current and future modifications of fractures can be resolved through new data collection, detailed data analysis, modeling, and analog studies.

Step 5—Abstraction of fracture data and models

> Independently evaluate the adequacy of DOE's abstraction and consideration of fracture data, and models of origin and their past, present, and future modifications in process level models.

Staff review to date has yielded the following inadequacies in abstraction of fracture data and models for process models: (i) sampling biases not corrected, (ii) nonrepresentative data sets used as basis for abstractions, (iii) fundamental fracture network characteristics ignored in discrete fracture network modeling, (iv) assumption of homogeneous and isotropic permeability in SZ aquifers is unsupported and nonconservative, (v) heterogeneity and anisotropy of permeability architecture in UZ under-represented, and (vi) oversimplification and lack of transparency of abstraction. The following discussions summarize these findings in additional detail.

Sampling biases not corrected

Raw DLS data for fractures in the ESF were used in conjunction with air permeability data to develop UZ hydraulic properties for the UZ site scale model of YM (chapter 7 of Bodvarsson, et al., 1997). The raw fracture data are, as discussed above under RM-1, not representative of the natural fracture network because of directional sampling, censorship, and truncation biases, which can yield erroneous abstractions for process models. Results from the drift scale flow model (U.S. Department of Energy, 1998b) have not only shown that drift seepage is sensitive to estimates of permeability and van Genuchten alpha, but also that heterogeneity of both parameters is critical to seepage rates.

Nonrepresentative data sets used as basis for abstractions

The report on the UZ site scale flow model for YM (Bodvarsson, et al., 1997) notes that fracture data from the ESF is only used to Station 40+00. This selective use of data avoids the intensely fractured zone encountered in the Main drift.

Flint, et al. (1996) use fracture data from surface studies in a supporting role. For analysis of spatial variation of shallow infiltration. Bodvarsson, et al. (1997, chapter 7) use results from Flint, et al. (1996) as input for the UZ site-scale flow model. Unfortunately, the surface data have not been gathered in the same systematic continuous manner that the subsurface data of the ESF, ECRB and other subsurface tunnels and may not provide an adequate technical basis for assessment of spatial distribution of water infiltration and influx into the subsurface fracture network. Surface data have been gathered over more than 10 yr by different investigators using different methodologies and with interludes between collection efforts. As described in section 4.3.1.2, anisotropic, spatially heterogeneous but persistent fracture networks exist and their interaction with topography, soil and vegetation bear directly on the infiltration (Flint, et al. (1996) used as input into the subsurface fracture network for the UZ site-scale flow model.

Fundamental fracture network characteristics ignored in discrete fracture network modeling

Use of a discrete fracture modeling approach to simulate flow behavior in the UZ can be quite useful for identifying probable network geometries, persistent flow pathways, and permeability anisotropies (e.g., Anna, 1997). Inputs from this approach have been applied to the analysis done for Chapter 7 of Bodvarsson, et al. (1997). However, the existing usage of synthetic fracture networks is not representative of the natural fracture network for two reasons:

First, for the Tiva Canyon Tuff models, data were dominantly used from the north portal of the ESF, which is located in proximity to eight north-south trending faults, including the Bow Ridge fault. In contrast, the Tiva Canyon Tuff above the repository only contains a comparatively minor north-south trending fault, the Ghost Dance fault. For the Topopah Spring Tuff models, the region of the main north-south drift of the ESF (with appropriate corroboration from ECRB data) where the high-intensity joint population trending northwest-southeast is present should be modeled separately. This fracture domain is not an artifact of the sampling methodology and should be treated as a separate domain.

Second, fractures were equally weighted by orientation and not other attributes such as fracture length and relative age. Sets were fitted statistically and forced to accommodate all orientations. Thus, sets have very broad orientation ranges unlike in nature, and the basic age attribute (cooling versus tectonic origin) of the fractures at YM, which key to any synthetic network construction because cooling joints are older and will tend to be longer and have tectonic joints abut against them, was ignored. Set selection procedures need to recognize the relative ages of fracture sets as determined form surface work and incorporate the physical effects of the relative age of joint sets into the synthetic networks. Also, set selection procedures should yield sets with narrower orientation ranges as are actually observed in surface fracture analyses.

Assumption of homogeneous and isotropic permeability in saturated zone aquifers is unsupported and nonconservative

The TSPA 3D SZ model assumes material properties in the hydrogeologic layers are homogeneous and isotropic. This approach is implemented because of limited data and therefore represents a considerable simplification of the complex distribution of hydraulic conductivities observed in cores and from localized pump-tests in hydrogeologic units at YM. The assumption of homogeneous and isotropic permeability of SZ aquifers (U.S. Department of Energy, 1998a), however, lacks a technical basis and is not conservative. Faults, which may act as conduits or barriers to flow, are only accounted for in the model by hydrogeologic unit offsets. Although not accounted for in the base case analyses, the potential impacts of high permeability faults on SZ flow have been considered in the sensitivity analyses. The presence of these features were found to influence groundwater flow paths and effect performance. More elaborate approaches for accounting for faults have not yet been attempted. In areas where the maximum anisotropy axis is not parallel to the potentiometric gradient, groundwater flow directions could be oblique to the hydraulic gradient. In this way, incorporation of anisotropy would change the configuration of flow tubes currently used to model groundwater flow at YM in the TSPA code. The assumption of homogeneous and isotropic aquifer properties leads to flow paths that are controlled by the potentiometric gradient, which at YM results in relatively short groundwater travel paths to the unconsolidated alluvial aquifer in Jackass Flat, and relatively long travel distances in alluvium where sorption of radionuclides may be enhanced. The presence of faults and fractures as flow conduits may modify these groundwater flow paths, resulting in more southward groundwater flow and increased travel distances in the unconfined welded tuff aquifer.

In faulted aquifers, such as those at Yucca Mountain, Nevada, geologic structures (faults and fractures) exert three major controls on subregional to regional conductivity and flow: (i) fault offsets alter the overall architecture of the aquifers and control aquifer communication between fault blocks (Allan, 1989), (ii) fault zones commonly form relatively impermeable barriers to cross-fault flow and permeable pathways for along-fault flow (Caine, et al., 1996), and (iii) relatively small faults and fractures lead to permeability anisotropy in fault blocks (Ferrill, et al., 1999b). In addition, fault and fracture conductivity (and permeability anisotropy) may be influenced by the *in situ* stress field (e.g., Barton, et al.,1995; Finkbeiner, et al., 1997; Ferrill, et al., 1999b, in press). Fault zone permeability properties depend on rock type, deformation mechanisms (functions of lithology, deformation conditions and amount of deformation), amount of cementation (in some case, a function of time), and the *in situ* stress field (Caine, et al., 1996; Evans, et al., 1997). At YM, hydraulic conductivities within the Miocene Tuff layers appear to be strongly anisotropic at both the local and regional scales (Geldon, et al., 1997; Bredehoeft, 1997; Ferrill, et al., 1999b). To incorporate fault zone permeabilities into flow models, additional constraints on fault zone properties at YM or appropriate analogs are necessary.

Heterogeneity and anisotropy of permeability architecture in unsaturated zone underrepresented

Much of the fracture network characterization and application of the network to KTIs and subissues tends to amalgamate data sets and assume spatial homogeneity. However, existing work indicates (Barton, et al., 1993; Sweetkind and Williams-Stroud, 1996) that the network has significant spatial heterogeneities in fracture characteristics. The two most prominent cases are increased joint intensities near normal faults and cooling joint swarms. Although cooling joint swarms were identified by earlier workers in at least the Tiva Canyon Tuff (Barton, et al., 1993), the current abstractions of the fracture network do not incorporate the strong anisotropy and heterogeneity of the network. Fracture swarms are likely to be loci of increased infiltration at the surface, and, coupled with vertical and/or lateral connectivity, may be under characterized fast paths for groundwater flow at YM.

On a more detailed scale, insufficient data exist to substantiate abstractions of aperture variation along fractures in the UZ. Although single aperture measurements are available from ESF fracture data sets, aperture distribution and variations along fractures remain unconstrained. Aperture distribution along fractures is a key consideration in modeling of the flow along fractures in the UZ, and largely determines the type of flow in fractures: sheet or rivulet surface flow on a single fracture wall, than induced by local filling of the fracture gap by capillary forces, and locally saturated flow down the fracture. Detailed characterization of fracture aperture distribution for different types of fractures (cooling joints, tectonic joints, and unloading joints) is needed to constrain models of UZ fracture flow at YM.

Oversimplification and Lack of Transparency of Abstraction

Recent numerical analyses of rockfall in drifts (RDTME IRSR, U.S. Nuclear Regulatory Commission, 1999b) have shown that rockfall processes are sensitive to variation in fracture orientation within joint sets. When all joints in a set are modeled to be perfectly parallel, drifts tend to be more stable. Slight natural variation in orientation, which is typical within natural joint sets, leads to increased drift instability. Current DOE abstractions assume single orientations for fractures in a set (e.g., U.S. Department of Energy, 1998b). In one case, (table 4-12 in U.S. Department of Energy, 1998b) multiple sets are represented in a single orientation; an abstraction apparently based on a previous abstraction (U.S. Department of Energy, 1997b). Abstractions need to be both representative of the natural fractures network, and clearly tied to fracture characterization and models. Simplifications need to be technically justified.

Path to Resolution

Technical bases must be clearly presented where DOE contends that current abstractions and consideration of fracture data are adequate, and that abstractions and considerations of data are sufficient to provide technical bases for adequate and conservative bounding analyses, and for the approximation of adequate and conservative parameter distributions in PA. Inadequacies in abstraction and consideration of fracture data and models can be resolved through additional focused data collection, utilization of improved fracture characterization (e.g., data corrected for sampling biases), basing abstractions on representative data sets, and faithfully honoring available data. The abstraction process may strongly benefit from involving members of fracture characterization teams. It is expected that concerns identified during the abstraction process may provide additional focus for fracture characterization and modeling activities described under Steps 1–4 above.

5.3.2 Additional Fracture and Structural Framework Related Items

Site Characterization Analysis (SCA) Items

There are no SCA open items on this subissue.

5.4 TECTONIC FRAMEWORK OF THE GEOLOGIC SETTING

The goal of the identification of viable tectonic models and of current crustal conditions has been to provide technical bases for PVHA, PSHA, PFDHA, SZ and UZ hydrology, repository design, analyses of mechanical disruption of WPs, and related issues. Viable tectonic models have been selected from tectonic models published in the scientific literature and supported by data from and conditions in the YM region. Related crustal conditions were determined using available technologies, and data collection continues for the YM region.

5.4.1 Analysis of Subissue Resolution

Resolution of the tectonics and crustal conditions subissue requires that staff ensure that the ACs have been met. This depends not only upon the identification and evaluation of viable tectonic models and crustal conditions, but also upon the adequate abstraction and incorporation of the models and conditions to the dependent subissues. Staff apply the following RMS to confirm that pertinent AC are met for the faulting subissue.

Step 1—Determination of Tectonic Models

> Independently evaluate the adequacy of DOE's determination of viable tectonic models for YM and surrounding region.

Given the present state of knowledge, staff conclude that DOE's determination of viable tectonic models as presented in DOE's PSHA (U.S. Geological Survey, 1998) is adequate. At present, staff consider five of the eleven models discussed at the May 7–8, 1996 Appendix Seven meeting on conceptual tectonic models as viable (appendix C-1). DOE's PSHA expert elicitation considered the full range of viable tectonic models, and staff have no further questions at this time as to DOE's use of the full range of variable tectonic models. Staff will continue to monitor DOE's program to ensure that this full range of tectonic models is applied uniformly and with continuity across the entire DOE analysis of YM, as appropriate.

Step 2–Geological and Geophysical Data

> Independently evaluate the adequacy of DOE's consideration of existing geophysical, geological, seismological, and geodetic data in assessment of viable tectonic models and current crustal conditions.

Staff considers the treatment of tectonic models and current crustal conditions in DOE's PSHA (U.S. Geological Survey, 1998) adequate. DOE is encouraged to maintain this level of adherence to existing data and reasonable explanations for inconsistencies in the treatment of tectonic models and crustal conditions in all related subissues. DOE's current assessment of crustal conditions is adequate. Although the data of Wernicke, et al. (1998) indicate anomalous strain rates, analyses by DOE and independent analyses by NRC staff and contractors indicate that the anomalous rates indicated by Wernicke, et al. (1998) may be either incorrect, or of no extraordinary consequence. Staff anticipate that further surveys by Wernicke, et al., will yield new data, and that these new data will be incorporated into the assessment of current crustal conditions as warranted by the results. However, staff do not consider adequate the assessment of the viable tectonic models and the promulgation of the "preferred" or "favored" tectonic model in DOE's YM Site Description (U.S. Department of Energy, 1998c). Until such time as new evidence or improved interpretations become available, re-classification of the five viable tectonic models, or introduction of "preferred" or "favored" models that are not supported by the current state of knowledge is not warranted. Staff recommends that the classification of specific models as "preferred" or "favored" be avoided as these terms present a negative connotation. DOE is encouraged to introduce "new" models through publication in refereed scientific journals to allow review by the greater scientific community.

Step 3–Characterization of Tectonic Models

> Independently evaluate DOE's characterization of viable tectonic models and related crustal conditions to ensure that sufficiently detailed bases exist for abstractions.

Although the abstraction of tectonic models and crustal conditions are not complete for all affected subissues, staff concludes that DOE's characterization of the viable tectonic models as presented in DOE's PSHA (U.S. Geological Survey, 1998) is adequate. Tectonic, structural and seismic elements and associated uncertainties are adequately described, abstracted and implemented for the purpose of seismic hazard assessment. DOE's PSHA expert elicitation considered the full range of viable tectonic models as supported by existing data to bound the seismic hazard at YM.

Step 4–Abstraction and Continuity of Tectonic Models

> Independently evaluate the abstraction and continuity of viable tectonic models and crustal conditions across all subissues affecting performance.

Staff have reviewed the application of tectonic models to development of the DOE PSHA, including the fault displacement hazard and have no further questions at this time regarding the implementation of tectonic models to those issue (see sections 5.1 and 5.2). Implementation of tectonic model development of the site scale GFM3.1 model is also adequate and staff have no further questions about the GFM3.1 model (see discussion below). Application to other subissues such as fracturing are not yet resolved (see section 5.3). In addition, staff is currently evaluating the applicability and continuity of tectonic models across subissues in all other relevant KTIs. Pending completion of those analyses and resolution of fracture framework ACs, staff consider this subissue open. Applying the tectonic framework review methods (section 4.4) to the preliminary uniform AC (section 4.1), staff conclude that AC 1, 2, 3, and 4 are resolved, and that staff have no further questions at this time for these AC. AC 5 remains open until staff review tectonic framework and related abstractions for all related subissues.

Path to Resolution

Staff will review the abstractions of tectonic models and crustal conditions for affected subissues and implementation of tectonic models and crustal conditions for continuity across issues, and for continuity from probability estimations through to consequence analyses. Staff encourages that the abstraction and implementation of tectonic models and crustal conditions be complete, and completely documented, including the incorporation of new concepts.

Geologic Framework Model Version 3.1 (GFM3.1)

The following item is resolved (see discussion in section 4.4.1.2 and appendix E):

DOE's GFM3.1 is an adequate tool for various site-scale analyses of stratigraphy, faults, fault blocks, and their relationship to typography and to the 3D distribution of parameters associated with hydrologic and rock properties. GFM3.1 is the framework for the soon-to-be-released ISM3.0. The NRC staff have developed the capability to fully utilize GFM3.1 and will use it to conduct independent analyses and as a review tool for various DOE models that have incorporated GFM3.1. Staff recommends that GFM3.1 be incorporated with the viable tectonic models to ensure confidence in ISM3.0.

5.4.2. Site Characterization Analysis (SCA) Items

To date, staff has identified four comments (Numbers 8, 47, 68, and 98) in the area of tectonic models that are open items (appendix D).

Site Characterization Analysis (SCA) - Other Geoscience

To date, NRC staff has identified two comments (Numbers 32 and 51) and one question (Number 8) in areas of geology and geophysics related to SDS KTI in the SCA of DOE's Site Characterization Plan. All are open items. (appendix D, "Other Geoscience"). ['Other Geoscience' is an arbitrary grouping of items from the SCA that are not specific to the four subissues categories].

6.0 REFERENCES CITED

Abrahamson, N.A., and K.M. Shedlock, *Overview*, Seismological Research Letters 68(1), 9–23, 1997.

Abrahamson, N.A., and W.J. Silva, *Empirical response spectral attenuation relations for shallow crustal earthquakes*, Seismological Research Letters 68, 94–127, 1997.

Albin, A.L., W.L. Singleton, T.C. Moyer, A.C. Lee, R.C. Lung, G.L.W. Eatman, and D.L. Barr, *Geology of the Main Drift—Station 28+00 to 55+00, Exploratory Studies Facility, Yucca Mountain Project, Yucca Mountain, Nevada, Bureau of Reclamation and U.S. Geological Survey*, Prepared in cooperation with the Nevada Field Office, U.S. Department of Energy, under Interagency Agreement DE-A108-92NV10874, MOL.19970625.0096, 29, 30, 33, 1997.

Alexander, L.L., and J.W. Handschy, *Fluid flow in a faulted reservoir system: Fault trap analysis for the block 330 field in Eugene Island, south addition, offshore Louisiana*, American Association of Petroleum Geologists Bulletin 82(3), 387–411, 1998.

Allan, U.S., *Model for hydrocarbon migration and entrapment within faulted structures*, American Association of Petroleum Geologists Bulletin 73(7), 803–811, 1989.

Anderson, E.M., *The dynamics of faulting*, Oliver & Boyd, Ltd., Edinburgh, 1951.

Anderson, J.G., S.G. Wesnousky, and M.W. Stirling, *Earthquake size as a function of fault slip rate*, Bulletin of the Seismological Society of America 86, 683–690, 1996.

Anderson, J.G., J.N. Brune, J.N. Louie, Y. Zeng, M. Savage, G. Yu, Q. Chen, and D. dePolo, *Seismicity in the western Great Basin apparently triggered by the Landers, California, earthquake, 28 June 1992*, Bulletin of the Seismological Society of America 84, 863–891, 1994.

Anderson, L.W., and R.E. Klinger, *Preliminary evaluation of the Bare Mountain fault zone, Nye County, Nevada*, Administrative Report in Support of Yucca Mountain Site Characterization Activity 8.3.1.17.4.3, Denver, CO, Bureau of Reclamation, 1994.

Anderson, R.E., *Thin-skinned distension in Tertiary rocks of southwestern Nevada*, Geological Society of America Bulletin 82, 43–58, 1971.

Anderson, R.E., A.J. Crone, M.N. Machette, L.A. Bradley, and S.F. Diehl, *Characterization of Quaternary and suspected Quaternary faults, Amargosa area, Nevada and California*, U.S. Geological Survey Open-File Report 95-613, 41 plus appendices, 1995b.

Anderson, R.E., R.C. Buckman, A.J. Crone, K.M. Haller, M.N. Machette, S.F. Personius, T.P. Barnhard, M.J. Cecil, and R.L. Dart, *Characterization of Quaternary and suspected Quaternary faults, regional studies, Nevada and California*, U.S. Geological Survey Open-File Report 95-599, 56 plus appendices, 1995a.

Anna, L.O., *Preliminary three-dimensional discrete fracture model of the Topopah Spring Tuff in the exploratory studies facility, Yucca Mountain area, Nye County, Nevada*, U.S. Geological Survey Open-File Report 97-834, Lakewood, CO, U.S. Geological Survey, 1997.

Anna, L.O., and P. Wallman, *Characterizing the fracture network at Yucca Mountain, Nevada, Part 2; Numerical simulation of flow in a three-dimensional discrete fracture network*, Fractured Reservoirs: Descriptions, Predictions, and Applications: Rocky Mountain Association of Geologists 1997 Guidebook, T.E. Hoak, P.K. Blomquist, and A. Klawitter, eds, Denver, CO, Rocky Mountain Association of Geologists, 199–208, 1997.

Arabasz, W.J., and D.R. Julander, *Geometry of seismically active faults and crustal deformation within the Basin and Range Province, northeastern Nevada. Extensional tectonics of the Southwestern United States: A Perspective on Processes and Kinematics*, L. Mayer, ed, Geological Society of America Special Paper 208, Boulder, CO, Geological Society of America, 43–74, 1986.

Armstrong, R.L., *Sevier orogenic belt in Nevada and Utah*, Geological Society of America Bulletin 79, 439–458, 1968.

Atwater, T., *Implications of plate tectonics for the Cenozoic tectonic evolution of western North America*, Geological Society of America Bulletin 81, 3,513–3,536, 1970.

Axen, G.J., W.J. Taylor, and J.M. Bartlet, *Space-time patterns and tectonic controls of tertiary extension and magmatism in the Great Basin of the western United States*, Geological Society of America Bulletin 105, 56–76, 1993.

Barton, C.C., and P.A. Hsieh, *Physical and Hydrologic-Flow Properties of Fractures*, Washington, DC, American Geophysical Union, 1989.

Barton, C.C., and E. Larsen, Fractal geometry of two-dimension fracture networks at Yucca Mountain, Fundamentals of Rock Joints: Proceedings of the International Symposium on Fundamentals of Rock Joints, O. Stephanson, ed, Sweden, Bjorkliden, 77–84, 1985.

Barton, C.C., T.M. Howard, and E. Larsen, *Tubular structures on the faces of cooling joints—A new volcanic feature*, EOS, Transactions of the American Geophysical Union 65, 1,148, 1984.

Barton, C.C., E. Larsen, W.R. Page, and T.M. Howard, *Characterizing Fractured Rock for Fluid-Flow, Geomechanical, and Paleostress Modeling: Methods and Preliminary Results from Yucca Mountain, Nevada*, U.S. Geological Survey Open-File Report 93-269, Denver, CO, U.S. Geological Survey, 1993.

Barton, C.C., M.D. Zoback, and D. Moos, *Fluid flow along potentially active faults in crystalline rock*, Geology 23(8), 683–686, 1995.

Bell, M.J., Letter (July 25) to S. J. Brocoum, U.S. Department of Energy, Washington, D.C., U.S. Nuclear Regulatory Commission, 1996.

Bellier, O., and M.L. Zoback, *Recent state of stress change in the Walker Lane Zone, western Basin and Range Province, United States*, Tectonics 14, 564–593, 1995.

Bennett, R.A., J.L. Davis, P. Elósegui, B.P. Wernicke, J.K. Snow, M.J. Abolins, M.A. House, G.L. Stirewalt, and D.A. Ferrill, *Global positioning system constraints on fault slip rates in the Death Valley region, California and Nevada*, Geophysical Research Letters 24, 3,037–3,076, 1997a.

Bennett, R.J., J.R. Murphy, and B.W. Baker, *Empirical Ground Motion Predictions for Yucca Mountain Repository Using Experience from NTS Underground Nuclear Explosions*, presented at Summary of Methods, Models, and Preliminary Interpretations Workshop on Ground Motion at Yucca Mountain, Civilian Radioactive Waste Management System, Management and Operation Contractor, Salt Lake City, UT, January 9–10, 1997.

Bernreuter, D.L., A.C. Boissonade, and C.M. Short, Investigations of technique for the development of seismic design basis using probabilistic seismic hazard analysis, NUREG/CR–6606, 1998.

Bodin G.E., and J. Gomberg, *Triggered seismicity and deformation between Landers, California, and Little Skull Mountain, Nevada, earthquakes*, Bulletin of the Seismological Society of America 84, 835–843, 1994.

Bodvarsson, G.S., T.M. Bandurraga, and Y.S. Wu, *The site-scale unsaturated zone model of Yucca Mountain, Nevada, for the viability assessment*, LBNL–40376/UC–814, Berkeley, CA, Lawrence Berkeley National Laboratory, 1998.

Bohannon, R.G, and T. Parsons, *Tectonic implications of post-30 Ma Pacific and North American relative plate motions*, Geological Society of America Bulletin 107, 937–959, 1995.

Boore, D.M., W.B. Joyner, and T.E. Fumal, *Estimation of Response Spectra and Peak Accelerations from Western North American Earthquakes: An Interim Report*, U.S. Geological Survey Open-File Report 93-509, Denver, CO: U.S. Geological Survey, 1993.

Boore, D.M., W.B. Joyner, and T.E. Fumal, *Equations for estimating horizontal response spectra and peak acceleration from western North American earthquakes: A summary of recent work*, Seismological Research Letters 86, 128–153, 1997.

Bowring, S.A., and K.E. Karlstrom, *Growth and stabilization of the Proterozoic lithosphere in the southwestern United States*, Geology 18, 1,203–1,206, 1990.

Bradshaw, T.K., and E.I. Smith, *Polygenetic Quaternary volcanism at Crater Flat, Nevada*, Journal of Volcanology and Geothermal Research 63, 165–182, 1994.

Bredehoeft, J.D., *Fault permeability near Yucca Mountain*, Water Resources Research 33, 2,459–2,463, 1997.

Brethauer, G.E., D.L. Healy, and C.H. Miller, *Statistical Analysis of the Gravity Method of Calculating the Depth of the Pre-Cenozoic Surfaces in Yucca Flat, Nevada Test Site*, Geological Prospecting 29, 31–38, 1981.

Brocher, T.M., M.D. Carr, K.F. Fox, and P.E. Hart, *Seismic reflection profiling across Tertiary extensional structures in the eastern Amargosa Desert, Basin and Range Quadrangle, Nevada*, Geological Society of America Bulletin 105, 30–46, 1993.

Brocher, T.M., P.E. Hart, W.C. Hunter, and V.E. Langenheim, *Hybrid-source seismic reflection profiling across Yucca Mountain, Nevada, regional lines 2 and 3*, U.S. Geological Survey Open-File Report 96-02, Menlo Park, CA, U.S. Geological Survey, 1996.

Brocher, T.M., W.C. Hunter, and V.E. Langenheim, *Implications of seismic reflection and potential field geophysical data on the structure frame work of Yucca Mountain-Crater Flat Region, Nevada*, Geological Society of America Bulletin 110, 947–971, 1998.

Bruhn, R.L., and R.A. Schultz, *Geometry and slip distribution in normal fault systems: Implications for mechanics and fault-related hazards*, Journal of Geophysical Research 101, 3,401–3,412, 1996.

Buesch, D.C., R.W. Spengler, T.C. Moyer, and J.K. Gelsin, *Proposed Stratigraphic Nomenclature and Macroscopic Identification of Lithostratigraphic Units of the Paintbrush Group Exposed at Yucca Mountain, Nevada*, U.S. Geological Survey Open-File Report 94-469, Denver, CO, U.S. Geological Survey, 1996.

Burchfiel, B.C., and G.A. Davis, *Structural framework and evolution of the southern part of the Cordilleran orogeny, western United States*, American Journal of Science 272, 97–118, 1972.

Burchfiel, B.C., D.S. Cowen, and G.A. Davis, *Tectonic overview of the Cordilleran orogen in the western United States*, The Cordilleran Orogen, Conterminous U.S.: The Geology of North America Volume G-3, B.C. Burchfiel, P.W. Lipman, and M.L. Zoback, eds, Boulder, CO, Geological Society of America, 407–479, 1982.

Burchfiel, B.C., K.V. Hodges, and L.H. Royden, *Geology of Panamint Valley-Saline Valley pull-apart system, California, Palinspastic evidence for low-angle geometry of a Neogene range-bounding fault*, Journal of Geophysical Research 93, 10,422–10,426, 1987.

Byerlee, J.D., *Friction of rocks*, Pure and Applied Geophysics 116, 615–626, 1978.

Byers, F.M., Jr., W.J. Carr, P.P. Orkild, W.D. Quinlivan, and K.A. Sargent, *Volcanic Suites and Related Cauldrons of the Timber Mountain-Oasis Valley Caldera Complex, Southern Nevada*, U.S. Geological Survey Professional Paper 919, Reston, VA, U.S. Geological Survey, 1976.

Caine, J.S., J.P. Evans, and C.B. Forster, *Fault zone architecture and permeability structure*, Geology 24, 1,025–1,028, 1996.

Camilleri, P.A., and K.R. Chamberlain, *Mesozoic tectonics and metamorphism in the Pequop Mountains and Wood Hills region, northeast Nevada: Implications for the architecture and evolution of the Sevier orogen*, Geological Society of America Bulletin 109, 74–94, 1997.

Campbell, K.W., *Near-source attenuation of peak horizontal acceleration*, Bulletin of the Seismological Society of America 71, 2,039–2,070, 1981.

Campbell, K.W., *Predicting strong ground motion in Utah*, Evaluation of Regional and Urban Earthquakes and Risk in Utah, W.W. Hays, P.L. Gori, eds. U.S. Geological Survey Professional Paper 87-585II, L1-L90, Washington, D.C.: U.S. Geological Survey, 1987.

Campbell, K.W., *Empirical near-source attenuation relationships for horizontal and vertical components of peak ground acceleration, peak ground velocity, and pseudo-absolute acceleration response spectra*, Seismological Research Letters 68, 154–179, 1997.

Carlos, B.A., S.J. Chipera, D.L. Bish, and S.J. Craven, *Fracture-lining manganese oxide minerals in silicic tuff, Yucca Mountain, Nevada, U.S.A.*, Chemical Geology 107, 47–69, 1993.

Carlsson, A., and T. Olsson, *Hydraulic conductivity and its stress dependence*, Proceedings of the 1979 Workshop Low-Flow, Low-Permeability Measurements in Largely Impermeable Rocks, Paris, France, 249–259, 1979.

Carr, W.J., *Volcano-tectonic history of Crater Flat, southwestern Nevada, as suggested by new evidence from drill hole USW-VH-1*, USGS Open-File Report 82-457, Denver, CO, U.S. Geological Survey, 1982.

Carr, W.J., *Regional Structural Setting of Yucca Mountain, Southwestern Nevada, and Late Cenozoic Rates of Tectonic Activity in Part of the Southwestern Great Basin, Nevada and California*, USGS Open-File Report 84-854, Denver, CO, U.S. Geological Survey, 1984.

Carr, W.J., *Volcano-tectonic setting of Yucca Mountain and Crater Flat, southwestern Nevada in geologic and hydrologic investigations of a potential nuclear waste disposal site at Yucca Mountain, southern Nevada*, M. Carr, and J. Yount, eds, U.S. Geological Survey Bulletin 1790. Denver, CO, U.S. Geological Survey, 35–49, 1988.

Carr, W.J., *Styles of extension in the Nevada test site region, southern Walker Lane belt; An integrated volcano-tectonic and detachment fault model*, Geological Society of America Memoir 176, Boulder, CO, Geological Society of America, 283–303, 1990.

Carr, W.J., *Structures in continuously cored, deep drill holes at Yucca Mountain, Nevada, with notes on calcite occurrence*, SAND91-7037, Albuquerque, NM, Sandia National Laboratories, 1992.

Carr, W.J., and L.D. Parrish, *Geology of Drill Hole USW VH-2, and Structure of Crater Flat, Southwestern, Nevada*, USGS Open-File Report 85-475, Denver, CO, U.S. Geological Survey, 1985.

Carr, W.C., S.M. Keller, and J.A. Grow, *Lithologic and Geophysical Logs of Drill Holes Felderhoff Federal 5-1 and 25-1, Amargosa Desert, Nye County, Nevada*, U.S. Geological Survey Open-File Report 95-115, Denver, CO, U.S. Geological Survey, 1995.

Carr, W.J., F.M. Byers, Jr., and P.P. Orkild, *Stratigraphy and Volcano-Tectonic Relations of Crater Flat Tuff and Some Older Volcanic Units, Nye County, Nevada*, U.S. Geological Survey Professional Paper 1323, Reston, VA, U.S. Geological Survey, 1986a.

Carr, W.J., S.J. Wadell, G.S. Vick, J.M. Stock, S.A. Monsen, A.G. Harris, B.W. Cork, and F.M. Byers, Jr., *Geology of Drill Hole UE25p#1: A Test Hole into Pre-Tertiary Rocks Near Yucca Mountain, Southern Nevada,* USGS Open-File Report 86-175, Denver, CO, U.S. Geological Survey, 1986b.

Carrigan, C.R., G.C.P. King, G.E. Barr, and N.E. Bxleil, *Potential for water-table excursions induced by seismic events at Yucca Mountain, Nevada*, Geology 19(12), 1,157–1,160, 1991.

Cartwright, J.A., and C.S. Mansfield, *Lateral displacement variations and lateral tip geometry of normal faults in the Canyonlands National Park, Utah*, Journal of Structural Geology 20, 2–19, 1998.

Caskey, S.J., and R.A. Schweickert, *Mesozoic deformation in the Nevada Test Site and vicinity: Implications for the structural framework of the Cordilleran fold and thrust belt and Tertiary extension north of Las Vegas Valley*, Tectonics 11, 1,314–1,331, 1992.

Castagna, J., *Exploration questions: the sequel*, The Leading Edge, January 1996.

Chekuri, V.S., S.W. Tyler, and J.W. Fordham, *The role of fracture coatings on water imbibition into unsaturated tuff from Yucca Mountain*, Nevada Agency for Nuclear Projects/Nuclear Waste Project Office NWPO-TR-024-95, Carson City, NV, Nevada Agency for Nuclear Projects, 1995.

Chester F.M., and J.M. Logan, *Composite planar fabric of gouge from the Punchbowl Fault, California*, Journal of Structural Geology 9, 621–634, 1986.

Christiansen, R.L., P.W. Lipman, W.J. Carr, F.M. Byers, Jr., P.P. Orkild, and K.A. Sargent, *Timber Mountain-Oasis Valley caldera complex of southern Nevada*, Geological Society of America Bulletin 88, 943–959, 1977.

Civilian Radioactive Waste Management System Management and Operational Contractor, *Yucca Mountain Site Geotechnical Report*, B00000000-01717-5705-00043 REV01. Las Vegas, NV, 1997.

Civilian Radioactive Waste Management System Management and Operational Contractor, *Repository Ground Support Analysis for Viability Assessment*, BCAA00000-01717-0200-0004 REV01. Las Vegas: NV, 1998a.

Civilian Radioactive Waste Management System Management and Operational Contractor, *Yucca Mountain Site Description*, B00000000-01717-5700-00019 REV00. Las Vegas: NV, 1998b.

Connor, C.B., and B.E. Hill, *Three nonhomogeneous Poisson models for the probability of basaltic volcanism: Application to the Yucca Mountain region, Nevada*, Journal of Geophysical Research 100, 10,107–10,125, 1995.

Connor, C.B., B.E. Hill, K.H. Spivey, and P. Hunka, Volcanism Research. *NRC High-Level Radioactive Waste Research at CNWRA, July–December 1993*, 10-1 to 10-26, B. Sagar, ed. San Antonio, TX, Center for Nuclear Waste Regulatory Analyses, 121–139, 1993.

Connor, C.B., S. McDuffie, and B.E. Hill, Field volcanism research, *NRC High-Level Radioactive Waste Research at CNWRA, July-December 1993.* B. Sagar, ed. San Antonio, Texas: Center for Nuclear Waste Regulatory Analyses: 10-1 to 10-26, 1994.

Connor, C.B., J.A. Stamatakos, D.A. Ferrill, B.E. Hill, S.B.L. Magsino, P. La Femina, and R.H. Martin, *Integrating structural models into volcanic hazard assessments: An example from Yucca Mountain, Nevada,* EOS Transactions of the American Geophysical Union, San Francisco Annual Meeting, Washington, DC, American Geophysical Union, F20, 1996.

Connor, C.B., S. Lane-Magsino, J.A. Stamatakos, R.H. Martin, P.C. La Femina, B.H. Hill, and S. Lieber, *Magnetic surveys help reassess volcanic hazards at Yucca Mountain, Nevada.* EOS, Transactions of the American Geophysical Union 78, 73, 77–78, 1997.

Connor, C.B., J.A. Stamatakos, D.A. Ferrill, B.E. Hill, G.I. Ofoegbu, and F.M. Conway, *Volcanic hazards at the proposed Yucca Mountain, Nevada, high level-radioactive waste repository I: Geologic factors controlling patterns of small-volume basaltic volcanism,* Journal of Geophysical Research, 1999, in review.

Conway, F.M., D.A. Ferrill, C.M. Hall, A.P. Morris, J.A. Stamatakos, C.B. Connor, A.N. Halliday, and C. Condit, *Timing of basaltic volcanism along the Mesa Butte Fault in the San Francisco volcanic field, Arizona from $^{40}Ar/^{39}Ar$ ages: Implications for longevity of cinder cone alignments,* Journal of Geophysical Research 102, 815–824, 1997.

Coppersmith, K.J., *Update on data related to fault displacement and vibratory ground motion hazard at Yucca Mountain for use in EPRI performance assessment, in Yucca Mountain total system performance assessment, Phase 3*, Prepared by Kessler, J., and R. McGuire, EPRI TR-107191 3055-02 Final Report, Palo Alto, CA, Electric Power Research Institute, 11-1 to 11-15, 1996.

Coppersmith, K.J., and R.R. Youngs, *Risk-Based Approach to High-Level Waste Repository Evaluation Plan 2,* EPRI TR-100384, 1992.

Cornell C.A., and E.H. Van Marke, *The major influences on seismic risk,* Proceedings, Third World Conference on Earthquake Engineering, Santiago Chile, A1: 3–14, 1969.

Cornwall, H.R., *Geology and mineral deposits of Nye County, Nevada,* Nevada Bureau of Mines and Geology Bulletin 77, Reno, NV, Nevada Bureau of Mines, 1972.

Cornwall, H.R., and F.J. Kleinhample, *Geology of the Bare Mountain Quadrangle,* U.S. Geological Quadrangle Map GQ-157, Scale 1:62,500, Reston, VA, U.S. Geological Survey, 1961.

Cornwall, H.R., and F.J. Kleinhample, *Geology of the Bullfrog quadrangle and ore deposits related to the Bullfrog Hills caldera, Nye County, Nevada and Inyo County, California,* U.S. Geological Survey Professional Paper 454-J, Reston, VA, U.S. Geological Survey, 1964.

Crider, J.G., and D.D. Pollard, *Fault linkage: Three-dimensional mechanical interaction between echelon normal faults,* Journal of Geophysical Research 103(B10), 24,373–24,391, 1998.

Crowe, B., F. Perry, J. Geissman, L. McFadden, S. Wells, M. Murrell, J. Poths, G.A. Valentine, L. Bowker, and K. Finnegan, *Status of volcanism for the Yucca Mountain site characterization project*, Los Alamos National Laboratory Report 12908-MS, Los Alamos, NM, Los Alamos National Laboratory, 2-18 to 2-21, 1995.

Crowe, B.M., D.T.. Vaniman, and W.J. Carr, *Status of Volcanic Hazard Studies for the Nevada Nuclear Waste Storage Investigation*, Los Alamos National Laboratory Report LA-9325-MS, Los Alamos, NM, Los Alamos National Laboratory, 1983.

Czarnecki. J.B., C.C. Faunt, C.W. Gable, and G.A. Zyvoloski, *Hydrogeology and Preliminary Three-Dimensional Finite-element Groundwater Flow Model of the Site Saturate Zone, Yucca Mountain, Nevada,* Yucca Mountain Project Milestone Report SP23NM3, Denver, CO: U.S. Geological Survey, 1997.

Davies, R.K., M Crawford, W.F. Dula, Jr., M. Cole, and G. Dorn, *Outcrop interpretation of seismic-scale normal faults in southern Oregon: Description of structural styles and evaluation of subsurface interpretation methods,* The Leading Edge 16, 1,135–1,141, 1997.

Davis, G.A., and P.J. Coney, *Geologic development of the metamorphic core complexes,* Geology 7, 120–124, 1979.

Dawers, N.H., and M.H. Anders, *Displacement-length scaling and fault linkage,* Journal of Structural Geology 17, 607–614, 1995.

Day, W.C., C.J. Potter, D.S. Sweetkind, R.P. Dickerson, and C.A. San Juan, *Bedrock geologic map of the central block area, Yucca Mountain, Nye County, Nevada,* U.S. Geological Survey Miscellaneous Investigations Series Map I-2601, Denver, CO, U.S. Geological Survey, Scale 1:6000, 1997.

Day, W.C., R.P. Dickerson, C.J. Potter, D.S. Sweetkind, C.A. San Juan, R.M. Drake, II, and C.J. Fridrich, *Geologic map of the Yucca Mountain Area, Nye County, Nevada, Scale 1:24,000,* U.S. Geological Survey, Geological Investigations Series I-2627, 1998.

dePolo, C.M., *The maximum background earthquake in the Basin and Range,* Bulletin of the Seismological Society of America 84, 466–472, 1994.

dePolo, C.M., D.G. Clark, D.B. Slemmons, and A.R. Ramelli, *Historical surface faulting in the Basin and Range Province, western North America, Implications for fault segmentation,* Journal of Structural Geology, 13: 123–126, 1991.

Dickenson, W.R., *Kinematics of Transrotational Tectonism in the California Transverse Ranges and Its Contribution to Cumulative Slip Along the San Andreas Transform Fault System,* Geological Society of America Special Paper 305, Boulder, CO, Geological Society of America, 1996.

Dokka, R.K., and C.J. Travis, *Role of the eastern California shear zone in accommodating Pacific-North American plate motion,* Geophysical Research Letters 17, 1,223–1,326, 1990.

Dula, W.F., Jr., *Geometric models of listric normal faults and rollover folds*, American Association of Petroleum Geologists Bulletin 75, 1,609–1,625, 1990.

Dunne, W.M., and D.A. Ferrill, *Fractal strain distribution and its implications for cross-section balancing, Discussion*, Journal of Structural Geology 17, 757–760, 1995.

Dupin, J.-M., W. Sassi, and J. Angelier, *Homogeneous stress hypothesis and actual fault slip, a distinct element analysis*, Journal of Structural Geology 15, 1,033–1,043, 1993.

Eldredge, S., V. Bachtadse, and R. Van der Voo, *Paleomagnetism and the orocline hypothesis*, Tectonophysics 119, 153–179, 1985.

Engelder, T., *Stress Regimes in the Lithosphere*, Princeton, NJ, Princeton University Press, 1993.

Engelder, T., and M.P. Fischer, *Loading configurations and driving mechanisms for joints based on the Griffith energy-balance concept*, Tectonophysics 256, 253–277, 1996.

Evans, J.P., C.B. Foster, and J.V. Goddard, *Permeability of fault-related rocks, and implications for hydraulic structure of fault zones*, Journal of Structural Geology 19, 1,393–1,404,1997.

Farrell, D.A., A. Armstrong, J.R. Winterle, D.R. Turner, D.A. Ferrill, J.A. Stamatakos, N.M. Coleman, M.B. Gray, and S.K. Sandberg, *Structural controls on groundwater flow in the Yucca Mountain region*, CNWRA Report, San Antonio, TX: Center for Nuclear Waste Regulatory Analyses, 1999.

Faulds, J.E., J.W. Bell, D.L. Feuerbach, and A.R. Ramelli, *Geologic map of the Crater Flat Area, Nevada*, Nevada Bureau of Mines and Geology Map 101, Scale 1:24,000, Reno, NV, Nevada Bureau of Mines and Geology, University of Nevada, Reno, 1994.

Fedotov, S.A., and Y.K. Markhinin, *The Great Tolbachik Fissure Eruption*, Cambridge, United Kingdom, Cambridge University Press, 1983.

Ferrill, D.A., and W.M. Dunne, *Cover deformation above a blind duplex, an example from West Virginia, U.S.A.*, Journal of Structural Geology 11, 421–431, 1989.

Ferrill, D.A, and R.H. Groshong, Jr., *Kinematic model for the curvature of the northern Subalpine Chain, France*, Journal of Structural Geology 15, 523–541, 1993.

Ferrill, D.A., and A.P. Morris, *Geometric considerations of deformation above curved normal faults and salt evacuation surfaces*, The Leading Edge 16, 1,129–1,133, 1997.

Ferrill, D.A., S.R. Young, G.L. Stirewalt, A.P. Morris, and D.B. Henderson, *Tectonic processes in the central Basin and Range region*, NRC High-Level Radioactive Waste Research at Center for Nuclear Waste Regulatory Analyses, January–June 1994, B. Sagar, ed, CNWRA 94-015, San Antonio, TX, Center for Nuclear Waste Regulatory Analyses, 139–160, 1994.

Ferrill, D.A., D.B. Henderson, J.A. Stamatakos, K.H. Spivey, and A.P. Morris, *Tectonic processes in the central Basin and Range*, NRC High-Level Radioactive Waste Research at CNWRA, January-June, 1995, B. Sagar, ed, CNWRA 95-01S, San Antonio, TX, Center for Nuclear Waste Regulatory Analyses, 6.1–6.27, 1995a.

Ferrill, D.A., A.P. Morris, D.B. Henderson, and R.H. Martin, Tectonic Processes in the central Basin and Range region, In B. Sagar ed, *NRC High-Level Radioactive Waste Research at CNWRA, July-December 1994*, San Antonio, TX, Center for Nuclear Waste Regulatory Analyses: 121–139, 1995b.

Ferrill, D.A., J.A. Stamatakos, S.M. Jones, B. Rahe, H.L. McKague, R.H. Martin, and A.P. Morris, *Quaternary slip history of the Bare Mountain fault (Nevada) from the morphology and distribution of alluvial fan deposits*, Geology 24, 559–562, 1996a.

Ferrill, D.A., G.L. Stirewalt, D.B. Henderson, J.A. Stamatakos, K.H. Spivey, and B.P. Wernicke, *Faulting in the Yucca Mountain Region, Critical Review and Analyses of Tectonic Data from the Central Basin and Range*, NUREG/CR-6401, Washington, D.C., U.S. Nuclear Regulatory Commission, 1996b.

Ferrill, D.A., J.A. Stamatakos, and A.P. Morris, *Structural controls on progressive deformation of the Yucca Mountain (Nevada) region*, Geological Society of America Abstracts with Programs 28, A–192, 1996c.

Ferrill, D.A., C.B. Connor, J.A. Stamatakos, H.L. McKague, B.E. Hill, G.I. Ofoegbu, and R. Terhune, *Modeling fault-dike interaction: Implications for lateral diversion of dikes and alignment of volcanoes in the Yucca Mountain (Nevada) Region*, IM 20-5708-471-760, San Antonio, TX, Center for Nuclear Waste Regulatory Analyses, 1997a.

Ferrill, D.A., J.A. Stamatakos, and H.L. McKague, *Quaternary slip history of the Bare Mountain fault (Nevada) from the morphology and distribution of alluvial fan deposits, REPLY*, Geology 25, 190, 1997b.

Ferrill, D.A., A.P. Morris, S.M. Jones, and J.A. Stamatakos, *Extensional layer-parallel shear and normal faulting*, Journal of Structural Geology 20, 355–362, 1998a.

Ferrill, D.A., A. P. Morris, J.A. Stamatakos, and D. Sims, *Crossing conjugate normal faults*, IM 20 1402-47771-950 (invited manuscript to American Association of Petroleum Geologists Book, "Recognition and Characterization of Reservoir Scale Structures"), 1998b.

Ferrill, D.A., J.A. Stamatakos, and D. Sims, *Normal fault corrugation: Implications for growth and seismicity of active normal faults*, Journal of Structural Geology, In press, 1999a.

Ferrill, D.A., J.R. Winterle, G. Wittmeyer, D. Sims, S. Colton, A. Armstrong, and A.P. Morris, *Stressed rock strains groundwater at Yucca Mountain, Nevada*, GSA Today 9, 1–8, 1999b.

Finkbeiner, T., C.A. Barton, and M. Zoback, *Relationships among in-situ stress, fractures and faults, and fluid flow, Monterey formation, Santa Maria Basin, California*, American Association of Petroleum Geologists Bulletin 81, 1,975–1,999, 1997.

Fleck, R.J., B.D. Turrin, D.A. Sawyer, R.G. Warren, D.E. Champion, M.R. Hudson, and S.A. Minor, *Age and character of basaltic rocks of the Yucca Mountain region, southern Nevada*, Journal of Geophysical Research 101, 8,205–8,227, 1996.

Flint, L.E., and A.L. Flint, *Shallow infiltration processes at Yucca Mountain, Nevada-Neutron logging data 1984-93*, U.S. Geological Survey Water-Resources Investigations Report 95-4035, Denver, CO, U.S. Geological Survey, 1995.

Flint, A.L., J.A. Hevesi, and L.E. Flint, *Conceptual and Numerical Model of Infiltration for the Yucca Mountain Area, Nevada*, U.S. Geological Survey Water Resources Investigation Report, Milestone 3GUI623M, Denver, CO, U.S. Geological Survey, 1996.

Frankel, A., *Mapping Seismic hazard in the central and eastern United States*, Seismological Research Letters 66, 8–21, 1995.

Freeze, R.A., and J.A. Cherry, *Groundwater*, Englewood Cliffs, NJ, Prentice-Hall, Inc., 604, 1979.

Freund, R., *Kinematics of transform and transcurrent faults*, Tectonophysics 21, 93–134, 1974.

Fridrich, C.J., *Tectonic Evolution of the Crater Flat Basin Yucca Mountain Region, Nevada, Denozoic Basins of the Death Valley Region*, U.S. Geological Survey Open-File Report 98-33, Denver, CO, U.S. Geological Survey 43, 1998.

Fridrich, C.J., W.W. Dudley, Jr., and J.S. Stuckless, *Hydrogeologic analysis of the saturated-zone ground-water system, under Yucca Mountain, Nevada*, Journal of Hydrology 154, 133–168, 1994.

Fridrich, C.J., J.W. Whitney, M.R. Hudson, and B.M. Crowe, *Late Cenozoic extension, vertical axis rotation, and volcanism in the Crater Flat basin, southwest Nevada, Cenozoic basins of the Death Valley region*, L. Wright and B. Troxel, ed's, Geological Society of America Special Paper, 1999, In press.

Frizzell, V.A. Jr., and J. Shulters, *Geologic Map of the Nevada Test Site, Southern Nevada*, U.S. Geological Survey Miscellaneous Investigations Series, Map I-2046, scale 1:100,000, Denver, CO, U.S. Geological Survey, 1990.

Gabrielse, H., W.S. Snyder, and J.H. Stewart, *Sonoma orogeny and Permian to Triassic tectonism in western North America*, Geology 11, 484–486, 1983.

Gauthier, J.H., ML. Wilson, D.J. Borns, and B.W. Arnold, *Impact of seismic activity on long-term repository performance at Yucca Mountain*, Proceedings of the Topical Meeting on Methods of Seismic Hazard Evaluation, Focus 95, Las Vegas, NV, 1995.

Gay, N.C., and W.D. Ortlepp, *Anatomy of a mining-induced fault zone*, Geological Society of America Bulletin Part I, 90, 47–58, 1979.

Geldon, A.L., A.M.A. Umari, M.F. Fahy, J.D. Earle, J.M. Gemmell, and J. Darnell, *Results of hydraulic and conservative tracer tests in miocene tuffaceous rocks at the C-Hole complex, 1995 to 1997, Yucca Mountain, Nye County, Nevada*, 1997 Milestone Report SP23PM3, Las Vegas, NV, U.S. Geological Survey, 1997.

Ghosh, A., R.D. Manteufel, and G.L. Stirewalt, *FAULTING Version 1.0 – A code for simulation of direct fault disruption*, Technical description and User's Guide, CNWRA 97-002, San Antonio, TX, Center for Nuclear Waste Regulatory Analyses, 1997.

Gillett, S.L., and J.W. Geissman, *Regional Late Paleozoic remagnetization of shallow-water carbonate rocks in the Great Basin, The usefulness of "micro"-fold tests from late compaction fabrics*, Application of Paleomagnetism to Sedimentary Geology, Society for Sedimentary Geology (SEPM) Special Publication 49, 129–147, 1993.

Gillett, S.L., and D.R. Van Alstine, *Remagnetization and tectonic rotation of Upper Precambrian and Lower Paleozoic strata from the Desert Range, southern Nevada*, Journal of Geophysical Research 87, 10,929–10,953, 1982.

Gilmore, T.D., *Geodetic leveling data used to define historical height changes between Tonopah Junction and Las Vegas, Nevada*, U.S. Geological Survey Open-File Report 92-450, Menlo Park, CA, U.S. Geological Survey, 1992.

Goddard, J.V., and J.P. Evans, *Chemical changes and fluid-rock interactions in faults of crystalline thrust sheets, northwestern Wyoming, USA*, Journal of Structural Geology 17, 533–547, 1995.

Gray, M.B., and J.A. Stamatakos, *A new model for evolution of fold and thrust belt curvature from integrated structural and paleomagnetic results around the Pennsylvania Salient*, Geology 25, 1,067–1,070, 1998.

Gray, M.B., J.A. Stamatakos, and D.A. Ferrill, *Microstructural and microtextural analyses of faulting at Yucca Mountain, Nevada*, EOS, Transactions of the American Geophysical Union 79(45), F823, 1998.

Groshong, Jr., R.H., *Low-temperature deformation mechanisms and their interpretation*, Geological Society of America Bulletin 100, 1,329–1,360, 1988.

Groshong, Jr., R.H., *Unique determinations of normal fault shape from hanging-wall bed geometry in detached half grabens*, Eclogae Geologica Helvetica 83, 455–471, 1990.

Grow, J.A., C.E. Barker, and A.G. Harris, *Oil and gas exploration near Yucca Mountain, southern Nevada*, Proceedings of Fifth Annual International Conference on High-Level Radioactive Waste Management, La Grange Park, IL, American Nuclear Society International, 1,298–1,315, 1994.

Gutenberg, B., and C.F. Richter, *Seismicity of the Earth*, Princeton, NJ, Princeton University Press, 1954.

Gutenberg, B., and C.F. Richter, *Earthquake magnitude, intensity, energy, and acceleration*, Bulletin of the Seismological Society of America 46, 105–145, 1956.

Hamilton, W.B., Crustal extension in the Basin and Range province, southwestern United States, *Continental Extensional Tectonics*, M.P. Coward, J.F. Dewey, and P.L. Hancock, eds, London, England, Geological Society Special Publications 28, 155–176, 1987.

Hamilton, W.B., Detachment faulting in the Death Valley Region, California and Nevada, *Geologic and hydrologic investigations of a potential nuclear waste disposal site at Yucca Mountain, southern Nevada*, M.D. Carr and J.C. Yount, eds, U.S. Geological Survey Bulletin 1790, 51–85, 1988.

Hanks, T.C., and H. Kanamori, *A moment-magnitude scale*, Journal of Geophysical Research 84, 2,348–2,350, 1979.

Hardyman, R.F., and J.S. Oldow, *Tertiary tectonic framework and Cenozoic history of the central Walker Lane, Nevada, Geology and Ore Deposits of the Great Basin*, G.L. Raines, R.E. Lisle, R.W. Schafer, W.H. Wilkinson, eds, Las Vegas, NV, Geological Society of Nevada Symposium Proceedings 1, 279–301, 1991.

Harmsen, S.C., *Seismicity and focal mechanisms for the southern Great Basin of Nevada and California in 1990*, USGS Open-File Report 91-367, U.S. Geological Survey, 1991.

Harmsen, S.C., *Seismicity and focal mechanisms for the southern Great Basin of Nevada and California in 1991*, USGS Open-File Report 92-340, U.S. Geological Survey, 1993.

Harmsen, S.C., *The Little Skull Mountain, Nevada, earthquake of 29 June 1992: Aftershock focal mechanisms and tectonic stress field implications*, Bulletin of the Seismological Society of America 84, 1,484–1,505, 1994.

Harmsen, S.C., and C.G. Bufe, *Seismicity and focal mechanisms for the southern Great Basin of Nevada and California, 1987 through 1989*, USGS Open-File Report 91-572, U.S. Geological Survey, 1992.

Henderson, D.B., D.A. Ferrill, and K.C. Clarke, *Mapping geological faults using image processing techniques applied to hill-shaded digital elevation models*, Proceedings of the IEEE Southwest Symposium on Image Analysis, San Antonio, TX, 1996.

Higgs, W.G., G.D. Williams, and C.M. Powell, *Evidence for flexural shear folding associated with extension al faults*, Geological Society of America Bulletin 103, 710–717, 1991.

Hill, B.E., and C.B. Connor, *Volcanic systems of the Basin and Range*, NRC High-Level Radioactive Waste Research at CNWRA, July–December, 1995, B. Sagar ed, CNWRA 95-02S, San Antonio, TX, Center for Nuclear Waste Regulatory Analyses, 5-1 to 5-21, 1996.

Hill, C.A., Y.V. Dublyansky, R.S. Harmon, and C.M. Schluter, *Overview of calcite/opal deposits at or near the proposed high-level nuclear waste site, Yucca Mountain, Nevada, USA, Pedogenic, hypogene, or both?* Environmental Geology 26, 69–88, 1995.

Hodges, K.V., and J.D. Walker, *Extension in the Cretaceous Sevier orogeny, North American Cordillera*, Geological Society of America Bulletin 104, 560–569, 1992.

Hoek, E., and E.T. Brown, *Underground Excavations in Rock*, The Institution of Mining and Metallurgy, London, Hertford, England, Stephen Austin and Sons, Ltd, 1980.

Hoisch, T.D., and C. Simpson, *Rise and tilt of metamorphic rocks in the lower plate of a detachment fault in the Funeral Mountains, Death Valley, California*, Journal of Geophysical Research 98, 6,805–6,827, 1993.

Hoisch, T.D., M.T. Heizler, and R.E. Zartman, *Timing of detachment faulting in the Bullfrog Hills and Bare Mountain area, southwestern Nevada, Inferences from $^{40}Ar/^{39}Ar$, K-Ar, U-Pb, and fission track thermochronology*, Journal of Geophysical Research 102, 2,815–2,833, 1997.

Holm, D.K., J.W. Geissman, and B. Wernicke, *Tilt and rotation of the footwall of a major normal fault system, Paleomagnetism of the Black Mountains, Death Valley extended terrain, California*, Geological Society of America Bulletin 105, 1,373–1,387, 1993.

Hudson, M.R., *Paleomagnetic data bearing on the origin of arcuate structures in the French Peak-Massachusetts Mountains area of southern Nevada*, Geological Society of America Bulletin 104, 581–594, 1992.

Hudson, M.R., D.A. Sawyer, and R.G. Warren, *Paleomagnetism and rotation constraints for the Miocene southwestern Nevada volcanic field*, Tectonics 13, 258–277, 1994.

Hudson, M.R., S.A. Minor, and C.J. Fridrich, *The distribution, timing, and character of steep-axis rotations in a broad zone of dextral shear in southwestern Nevada*, Geological Society of America Abstracts with Programs 28, Denver, CO, Geological Society of America, A451, 1996.

Hunter, R.L., and C.J. Mann, *Techniques for determining probabilities of events and processes affecting the performance of repositories*, SAND83-1342, NUREG/CR-3354, Albuquerque, NM, Sandia National Laboratory, 1990.

Idriss, I.M., *Earthquake ground motions at soft soil sites*, 2nd International Conference on Recent Advances in Geotechnical Earthquake Engineering and Soil Dynamics 3, 2,265–2,272, 1991.

Jaeger, J.C., and N.G.W. Cook, *Fundamentals of Rock Mechanics*, Chapman and Hall, New York, NY, 1979.

Janssen, B., *Modelisation numerique de l'extension de la croute terrestre avec des examples du basin and range, Etats-Unis*, These de doctorat, l'Universite Louis-Pasteur de Strasbourg, 1995.

Joyner, W.B., and D.M. Boore, *Peak horizontal acceleration and velocity from strong motion records including records from the 1979 Imperial Valley, California, earthquake*, Bulletin of the Seismological Society of America 71, 2,011–2,038, 1981.

Kane, M.F., and R.E. Bracken, *Aeromagnetic map of Yucca Mountain and Surrounding Regions, Southwest Nevada*, USGS Open-File Report 83-616, Reston, VA, U.S. Geological Survey, 1983.

King, G.C.P., R.S. Stein, and J. Lin, *Static stress changes and triggering of earthquakes*, Bulletin of the Seismological Society of America 84, 935–953, 1994.

Klinger, R.E., and L.W. Anderson, *Topographic profiles and their implications for late Quaternary activity on the Bare Mountain fault, Nye County, Nevada*, Geological Society of America Abstracts with Programs, A63, 1994.

Knipe, R.J., *Juxtaposition and seal diagrams to help analyze fault seals in hydrocarbon reservoirs*, American Association of Petroleum Geologists Bulletin 81(2),187–195, 1997.
Krantz, R.W., *Multiple fault sets and three-dimensional strain: Theory and application*, Journal of Structural Geology 10, 225–237, 1988.

Langenheim, V.E., and D.A. Ponce, *Ground magnetic studies along a regional seismic-reflection profile across Bare Mountain, Crater Flat and Yucca Mountain, Nevada*, USGS Open-File Report 95-834, U.S. Geological Survey, 1995.

Langenheim, V.E., S.F. Carle, D.A. Ponce, and J.D. Phillips, *Revision of an Aeromagnetic Survey in the Lathrop Wells Area, Nevada*, USGS Open-File Report 91-46, Reston, VA, U.S. Geological Survey, 1991.

Langenheim, V.E., K.S. Kirchoff-Stein, and H.W. Oliver, *Geophysical investigations of buried volcanic centers near Yucca Mountain, Nevada*, Proceedings of the Third International High Level Radioactive Waste Management Conference, La Grange Park, IL, American Nuclear Society, 1,840–1,846, 1993.

Le Cain, G.D., *Air-injection Testing in Vertical Boreholes in Welded and Nonwelded Tuff, Yucca Mountain, Nevada*, U.S. Geological Survey, Water-Resources Investigation Report, 96-4262, 1997.

Levy, S.S., D.S. Sweetkind, D.S. Fabryka-Martin, P.R. Dixon, J.L. Roach, L.E. Wolfsberg, D. Elmore, and P. Sharma, *Investigations of structural controls and mineralogic associations of Chlorine-36 fast pathways in the ESF*, Los Alamos Milestone SP2301M4, Los Alamos, NM, Los Alamos National Labs, 1997.

Lienkaemper, J.J., S.K. Pezzopane, M.M. Clark, and M.J. Rymer, *Fault fractures formed in association with the 1986 Chalfant Valley, California, earthquake sequence, Preliminary report*, Bulletin of the Seismological Society of America 77(1), 297–305, 1987.

Lin, M., M.P. Hardy, and S.J. Bauer, *Fracture analysis and rock quality designation estimation for the Yucca Mountain site characterization project*, SAND92-0449, 1993.

Luhr, J.F., and T. Simkin, *Parícutin, the Volcano Born in a Mexican Cornfield*, Phoenix, AZ, Geosciences Press Inc., 1993.

Majer, E.L., M. Feighner, L. Johnson, K. Lee, T. Daley, E. Karageorgi, P. Parker, T. Smith, K. Williams, A. Romero, and T. McEvilly, Milestone 0BB02, *Results of Geophysical Surveys Along North-South and South ESF Alignment* and Milestone 0BB03, *Summary Report, Interpretations of Multiple Geophysical Surveys*, Berkeley, CA, Ernest Orlando Lawrence Berkeley National Laboratory, 1997.

Maldonado, F., *Structural geology of the upper plate of the Bullfrog Hills detachment fault system, southern Nevada*, Geological Society of America Bulletin 102, 992–1,006, 1990.

Maldonado, F., and B.P. Hausback, *Geologic map of the northern quarter of the Bullfrog 15-minute quadrangle, Nye County, Nevada*, U.S. Geological Survey Miscellaneous Investigations Series Map I-2049 Scale 1:24,000, 1990b.

Marrett, R., J.A. Stamatakos, D.A. Ferrill, C.B. Connor, and B.E. Hill, *Extension rate estimates from faults, fracture opening, and earthquakes near Yucca Mountain, Nevada*, EOS, transactions of American Geophysical Union 80(17), F203, 1998.

Marshak, S., *Kinematics of orocline and arc formation in thin-skinned orogens*, Tectonics 7, 73–86, 1988.

Martinez, L.J., C.M. Meertens, and R.B. Smith, *Rapid deformation rates along the Wasatch fault zone, Utah, from first GPS measurements with implication for earthquake hazard*, Geophysical Research Letters 25, 567–570, 1998.

Mayer, J.R., and J.M. Sharp, Jr., *Fracture control of regional groundwater flow in a carbonate aquifer in a semi-arid region*, Geological Society of America Bulletin 110(2), 269–283, 1998.

McConnell, K.I., M.E. Blackford, and A.K. Ibrahim, *Staff Technical Position on Investigations to Identify Fault Displacement Hazards and Seismic Hazards at a Geologic Repository*, NUREG–1451, Washington, D.C.: U.S. Nuclear Regulatory Commission, 1992.

McDuffie, S.M., C.B. Connor, and K.D. Mahrer, *A simple 2-D stress model of dike-fracture interaction*, EOS, Transactions of the American Geophysical Union 75(16), 345, 1994.

McKague, H. L., *Identification of Type II Faults in the Yucca Mountain Area, Rev 2*, Letter Report, San Antonio, TX, Center for Nuclear Regulatory Analyses, 1996.

McKague, H.L., J.A. Stamatakos, and D.A. Ferrill, *Type I Faults in the Yucca Mountain Region*, CNWRA 96-007 Rev. 1, San Antonio, TX, Center for Nuclear Waste Regulatory Analyses, 1996.

McKenzie, D., and M.J. Bickle, *The volume and composition of melt generated by extension of the lithosphere*, Journal of Petrology 29, 625–679, 1988.

Menges, C.W., J.W. Whitney, J.A. Coe, J.R. Wesling, F.H. Swan, E.M. Taylor, and D.J. Ponti, *Summary of paleoseismic investigations of the Paintbrush Canyon, Bow Ridge, and Stagecoach Road faults of eastern Yucca Mountain, Nye County, Nevada*, U.S. Geological Survey Open-File Report 95-738, Denver, CO, U.S. Geological Survey, 1995.

Meremonte, M., J. Gomberg, and E. Cranswick, *Constraints on the 29 June 1992 Little Skull Mountain, Nevada, earthquake sequence provided by robust hypocenter estimate,* Bulletin of the Seismological Society 85, 1,039–1,049, 1995.

Minor, S.A., *Superposed local and regional paleostresses: Fault-slip analysis of neogene extensional faulting near coeval caldera complexes, Yucca Flat, Nevada,* Journal of Geophysical Research 100, 12,507–12,528, 1995.

Minor, S.A., M.R. Hudson, and C.J. Fridrich, *Fault-slip data, paleomagnetic data, and paleostress analyses bearing on the neogene tectonic evolution of northern Crater Flat Basin, Nevada,* U.S. Geological Survey Open File Report 97-285, Denver, CO, U.S. Geological Survey, 1997.

Mohanty, S., and T.J. McCartin, *Total systems performance assessment (TPA) Version 3.2 code: Module description user's guide,* San Antonio, TX, Center for Nuclear Waste Regulatory Analyses, 1998.

Mohanty, S., R. Codell, R.W. Rice, J. Weldy, Y. Lu, R.M. Byrne, T.J. McCartin, M.S. Jarzemba, and G.W. Wittmeyer, *System-level repository sensitivity analyses using TPA Version 3.2,* San Antonio, TX, Center for Nuclear Waste Regulatory Analyses, 1999.

Monsen, S.A., *Structural Evolution and Metamorphic Petrology of the Precambrian-Cambrian Strata, Northwest Bare Mountain, Nevada,* M.S. thesis, Davis, CA, University of California at Davis, 1983.

Monsen, S.A., M.D. Carr, M.C. Reheis, and P.A. Orkild, *Geologic map of Bare Mountain, Nye County, Nevada,* U.S. Geological Survey Miscellaneous Investigations Series Map I-2201, Scale 1:24,000, 1992.

Montazer, P., and W.E. Wilson, *Conceptual hydrologic model of flow in the unsaturated zone, Yucca Mountain, Nevada,* Water Resources Investigations Report 84-4345, Lakewood, CO, U.S. Geological Survey, 1984.

Morris, A.P., and D.A. Ferrill, *Constant-thickness deformation above curved normal faults,* Journal of Structural Geology 21, 67–83, 1999.

Morris, A.P., D.A. Ferrill, and D.B. Henderson, *Slip-tendency analysis and fault reactivation,* Geology 24, 275–278, 1996.

Mozley, P.S., and L.B. Goodwin, *Patterns of cementation along a Cenozoic normal fault: A record of paleoflow orientations,* Geology 23, 539–542, 1995.

Nakata, J.K., C.M. Wentworth, and M.N. Machette, *Quaternary Fault Maps of the Basin and Range and Rio Grande Rift Provinces, Western United States,* U.S. Geological Survey Open-File Report 82-579, Denver, CO, U.S. Geological Survey, Scale 1:2,500,000, 1982.

National Research Council, Commission of Physical Sciences, Mathematic, and Resources, *Probabilistic seismic hazard analysis,* National Academy Press, Washington, D.C., 1988.

National Research Council, *Rock Fractures and Fluid Flow*, National Academy Press, Washington, D.C., 1996.

Nelson, M.R., and C.H. Jones, *Paleomagnetism and crustal rotations along a shear zone, Las Vegas range, southern Nevada*, Tectonics 6, 13–33, 1987.

Nilsen, T.J., and J.H. Stewart, *The Antler Orogeny; Mid-Paleozoic tectonism in western North America*, Geology 8, 298–302, 1980.

Noble D.C., S.I. Weiss, and S.M. Green, *High-salinity fluid inclusions suggest that Miocene gold deposits of the Bare Mountain district, Nevada, are related to a large buried rare-metal rich magmatic system*, Geological Society of America Abstracts with Programs 21, Boulder, CO, Geological Society of America, A123, 1989.

Noble, D.C., S.I. Weiss, and E.H. McKee, *Magmatic and Hydrothermal Activity, Caldera Geology, and Regional Extension in the Western Part of the Southwestern Nevada Volcanic Field*, Geology and Ore Deposits of the Great Basin, G.L. Raines, R.E. Lisle, R.W. Shafer and W.W. Wilkerson, eds. Reno, NV, Geological Society of Nevada, 913–934, 1991.

Ofoegbu, G.I., and D.A. Ferrill, *Finite Element Modeling of Listric Normal Faulting*, CNWRA 95-008, San Antonio, TX, Center for Nuclear Waste Regulatory Analyses, 1995.

Ofoegbu, G.I., and D.A. Ferrill, *Mechanical analyses of a Yucca Mountain fault model, Proceedings of the Topical Meeting on Methods of Seismic Hazards Evaluation, Focus '95*, La Grange Park, IL, American Nuclear Society, 115–124, 1996.

Ofoegbu, G.I., and D.A. Ferrill, *Mechanical analyses of listric normal faulting with emphasis on seismicity assessment*, Tectonophysics 284, 65–77, 1998.

Oldow, J.S., *Spatial variability in the structure of the Roberts Mountain allochthon, western Nevada*, Geological Society of America Bulletin 95, 174–185, 1984.

Oldow, J.S., G. Kohler, and R.A. Donelick, *Late Cenozoic extensional transfer in the Walker Lane strike-slip belt, Nevada*, Geology 22, 637–640, 1994.

Oliver, H.W., and K.F. Fox, *Structure of Crater Flat and Yucca Mountain, southeastern Nevada, as interpreted from gravity data*, Proceedings of the Fourth Annual International Conference, Las Vegas, Nevada, La Grange Park, IL, American Nuclear Society, 1,812–1,817, 1993.

Paces, J.B., L.A. Neymark, B.D. Marshall, J.F. Whelan, and Z.E. Peterman, *Ages and origins of subsurface secondary minerals in the Exploratory Studies Facility (ESF)*, U.S. Geological Survey—Yucca Mountain Project Branch 1996 Milestone Report 3GQH450M, Denver, CO, U.S. Geological Survey, 1996.

Parsons, T., and G.A. Anderson, *The role of magma overpressure in suppressing earthquakes and topography: Worldwide Examples*, Science 253, 1,399–1,402.

Peacock, D.C.P., and D.J. Sanderson, *Displacements, segment linkage, and relay ramps in normal fault zones*, Journal of Structural Geology 13, 721–733, 1991.

Peacock, D.C.P., and D.J. Sanderson, *Geometry and development of relay ramps in normal fault systems*, American Association of Petroleum Geologists Bulletin 78, 147–165, 1994.

Pezzopane, S.K., *Preliminary table of characteristics of known and suspected quaternary faults in the Yucca Mountain Region*, U.S. Geological Survey Administrative Report, Denver, CO, U.S. Geological Survey, 1996.

Pezzopane, S.K., R.E. Carande, K.D. Smith, *Preliminary surface displacement of the Little Skull Mountain earthquake measured by satellite radar interferometry of the Yucca Mountain Region, Nevada*, EOS, Transactions, American Geophysical Union S1, 1999.

Piety, L.A., *Compilation of known and suspected quaternary faults within 100 km of Yucca Mountain*, Scale 1:250,000, U.S. Geological Survey Open File Report 94-112, Denver, CO, U.S. Geological Survey, 1995.

Ponce, D.A., and H.W. Oliver, *Gravity investigations, Major results of geophysical investigations at Yucca Mountain and Vicinity, southern Nevada*, USGS Open-File Report 95-74, H.W. Oliver, D.A. Ponce, and W.C. Hunter, eds, Menlo Park, CA, U.S. Geological Survey, 1995.

Ponce, D.A., S.B. Kohrn, and S. Waddell, *Gravity and magnetic data of Fortymile Wash, Nevada Test Site, Nevada*, USGS Open-File Report 92-343, Reston, VA, U.S. Geological Survey, 1992.

Poole, F.G., J.H. Stewart, A.P. Palmer, C.A. Sandberg, R.J. Madrid, R.J. Ross, Jr., L.F. Hintze, M.M. Miller, and C.T. Wrucke, *Latest Precambrian to latest Devonian time; Development of a continental margin, The Cordilleran Orogen, Conterminous U.S.*, The Geology of North America Volume G-3, B.C. Burchfiel, P.W., Lipman, and M.L. Zoback, eds, Boulder, CO, Geological Society of America, 407–479, 1992.

Potter, C.J., Personal communication, 1999.

Potter, C.J., W.C. Day, D.S. Sweetkind, and R.P. Dickerson, *Fault styles and strain accommodation in the Tiva Canyon Tuff, Yucca Mountain, Nevada*, EOS, Transactions, American Geophysical Union 77(17), S265, 1996.

Prave, A.R., and L.A. Wright, *Isopach patterns in the Lower Cambrian Zabriskie Quartzite: How useful in tectonic reconstructions?*, Geology 14, 251–254, 1986.

Rahe, B., D.A. Ferrill, and A.P. Morris, *Physical analog modeling of pull-apart basin evolution*, Tectonophysics 285, 21–40, 1997.

Ramsay, J.G., and M.I. Huber, *The techniques of modern structural geology volume 2: folds and fractures*, Academic Press, London, 700, 1987.

Ransome, F.L., W.H. Emmons, and G.H. Gary, *Geology and ore deposits of the Bullfrog District, Nevada*, U.S. Geological Survey Bulletin 407, 1910.

Reheis, M.C., Preliminary study of quaternary faulting on the east side of Bare Mountain, Nye County, Nevada, *Geologic and Hydrologic Investigations of a Potential Nuclear Waste Disposal Site at Yucca Mountain, Southern Nevada*, M.D. Carr, J.C. Yount, eds, U.S. Geological Bulletin 1790, 103–112, 1988.

Reheis, M.C., *Holocene faulting along the central Fish Lake Valley Fault Zone, California and Nevada*, Geological Society of America Abstracts with Programs-1994 Cordilleran Section Meeting, Boulder, CO, Geological Society of America 26, 83, 1994.

Reheis, M.C., and T.H. Dixon, *Kinematics of the Eastern California shear zone: evidence for slip transfer from Owens and Saline Valley fault zones to Fish Lake Valley Fault zone*, Geology 24, 339–342, 1996.

Reheis, M.C., and T.L. Sawyer, *Late Cenozoic history and slip rate of the Fish Lake Valley, Emigrant Peak, and Deep Springs fault zones, Nevada and California*, Geological Society of America Bulletin 109, 280–299, 1997.

Reiter, L., *Earthquake hazard analysis, Issues and Insights*, Columbia University Press, New York, 1991.

Richter, C.F., *Elementary Seismology*, W. H. Freeman, San Francisco, California, 1958.

Ritzi, Jr., R.W., and R.H. Andolsek, *Relation between anisotropic transmissivity and azimuthal resistivity surveys in shallow, fractured, carbonate flow system*, Ground Water 30(5), 774–780, 1992.

Robinson, G.D., *Structure of Pre-Cenozoic rocks in the vicinity of Yucca Mountain, Nye County, Nevada—A potential nuclear-waste disposal site*, U.S. Geological Survey Bulletin 1647, Denver, CO, U.S. Geological Survey, 1985.

Rogers, A.M., S.C. Harmsen, E.J. Corbett, K. Priestly, and D. dePolo, *The seismicity of Nevada and some adjacent parts of the Great Basin, Neotectonics of North America*, D.B. Slemmons, E.R. Engdalhl, M.D. Zoback, D.D. Blackwell, eds, Boulder, CO, Geological Society of America Bulletin 1, 153–184, 1991.

Rogers, N.W., C.J. Hawkesworth, and D.S. Ormerod, *Late Cenozoic basaltic magmatism in the Western Great Basin, California and Nevada*, Journal of Geophysical Research 100(B7), 10,287–10,301, 1995.

Rosenbaum, J.G., M.R. Hudson, and R.B. Scott, *Paleomagnetic constraints on the geometry and timing of deformation at Yucca Mountain, Nevada*, Journal of Geophysical Research 96, 1,963–1,979, 1991.

Rousseau, J.P., E.M. Kwicklis, and D.C. Gillis, eds, *Hydrology of the Unsaturated Zone, North Ramp Area of the Exploratory Studies Facility, Yucca Mountain, Nevada*, Water Resources Investigations Report, Denver, CO, U.S. Geological Survey Draft, 1996.

Savage, J.C., M. Lisowski, W.K. Gross, N.E. King, and J.L. Svarc, *Strain accumulation near Yucca Mountain, Nevada, 1983–1993,* Journal of Geophysical Research 99, 18,103–18,107, 1994.

Savage, J.C., J.L. Svarc, and W.H. Prescott, *Strain accumulation at Yucca Mountain, Nevada, 1983-1998,* EOS, Transaction, American Geophysical Union F203, 1998.

Sawyer, D.R., R.J. Fleck, M.A. Lanphere, R.G. Warren, D.E. Broxton, and M.R. Hudson, *Episodic caldera volcanism in the miocene southwestern Nevada volcanic field: Revised stratigraphic framework, $^{40}Ar/^{39}Ar$ geochronology, and implications for magmatism and extension,* Geological Society of America Bulletin 106, 1,304–1,318, 1994.

Scholz, C.H., N.H. Dawers, J.-Z. Yu, and M.H. Anders, *Fault growth and fault scaling laws, Preliminary results,* Journal of Geophysical Research 98, 21,951–21,961, 1993.

Schwartz, D.B., and K.J. Coppersmith, *Fault behavior and characteristic earthquakes: Examples from the Wasatch and San Andreas Faults,* Journal of Geophysical Research 89, 5,681–5,698, 1984.

Schwartz, S.Y., and R. Van der Voo, *Paleomagnetic study of thrust-sheet rotation during foreland impingement in the Wyoming-Idaho overthrust belt,* Journal of Geophysical Research 89, 10,077–10,086, 1984.

Schweickert, R.A., and M.M. Lahren, *Strike-slip fault system in Amargosa Valley and Yucca Mountain, Nevada,* Tectonophysics 272, 25–41, 1997.

Scott, R.B., *Tectonic setting of the Yucca Mountain region, southwest Nevada,* Geological Society of America Memoir 176, Boulder, CO, Geological Society of America, 251–282, 1990.

Scott, R.B., and J. Bonk, *Preliminary geologic map of Yucca Mountain, Nye County, Nevada with geologic sections,* scale 1:12000, USGS Open-File Report 84-494, Denver, CO, U.S. Geological Survey, 1984.

Senior Seismic Hazard Analysis Committee, *Recommendations for probabilistic seismic hazard analysis, Guidance on uncertainty and use of Experts,* NUREG/CR-6372, 1997.

Seront, B., T.F. Wong. J.S. Caine, C.B Forster, and R.H. Bruhn, *Laboratory characterization of hydromechanical properties of a seismogenic fault system,* Journal of Structural Geology 20, 865–881, 1998.

Serpa, L., and T.L. Pavlis, *Three-dimensional model of the late Cenozoic history of the Death Valley region, southeastern California,* Tectonics 15, 1,113–1,128, 1996.

Sibson, R.H., *Fault rocks and fault mechanisms,* Geological Society of London Journal 133, 191–231, 1977.

Silva, W.J., N. Abrahamson, G. Toro, and C. Costantino, *Description and validation of the stochastic ground motion model,* Brookhaven National Laboratory, Associated Universities, Inc., Upton, NY, 1997.

Simonds, W.F., J.W. Whitney, K. Fox, A. Ramelli, J.C. Yount, M.D. Carr, C.D. Menges, R. Dickerson, and R.B. Scott, *Map of Fault Activity of the Yucca Mountain Area, Nye County, Nevada*, scale 1:24,000, U.S. Geological Survey Miscellaneous Investigations Series Map, 1-2520, Denver, CO, U.S. Geological Survey, 1995.

Simonds, W.F., C.J. Fridrich, T.D. Hoisch, and W.B. Hamilton, *A synthesis of detachment fault studies in the Yucca Mountain region, Methods of Seismic Hazard Evaluation*, Proceedings of the Topical Meeting on Methods of Seismic Hazards Evaluation, Focus '95, La Grange Park, IL, American Nuclear Society, Inc., 107–114, 1996.

Slemons, D.B., *Carrara fault in southern Nevada from paleoseismic, geologic and geophysical evidence: Implications to the earthquake hazards and tectonics near Yucca Mountain, Nevada*, EOS, Transactions, American Geophysical Union 78, F453, 1997.

Smith, R.B., and W.J. Arabasz, *Seismicity of the intermountain seismic belt, Neotectonics of North America,* D.B. Slemmons, E.R. Engdalhl, M.D. Zoback, and D.D. Blackwell, eds, Boulder, CO, Geological Society of America Bulletin 1, 185–228, 1991.

Smith, R.B., W.C. Nagy, K.A. (Smith) Julander, J.J. Viveiros, C.A. Barker, and D.G. Gants, *Geophysical and tectonic framework of the eastern Basin and Range-Colorado Plateau-Rocky transition, Geophysical framework of the Continental United States*, L.C. Pakiser, and W.D. Mooney, eds, Geological Society of America Memoir 172, Boulder, CO, Geological Society of America, 1989.

Smith, E.I., D.L. Feuerbach, T.R. Naumann, and J.E. Faulds, *The area of most recent volcanism near Yucca Mountain, Nevada: Implications for volcanic risk assessment*, High-Level Radioactive Waste Management: Proceedings of the First Annual International Conference, La Grange, IL, American Nuclear Society 1: 81–90, 1990.

Smith, E.I., S. Morikawa, and A. Sanchez, Summary of the Activities of the Center for Volcanic and Tectonic Studies, University of Nevada, Las Vegas, for the Period 1986–1996, Carson City, NV, The Nuclear Waste Project Office, 1997.

Snow, J.K., *Large-magnitude Permian shortening and continental-margin tectonics in the southern Cordillera*, Geological Society of America Bulletin 104, 80–105, 1992a.

Snow, J.K., *Paleogeographic and structural significance of an upper Mississippian facies boundary in southern Nevada and east-central California, (Discussion)*, Geological Society of America Bulletin 104, 1,067–1,071, 1992b.

Snow, J.K., *Mass balance of Basin and Range extension as a tool for geothermal exploration*, Geothermal Resources Council Transactions 18, 23–30, 1994.

Snow, J.K., and A.R. Prave, *Covariance of structural and stratigraphic trends: Evidence for anticlockwise rotation within the Walker Lane Belt Death Valley region, California and Nevada*, Tectonics 13, 712–724, 1994.

Snow, J.K, and B. Wernicke, *Uniqueness of geological correlations: An example from the Death Valley extended terrane*, Geological Society of America Bulletin 101, 1,351–1,362, 1989.

Snow, J.K., J.W. Geissman, and B. Wernicke, *Paleomagnetic data from Paleozoic sedimentary rocks and Permo-Triassic intrusions, Death Valley area, southeast CA, Implications for Mesozoic and Cenozoic deformation*, EOS Transactions, American Geophysical Union 74, Washington, D.C., American Geophysical Union, 206, 1993.

Snyder, B.B., and W.J. Carr, *Preliminary results of gravity investigations at Yucca Mountain and vicinity, southern Nye County, Nevada*, U.S. Geological Survey Open-File Report 82-701, Denver, CO, U.S. Geological Survey, 1982.

Sommerville, P.G., N.F. Smith, R.W. Graves, and N.A. Abrahamson, *Modification of empirical strong ground motion attenuation relations to include the amplitude and duration effects of rupture directivity*, Seismological Research Letters 68, 199–222, 1997.

Sonder, L.J., C.H. Jones, S.L. Salyards, and K.M. Murphy, *Vertical axis rotations in the Las Vegas shear zone, southern Nevada: Paleomagnetic constraints on kinematics and dynamics of block rotations*, Tectonics 13, 769–788, 1994.

Spengler, R.W., C.A. Braun, L.G. Martin, and C.W. Weisenberg, *The Sundance Fault–A newly recognized shear zone at Yucca Mountain, Nevada*, United States Geological Survey Open-File Report 94-49, Denver, CO, U.S. Geological Survey, 1994.

Spudich, P. J.B. Fletcher, M. Hellweg, J. Boatwright, C. Sullivan, W.B. Joyner, T.C. Hanks, D.M. Boore, A. McGarr, L.M. Baker, and A.G. Lindh, *SEA96—A new predicative relation for earthquake ground motions in extensional tectonic regimes*, Seismological Research Letters 68, 190–198, 1997.

Stamatakos, J.A. D.A. Ferrill, *Paleomagnetism of Ordovician Pogonip Group Carbonates in southwestern Nevada, Implications for tectonism of the Yucca Mountain region*, EOS Transactions of the American Geophysical Union, San Francisco Annual Meeting, Washington, D.C., American Geophysical Union, F173, 1996.

Stamatakos, J.A., and D.A. Ferrill, *Comment on "Strike-slip fault system in Amargosa Valley and Yucca Mountain, Nevada by R.A. Schweickert and M.M. Lahren*, Tectonophysics 294, 151–160, 1998.

Stamatakos, J.A., and A.M. Hirt, *Paleomagnetic considerations of the development of the Pennsylvania salient in the central Appalachians*, Tectonophysics 231, 237–255, 1994.

Stamatakos, J.A., C.B. Connor, and R.H. Martin, *Quaternary basin evolution and basaltic volcanism of Crater Flat, Nevada, from detailed ground magnetic surveys of the Little Cones.* Journal of Geology 105, 319–330, 1997a.

Stamatakos, J.A., P.S. Justus, D.A. Ferrill, R. Chen, and G.I. Ofoegbu, *Structural deformation and seismicity*, NRC High-Level Radioactive Waste Program Annual Progress Report, Fiscal year 1996, Sagar, B., ed, NUREG/CR-6513, No. 1, CNWRA 96-OIA, San Antonio, TX, Center for Nuclear Waste Regulatory Analyses, 1997b.

Stamatakos, J.C., C.B. Connor, B.E. Hill, S.L. Magsino, D.A. Ferrill, K.P. Kodama, and P.S. Justus, *The Carrara fault in southwestern Nevada revealed from detailed gravity and magnetic results: Implications for seismicity, volcanism, and tectonics near Yucca Mountain, Nevada*, EOS, Transactions, American Geophysical Union 78, F453, 1997c.

Stamatakos, J.A., D.A. Ferrill, and K.P. Spivey, *Paleomagnetic constraints on the tectonic evolution of Bare Mountain, Nevada*, Geological Society of America Bulletin, In review, 1999.

Stevens, C.H., P. Stone, and P. Belasky, *Paleogeographic and structural significance of an Upper Mississippian facies boundary in southern Nevada and east-central California*, Geological Society of America Bulletin 103, 876–885, 1991.

Stewart, J.H., *Upper Precambrian and Lower Cambrian Strata in the Southern Great Basin, California and Nevada*, U.S. Geological Survey Professional Paper 620, Denver, CO, U.S. Geological Survey, 1970.

Stewart, J.H., *Basin-Range Structure in Western North America, A Review*, Cenozoic Tectonic and Regional Geophysics of the Western Cordillera, R.B. Smith and G.P. Eaton, eds, Boulder, CO, Geological Society of America Memoir 152, 1–31, 1978.

Stewart, J.H., *Tectonic of the Walker Lane belt, western Great Basin - Mesozoic and Cenozoic deformation in a zone of shear*, Metamorphism and Crustal Evolution of the Western United States, Vol. VII, W.G. Ernst, ed, Englewood Cliffs, NJ, Prentice-Hall, Inc, 684–713, 1988.

Stirewalt, G.L., and D.B. Henderson, *A three-dimensional geological framework model for Yucca Mountain, Nevada, with hydrologic application, Report to accompany 1995 model transfer to the U.S. Nuclear Regulatory Commission*, CNWRA 94-023, San Antonio, TX, Center for Nuclear Waste Regulatory Analyses, 1995.

Stock, J.M., and J.H. Healy, *Stress field at Yucca Mountain, Nevada, Geologic and Hydrologic Investigations of a Potential Nuclear Waste Disposal Site at Yucca Mountain, Southern Nevada*, M.D. Carr and J.C. Yount, eds, U.S. Geological Survey Bulletin 1790, 87–94, 1988.

Stock, J.M., J.H. Healy, S.H. Hickman, and M.D. Zoback, *Hydraulic fracturing stress measurements at Yucca Mountain, Nevada and relationship to regional stress fields*, Journal of Geophysical Research 90, 8,691–8,706, 1985.

Stock, J.M., J.H. Healy, J. Soitek, and L. Mastin, *Report on televiewer and stress measurements in holes USW G-3 and UE-25pl, Yucca Mountain, Nye County, Nevada*, U.S. Geological Survey Open-File Report 86-369, Washington D.C., U.S. Geological Survey, 1986.

Stothoff, S.A., D. Or, D.P. Groeneveld, and S.B. Jones, *The effect of vegetation on infiltration in shallow soils underlain by fissured bedrock*, San Antonio, TX, Center for Nuclear Waste Regulatory Analyses, 1997.

Stover, C.W., and J.L. Coffman, *Seismicity of the United States, 1568-1989 (revised)*, U.S. Geological Survey Professional Paper 1527, Menlo Park, CA, U.S. Geological Survey, 1993.

Stuckless, J.S., Z.E. Peterman, R.M. Forester, J.F. Whelan, D.T. Vaniman, B.D. Marshall, and E.M. Taylor, *Characterization of fault-filling deposits in the vicinity of Yucca Mountain, Nevada,* Waste Management 1992 Conference Proceedings, Tucson, AZ, March 1-5, 1992, Tucson, AZ, Waste Management, 929–935, 1992.

Su, F., J.G. Anderson, J.N. Brune, and Y. Zeng, *A comparison of direct S wave and code wave site amplification determined from aftershocks of the Little Skull Mountain Earthquake,* Bulletin of the Seismological Society of America 86, 1,006–1,018, 1996.

Suppe, J., *Geometry and kinematics of fault-bend folding,* American Journal of Science 283, 684–721, 1983.

Swadley, W.C., and L.D. Parrish, *Surficial geologic map of the Bare Mountain Quadrangle, Nevada,* U.S. Geological Survey Miscellaneous Investigations Series Map I-1826, Denver, CO, U.S. Geological Survey, 1988.

Swadely, W.C., D.L. Hoover, and J.N. Rosholt, *Preliminary report on Late Cenozoic faulting and stratigraphy in the vicinity of Yucca Mountain, Nye County, Nevada,* U.S. Geological Survey Open File report 84-788, Denver, CO, U.S. Geological Survey, 1984.

Sweetkind, D.S., and S.C. Williams-Stroud, *Characteristics of fracture at Yucca Mountain, Nevada,* Synthesis Report, U.S. Geological Survey, 1995a.

Sweetkind, D.S., and S.C. Williams-Stroud, *Controls on the genesis of fracture networks, Paintbrush Group, Yucca Mountain, Nevada,* EOS, Transactions, American Geophysical Union 76, F597, 1995b.

Sweetkind, D.S., and S.C. Williams-Stroud, *Characteristics of Fractures at Yucca Mountain, Nevada: Synthesis Report,* Administrative Report, Denver, CO: U.S. Geological Survey, 1996.

Sweetkind, D.S., E.R. Verbeek, J.K. Geslin, and T.C. Moyer, *Fracture character of the Paintbrush Tuff Nonwelded Hydrologic Unit, Yucca Mountain, Nevada,* U.S. Geological Survey Administrative Report to the U.S. Department of Energy, Denver, CO, U.S. Geological Survey, 1995a.

Sweetkind, D.S., E.R. Verbeek, F.R. Singer, F.M. Byers, Jr., and L.G. Martin, Surface fracture network at pavement P2001, Fran Ridge, Near Yucca Mountain, Nye County, Nevada, *Administrative Report,* Denver, CO, U.S. Geological Survey, 1995b.

Sweetkind, D.S., C.J. Potter, and E.R. Verbeek, *Interaction between faults and the fracture network at Yucca Mountain, Nevada,* EOS, Transactions, American Geophysical Union 77(17), S266, 1996.

Sweetkind, D.S., L.O. Anna, S.C. Williams-Stroud, and J.A. Coe, *Characterizing the fracture network at Yucca Mountain, Nevada, Part 1, Integration of field data for numerical simulations, Fractured Reservoirs,* Characterization and Modeling Guidebook-1997, T.E. Hoak, P.K. Blomquist, A. Klawitter, eds, Denver, CO, Rocky Mountain Association of Geologists, 185–196, 1997a.

Sweetkind, D.S., D.L. Barr, D.K. Polacsek, and L.O. Anna, *Administrative report: Integrated fracture data in support of process models, Yucca Mountain, Nevada*, 1997 Milestone Report SPG32M3, Denver, CO, U.S. Geological Survey, 1997b.

Terzaghi, R., *Sources of Error* in Joint Surveys, Geotechnique 15, 287, 1965.

Throckmorton, C.K., and E.R. Verbeek, *Joint networks in the TIVA Canyon and Topopah Spring Tuffs of the Paintbrush Group, southwestern Nevada*, U.S. Geological Survey Open-File Report 95-2, Denver, CO, U.S. Geological Survey, 1995.

Trexler, J.H., Jr., J.C. Cole, and P.H. Cashman, *Middle Devonian-Mississippian stratigraphy on and near the Nevada test site, Implications for hydrocarbon potential*, American Association of Petroleum Geologists 80, 1,736–1,762, 1996.

Trudgill, B., and J. Cartwright, *Relay-ramp forms and normal-fault linkages, Canyonlands National Park, Utah*, Geological Society of America Bulletin 106, 1,143–1,157, 1994.

Twiss, R.J., and E.M. Moores, Structural Geology, New York, NY, W.H. Freeman and Company, 1992.

U.S. Department of Energy, *Controlled Design Assumptions Document, Rev.2*, B000 000 00-01717-4600-00032, December 19, 1995a.

U.S. Department of Energy, Total System Performance Assessment-1995: *An Evaluation of the Potential Yucca Mountain Repository*, B000000000-01717-2200-00136 Rev. 01. TRW Environmental Safety Systems, Inc., 1995b.

U.S. Department of Energy, *Methodology to Assess Fault Displacement and Vibratory ground motion Hazards at Yucca Mountain*, YM/TR-002-NP, Revision 1, August 1997a.

U.S. Department of Energy, *Preclosure Seismic Design Methodology for Geologic Repository at Yucca Mountain*, Topical/Report YM/TR-003-NP, Revision 2, August 1997b.

U.S. Department of Energy, *Repository safety strategy, U.S. Department of Energy's strategy to protect public health and safety after closure of a Yucca Mountain repository, Revision 1*, YMP/96-01, Rev. 1, Washington, D.C., U.S. Department of Energy, 1998a.

U.S. Department of Energy, *Viability Assessment of a Repository at Yucca Mountain: Total System Performance Assessment*, December 1998, Vol. 1. DOE/RW-0508. Las Vegas Nevada: U.S. Department of Energy, Office of the Civilian Radioactive Waste Management, 1998b.

U.S. Department of Energy, *Site Description*, B00000000-01717-5700-00019 Rev. 00, TRW Environmental Safety Systems, Inc., 1998c.

U.S. Geological Survey, *Seismotectonic framework and characterization of faulting at Yucca Mountain, Nevada*, Denver, CO, J.W. Whitney, Report Coordinator, U.S. Geological Survey, 1996.

U.S. Nuclear Regulatory Commission, *Standard review plan for the review of safety analysis reports for nuclear power plants*, NUREG-0800, Washington, D.C., U.S. Nuclear Regulatory Commission, 1997a.

U.S. Geological Survey, *Probabilistic seismic hazard analyses for fault displacement and vibratory ground motion at Yucca Mountain, Nevada, Final Report*, I.G. Wong and C. Stepp Report Coordinators, SP32IM3, WBS Number 1.2.3.2.8.3.6, Oakland, CA, U.S. Department of Energy, 1998.

U.S. Nuclear Regulatory Commission, *Identification and characterization of seismic sources and determination of safe shutdown earthquake ground motion*, Regulatory Guide 1.165, Washington, D.C., U.S. Nuclear Regulatory Commission, 1997b.

U.S. Nuclear Regulatory Commission, *Senior Seismic Hazard Analysis Committee, Recommendations for Probabilistic Seismic Hazard Analysis: Guidance on Uncertainty and Use of Experts*, NUREG/CR–6372, Washington, D.C., 1997c.

U.S. Nuclear Regulatory Commission, *NRC Sensitivity and Uncertainty Analyses for a Proposed HLW Repository at Yucca Mountain, Nevada, Using TPA 3.1: Conceptual Models and Data*, NUREG-1668, Volume 1, 1998a.

U.S. Nuclear Regulatory Commission, *NRC Sensitivity and Uncertainty Analyses for a Proposed HLW Repository at Yucca Mountain, Nevada, Using TPA 3.1: Results and Conclusions*, NUREG-1668, Volume 2, 1998b.

U.S. Nuclear Regulatory Commission, *Issue Resolution Status Report, Key Technical Issue: Igneous Activity, Revision 2*, Washington, D.C.: U.S. Nuclear Regulatory Commission, Division of Waste Management, 1999a.

U.S. Nuclear Regulatory Commission, *Issue Resolution Status Report, Key Technical Issue: Repository Design and Thermal-Mechanical Effects, Revision 2*, Washington, D.C.: U.S. Nuclear Regulatory Commission, Division of Waste Management, In progress, 1999b.

U.S. Nuclear Regulatory Commission, *Issue Resolution Status Report, Key Technical Issue: Unsaturated and Saturated Flow Under Isothermal Conditions, Revision 2*, Washington, D.C.: U.S. Nuclear Regulatory Commission, Division of Waste Management, 1999c.

U.S. Nuclear Regulatory Commission, *Issue Resolution Status Report, Key Technical Issue: Total System Performance Assessment and Integration, Revision 2*, Washington, D.C.; U.S. Nuclear Regulatory Commission, Division of Waste Management, In progress, 1999d.

U.S. Nuclear Regulatory Commission, *Issue Resolution Status Report, Key Technical Issue: Evolution of the Near-Field Environment, Revision 2*, Washington, D.C.: U.S. Nuclear Regulatory Commission, Division of Waste Management, 1999e.

U.S. Nuclear Regulatory Commission, *Issue Resolution Status Report, Key Technical Issue: Radionuclide Transport, Revision 1*, Washington, D.C.: U.S. Nuclear Regulatory Commission, Division of Waste Management, In progress, 1999f.

U.S. Nuclear Regulatory Commission, *Issue Resolution Status Report, Key Technical Issue: Thermal Effects on Flow, Revision 2,* Washington, D.C.: U.S. Nuclear Regulatory Commission, Division of Waste Management, In progress, 1999g.

Young, S.R., G.L. Stirewalt, and A.P. Morris, *Geometric Models of Faulting at Yucca Mountain,* CNWRA 92-008, 1992.

Van der Voo, R., J.A. Stamatakos, and J.M. Parés, *Kinematic constraints on thrust-belt curvature from syndeformational magnetizations in the Lagos del Valle Syncline in the Cantabrian Arc, Spain,* Journal of Geophysical Research 102, 10,105–10,119, 1997.

Vaniman, D.T., and B.M. Crowe, *Geology and Petrology of Basalts of Crater Flat, Applications to Volcanic Risk Assessment for the Nevada Nuclear Waste Storage Investigations,* Los Alamos National Laboratory Report LA-8845-MS, Los Alamos, NM, Los Alamos National Laboratory, 1981.

Veneziano, D., and J. Van Dyck, *Statistical discrimination of "aftershocks" and their contribution to seismic hazard,* Seismic Hazard Methodology for Nuclear Facilities in the Eastern United States, EPRI Research Project No. P1010–29, Appendix A–4, A121–A186, 1985.

Wang, J.S.Y., P.J. Cook, R.C. Trautz, R. Salve, A.L. James, S. Finsterle, T.K. Tolunaga, R. Solbau, and J. Clyde, *Field Testing and Observation of Flow Paths in Niches, Phase I Status Report of the Drift Seepage Test and Niche Moisture Study,* Yucca Mountain Project Milestone SPC314M4, Lawrence Berkeley National Laboratory, Berkeley, CA., 1997.

Wang, J.S.Y., R.C. Trautz, P.J. Cook, S. Finsterle, A.L. James, J. Birkholzer, and C.F. Ahlers, *Testing and Modeling of Seepage into Drift Input of Exploratory Study Facility Seepage Test Results to Unsaturated Zone Models,* Yucca Mountain Project Milestone SP33PLM4, Lawrence Berkeley National Laboratory, CA, 1998.

Weiss, S.I., *Hydrothermal activity, epithermal mineralization and regional extension in the southwestern Nevada volcanic field,* Ph.D. dissertation, Reno, Nevada, University of Nevada at Reno, 1996.

Wells, D.L., and K.J. Coppersmith, *Likelihood of surface rupture as a function of magnitude,* Seismological Research Letters 64, 54, 1993.

Wells, D.L., and K.J. Coppersmith, *New empirical relationships among magnitude, rupture length, rupture width, rupture area, and surface displacement,* Bulletin of the Seismological Society of America 84, 974–1,002, 1994.

Wernicke, B.P., *Low-angle normal faults in the Basin and Range province, Nappe tectonics in an extending orogen,* Nature 291, 645–648, 1981.

Wernicke, B.P., *Cenozoic extensional tectonics of the western Cordillera, The Cordilleran Orogen, Conterminous U.S.,* The Geology of North America, B.C. Burchfiel, P.W., Lipman, and M.L. Zoback, eds, Boulder, CO, Geological Society of America, G-3, 553–581, 1992.

Wernicke, B.P., *Low-angle normal faults and seismicity, A review*, Journal of Geophysical Research 100, 20,159–20,174, 1995.

Wernicke, B.P., R.L. Christiansen, P.C. England, and L.J. Sonder, *Tectonomagmatic evolution of Cenozoic extension in the North American Cordillera Continental Extensional Tectonics*, M.P. Coward, J.F. Dewey, and P.L. Hancock, eds, London, England, Geological Society Special Publications 28, 203–221, 1987.

Wernicke, B.P., G.A. Axen, and J.K. Snow, *Basin and Range extensional tectonics at the latitude of Las Vegas, Nevada*, Geological Society of America Bulletin 100, 1,738–1,757, 1988.

Wernicke, B., J.L. Davis, R.A. Bennett, P. Elósegui, M.J.A. Bolins, R.J. Brady, M.A. House, N.A. Niemi, and J.K. Snow, *Anomalous strain accumulation in the Yucca Mountain Area, Nevada*, Science 279, 2,096–2,100, 1998.

Wesnousky, S.G., 1986, *Earthquakes, Quaternary faults, and seismic hazards in California*, Journal of Geophysical Research 91(B12), 12,587–12,631.

Wesnousky, S.G., and C.H. Jones, *Oblique slip, slip partitioning, spatial and temporal changes in the regional stress field, and the relative strength of active faults in the Basin and Range, western United States*, Geology 22, 1,031–1,034, 1994.

Willemse, E.J.M., *Segmented normal faults: Correspondence between three-dimensional mechanical models and field data*, Journal of Geophysical Research 102, 675–692, 1997.

Willemse, E.J.M., D.D. Pollard, and A. Aydin, *Three-dimensional analyses of slip distributions on normal fault arrays with consequences for fault scaling*, Journal of Structural Geology 18, 295–309, 1996.

Winograd, I.J., and W. Thordarson, *Hydrogeologic and hydrochemical framework, South-Central Great Basin, Nevada-California, with Special Reference to the Nevada Test Site*, Geological Survey Professional Paper 712-C, 1975.

Wittmeyer, G.W., and D.A. Ferrill, *Effect of contemporary regional stress on the anisotropy of transmissivity in fractured rock aquifers*, EOS, Transactions, American Geophysical Union 75(44), 258, 1994.

Wittmeyer, G.W., W.M. Murphy, and D.A. Ferrill, *Regional hydrologic processes of the Death Valley Region, NRC High-Level Radioactive Waste Research at CNWRA, January-June 1994*, B. Sagar, ed, San Antonio, TX, Center for Nuclear Waste Regulatory Analyses, 189–212, 1994.

Wright, L.A., and B.W. Troxel, *Shallow-fault interpretations of Basin and Range structure, southwestern Great Basin*, Gravity and Tectonics, K.A. de Jong and R. Scholten, eds, New York, NY, John Wiley and Sons, 97-407, 1973.

Wu, S., *Fractal strain distribution and its implications for cross-section balancing*, Journal of Structural Geology 15, 1,497–1,507, 1993.

Yielding, G., B. Freeman, and D.T. Needham, *Quantitative fault seal prediction*, American Association of Petroleum Geologists Bulletin 81(6), 897–917, 1997.

Yielding, G., J.A. Overland, and G. Byberg, *Characterization of fault zones for reservoir modeling: An example from the Gullfaks Field, Northern North Sea*, American Association of Petroleum Geologists Bulletin 83(6), 925–951, 1999.

Young, S.R., A.P. Morris, and G.L Stirewalt, *Preliminary Structural Interpretation of Reflection Seismic Line AV-1*, CNWRA 92-024, San Antonio, TX, Center for Nuclear Waste Regulatory Analyses, 1992a.

Young, S.R., G.L. Stirewalt, and A.P. Morris, *Geometric models of faulting at Yucca Mountain*, CNWRA, 92-008, San Antonio, TX, Center for Nuclear Waste Regulatory Analyses, 1992b.

Young, S.R., A.P. Morris, and G.L. Stirewalt, *Geometric analysis of alternative models of faulting at Yucca Mountain, Nevada*, International High-Level Radioactive Waste Management Conference Proceedings, La Grange Park, IL, American Nuclear Society, 1,818–1,825, 1993.

Youngs, R.R., and K.J. Coppersmith, *Implications of fault slip rates and earthquake recurrence models to probabilistic seismic hazard estimates*, Bulletin of the Seismological Society of America 75, 939–964, 1985.

Youngs, R.R., F.H. Swan, III, M.S. Power, D.P. Schwartz, and R.K. Green, Probabilistic analysis of earthquake ground-shaking along the Wasatch front, Utah, in W.W. Hays and P.L. Gori., eds., *Assessment of Regional Earthquake Hazards and Risk along the Wasatch Front, Utah*, U.S. Geological Survey Open-File Report 87-585, II, M-1–M-100, 1987.

Zeng, Y., J.G. Anderson, and G. Yu, *A composite source model for computing realistic strong ground motion*, Geophysical Research Letters 21, 725–728, 1994.

Zhang, X., and D.J. Sanderson, *Numerical modeling of the effects of fault slip on fluid flow around extensional faults*, Journal of Structural Geology 18(1), 109–119, 1996.

Zhang, P., M. Ellis, D.B. Slemmons, and F. Mao, *Right-lateral displacement and Holocene slip rate associated with prehistoric earthquakes along the southern Panamint Valley fault zone: implications for southern Basin and Range tectonics and coastal California deformation*, Journal of Geophysical Research 95, 4,857–4,872, 1990.

Zhang, Y., S.L. Gillett, R.E. Karlin, and R.A. Schweickert, *Paleomagnetism of the Miocene dikes in Bare Mountain, southwestern Nevada, Implications for regional tectonics*, Geological Society of America Cordilleran and Rocky Mountain Section Meetings Abstracts with Programs 23(5), Boulder, CO, Geological Society of America, A169, 1993.

Zoback, M.L., *First- and second-order patterns of stress in lithosphere: The world stress map project*, Journal of Geophysical Research 97(B8), 11,703–11,728, 1992.

Zoback, M.L., R.E. Anderson, and G.A. Thompson, *Cainozoic evolution of the state of stress and style of tectonism of the Basin and Range province of the western United States*, Philosophical Transactions of the Royal Society of London, London, England, Royal Society of London, A300, 407–434, 1981.

Zoback, M.L., and 36 project participants, *World stress map maximum horizontal stress orientations*, Journal of Geophysical Research 97, 11,703–11,728, 1992.

APPENDIX A

FLOW-DOWN DIAGRAM REVISED

FLOWDOWN DIAGRAM FOR TOTAL SYSTEM PERFORMANCE ASSESSMENT

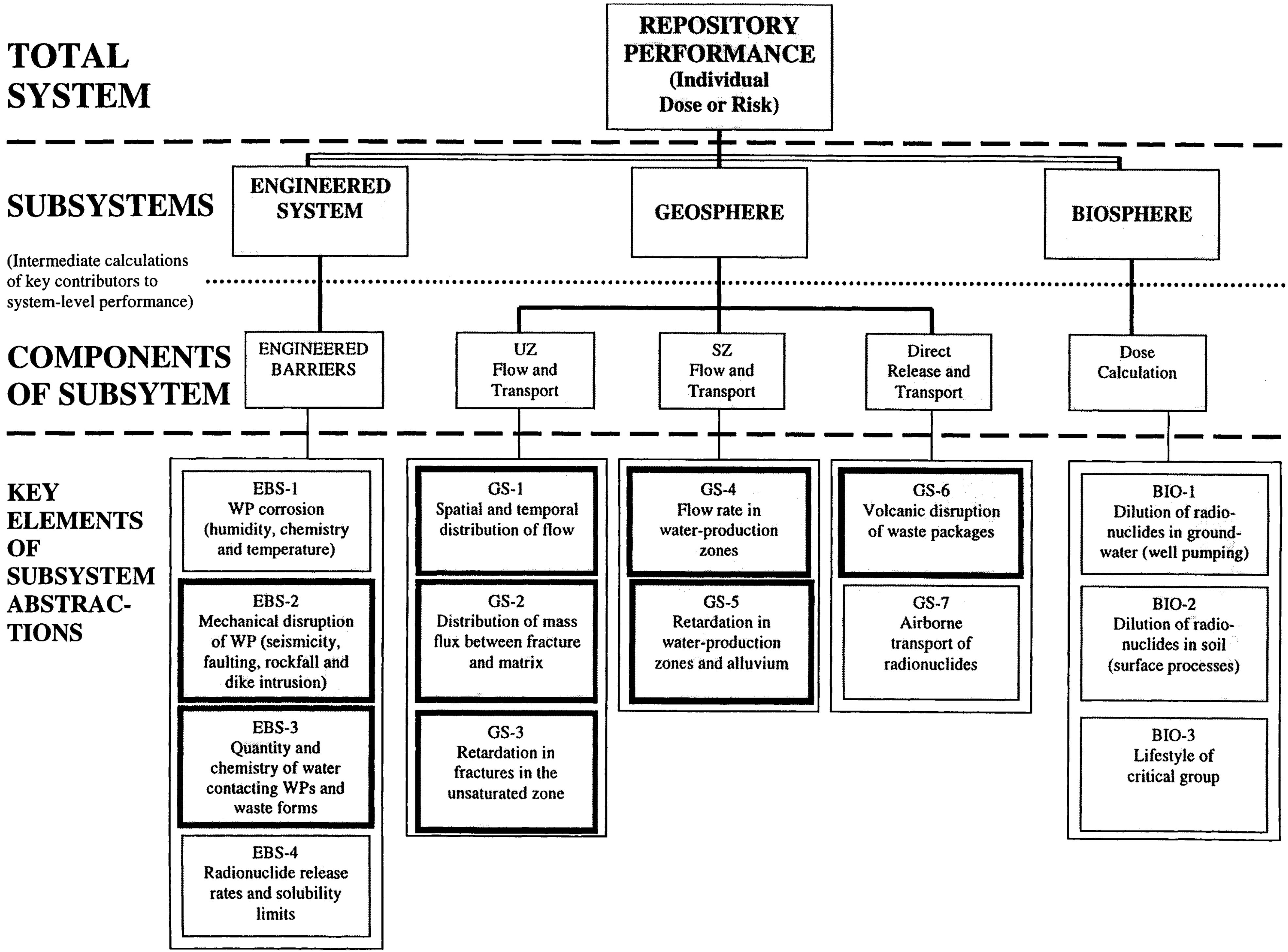

APPENDIX B

CLASSIFICATION OF QUATERNARY FAULTS WITHIN 100 KM of YUCCA MOUNTAIN (REVISED 05/18/98)

Table B-1. Faults Classified as Type I by McKague, et al. (1996) and as Relevant or Potentially Relevant by Pezzopane in U.S. Geological Survey (USGS) (1996) and Having Peak Accelerations ≥ 0.1 g Based on Attenuation Equations of Boore, et al. (1997) and/or Spudich, et al. (1997)

Name of Fault	Organiza-tion	Fault Length (km)	Maximum Magnitude	Distance to Fault (km)	Peak Acceleration (g)					Comments	Considered as Seismic Source in USGS (1998)*
					USGS (1996)		Boore et al. (1997)	Spudich et al. (1997	McKague et al. (1996)		
					Median	84th					
Amargosa River-Pahrump	DOE	130	7.5	38	0.18	0.28	0.14	0.10		Pahrump fault in McKague, et al., 1996	Y
	NRC	130	7.5	40			0.13	0.10	0.20		
Ash Meadow	DOE	60	7.1	34	0.16	0.26	0.12	0.09			Y
	NRC	60	7.1	34			0.12	0.09	0.20		
Bare Mountain	DOE	16	6.5	14	0.27	0.44	0.28	0.27			Y
	NRC	21	6.6	15			0.28	0.26	0.31		
Black Cone	DOE	7	6.1	8.5	0.35	0.58	0.29	0.30		Formerly Simonds Number 10 (McKague et al., 1996, appendix A; BC on Figure B-1	Y
	NRC	6	6.0	6			0.29	0.30	0.45		
Boomerang Point	DOE	5	5.9	2.5	0.48	0.79	0.25	0.25		In USGS (1998, appendix E), AAR team evaluated this fault. Based on lack of geomorphic expression in bedrock indicating significant Quaternary activity and estimated Mw, this fault was not considered as a seismic source. Fault is indicated as BP on figure B-1.'	N
	NRC	5	5.9	2			0.25	0.25	0.56		
Bow Ridge	DOE	10	6.2	2.5	0.52	0.85	0.31	0.31			Y
	NRC	8	6.1	2.3			0.26	0.26	0.61		
Cane Springs	DOE	27	6.7	29	0.17	0.27	0.11	0.08			Y
	NRC	14	6.4	29			0.09	0.07	0.13		

*Y—considered as a seismic source in USGS (1998); C—considered as a seismic source when combined with other faults; N—not considered as a seismic source

Table B-1. Faults Classified as Type I by McKague, et al. (1996) and as Relevant or Potentially Relevant by Pezzopane in U.S. Geological Survey (USGS) (1996) and Having Peak Accelerations ≥ 0.1 g Based on Attenuation Equations of Boore, et al. (1997) and/or Spudich, et al. (1997) (cont'd)

Name of Fault	Organization	Fault Length (km)	Maximum Magnitude	Distance to Fault (km)	Peak Acceleration (g)					Comments	Considered as Seismic Source in USGS (1998)*
					USGS (1996)		Boore et al. (1997)	Spudich et al. (1997	McKague et al. (1996)		
					Median	84th					
Crater Flat	DOE	18	6.5	6	0.48	0.79	0.27	0.26		The Crater Flat fault is considered the Crater Flat Fault System in DOE (1998). It is composed of the Northern Crater Flat Fault (NCF), Central Crater Flat Fault (CCF), and theSouthern Crater Flat Fault (SCF). In McKague, et al. (1996, figure 1-2), Faults 11 and 12 are now considered part of the Crater Flat Fault System and have been renamed accordingly. Simonds 11 is now labeled in NCF-11, and Simonds 12 is now labeled NCF-12 in figure B-1.	C
	NRC	12	6.3	1.0			0.19	0.17	0.36		
Death Valley	DOE	100	7.4	55	0.12	0.19	0.1	0.07			C
	NRC	61	7.2	50			0.09	0.07	0.12		
Fatigue Wash	DOE	17	6.5	3.5	0.56	0.92	0.12	0.08			Y
	NRC	33	6.8	2			0.11	0.08	0.79		
Furnace Creek	DOE	145	7.6	50	0.14	0.23	0.12	0.08			Y
	NRC	123	7.5	49			0.11	0.08	0.15		
Ghost Dance-Abandoned Wash	DOE	5	5.9	0.00001	0.48	0.79	0.26	0.27		Listed as Ghost Dance in McKague, et al. (1996)	Y
	NRC	9	6.2	0.4			0.31	0.31	0.69		
Iron Ridge	DOE	9	6.2	2.5	0.52	0.85	0.29	0.29		Fault is indicated as IR in figure B-1.	Y
	NRC	9	6.2	3			0.28	0.29	0.59		

*Y—considered as a seismic source in USGS (1998); C—considered as a seismic source when combined with other faults; N—not considered as a seismic source

Table B-1. Faults Classified as Type I by McKague, et al. (1996) and as Relevant or Potentially Relevant by Pezzopane in U.S. Geological Survey (USGS) (1996) and Having Peak Accelerations ≥ 0.1 g Based on Attenuation Equations of Boore, et al. (1997) and/or Spudich, et al. (1997) (cont'd)

Name of Fault	Organiza-tion	Fault Length (km)	Maximum Magnitude	Distance to Fault (km)	Peak Acceleration (g)					Comments	Considered as Seismic Source in USGS (1998)*
					USGS (1996)		Boore et al. (1997)	Spudich et al. (1997	McKague et al. (1996)		
					Median	84th					
Midway Valley	DOE	8	6.1	3	0.50	0.83	0.29	0.30		Fault is indicated as MVF in figure B-1.	Y
	NRC	8	6.1	3			0.29	0.30	0.58		
Mine Mountain	DOE	27	6.7	19	0.23	0.38	0.15	0.12			Y
	NRC	6	6.0	24			0.09	0.07	0.12		
Oasis Valley	DOE	20	6.6	24	0.17	0.28	0.12	0.1			Y, C
	NRC	16	6.5	24			0.11	0.09	0.18		
Paintbrush Canyon	DOE	24	6.7	4	0.60	0.97	0.41	0.40		Fault is indicated as PBC in figure B-1.	
	NRC	24	6.7	4			0.41	0.40	0.66		
Rock Valley	DOE	65	7.2	27	0.22	0.35	0.15	0.12			Y
	NRC	43	7.0	25			0.14	0.11	0.23		
Rocket Wash-Beatty Wash	DOE	17	6.5	19	0.23	0.39	0.14	0.11		Not considered relevant by RYA Team possibly because of lack of significant Quaternary displacement (DOE, 1998, appendix, RYA-13).	N
	NRC	17	6.5	19			0.14	0.11	0.23		
Solitario Canyon	DOE	20	6.6	1	0.58	0.94	0.38	0.38		Fault is indicated as SC in figure B-1.	Y
	NRC	19	6.6	1			0.38	0.38	0.76		
Stagecoach Road	DOE	9	6.2	10	0.36	0.60	0.30	0.31		Fault is indicated as SCR in figure B-1.	Y, C
	NRC	8	6.1	11			0.28	0.28	0.30		

*Y—considered as a seismic source in USGS (1998); C—considered as a seismic source when combined with other faults; N—not considered as a seismic source

Table B-1. Faults Classified as Type I by McKague, et al. (1996) and as Relevant or Potentially Relevant by Pezzopane in U.S. Geological Survey (USGS) (1996) and Having Peak Accelerations ≥ 0.1 g Based on Attenuation Equations of Boore, et al. (1997) and/or Spudich, et al. (1997) (cont'd)

Name of Fault	Organization	Fault Length (km)	Maximum Magnitude	Distance to Fault (km)	Peak Acceleration (g): USGS (1996) Median	Peak Acceleration (g): USGS (1996) 84th	Peak Acceleration (g): Boore et al. (1997)	Peak Acceleration (g): Spudich et al. (1997	Peak Acceleration (g): McKague et al. (1996)	Comments	Considered as Seismic Source in USGS (1998)*
Wahmonie	DOE	15	6.4	22	0.18	0.30	0.12	0.09			Y
	NRC	15	6.4	22			0.12	0.09	0.19		
Windy Wash	DOE	25	6.7	4.5	0.56	0.91	0.33	0.32		Fault is indicated as WW in figure B-1.	Y
	NRC	28	6.8	4			0.36	0.35	0.69		

*Y—considered as a seismic source in USGS (1998); C—considered as a seismic source when combined with other faults; N—not considered as a seismic source

Table B-2. Faults Classified as Type I by McKague, et al. (1996) and as Relevant or Potentially Relevant by Pezzopane in U.S. Geological Survey (USGS) (1996) and Having Peak Accelerations < 0.1 g Based on Attenuation Equations of Boore, et al. (1997) and Spudich, et al. (1997)

Name of Fault	Organiza-tion	Fault Length (km)	Maximum Magnitude	Distance to Fault (km)	Peak Acceleration (g)					Comments	Considered as Seismic Source in USGS (1998)*
					USGS (1996)		Boore et al. (1997)	Spudich et al. (1997	McKague et al. (1996)		
					Median	84th					
Amargosa River	DOE	15	6.4	38	0.09	0.15	0.08	0.06			Y
	NRC	15	6.4	40			0.07	0.05	0.1		
Belted Range	DOE	54	7.1	55	0.09	0.15	0.08	0.06			Y
	NRC	54	7.1	55			0.08	0.06	0.1		
Carpetbag	DOE	30	6.8	43	0.10	0.17	0.09	0.06			Y
	NRC	30	6.8	43			0.09	0.06	0.11		
Eleana Range	DOE	13	6.4	37	0.09	0.16	0.08	0.06			Y
	NRC	13	6.4	37			0.08	0.06	0.1		
Kawich Range	DOE	84	7.3	57			0.09	0.06			Y
	NRC	84	7.3	57			0.09	0.06	0.11		
Keane Wonder	DOE	25	6.7	43	0.10	0.16	0.08	0.06			Y
	NRC	33	6.8	42			0.09	0.06	0.12		
Plutonium Valley—North Halfpint Range	DOE	26	6.7	46	0.09	0.14	0.08	0.06			N
	NRC	26	6.7	46			0.08	0.06	0.10		
Sarcobatus Flat	DOE	51	7.1	52	0.10	0.17	0.09	0.06			Y
	NRC	51	7.1	52			0.09	0.06	0.12		
Tolicha Peak	DOE	22	6.6	42	0.10	0.16	0.08	0.06			C
	NRC	22	6.6	42			0.08	0.06	0.10		

*Y—considered as a seismic source in USGS (1998); C—considered as a seismic source when combined with other faults; N—not considered as a seismic source

Table B-2. Faults Classified as Type I by McKague, et al. (1996) and as Relevant or Potentially Relevant by Pezzopane in U.S. Geological Survey (USGS) (1996) and Having Peak Accelerations < 0.1 g Based on Attenuation Equations of Boore, et al. (1997) and Spudich, et al. (1997) (cont'd)

Name of Fault	Organization	Fault Length (km)	Maximum Magnitude	Distance to Fault (km)	Peak Acceleration (g)					Comments	Considered as Seismic Source in USGS (1998)*
					USGS (1996)		Boore et al. (1997)	Spudich et al. (1997	McKague et al. (1996)		
					Median	84th					
West Spring Mountain	DOE	60	7.1	53	0.10	0.16	0.09	0.06			Y
	NRC	60	7.1	53			0.09	0.06	0.11		
Yucca	DOE	32	6.8	40	0.11	0.18	0.09	0.07			
	NRC	31	6.8	43			0.09	0.06	0.10		
Yucca Lake	DOE	17	6.5	36	0.10	0.17	0.08	0.06			
	NRC	17	6.5	36			0.08	0.06	0.11		

*Y—considered as a seismic source in USGS (1998); C—considered as a seismic source when combined with other faults; N—not considered as a seismic source

Table B-3. Faults Classified as Relevant or Potentially Relevant by Pezzopane in U.S. Geological Survey (USGS) (1996) and Having Peak Accelerations ≥ 0.1 g Based on Attenuation Equations of Boore, et al. (1997) and/or Spudich, et al. (1997)

Name of Fault	Organiza-tion	Fault Length (km)	Maximum Magnitude	Distance to Fault (km)	Peak Acceleration (g) USGS (1996) Median	Peak Acceleration (g) USGS (1996) 84th	Boore et al. (1997)	Spudich et al. (1997	McKague et al. (1996)	Comments	Considered as Seismic Source in USGS (1998)*
Death Valley—Furnace Creek	DOE	205	6.2	48	0.06	0.10	0.13	0.09			Y
	NRC	N/A	N/A	N/A			N/A	N/A	N/A		
Death Valley—Furnace Creek—Fish Lake Valley	DOE	288	7.8	50	0.16	0.26	0.14	0.10			Y
	NRC	N/A	N/A	N/A			N/A	N/A	N/A		
Drill Hole Wash	DOE	4	5.8	1.5	0.46	0.74	0.25	0.25		Not considered Type I fault by McKague, et al. (1996) because of orientation in modern *in situ* stress field.	N
	NRC	N/A	N/A	N/A			N/A	N/A	N/A		
Dune Wash	DOE	3	5.6	2	0.44	0.74	0.23	0.22			C
	NRC	N/A	N/A	N/A			N/A	N/A	N/A		
Ghost Dance	DOE	3	5.6	0	0.44	0.74	0.23	0.23		See Ghost Dance—Abandoned Wash Fault	Y
	NRC	N/A	N/A	N/A			N/A	N/A	N/A		
Pagany Wash	DOE	4	5.8	2.5	0.46	0.77	0.25	0.25		Not considered Type I fault by McKague, et al. (1996) because of orientation in modern *in situ* stress field.	N
	NRC	N/A	N/A	N/A			N/A	N/A	N/A		
Paint Brush Canyon—Stagecoach Road	DOE	33	6.8	4	0.62	1.00	0.43	0.43		The DOE represents combined Paintbrush Canyon—Stagecoach Road Fault System.	Y
	NRC	N/A	N/A	N/A			N/A	N/A	N/A		
Sever Wash	DOE	4	5.8	3	0.46	0.77	0.25	0.25		Not considered Type I fault by McKague, et al. (1996) because of orientation in modern *in situ* stress field.	N
	NRC	N/A	N/A	N/A			N/A	N/A	N/A		

*Y—considered as a seismic source in USGS (1998); C—considered as a seismic source when combined with other faults; N—not considered as a seismic source

Table B-3. Faults Classified as Relevant or Potentially Relevant by Pezzopane in U.S. Geological Survey (USGS) (1996) and Having Peak Accelerations ≥ 0.1 g Based on Attenuation Equations of Boore, et al. (1997) and/or Spudich, et al. (1997) (cont'd)

Name of Fault	Organization	Fault Length (km)	Maximum Magnitude	Distance to Fault (km)	Peak Acceleration (g) USGS (1996) Median	Peak Acceleration (g) USGS (1996) 84th	Boore et al. (1997)	Spudich et al. (1997	McKague et al. (1996)	Comments	Considered as Seismic Source in USGS (1998)*
Sundance	DOE	1	1.5	0	0.38	0.66	.17	.18		Not used by McKague, et al., 1996 because of short length.	N
	NRC	N/A	N/A	N/A					N/A		
Yucca Wash	DOE	9	6.2	5	0.47	0.76	0.25	0.24		Not considered Type I fault by McKague, et al. (1996) because of orientation in modern *in situ* stress field.	N
	NRC										

*Y—considered as a seismic source in USGS (1998); C—considered as a seismic source when combined with other faults; N—not considered as a seismic source

Table B-4. Faults Classified as Relevant or Potentially Relevant by Pezzopane in U.S. Geological Survey (USGS) (1996) and Having Peak Accelerations < 0.1 g Based on Attenuation Equations of Boore, et al. (1997) and Spudich, et al. (1997)

Name of Fault	Organiza-tion	Fault Length (km)	Maximum Magnitude	Distance to Fault (km)	Peak Acceleration (g)					Comments	Considered as Seismic Source in USGS (1998)*
					USGS (1996)		Boore et al. (1997)	Spudich et al. (1997	McKague et al. (1996)		
					Median	84th					
Abandoned Wash	DOE									See Ghost Dance—Abandoned Wash fault.	Y
	NRC										
Area Three	DOE	12	6.3	44	0.07	0.12	0.07	0.02			N
	NRC	N/A	N/A	N/A					N/A		
Bullfrog Hills	DOE	7	6.1	38	0.07	0.12	0.07	0.02			N
	NRC								N/A		
Buried Hills	DOE	26	6.7	53	0.08	0.13	0.07	0.02			Y
	NRC								N/A		
Checkpoint Pass	DOE	7	6.1	44	0.06	0.11	0.06				N
	NRC								N/A		
Cockeyed Ridge—Papoose Lake	DOE	21	6.1	44	0.06	0.11	0.07	0.05			Y
	NRC	N/A	N/A	N/A					N/A		
Crossgrain Valley	DOE	9	6.6	53	0.07	0.12	0.06	0.04			Y
	NRC	N/A	N/A	N/A					N/A		
East Pintwater Range	DOE	58	7.1	81	0.06	0.10	0.06	0.04			Y
	NRC	N/A	N/A	N/A					N/A		
Emigrant Valley North	DOE	28	6.8	60	0.07	0.11	0.07	0.05			Y
	NRC	N/A	N/A	N/A			N/A	N/A	N/A		

*Y—considered as a seismic source in USGS (1998); C—considered as a seismic source when combined with other faults; N—not considered as a seismic source

Table B-4. Faults Classified as Relevant or Potentially Relevant by Pezzopane in U.S. Geological Survey (USGS) (1996) and Having Peak Accelerations < 0.1 g Based on Attenuation Equations of Boore, et al. (1997) and Spudich, et al. (1997) (cont'd)

Name of Fault	Organization	Fault Length (km)	Maximum Magnitude	Distance to Fault (km)	Peak Acceleration (g): USGS (1996) Median	Peak Acceleration (g): USGS (1996) 84th	Peak Acceleration (g): Boore et al. (1997)	Peak Acceleration (g): Spudich et al. (1997	Peak Acceleration (g): McKague et al. (1996)	Comments	Considered as Seismic Source in USGS (1998)*
Grapevine	DOE	20	6.6	58	0.06	0.10	0.06	0.04			Y
	NRC	N/A	N/A	N/A			N/A	N/A	N/A		
Grapevine Mountain	DOE	31	6.8	67	0.06	0.10	0.06	0.04			Y
	NRC	N/A	N/A	N/A			N/A	N/A	N/A		
Hunter Mountain—Panamint Valley	DOE	185	7.7	95	0.07	0.12	0.08	0.05			Y
	NRC	N/A	N/A	N/A			N/A	N/A	N/A		
Indian Springs Valley	DOE	28	6.8	67	0.06	0.10	0.06	0.04			N
	NRC	N/A	N/A	N/A			N/A	N/A	N/A		
Kawich Valley	DOE	43	7.0	61	0.06	0.10	0.70	0.05			N
	NRC	N/A	N/A	N/A			N/A	N/A	N/A		
Mercury Ridge	DOE	10	6.2	48	0.08	0.13	0.06	0.04			N
	NRC	N/A	N/A	N/A			N/A	N/A	N/A		
Oak Springs Butte	DOE	21	6.6	57	0.06	0.11	0.06	0.04			Y
	NRC	N/A	N/A	N/A			N/A	N/A	N/A		
Pahrump	DOE	70	7.2	70	0.08	0.12	0.07	0.04			Y
	NRC	N/A	N/A	N/A			N/A	N/A	N/A		
Pahute Mesa	DOE	9	6.2	48	0.06	0.10	0.06	0.04			Y
	NRC	N/A	N/A	N/A			N/A	N/A	N/A		

*Y—considered as a seismic source in USGS (1998); C—considered as a seismic source when combined with other faults; N—not considered as a seismic source

Table B-4. Faults Classified as Relevant or Potentially Relevant by Pezzopane in U.S. Geological Survey (USGS) (1996) and Having Peak Accelerations < 0.1 g Based on Attenuation Equations of Boore, et al. (1997) and Spudich, et al. (1997) (cont'd)

Name of Fault	Organiza-tion	Fault Length (km)	Maximum Magnitude	Distance to Fault (km)	Peak Acceleration (g)					Comments	Considered as Seismic Source in USGS (1998)*
					USGS (1996)		Boore et al. (1997)	Spudich et al. (1997	McKague et al. (1996)		
					Median	84th					
Panamint Valley	DOE	100	7.4	95	0.06	0.10	0.06	0.04			Y
	NRC	N/A	N/A	N/A			N/A	N/A	N/A		
South Ridge	DOE	19	6.6	50	0.08	0.12	0.07	0.05			N
	NRC	N/A	N/A	N/A			N/A	N/A	N/A		
Spotted Range	DOE	30	6.8	59	0.07	0.12	0.07	0.05			Y
	NRC	N/A	N/A	N/A			N/A	N/A	N/A		
West Pintwater Range	DOE	60	7.1	76	0.07	0.12	0.07	0.04			Y
	NRC	N/A	N/A	N/A			N/A	N/A	N/A		
West Specter Range	DOE	9	6.2	33	0.10	0.16	0.08	0.06			Y
	NRC	N/A	N/A	N/A			N/A	N/A	N/A		

*Y—considered as a seismic source in USGS (1998); C—considered as a seismic source when combined with other faults; N—not considered as a seismic source

Table B-5. Faults Classified as Relevant or Potentially Irrelevant by Pezzopane in U.S. Geological Survey (USGS) (1996) and as Type III by McKague, et al. (1996) and Having Peak Accelerations < 0.1 g Based on Attenuation Equations of Boore, et al. (1997) and Spudich, et al. (1997)

Name of Fault	Organiz-tion	Fault Length (km)	Maximum Magnitude	Distance to Fault (km)	Peak Acceleration (g) USGS (1996) Median	Peak Acceleration (g) USGS (1996) 84th	Boore et al. (1997)	Spudich et al. (1997	McKague et al. (1996)	Comments	Considered as Seismic Source in USGS (1998)*
Bonnie Claire	DOE	27	6.7	74	0.05	0.08	0.05	0.03			N
	NRC	N/A	N/A	N/A							
Boundary	DOE	7	6.1	51	0.05	0.09	0.05	0.04			N
	NRC	N/A	N/A	N/A							
Cactus Flat	DOE	50	7.1	84	0.06	0.09	0.06	0.04			N
	NRC	N/A	N/A	N/A							
Cactus Flat—Mellan	DOE	35	6.9	80	0.05	0.09	0.06	0.04			N
	NRC	N/A	N/A	N/A							
Cactus Range—Wellington Hills	DOE	29	6.8	87	0.05	0.07	0.05	0.03			N
	NRC	N/A	N/A	N/A							
Cactus Springs	DOE	14	6.4	59	0.05	0.09	0.05	0.04			N
	NRC	N/A	N/A	N/A							
Chalk Mountain	DOE	20	6.6	87	0.04	0.07	0.05	0.03			N
	NRC	N/A	N/A	N/A							
Chert Ridge	DOE	14	6.4	65	0.05	0.08	0.05	0.03			N
	NRC	N/A	N/A	N/A							
Chicago Valley	DOE	20	6.6	90	0.04	0.06	0.04	0.03			N
	NRC	N/A	N/A	N/A							

*Y—considered as a seismic source in USGS (1998); C—considered as a seismic source when combined with other faults; N—not considered as a seismic source

Table B-5. Faults Classified as Relevant or Potentially Irrelevant by Pezzopane in U.S. Geological Survey (USGS) (1996) and as Type III by McKague, et al. (1996) and Having Peak Accelerations < 0.1 g Based on Attenuation Equations of Boore, et al. (1997) and Spudich, et al. (1997) (cont'd)

Name of Fault	Organiz-tion	Fault Length (km)	Maximum Magnitude	Distance to Fault (km)	Peak Acceleration (g)					Comments	Considered as Seismic Source in USGS (1998)*
					USGS (1996)		Boore et al. (1997)	Spudich et al. (1997	McKague et al. (1996)		
					Median	84th					
Emigrant Valley South	DOE	20	6.6	66	0.06	0.09	0.06	0.04			N
	NRC	N/A	N/A	N/A							
Fallout Hills	DOE	8	6.1	70	0.04	0.06	0.04	0.03			N
	NRC	N/A	N/A	N/A							
Fish Lake Valley	DOE	83	7.3	135	0.04	0.06	0.05	0.03			N
	NRC	N/A	N/A	N/A							
Garlock	DOE	251	7.9	150	0.05	0.08	0.06	0.03			N
	NRC	N/A	N/A	N/A							
Gold Flat	DOE	16	6.5	60	0.06	0.09	0.06	0.04			N
	NRC	N/A	N/A	N/A							
Groom Range Central	DOE	31	6.8	82	0.05	0.08	0.05	0.03			N
	NRC	N/A	N/A	N/A							
Groom Range East	DOE	20	6.6	85	0.04	0.07	0.05	0.03			N
	NRC	N/A	N/A	N/A							
Hunter Mountain	DOE	85	7.3	95	0.06	0.09	0.06	0.04			Y
	NRC	N/A	N/A	N/A							
Jumbled Hills	DOE	27	6.7	77	0.05	0.06	0.05	0.03			N
	NRC	N/A	N/A	N/A							

*Y—considered as a seismic source in USGS (1998); C—considered as a seismic source when combined with other faults; N—not considered as a seismic source

Table B-5. Faults Classified as Relevant or Potentially Irrelevant by Pezzopane in U.S. Geological Survey (USGS) (1996) and as Type III by McKague, et al. (1996) and Having Peak Accelerations < 0.1 g Based on Attenuation Equations of Boore, et al. (1997) and Spudich, et al. (1997) (cont'd)

Name of Fault	Organiz-tion	Fault Length (km)	Maximum Magnitude	Distance to Fault (km)	Peak Acceleration (g)					Comments	Considered as Seismic Source in USGS (1998)*
					USGS (1996)		Boore et al. (1997)	Spudich et al. (1997	McKague et al. (1996)		
					Median	84^{th}					
La Madre	DOE	33	6.8	82	0.05	0.08	0.05	0.03			N
	NRC	N/A	N/A	N/A							
North Desert Range	DOE	24	6.7	81	0.05	0.07	0.05	0.03			N
	NRC	N/A	N/A	N/A							
Owens Valley	DOE	110	7.4	126	0.04	0.07	0.05	0.03			N
	NRC	N/A	N/A	N/A							
Pahranagat	DOE	91	7.4	106	0.05	0.09	0.06	0.04			N
	NRC	N/A	N/A	N/A							
Penoyer	DOE	56	7.1	97	0.05	0.08	0.05	0.03			N
	NRC	N/A	N/A	N/A							
Racetrack Valley	DOE	22	6.6	97	0.03	0.06	0.04	0.03			N
	NRC	N/A	N/A	N/A							
Ranger Mountain	DOE	5	5.9	49	0.05	0.08	0.05	0.03			N
	NRC	N/A	N/A	N/A							
San Andreas	DOE	420	8.1	291	0.03	0.05	0.04	0.02			N
	NRC	N/A	N/A	N/A							

*Y—considered as a seismic source in USGS (1998); C—considered as a seismic source when combined with other faults; N—not considered as a seismic source

Table B-5. Faults Classified as Relevant or Potentially Irrelevant by Pezzopane in U.S. Geological Survey (USGS) (1996) and as Type III by McKague, et al. (1996) and Having Peak Accelerations < 0.1 g Based on Attenuation Equations of Boore, et al. (1997) and Spudich, et al. (1997) (cont'd)

Name of Fault	Organiz-tion	Fault Length (km)	Maximum Magnitude	Distance to Fault (km)	Peak Acceleration (g)					Comments	Considered as Seismic Source in USGS (1998)*
					USGS (1996)		Boore et al. (1997)	Spudich et al. (1997	McKague et al. (1996)		
					Median	84th					
Simonds Number 1	DOE	N/A	N/A	N/A	N/A	N/A				In DOE (1998) (appendix E), AAR team evaluated this fault. Based on lack of geomorphic expression in bedrock indicating significant Quaternary activity and estimated Mw this fault was not considered as a seismic source. See figure B-1. NRC concurs in this assessment	N
	NRC	3	5.6	7			0.16	0.15	0.32		
Simonds Number 2	DOE	N/A	N/A	N/A	N/A	N/A				In DOE (1998) (appendix E), AAR team evaluated this fault. Based on lack of geomorphic expression in bedrock indicating significant Quaternary activity and estimated Mw, this fault was not considered as a seismic source. See figure B-1. NRC concurs in this assessment.	N
	NRC	7	6.1	6			0.22	0.21	0.44		
Simonds Number 3	DOE	N/A	N/A	N/A	N/A	N/A				In DOE (1998) (appendix E), AAR team evaluated this fault. Based on lack of geomorphic expression in bedrock indicating significant Quaternary activity and estimated Mw, this fault was not considered as a seismic source. See figure B-1. NRC concurs in this assessment.	N
	NRC	5	5.9	5			0.21	0.20	0.44		

*Y—considered as a seismic source in USGS (1998); C—considered as a seismic source when combined with other faults; N—not considered as a seismic source

Table B-5. Faults Classified as Relevant or Potentially Irrelevant by Pezzopane in U.S. Geological Survey (USGS) (1996) and as Type III by McKague, et al. (1996) and Having Peak Accelerations < 0.1 g Based on Attenuation Equations of Boore, et al. (1997) and Spudich, et al. (1997) (cont'd)

Name of Fault	Organiz-tion	Fault Length (km)	Maximum Magnitude	Distance to Fault (km)	Peak Acceleration (g)					Comments	Considered as Seismic Source in USGS (1998)*
					USGS (1996)		Boore et al. (1997)	Spudich et al. (1997	McKague et al. (1996)		
					Median	84th					
Simonds Number 4	DOE	N/A	N/A	N/A	N/A	N/A				In DOE (1998) (appendix E), AAR team evaluated this fault. Based on lack of geomorphic expression in bedrock indicating significant Quaternary activity and estimated Mw, this fault was not considered as a seismic source. See figure B-1. NRC concurs in this assessment.	N
	NRC	5	5.9	5			0.21	0.20	0.45		
Simonds Number 5	DOE	N/A	N/A	N/A	N/A	N/A				In DOE (1998) (appendix E), AAR team evaluated this fault. Based on lack of geomorphic expression in bedrock indicating significant Quaternary activity and estimated Mw, this fault was not considered as a seismic source. See figure B-1. NRC concurs in this assessment.	N
	NRC	5	5.9	6			0.20	0.19	0.42		
Simonds Number 6	DOE	N/A	N/A	N/A	N/A	N/A				In DOE (1998) (appendix E), AAR team evaluated this fault. Based on lack of geomorphic expression in bedrock indicating significant Quaternary activity and estimated Mw, this fault was not considered as a seismic source. See figure B-1. NRC concurs in this assessment.	N
	NRC	5	5.9	8			0.17	0.16	0.32		

*Y—considered as a seismic source in USGS (1998); C—considered as a seismic source when combined with other faults; N—not considered as a seismic source

Table B-5. Faults Classified as Relevant or Potentially Irrelevant by Pezzopane in U.S. Geological Survey (USGS) (1996) and as Type III by McKague, et al. (1996) and Having Peak Accelerations < 0.1 g Based on Attenuation Equations of Boore, et al. (1997) and Spudich, et al. (1997) (cont'd)

Name of Fault	Organiz-tion	Fault Length (km)	Maximum Magnitude	Distance to Fault (km)	Peak Acceleration (g) USGS (1996) Median	Peak Acceleration (g) USGS (1996) 84th	Boore et al. (1997)	Spudich et al. (1997	McKague et al. (1996)	Comments	Considered as Seismic Source in USGS (1998)*
Simonds Number 7	DOE	N/A	N/A	N/A	N/A	N/A				In DOE (1998) (appendix E), AAR team evaluated this fault. Based on lack of geomorphic expression in bedrock indicating significant Quaternary activity and estimated Mw, this fault was not considered as a seismic source. See figure B-1. NRC concurs in this assessment.	N
	NRC	7	6.1	9			0.18	0.16	0.36		
Simonds Number 8	DOE	N/A	N/A	N/A	N/A	N/A				In DOE (1998) (appendix E), AAR team evaluated this fault. Based on lack of geomorphic expression in bedrock indicating significant Quaternary activity and estimated Mw, this fault was not considered as a seismic source. See figure B-1. NRC concurs in this assessment.	N
	NRC	4	5.8	9			0.15	0.14	0.28		
Simonds Number 16	DOE	N/A	N/A	N/A	N/A	N/A				In DOE (1998) (appendix E), AAR team evaluated this fault. Based on lack of geomorphic expression in bedrock indicating significant Quaternary activity and estimated Mw, this fault was not considered as a seismic source. See figure B-1. Corresponds with Simonds Number 16 Fault in McKague, et al. (1996), appendix A.	N
	NRC	4	5.8	7			0.20	0.18	0.34		

*Y—considered as a seismic source in USGS (1998); C—considered as a seismic source when combined with other faults; N—not considered as a seismic source

Table B-5. Faults Classified as Relevant or Potentially Irrelevant by Pezzopane in U.S. Geological Survey (USGS) (1996) and as Type III by McKague, et al. (1996) and Having Peak Accelerations < 0.1 g Based on Attenuation Equations of Boore, et al. (1997) and Spudich, et al. (1997) (cont'd)

Name of Fault	Organiz-tion	Fault Length (km)	Maximum Magnitude	Distance to Fault (km)	Peak Acceleration (g)					Comments	Considered as Seismic Source in USGS (1998)*
					USGS (1996)		Boore et al. (1997)	Spudich et al. (1997	McKague et al. (1996)		
					Median	84th					
Stonewall Mountain	DOE	22	6.6	92	0.04	0.06	0.04	0.03			N
	NRC	N/A	N/A	N/A							
Stumble	DOE	33	6.8	74	0.05	0.09	0.06	0.04			N
	NRC	N/A	N/A	N/A							
Three Lakes Valley	DOE	27	6.7	84	0.04	0.07	0.05	0.03			N
	NRC	N/A	N/A	N/A							
Tikaboo	DOE	33	6.8	92	0.04	0.07	0.05	0.03			N
	NRC	N/A	N/A	N/A							
Tin Mountain	DOE	29	6.8	90	0.04	0.07	0.05	0.03			N
	NRC	N/A	N/A	N/A							
Towne Pass	DOE	38	6.9	76	0.06	0.09	0.06	0.04		Considered a seismic source when combined with Emigrant Fault.	C
	NRC	N/A	N/A	N/A							
White Mountains and Cedar Mountain	DOE	115	7.5	185	0.03	0.05	0.04	0.02			N
	NRC	N/A	N/A	N/A							

*Y—considered as a seismic source in USGS (1998); C—considered as a seismic source when combined with other faults; N—not considered as a seismic source

Table B-6. Faults Classified as Type I by McKague, et al. (1996) But Not Explicitly Considered by Pezzopane in U.S. Geological Survey (USGS) (1996) and Having Peak Accelerations ≥ 0.1 g Based on Attenuation Equations of Boore, et al. (1997) and/or Spudich, et al. (1997)

Name of Fault	Organization	Fault Length (km)	Maximum Magnitude	Distance to Fault (km)	Peak Acceleration (g)					Comments	Considered as Seismic Source in USGS (1998)*
					USGS (1996)		Boore et al. (1997)	Spudich et al. (1997	McKague et al. (1996)		
					Median	84th					
Northern Crater Flat (NCF 11)	DOE	N/A	N/A	N/A	N/A	N/A				Formerly Simonds 11 [McKague, et al. (1996); appendix A]. Fault indicated as NCF-11 in figure B-1.	C
	NRC	5	5.9	6			0.20	0.19	0.3		
Northern Crater Flat (NCF 12)	DOE	N/A	N/A	N/A	N/A	N/A				Formerly Simonds 12 [See McKague, et al. (1996); appendix A]. Fault indicated as NCF-12 in figure B-1.	C
	NRC	8	6.1	6			0.22	0.21	0.47		
West Dune Number 1	DOE	N/A	N/A	N/A	N/A	N/A				Formerly Simonds 14 [McKague, et al. (1996); appendix A]. Fault indicated as WD-1 in figure B-1.	Y
	NRC	8	6.1	2			0.28	0.28	0.64		
West Dune Number 2	DOE	N/A	N/A	N/A	N/A	N/A				Formerly Simonds 15 [McKague, et al. (1996); appendix A]. Fault indicated as WD-2 in figure B-2.	Y
	NRC	4	5.8	4			0.21	0.21	0.47		
South Windy Wash	DOE	N/A	N/A	N/A	N/A	N/A				Formerly Simonds 17 [McKague, et al. (1996); appendix A]. Fault indicated as SWW in figure B-1.	Y
	NRC	10	6.2	8			0.20	0.19	0.40		
South Crater Flat (SCF)	DOE	N/A	N/A	N/A	N/A	N/A				In DOE, 1998 (Appendix E) AAR team identifies this as the South Crater Flat Fault. Formerly fault 14, McKague, et al., 1996, (Appendix A).	C
	NRC	8	6.1	8			0.19	0.18	0.39		

*Y—considered as a seismic source in USGS (1998); C—considered as a seismic source when combined with other faults; N—not considered as a seismic source

Table B-7. Faults Used as Seismic Source Experts [U.S. Department of Energy (DOE), 1998]. Fault Length is Maximum Value from U.S. Department of Energy, 1998.

Name of Fault	Organization	Fault Length (km)	Maximum Magnitude	Distance to Fault (km)	Peak Acceleration (g)					Comments	Considered as Seismic Source in USGS (1998)*
					USGS (1996)		Boore et al. (1997)	Spudich et al. (1997	McKague et al. (1996)		
					Median	84th					
Ash Hill	DOE	90	N/A	N/A	N/A	N/A				Location shown on DOE, 1998; Figure 4-67	Y
	NRC	N/A	N/A	N/A							
H 95 (Carrara)	DOE	27	6.5–7.0	N/A	N/A	N/A				Location shown on DOE, 1998; Figure 4-67.	Y
	NRC	N/A	N/A	N/A							
East Busted Butte	DOE		N/A	N/A	N/A	N/A				Location shown on DOE, 1998; Figure 4-18.	Y
	NRC	N/A	N/A	N/A							
East Death Valley	DOE	75	7.2	N/A	N/A	N/A				May be same as DV shown in DOE, 1998; Figure 4-31.	?
	NRC	N/A	N/A	N/A							
East Lathrop Cone	DOE	9	N/A	N/A	N/A	N/A				Location shown on DOE, 1998; Figure 4-18.	Y
	NRC	N/A	N/A	N/A							
East Spector Range	DOE	15	N/A	N/A	N/A	N/A				Location shown on DOE, 1998; Figure 4-31.	Y
	NRC	N/A	N/A	N/A							
Emigrant/ Towne Pass	DOE	47	7.0	N/A	N/A	N/A				Location shown on DOE, 1998; Figure 4-31.	C
	NRC	N/A	N/A	N/A							
Peace Camp	DOE	31	6.5–7.1	N/A	N/A	N/A				Location shown on DOE, 1996; Figure 4-41.	C
	NRC	N/A	N/A	N/A							
South Silent Canyon	DOE	17	N/A							Location shown on DOE, 1998; Figure 4-67.	Y
	NRC										

*Y—considered as a seismic source in USGS (1998); C—considered as a seismic source when combined with other faults; N—not considered as a seismic source

Table B-7. Faults Used as Seismic Source Experts (U.S. Department of Energy, 1998). Fault Length is Maximum Value from U.S. Department of Energy, 1998. (cont'd)

Name of Fault	Organization	Fault Length (km)	Maximum Magnitude	Distance to Fault (km)	Peak Acceleration (g)					Comments	Considered as Seismic Source in USGS (1998)*
					USGS (1996)		Boore et al. (1997)	Spudich et al. (1997	McKague et al. (1996)		
					Median	84th					
Tolicha Pass	DOE									May be same as Tolich Peak fault.	Y
	NRC										
Yucca Butte	DOE	49	N/A	N/A	N/A	N/A				Location shown on DOE, 1998; Figure 4-67.	Y
	NRC	N/A	N/A	N/A							

*Y—considered as a seismic source in USGS (1998); C—considered as a seismic source when combined with other faults; N—not considered as a seismic source

APPENDIX C

CLASSIFICATION OF TECTONIC MODELS AT YUCCA MOUNTAIN VICINITY

Appendix C-1. Summary of Viable Tectonic Models

Model Name	References	Comments
Half Graben with Moderate Depth Detachment	Young, et al. (1992b) Ferrill, et al (1996b)	Supported by CNWRA balanced cross sections (e.g., Young, et al., 1992b). Also consistent with pull-apart model (Stamatakos and Ferrill, 1996a). Supported by regional observations (e.g., Wright and Troxel, 1973; Burchfiel, et al., 1987). Seismic data (e.g., Brocher, et al., 1996) neither support nor refute the models because validity of seismic data below 6 km depth is questionable (cf. Brocher, et al., 1996; Majer, et al., 1997).
Half Graben with Deep Depth Detachment	Young et al. (1992b) Ferrill, et al. (1996b)	Supported by CNWRA balanced cross sections (e.g., Young, et al., 1992b). Also consistent with pull-apart model (Stamatakos and Ferrill, 1996a). Supported by regional observations (e.g., Wright and Troxel, 1973; Burchfiel, et al., 1987). Seismic data (e.g., Brocher, et al., 1996) neither support nor refute the model because validity of seismic data below 6 km depth is questionable (cf. Brocher, et al., 1996; Majer, et al., 1997).
Crater Flat Pull-Apart Basin	Fridrich (in press)	Supported by regional seismo-tectonic framework (e.g., Oldow, et al., 1994). Fault geometries at depth unspecified. Requires existence of additional blind seismic sources (McKague, et al., 1996). Requires blind strike-slip fault south of CF (Stamatakos and Ferrill, 1996a).
Elastic-Viscous Graben	Janssen (1995)	Consistent with pull-apart basin interpretation. Assumes mobile ductile middle crust and internally deformable upper crustal blocks. Requires very thin effective elastic crust (thickness of only 2 km) and blind large-displacement faults in CF and external to the model (See Section 4.3).
Amargosa Desert Fault	Schweickert and Lahren (1997)	Explains selected geometric features (e.g., State Line fault and CF basaltic cone alignment) but requires unrecognized shallow detachments within calderas north of CF (e.g., Hardyman and Oldow, 1991). Inconsistent with thermochronological data (e.g., Ferrill, et al., 1996b).

Appendix C-1. Summary of Viable Tectonic Models (cont'd)

Model Name	References	Comments
Collapsed Caldera	Carr (1982, 1988); Carr and Parrish (1985)	Inconsistent with geometric and kinematic data. Geophysical data (Brocher, et al., 1996; Rosenbaum, et al., 1991) and structural data (e.g., Scott, 1990; Young, et al., 1992b; Ferrill, et al., 1996b) show CF and BM fault bound half graben. Thermochronological data show CF and BM fault probably existed prior to Miocene volcanism (e.g., Ferrill, et al., 1996b).
Kawich-Greenwater Rift	Carr (1984)	Inconsistent with kinematic data. Rifting assumes contemporaneous faulting and volcanism, but BM fission track data indicate significant uplift (faulting) prior to Miocene volcanism (e.g., Ferrill, et al., 1996b).
Yucca Synclinorium	Robinson (1985)	Inconsistent with nearly all geological and geophysical studies.
Planar-Domino Faults	Stewart (1978)	Inconsistent with known geometry and kinematics of faults (e.g., Fridrich, in press; Ferrill, et al., 1996b). Domino faulting layering requires all fault blocks to have similar dips and faulting to be coeval.
Regional Detachment	Wernicke (1992) Snow (1994)	Inconsistent with existing kinematic and geometric data. No evidence for shallow detachment east of BM (e.g., Simonds, et al., 1995b; Ferrill, et al., 1996b). Paleomagnetic data (e.g., Stamatakos and Ferrill, 1996b) show no large-scale vertical-axis rotation of BM as indicated in model of Snow (1994).
Shallow Detachment	Scott (1990) Hamilton (1988)	Inconsistent with geometric and kinematic data. Balanced cross sections require a minimum detachment depth of 6 km (e.g., Young, et al., 1992b; Ferrill, et al., 1996b). No detachment visible on seismic data (Brocher, et al., 1996). Thermochronology data (e.g., Ferrill, et all, in review) indicate BM exhume prior to Bullfrog Hills-Flurospar Canyon detachment faulting (Ferrill, et al., 1996b).

Appendix C-1. Summary of Viable Tectonic Models (cont'd)

Model Name	References	Comments
Half Graben with Moderate Detachment		Has least adverse effect on repository performance. Connectivity between the BM fault and the CF-YM detachment fault can lead to compensatory slip on the CF-YM faults in response to slip on the Bmm fault. However, the response behavior depends on the details of the strain accommodation mechanism in the BM fault hanging wall (e.g., flexural shear and outer arc extension versus oblique simple shear or vertical simple shear). Since the CF-YM faults extend to a lesser depth in this model, the potential rupture area (the area with high slip tendency) and earthquake magnitudes are smaller than those for a deep detachment (Ofoegbu and Ferrill, 1995; McKague, et al., 1996). Moreover, faults with dips coalescing into a moderate detachment are less likely to serve as magma pathways.
Half Graben with Deep Detachment		Possibility of the CF-YM domain producing large magnitude earthquakes in the future. The CF-YM faults extend to considerable depth (~15 km), hence they have large potential rupture areas with high slip tendency and can produce large-magnitude earthquakes (McKague, et al., 1996). In addition, slip on the BM may trigger slip on one or more CF-YM faults because of the supposed link at depth. Faults that maintain steep dips to the base of the seismogenic crust are also good candidates for capturing igneous dikes, thus serving as preferred magma pathways.
Crater Flat Pull-Apart Basin		Mix of strike-slip and dip-slip faulting could increase seismic hazard because the current PSHA (Wong, et al, 1995) considers only dip-slip motion on most CF-YM faults. More importantly, the hypothesized regional strike-slip system is a major seismic source that could dominate the PSHA. Such a source is not considered in the existing PSHA (Wong, et al., 1995). The pull-apart model has CF-YM faults maintaining steep dips to depth, so the structures are favorable for dike capture.
Elastic-Viscous Graben		Possibility for large rupture areas and attendant earthquakes associated with planar faults extending as deep as 15 km. Faults could also serve as easily exploitable magma pathways. In contrast to the detachment models, slip on the CF-YM faults is not directly linked to movement on the BM. The planar model also predicts a significant west-dipping blind fault with 3 km of offset beneath CF (in order to contain deformation within CF).

Appendix C-1. Summary of Viable Tectonic Models (cont'd)

Model Name	References	Comments
Amargosa Shear or Amargosa Desert Fault		Raises the possibility of the most significant adverse effect on repository performance. As with the pull-apart models, the Amargosa shear requires a major strike-slip fault capable of generating earthquakes with maximum magnitudes up to $M_w = 8.0$, which would greatly affect PSHA. Furthermore, such a fault could have a major impact on rock hydrologic properties between CF and Amargosa Valley. The link with igneous activity suggests that a strike-slip event may be able to trigger another phase of basaltic activity in CF.

APPENDIX D

SITE CHARACTERIZATION ANALYSIS COMMENTS REVISED

Site Characterization Analysis Open Items Reconsidered

Based on several meetings, workshops, field trips, and visits to the Experimental Studies Facility (ESF), the staff considers that most of the Site Characterization Analysis (SCA) openitems are being considered by the U.S. Department of Energy (DOE). The staff believes that the recentlycollected data and the results of the several workshops that will be discussed in FY1998 and FY1999 reports will form suitable bases on which to reconsider SCA open items.

Items are organized by Comment and Question, numerically, according to subissues in this Issue Resolution Status Report, and Subissue: Other Geoscience.

Numbers in parentheses refer to pages in NUREG-1347, *NRC Staff Site Characterization Analysis of the DOE's Site Characterization Plan, Yucca Mountain*, NV, 1989

- **FAULTING SUBISSUE**

Comment 36	Resolved
Comment 48	Resolved
Comment 59	Resolved
Comment 60	Resolved
Comment 61	Resolved
Comment 62	Resolved
Comment 63	Resolved
Comment 64	Resolved
Comment 69	Resolved
Comment 71	Resolved

- **SEISMICITY SUBISSUE**

Comment 66	Resolved
Comment 67	Resolved

- **FRACTURING SUBISSUE**

None

- **TECTONICS SUBISSUE**

Comment 8	Resolved
Comment 47	Resolved
Comment 68	Resolved
Comment 98	Resolved

- **OTHER GEOSCIENCES SUBISSUES**

Comment 32	Open
Comment 51	Open
Question 8	Open

****

COMMENT 8 Alternative Tectonic Models

"Alternative tectonic models for the site do not appear to be fully integrated into the site characterization plan and, as a result alternatives are apparently not considered in the preliminary performance allocations and the design of the Engineered Barrier System (EBS). The site characterization program appears to be directed toward providing data that confirm the preferred tectonic model rather than determining what the preferred model should be." (p. 4-14)

RECOMMENDATIONS

"Alternative tectonic models should be thoroughly integrated into preliminary performance allocations and the design of the EBS. Consideration should be given to prioritizing investigations giving high priority to those investigations associated with tectonic features, events, or processes that could lead to the determination of whether the site has unacceptable adverse conditions or to a substantial change in the site characterization program." (p. 4-16)

DISPOSITION

Resolved. DOE has considered a range of alternative tectonic models in its Probabilistic Seismic Hazard Analysis (PSHA). These are reflected in its acceptable seismic hazard curve. Staff has no questions at this time.

****

COMMENT 32 Geophysical Data Integration

"The program for geophysical integration as presented in the Site Characterization Plan (SCP) is insufficiently described. The correlation between the different geophysical investigations is not presented and, in addition, the approach that will be used to integrate the geophysical activities and how these different activities will complement each other does not appear to be discussed in the SCP." (p. 4-35)

RECOMMENDATIONS

*"Integrate and evaluate existing geologic and geophysical data and provide overlays of the existing coverage and evaluations.

*Based on this integration, provide a coherent geophysical program to be implemented in the Yucca Mountain (YM) area that would provide sufficient characterization of the site." (p. 4-35)

DISPOSITION

Open. The DOE has completed reports on its geophysical surveys (seismic reflection, gravity, and magnetic data). The results were utilized in several workshops held during 1996 and 1997. The DOE submitted results of gravity and magnetic surveys of YM area (Earthfield Technology, 1995). The Center for Nuclear Waste Regulatory Analyses (CNWRA) recently collected gravity and magnetic data and plan to integrate the results from the different geophysical methods.

The resolution of this issue is pending the outcome of staff reviews of the DOE reports and of the CNWRA results.

****

COMMENT 36 **Faults in Perimeter Drift**

"The technical rationale for this investigation states that the perimeter drift defines an area of a significantly lower concentration of faults than has been mapped in surrounding areas. However, based on other parts of the SCP, this concept may not be accurate. Further, there is no apparent indication that studies in the SCP address the potential impact on system performance of the presence within the perimeter drift (i.e., in emplacement areas) of a significant number of faults, some of which may be favorably oriented for failure under the present stress regime." (p. 4-38)

RECOMMENDATIONS

*"Rectify the apparent contradiction as to whether a zone of imbricate faulting is present within the perimeter drift.

*If the imbricate fault zone is present within the perimeter drift, an assessment should be made to demonstrate that the requirements of 10 CFR 60.133(h) will be met." (p. 4-38)

DISPOSITION

Resolved. The DOE ESF reports, Repository Safety Strategy, Total System Performance Assessment-Viability Assessment (TSPA-VA) Plan, the plan to conduct perimeter drifting, and proposed enhanced drifting and drilling alleviate this concern. Also the DOE is planning to move the perimeter drift to a location west of Ghost Dance fault, leaving the imbricate fault zone outside the perimeter. No staff questions at this time.

****

COMMENT 47 **Integrate Tectonics Into Performance Assessment (PA)**

"The approach to incorporating data derived in the postclosure tectonics program into an assessment of whether performance issues related to the waste package and EBS requirements (10 CFR 60.113(a)) will be met is confusing and may result in an inaccurate assessment of performance." (p. 4-44)

RECOMMENDATION

* "Consideration should be given to establishing a direct path for the integration of data collected in the Postclosure Tectonics program into issues 1.4 (Will waste package meet the performance objective) and 1.5 (Will the waste package and repository EBS meet the performance objective)." (p. 4-44)

DISPOSITION

Resolved. The DOE has integrated seismicity into TSPA-VA regarding disruption of waste packages by rockfall. DOE's Repository Safety Strategy considers faulting, but does not show plans to conduct a faulting-disrupts-waste package analysis. DOE will need to demonstrate that faulting is not significant to PA, as it currently implies. Staff has no questions at this time.

****

COMMENT 48 **Fault Slip Rate**

"The use of fault slip rates to determine the level of hazard posed to repository facilities by faults does not appear to be a conservative approach and may result in overly optimistic predictions about the effects of faulting on system performance." (p. 4-45)

RECOMMENDATIONS

*"Demonstrate that the use of slip rates for determining hazard does not provide overly optimistic predictions of the effects of faulting on repository performance.

*Consider alternative methods (e.g., maximum event offset) or a combination of methods (e.g., maximum event offset and slip rates) to assess the level of hazard to the surface facilities and EBS posed by faulting." (p. 4-45)

DISPOSITION

Resolved. Results of the DOE's expert elicitation on PSHA regarding development of a reasonable range or slip rates is acceptable. No staff questions at this time.

****

COMMENT 51 **Correlate Deep & Shallow Geophysical Surveys**

"Geophysical survey programs as indicated in the SCP may not be sufficient to identify and characterize both the deep crustal and shallow geologic features and their interrelationship." (p. 4-47)

RECOMMENDATIONS

*"Provide a geophysical investigation program plan that is comprehensive, integrated, and sufficient to identify and understand the interrelationships of the deep crustal structure and shallow geologic structural features, and to assure that no significant structural features have gone undetected.

*Consider including a gridded program of exploratory surveys and measurements that would allow for cross-line correlations and more complete spatial definition of anomalies at the site and specifically at the locations of the exploratory shafts." (p. 4-47)

DISPOSITION

Open. The DOE collected more seismic reflection, gravity, and magnetic data since the issuance of the SCP (e.g., Earthfield Technology, 1995). CNWRA also collected gravity and magnetic data in the vicinity of YM. Staff expects that these data will be sufficient to characterize the shallow and deep structures and their interrelationship. The resolution of this issue is pending the outcome of the review of the DOE and CNWRA reports.

****

COMMENT 59 **Sequencing Fault Investigations**

"The information presented for the program of investigations for faulting does not allow the NRC staff to determine what investigations will actually be conducted. In addition, the sequencing of many geophysical and geologic activities related to faulting may lead to data collection activities that are inadequate to support assessments of performance and design bases." (p. 4-53)

RECOMMENDATION

*"Consideration should be given to re-examining the sequence of all activities dependent on input from other activities." (p. 4-53)

DISPOSITION

Resolved. The DOE geological and geophysical site characterization activities that bear on fault characterization are largely completed. Results of DOE's expert elicitation for PSHA regarding faulting investigations is acceptable. No staff questions at this time.

****

COMMENT 60 **Fault Parameters**

"The NRC staff does not consider that the basis and rationale for the design and performance parameters, characterization parameters, and goals proposed in the SCP for fault displacement, in particular for fault investigations for facilities important to safety (FITS), have been justified. The staff is concerned, as these values appear to be used to limit the exploration program prior to having sufficient data to evaluate the site." (p. 4-53)

RECOMMENDATION

*"The DOE needs to strengthen its justification for the design and performance parameters, characterization parameters, and goals for preclosure fault displacement as related to FITS, or revise these values. The justification should include a discussion of the interrelationship of the characterization parameters, performance and design parameters, and goals with the design criteria and the performance objectives of 10 CFR Part 60." (p. 4-54)

DISPOSITION

Resolved. Results of DOE's expert elicitatio for PSHA provided an adequate basis for fault design parameters. Staff has no questions at this time.

****

COMMENT 61 **Location of New Faults**

"The program of investigations for faulting appears to assume that any future faulting will follow old faulting patterns. The NRC staff considers that this is not a reasonably conservative assumption and does not consider that this assumption is technically justified." (p. 4-55)

RECOMMENDATION

*"The DOE needs to review its assumptions used to plan the exploration program for FITS to assure unconservative assumptions, such as future faulting only occurring at the exact locations of past faulting, do not bias the program." (p. 4-55)

DISPOSITION

Resolved. Results of DOE's expert elicitation for PSHA provided adequate basis for assessing potential for future faulting. Staff has no questions at this time.

****

COMMENT 62 **Fault Standoff**

The information presented for the program of investigations for study of faulting at the surface facilities does not allow the NRC staff to determine how the DOE is proposing to use standoff distances in designing the program of investigations and in performing the resultant design and analysis." (p. 4-56)

RECOMMENDATION

*"The DOE needs to demonstrate that:

(i) the program of investigations for faulting at or near FITS will adequately evaluate all faults that have a potential of movement; and/or

(ii) that the evaluation of the effects of faulting, taking into account the degree of resolution of the investigation, will not underestimate the effects; and

(iii) the effect of faulting will not compromise the ability of the FITS to meet the performance objectives." (p. 4-56)

DISPOSITION

Resolved. The DOE is planning to avoid areas where concentration of active faults are located and relocate the repository perimeter west of the Ghost Dance fault. The DOE plans to design

for faults that it cannot avoid (U.S. Department of Energy, 1995, key 023). No staff questions at this time.
****

COMMENT 63 **Integrating Fault Data**

"The information presented for the program of investigations for study of faulting at the surface facilities does not appear to have integrated pre-existing information and makes assumptions about pre-existing information and ongoing investigations that the NRC cannot evaluate because the NRC has not seen the background information." (p. 4-56)

RECOMMENDATION

* "Prior to the NRC staff's being able to evaluate the program of site investigations, the DOE needs to complete at least the planning step of integration of the site program. This step should include not only a separate integration of drilling or a separate integration of geophysics, but a complete integration of the planned program of investigations. This integration should show how ongoing activities and pre-existing information has been incorporated into the program and should demonstrate what assumptions are being made on the qualification of pre-existing data." (p. 4-57)

DISPOSITION

Resolved. Results of DOE's expert elicitation for PSHA indicates acceptable identification and inclusion of relevant faults in fault hazard analysis. Site specific analysis will be needed. Staff has no questions at this time.
****

COMMENT 64 **Significant Faults**

"The characterization parameters for the identification and characterization of "significant Quaternary faults" in the area of the repository block do not appear to fulfill the requirements in 10 CFR 60, such as investigating and evaluating the effects of potentially adverse natural conditions." (p. 4-57)

RECOMMENDATION

*"The site characterization program and performance allocation process should be designed to assure that any fault that could have an adverse impact on waste isolation will be characterized." (p. 4-58)

DISPOSITION

Resolved. Staff have resolved the disposition of potentially significant Quaternary faults (Section 5.1.1.1).
****

COMMENT 66 **10,000-Year Earthquake**

"Since the 10,000-yr cumulative slip earthquake (10-kyr CSE) methodology assumes that average cumulative slip over 10,000 yr is released in a single event, it appears that recurrence is implied to be fixed at 10,000 yr. It is questionable whether such a methodology can properly characterize fault activity and the related seismic activity in the site region." (p. 4-58)

RECOMMENDATION

*"Recurrence-rate estimates should be given special emphasis. In particular, differences between the true maximum magnitude and the 10-kyr CSE, based on evaluations of the recurrence interval associated with the maximum earthquake determined from magnitude-frequency relationships, should be thoroughly explained. The planned site characterization activities, which are designed to provide all types of information that are material to the characterization of seismic hazard, should be conducted in a manner that will allow for a clear comparison of the 10-kyr CSE methodology with other alternative methodologies." (p. 4-59)

DISPOSITION

Resolved. The DOE is not using the 10-kyr CSE concept. The DOE's current methodology presented in TR#1 (DOE, 1997; *YMP/TR-002-NP: Methodology to Assess Fault Displacement and Vibratory Ground Motion Hazards at YM*, August 1997) is acceptable. No staff questions at this time.

****

COMMENT 67 **Magnitude 5.5 Cutoff**

"The data compiled according to Activity 8.3.1.17.4.1.2 (i.e., having a magnitude cutoff of 5.5,) may not be sufficient to support an evaluation of the effects of local site geology on surface and subsurface motions."

RECOMMENDATION

*"The distinction between those parameters that are to be compiled for all recorded seismic events and those that are to be compiled for events greater than magnitude 5.5 should be dropped. If it is reasonable and practical, information for any of the 19 categories of parameters listed in Activity 8.3.1.17.4.1.2 should be compiled for earthquakes in the YM vicinity, without regard to their size." (p. 4-60)

DISPOSITION

Resolved. In a letter dated August 15, 1991 (D.E. Shelor to J. Lichen), DOE provided clarification as follows: smaller-magnitude earthquakes of less than 5.5 that may have an impact on the site will be considered in seismic analysis. This comment was closed by letter from R. Ballard to J. Holonich dated October 2, 1991.

****

COMMENT 68 **Detachment Fault Model**

"Other aspects of detachment faulting, in addition to those described in Section 8.3.1.17.4.5 regarding key questions to be answered on earthquake sources, do not appear to be treated as similarly potentially significant." (p. 4-60)

RECOMMENDATIONS

*"The significance of detachment faulting as a key element in assessing the potential for faulting at the site needs to be readdressed giving consideration to other key concerns related to detachment faulting.

*Consideration should be given to having the results of Study 8.3.1.17.4.5 input directly into postclosure tectonics performance issues." (p. 4-61)

DISPOSITION

Resolved. The DOE has considered detachment faults (U.S.Geological Society, 1996). Detachment fault models were adequately discussed in PSHA.

****

COMMENT 69 **NW-Trending Faults**

"The SCP does not appear to integrate and synthesize data resulting from the planned activities characterizing northwest-trending faults." (p. 4-61)

RECOMMENDATION

*"Consideration should be given to specifically outlining a program of study to integrate and synthesize all activities that will collect data on northwest-trending faults." (p. 4-61)

DISPOSITION

Resolved. Results of DOE's expert elicitation for PSHA provided acceptable consideration of north-west-trending faults. No staff questiosn at this time.

****

COMMENT 71 **Significant Fault**

"The tentative goal, design parameter, and expected value relating faulting (e.g., 'significant Quaternary fault') and performance allocation for System Element 1.1.2 are not sufficient for adequately characterizing the hazard posed by faulting in the repository." (p. 4-61)

RECOMMENDATIONS

*"Consideration should be given to using alternative fault models as a conceptual basis for assessing the preclosure hazard to the repository."

*Demonstrate that, from a scientific perspective, the program of drifting in the northern part of the repository combined with the systematic drilling program and feature sampling program will provide the information necessary to ensure that conditions and processes encountered are representative of conditions and processes throughout the site and that potentially adverse conditions will be adequately investigated." (p. 4-62)

DISPOSITION

Resolved. The staff considers Type I faults to be significant faults. The staff now considers that the DOE has adequately identified significant faults at YM and will continue to do so.
****

COMMENT 98 **Alternative Conceptual Models**

"Weighting alternative conceptual models according to the judgment that they are likely to be correct and using such 'probabilities' to weight consequences in the construction of the complementary cumulative distribution function (CCDF) is not a conservative estimate of repository performance, nor is it an advisable approach for demonstrating compliance." (p. 4-78)

RECOMMENDATIONS

*"The SCP should recognize that the approach of incorporating alternative conceptual model likelihoods into the computation of the CCDF of cumulative releases of radionuclides may not provide information about repository performance in an acceptable format because uncertainties are not delineated distinctly.

*"Plan to incorporate consideration of unresolved alternative conceptual models into the CCDF in a conservative fashion by choosing the alternative that gives the poorest performance (greatest releases of radionuclides) or by some combination of the two alternatives that ensures no underestimates of releases and develop the site characterization program accordingly." (p. 4-79)

DISPOSITION

Resolved. Based on expert elicitation, the DOE provided alternative models to be considered in the PA. Different weights were assigned to these models based on their credibility. The range in uncertainty in these models was adequately addressed in PSHA.
****

QUESTION 8 **Variability of Model Input**

"What measure of predictability will accompany the computer models, maps, and other illustrations? How will uncertainties be explicitly transmitted to the model users?" (p. 4-105)

RECOMMENDATION

"SCP updates should describe how local variability in the data will be presented in the block model." (p. 4-106)

DISPOSITION

Open. The DOE ISM 3.0 and related process models will address uncertainty in data and interpretations. The DOE requested NRC feedback on the adequacy of ISM 2.0 for its intended purposes. Appendix 7 interactions were held in July and September 1997 to provide preliminary staff feedback and to brief staff on the operation of the ISM 2.0 code. The DOE revised its request by submitting a geologic framework model (GFM3.0) for staff review. Technical exchanges on GFM3.0 held in May 1997 and GFM3.1 held in June 1999 by the DOE to brief the staff on operation of GFM3.0 and GFM3.1 codes, respectively, led to NRC adopting these models and codes. ISM3.0 Paseo Model Report will be revieed after its issuance in FY2000.

APPENDIX E

TESTS AND EVALUATIONS OF DOE'S GEOLOGIC FRAMEWORK MODEL VERSION 3.1

REVIEW AND EVALUATION OF THE U.S. DEPARTMENT OF ENERGY THREE-DIMENSIONAL GEOLOGICAL FRAMEWORK MODEL OF YUCCA MOUNTAIN, VERSION 3.1

Geological Framework Model Version 3.1 (GFM3.1), a modified version of GFM3.0 and its associated data files, was constructed by a U.S. Department of Energy (DOE) contractor using Quality Assurance (QA)-approved EarthVision (EV) software, Version 4.0 (EV4.0, Dynamic Graphics, Inc.). The staff and its contractors reviewed GFM3.0 last year [Appendix F, Issue Resolution Status Report Revision 1 (IRSR Revision 1) for the Key Technical Issue (KTI) of Structural Deformation and Seismicity (U.S. Nuclear Regulatory Commission, 1998] and found it to be largely be a credible representation of the stratigraphy, faults, fault blocks, geologic cross sections, and topography of Yucca Mountain (YM) at the site scale. In late 1998, the DOE issued the modified version GFM3.1. The DOE notified the staff of the new version and requested staff's review and evaluation.

OBJECTIVES OF THE GEOLOGIC FRAMEWORK MODEL VERSION 3.1 REVIEW AND EVALUATION

(1) To understand the main differences between GFM3.1 and GFM3.0 and the rationales for the revision;

(2) To test and evaluate the adequacy GFM3.1 for DOE's purposes of representing site stratigraphy and faults as a framework for its Integrated Site Model (ISM), Version 3.0;

(3) To consider replacing the Nuclear Regulatory Commission's (NRC's) EV Geological Site Model (GSM) with an adapted version of GFM3.1 as NRC's three-dimensional (3D)-model of the site, for independent NRC analyses.

STRUCTURE OF THE GEOLOGIC FRAMEWORK MODEL VERSION 3.1 REVIEW AND EVALUATION

Review and evaluation of GFM3.1 were jointly conducted by staff from the Center for Nuclear Waste Regulatory Analyses (CNWRA), and MANDEX, Inc. This review and evaluation, performed under the direction of NRC staff, was organized as follows:

- Part I - Review and Evaluation of Stratigraphic Horizons in GFM3.1.
- Part II - Review and Evaluation of Fault Surfaces in GFM3.1.

QUESTIONS USED TO FOCUS THE GEOLOGIC FRAMEWORK MODEL VERSION 3.1 REVIEW AND EVALUATION

The following questions define the scope of review and evaluation of GFM3.1:

- Are input data used in GFM3.1 to define stratigraphic horizons (Part I, Question 1) and faults at the surface and in the subsurface (Part II, Question 1) appropriate and sufficient?
- Do stratigraphic horizons (Part I, Question 2) and fault traces and fault surfaces (Part II, Question 2) as modeled in GFM3.1 fit the input data?

- Are all data essential for constructing stratigraphic horizons (Part I, Question 3) and fault surfaces and other structure models (Part II, Question 3) included in the database which accompanied GFM3.1?

- Considering the technical bases for the manner in which stratigraphic horizons (Part I, Question 4) and fault surfaces (Part II, Question 4) are represented in GFM3.1, are there alternative interpretations which should be incorporated into the model for thickness or distribution of stratigraphic horizons and fault geometries?

- Are there any observations on how stratigraphic horizons (Part I, Question 5) and fault surfaces (Part II, Question 5) are represented in GFM3.1 that may benefit from further clarification by the DOE?

SUMMARY OF OBSERVATIONS AND RESULTS FROM REVIEW AND EVALUATION OF GEOLOGIC FRAMEWORK MODEL VERSION 3.1

(1) Stratigraphy and the Paleozoic surface are not well constrained at depth or at the edges of the model;

(2) It is assumed that all boreholes are straight and plumb;

(3) Mismatches between true and modeled elevations of subsurface horizons are generally fewer and of smaller magnitude than observed in GFM3.0, and are typically ± 10 ft, owing in part to a difference in export procedures;

(4) Some fault geometries observed in the GFM3.1, including faults that terminate updip against other faults (orphans) and faults with changes in displacement with depth, are of uncertain geologic significance and require clarification;

(5) The topography of the upper surface of the Paleozoic (Pz) horizon has the form of a basement high in the eastern half of the GFM3.1. This basement high is difficult to reconcile given the fault geometries interpreted in GFM3.1.

(6) Only 10 of the 42 faults in the model have some information to control their position at depth.

(7) A fault located between the Black Glass Canyon fault and the Paintbrush Canyon fault, interpreted to have at least 400 feet of dip slip (Day, et al., 1998), is not represented in GFM3.1.

(8) Results of restoration of an east-west oriented cross section indicate that overall fault geometries are appropriate for producing the warped or folded hangingwall horizons;

(9) Distance/displacement diagrams constructed from data extracted from the GFM3.1 may indicate the presence of unmapped faults, or faults that are not encompassed by the GFM3.1, or that mapped displacements or fault dips are erroneous or not representative;

(10) Results of restoration of faults in cross sections imply that faulting was active during certain episodes in the Tertiary while silicic volcanism was active.

SUMMARY OF CONCLUSIONS FROM REVIEW AND EVALUATION OF GEOLOGIC FRAMEWORK MODEL VERSION 3.1

(1) The staff considers GFM3.1 to be an improved representation of the stratigraphy, faults, fault blocks, geologic cross sections, and topography of YM at the site scale.

(2) The staff considers GFM3.1 to be an interpretation of the geologic framework of YM that will continue to evolve as new data or improved or alternative interpretations are developed.

(3) The staff will adapt a version of GFM3.1 for NRC's use in conducting 3D analyses of the YM site, including reviews of subsequent ISMs.

The staff have made certain observations based on analyses of the model that may require explanation or clarification, particularly to enable the staff to fully evaluate ISM3.0. The illustrated evaluations of stratigraphy, faults, fault blocks, topography, and geologic cross sections detailed in the following two-part review are the source for observations made during this review. The observations notwithstanding, GFM3.1 was considered an appropriate improvement over GFM3.0. Note that critiques of the quality assurance or quality control of data were not performed for this review:

STATUS OF GEOLOGICAL FRAMEWORK MODEL 3.0 OBSERVATIONS (U.S. Nuclear Regulatory Commission, 1998)

(1) No change: Stratigraphy and the Paleozoic surface are not well constrained at depth or at the edges of the model.

(2) Resolved: Topographic elevations over about 85 percent of the model area have elevation differences of less than 5 m (comparing two sources of elevation data). Such differences are not detrimental because topography was not used to control subsurface stratigraphy.

(3) No change: Stratigraphic borehole controls assume straight and plumb boreholes.

(4) Improved: Mismatches between true and modeled elevations of subsurface horizons typically are less than 25 ft, although a few are greater than 50 ft. Possible explanations for these mismatches include new realizations of fault dips at depth, presence of unmapped faults, or results of sparse data.

(5) Resolved: A structure in Antler Wash shown on the U.S. Geological Survey (USGS) central block geologic map may need to be added to the model to help explain the hydrogeologic tracer data from C-wells. There are no geological or geophysical evidence to support a fault in Antler Wash.

(6) No change: The imbricate fault zone is presently modeled as a single fault. This representation may need to be changed if it is necessary to understand or explain phenomena in that zone.

(7) Improved: Warping or folding of horizons in the hangingwall of faults is explained by the presence of curved faults.

(8) Improved: Boomerang Point fault shows an apparent reversal of slip sense that may need to be explained.

(9) Resolved: Dune Wash fault is shown truncated against the Ghost Dance fault in one cross section, but not in sections to the north or south, and the surface traces of the two faults do not appear to intersect. This observation may need to be explained.

(10) No change: Many faults are shown with increasing displacements with depth, suggesting that they are growth faults. This may need to be explained and compared with other DOE models of fault development. However, poorly constrained stratigraphic horizon data in the northern and southern edges of the model may be a contributing factor.

(11) Improved: Complex fault interactions have been modeled at depth in some zones - a positive feature of the model. Some of the structural relationships shown, such as one fault 'beheading' another, have implications for understanding past, and perhaps future, faulting and may need to be explained in more detail.

POINTS FOR FURTHER DISCUSSION WITH THE U.S. DEPARTMENT OF ENERGY

(1) Assurances that all necessary DOE QA/QC procedures were followed.

(2) Clarification of assumptions made for the purpose of this review as needed to maintain confidence in future ISM results.

(3) Incorporate the missing fault between Black Glass Canyon and Paintbrush Canyon faults into the GFM3.1.

(4) Clarification of largest elevation discrepancies between borehole horizon elevations and interpolated GFM3.1 horizon grids.

(5) Clarification of rock-unit thickness variations across center of repository block and vertical dip-slip displacement variations along faults for ISM3.0, as needed.

(6) Constraint of interpretations of the upper surface of the Paleozoic rocks.

(7) Explanation of fault displacement inconsistencies with depth, including the Ghost Dance fault and faults showing reverse and reversing sense of displacement.

PART I - REVIEW AND EVALUATION OF STRATIGRAPHIC HORIZONS IN GEOLOGIC FRAMEWORK MODEL VERSION 3.1

Where appropriate, lithostratigraphic designations used in this review are identical to the lithostratigraphic designations in the GFM3.1.

(1) Are input data used in GFM3.1 to define stratigraphic horizons appropriate and sufficient?

The input data used to define stratigraphic horizons in GFM3.1 are appropriate, and may be sufficient. Horizons in GFM3.1 were derived from several data sources, including the EG&G digital topographic model (Personal communication with Rob Clayton, July 1998), the geologic map of Day and others (1998), well-log horizon picks, and geophysical (gravity) data. These data were combined in an EV geologic model that presents an interpretation of the stratigraphic units in the vicinity of the proposed repository. The relatively small number of boreholes and limited geophysical data sets available to the modelers necessitates an increased level of reliance on surface geologic mapping to establish shallow horizon relationships that are then confirmed at depth by geophysical well logs and samples. The deeper model horizons, i.e., Tund (Tertiary undefined) and Paleozoic, are not well-sampled by boreholes and were, in part, interpreted from gravity measurements. Thus, it should be explained in the GFM3.1 report that any utilization of GFM3.1 horizon data in other modeling and/or design work should be undertaken with an understanding of the accuracy of the input data and the extent to which GFM3.1 honors these data. As data from the GFM3.1 are incorporated into process and design models, it may become necessary to increase the amount of control of deeper model horizons, or of horizons near the fringe of the GFM.

This analysis of GFM3.1 assumes the well-log horizon picks used in building the model have been qualified by an appropriate QA process. Thus, the questions addressed in this analysis are whether there are sufficient data, and have they been honored such that GFM3.1 is an adequate representation of the real geology? Figure E-1 contains an image taken from GFM3.1 showing the location of the boreholes incorporated in the model. There is a higher density of boreholes in the center of the model than at the model edges. The position of stratigraphic units at the model boundaries are the result of data extrapolation calculations by the EV software application. Because of the better stratigraphic control in the center of the model it is assumed that the model is more representative there than at the edges.

(2) Do stratigraphic horizons as modeled in GFM3.1 fit the input data?

Analyses performed by staff indicate that, with few exceptions, modeled stratigraphic horizons and topography fit the input data. The CNWRA performed a brief comparison of the DOE GFM3.0 and CNWRA topography models in Revision 1 of the Structural Deformation and Seismicity Issue Resolution Status Report (U.S. Nuclear Regulatory Commission, 1998). Comparison of topography in the GFM3.1 with GFM3.0 indicates no modifications of the topographic horizon. The DOE has utilized a topography model produced by EG&G with a 100-ft grid node spacing. The CNWRA uses USGS 7.5-min digital elevation models with a 30-m grid node spacing. After making the appropriate coordinate system and projection conversions, the CNWRA topography model was subtracted from the DOE model.

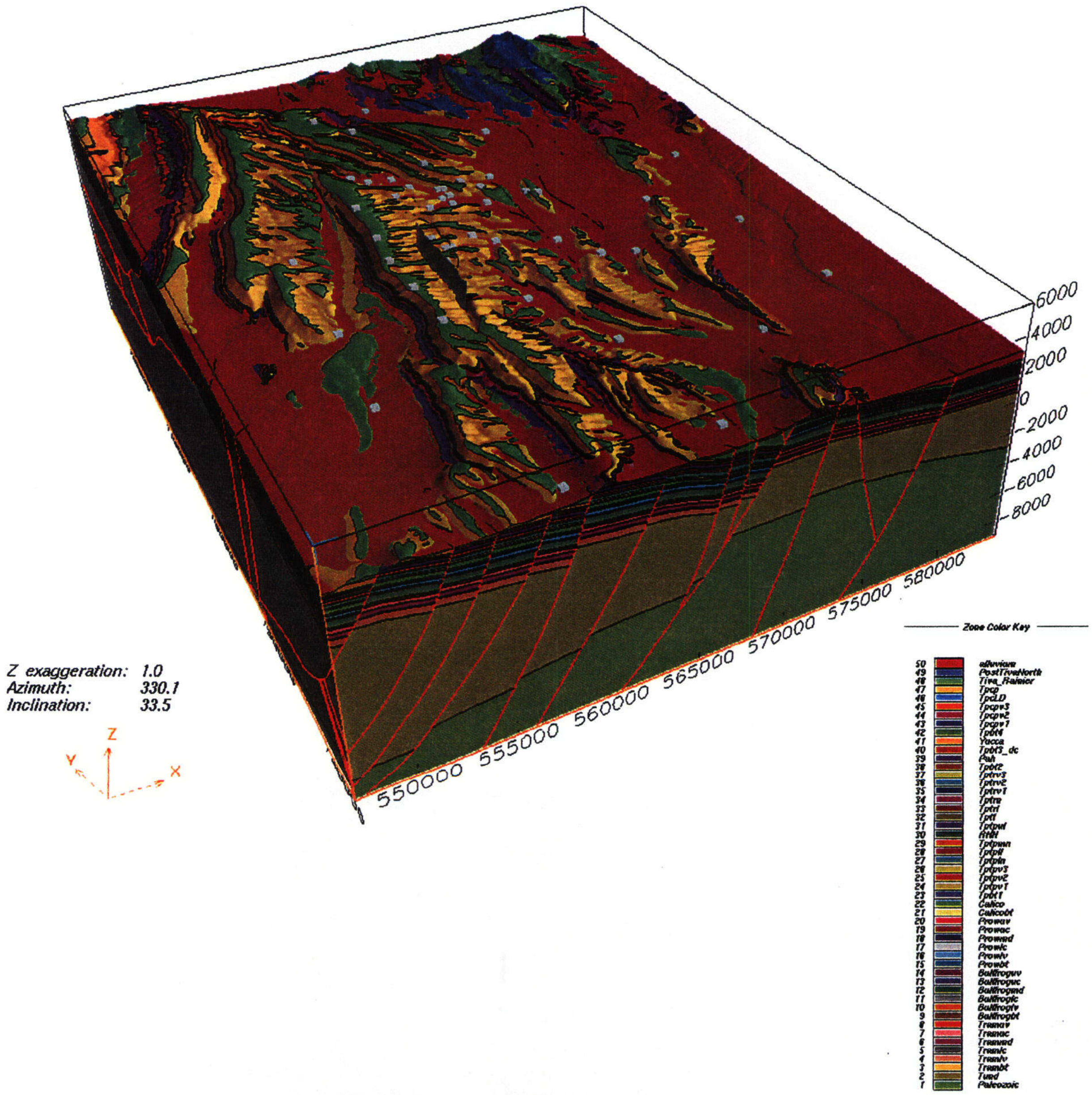

Figure E-1a. Oblique view of GFM3.1 looking northeast. Grey cubes show well locations. Coordinates are Nevada State Plane feet.

Figure E-1b. Plan view of GFM3.1 areal extent showing well locations.

Approximately 85 percent of the elevation differences are less than 5 m. These differences are not considered to be significant to GFM3.1 because topography is used to truncate stratigraphic units at the model surface. The topography was not used to control or influence the subsurface stratigraphy.

A subsurface horizon tie analysis was performed by the CNWRA to measure the agreement between borehole horizon picks and modeled horizon depths. The tie analysis compares the depth at which the borehole actually intersected a horizon and the modeled depth for that same coordinate. Borehole directional logs were not available to the CNWRA at the time this analysis was performed. All comparisons assume straight and plumb boreholes.

The data processing sequence used to generate the tie analysis differs from that used in evaluation of GFM3.0. Analyses of the GFM3.0 included extracting complete horizon grids from the GFM3.0 EV faces file. The analyses presented here are based upon exported horizon grids accompanying the GFM3.1 and, where erroneous correlations are greater than 10 ft, based upon the individual fault-block horizon grids used to construct the GFM3.1 rather than the horizon-export grids supplied with the model. The data processing sequence is:

1) Select export horizon grids supplied with the GFM3.1.

2) Compute the borehole-horizon intersection coordinate for each borehole penetrating the horizon. Repeat this process for several horizons in the stratigraphic column.

3) Compare the export horizon elevations with the elevations picked from the well logs.

4) Where differences between the export horizon grid and borehole-horizon intersections are greater than 10 ft, extract horizon elevations from horizon grids used to construct the GFM3.1.

Table 1 contains the original borehole picks provided with the GFM3.1 for the six horizons used in this analysis. Table 2 contains the modeled horizon elevations (i.e., horizon picks extracted from exported horizon grids), and table 3 contains the difference between the well log picks and modeled elevations.

Table 1. U.S. Department of Energy borehole/well log horizon elevation picks (ft)

#wellid	Tpbt4	Tptpul	RHH	Tptpll	Tac	Tund
a#4	3951.3					
a#5	3912	3586				
a#6	3908.8	3631				
b#1	3750	3499	3307	3174	2554	-21.3
c#2	3450	3257	3194	2989	2379	
G-1		3893.5	3750	3535.2	2924.5	791.8
G-2	4862	4119.8	3965.1	3817	3340	1115

Table 1. U.S. Department of Energy borehole/well log horizon elevation picks (ft) (cont'd)

#wellid	Tpbt4	Tptpul	RHH	Tptpll	Tac	Tund
G-3	4483.5	4308	4181	4026	3443.5	979.7
G-4	4025	3746	3548	3392	2756.6	
H-1	4184	3736	3624	3377	2769	612.6
H-3	4466	4326	4261	4017.9	3466	1228.9
H-4	3903	3720	3543	3393	2779	277.1
H-5	4413.5	4110	3920	3763	3146	1429.1
H-6	4011	3836	3686	3476	2915	1393.1
J-13	2688	2516		2314	1835	97
NRG#1						
NRG#2						
NRG#4	3761	3399				
NRG#5	3944	3542	3426	3205.5		
NRG-6	3933.4	3626.5	3472	3282		
NRG-7A	4105	3688.6	3548	3329.4	2709	
ONC#1	3218	3005	2888		2541	
p#1		3407	3202	3015	2385	792
SD-6	4466.6	4263.3	4129	3914	3348	
SD-7	4146.2	3982	3832	3668.7	3066.4	
SD-9	4181.5	3800	3645	3427.2	2793.1	
SD-12	4079.3	3872.8	3713	3556.1	2931.5	
UZ-1		3955	3840	3595		
UZ#4	3841					
UZ#5	3835					
UZ-6	4492.5	4315	4235	4008	3465	
UZ-7a	4030.3			3621		
UZ-14					3004.8	
UZ#16	3839.3	3629	3515	3331	2803	
WT-1	3509	3347	3227	3052	2556	
WT-2	4041	3847	3728	3541	2949	
WT#3					3021	
WT#4	3555	3176	3157	3051	2680	
WT#6				4063	3930	
WT-7	3556.5	3380	3261	2967	2488	

Table 1. U.S. Department of Energy borehole/well log horizon elevation picks (ft) (cont'd)

#wellid	Tpbt4	Tptpul	RHH	Tptpll	Tac	Tund
WT-10	2799	2637	2453			
WT-11	3318	3159	2948	2807	2381	
WT#12	3207	3048	2866	2766	2250	
WT#13	2946	2756	2646	2518		
WT#14		3255	3138	2996	2320	
WT#15	3204	2912	2713	2634		
WT#16	3585	3141		3141	2903	
WT#17	3490	3351	3275	3152	2689	
WT#18	4044	3484	3394	3214	2764	
WT#24	4623.4	3964.6	3784	3640.3	3133.2	

Table 2. GFM3.1 horizon elevation picks computed from exported horizon grids with EarthVision (ft)

#wellid	Tpbt4	Tptpul	RHH	Tptpll	Tac	Tund
a#4	3951.5	3552.6	3430.8	3208.0	2684.4	215.8
a#5	3912.1	3585.3	3444.1	3249.0	2672.9	153.5
a#6	3908.8	3631.6	3450.9	3286.8	2667.7	154.9
b#1	3750.0	3493.0	3302.1	3168.5	2551.4	-28.3
c#2	3450.3	3257.6	3194.8	2989.7	2379.0	373.6
G-1	4293.8	3892.5	3750.6	3533.6	2923.4	791.1
G-2	4862.2	4120.2	3965.3	3817.1	3339.7	1115.3
G-3	4483.5	4308.4	4181.4	4026.4	3443.4	979.7
G-4	4025.1	3746.2	3548.2	3392.2	2756.6	394.9
H-1	4184.1	3736.2	3624.2	3377.2	2768.9	612.3
H-3	4465.5	4325.8	4260.8	4017.7	3466.0	1229.0
H-4	3902.5	3720.8	3543.6	3393.8	2779.2	277.7
H-5	4413.5	4109.8	3919.5	3762.6	3146.1	1428.5
H-6	4011.1	3836.2	3686.3	3476.2	2915.1	1392.7
J-13	2688.0	2516.4	2422.2	2314.4	1835.0	96.9
NRG#1	3490.7	3201.9	3094.6	2983.4	2499.4	16.0
NRG#2	2162.0	3286.0	3181.0	3070.0	2610.0	76.8
NRG#4	3760.4	3398.6	3297.3	3151.6	2682.4	74.2
NRG#5	3944.0	3542.2	3426.2	3205.7	2693.0	178.7

Table 2. GFM3.1 horizon elevation picks computed from exported horizon grids with EarthVision (ft) (cont'd)

#wellid	Tpbt4	Tptpul	RHH	Tptpll	Tac	Tund
NRG-6	3933.9	3627.4	3472.8	3282.8	2695.8	219.3
NRG-7A	4105.2	3690.7	3550.1	3331.4	2709.0	437.5
ONC#1	3222.7	3009.1	2896.9	2736.3	2544.3	226.2
p#1	3554.1	3404.1	3199.2	3012.3	2384.3	791.4
SD-6	4466.6	4263.4	4129.1	3914.1	3348.0	1401.2
SD-7	4146.3	3982.5	3832.4	3669.1	3066.5	833.6
SD-9	4181.4	3799.9	3644.9	3427.1	2793.1	607.7
SD-12	4079.4	3873.1	3713.2	3556.4	2931.6	727.6
UZ-1	4390.2	3955.6	3840.4	3595.6	2997.0	1053.8
UZ#4	3841.1	3372.9	3305.3	3132.9	2758.4	210.2
UZ#5	3835.3	3375.0	3305.1	3131.8	2755.7	202.3
UZ-6	4492.5	4315.4	4235.4	4008.3	3465.1	1394.4
UZ-7a	4049.9	3903.0	3777.3	3608.8	3017.6	733.4
UZ-14	4399.8	3964.4	3849.7	3604.1	3007.6	1077.9
UZ#16	3838.9	3628.9	3514.9	3330.8	2802.9	365.4
WT-1	3508.8	3347.1	3227.1	3052.1	2556.3	867.3
WT-2	4041.8	3846.4	3727.3	3541.4	2949.3	716.6
WT#3	3811.9	3708.6	3646.6	3511.5	3020.9	1299.7
WT#4	3556.0	3176.7	3157.7	3051.2	2680.4	207.0
WT#6	4682.1	3975.2	3929.1	3929.3	3927.6	1645.3
WT-7	3556.6	3380.3	3261.3	2967.2	2486.5	552.2
WT-10	2798.7	2637.0	2453.3	2237.7	1808.0	668.4
WT-11	3318.0	3159.4	2948.4	2807.4	2381.1	1070.5
WT#12	3207.0	3048.4	2866.4	2766.4	2249.9	564.9
WT#13	2945.4	2755.6	2645.6	2517.6	1925.4	529.4
WT#14	3469.0	3235.7	3118.7	2976.7	2320.0	523.0
WT#15	3204.0	2912.2	2713.2	2634.2	2147.7	230.2
WT#16	3584.8	3141.0	3141.0	3141.2	2903.4	761.5
WT#17	3490.0	3351.3	3275.3	3152.3	2689.1	579.9
WT#18	4043.4	3483.4	3393.3	3213.3	2763.8	399.7
WT#24	4623.0	3964.3	3783.8	3640.0	3132.7	952.1

Table 3. Model to borehole correlation difference computed by subtracting the model horizon elevations in table 2 from well log horizon picks in table 1 (ft)

#wellid	Tpbt4	Tptpul	RHH	Tptpll	Tac	Tund
a#4	-0.2					
a#5	-0.1	0.7				
a#6	0.0	-0.6				
b#1	0.0	6.0	4.9	5.5	2.6	7.0
c#2	-0.3	-0.6	-0.8	-0.7	0.0	
G-1		1.0	-0.6	1.6	1.1	0.7
G-2	-0.2	-0.4	-0.2	-0.1	0.3	-0.3
G-3	0.0	-0.4	-0.4	-0.4	0.1	0.0
G-4	-0.1	-0.2	-0.2	-0.2	0.0	
H-1	-0.1	-0.2	-0.2	-0.2	0.1	0.3
H-3	0.5	0.3	0.2	0.2	0.0	-0.1
H-4	0.5	-0.8	-0.6	-0.8	-0.2	-0.6
H-5	0.0	0.2	0.5	0.4	-0.1	0.6
H-6	-0.1	-0.2	-0.3	-0.2	-0.1	0.4
J-13	0.0	-0.4		-0.4	0.0	0.1
NRG#1						
NRG#2						
NRG#4	0.6	0.4				
NRG#5	0.0	-0.2	-0.2	-0.2		
NRG-6	-0.5	-0.9	-0.8	-0.8		
NRG-7A	-0.2	-2.1	-2.1	-2.0	0.0	
ONC#1	-4.7	-4.1	-8.9		-3.3	
p#1		2.9	2.8	2.7	0.7	0.6
SD-6	0.0	-0.1	-0.1	-0.1	0.0	
SD-7	-0.1	-0.5	-0.4	-0.4	-0.1	
SD-9	0.1	0.1	0.1	0.1	0.0	
SD-12	-0.1	-0.3	-0.2	-0.3	-0.1	
UZ-1		-0.6	-0.4	-0.6		
UZ#4	-0.1					
UZ#5	-0.3					
UZ-6	0.0	-0.4	-0.4	-0.3	-0.1	
UZ-7a	-19.6			12.2		
UZ-14					-2.8	

Table 3. Model to borehole correlation difference computed by subtracting the model horizon elevations in table 2 from well log horizon picks in table 1 (ft) (cont'd)

#wellid	Tpbt4	Tptpul	RHH	Tptpll	Tac	Tund
UZ#16	0.4	0.1	0.1	0.2	0.1	
WT-1	0.2	-0.1	-0.1	-0.1	-0.3	
WT-2	-0.8	0.6	0.7	-0.4	-0.3	
WT#3					0.1	
WT#4	-1.0	-0.7	-0.7	-0.2	-0.4	
WT#6				133.7	2.4	
WT-7	-0.1	-0.3	-0.3	-0.2	1.5	
WT-10	0.3	0.0	-0.3			
WT-11	0.0	-0.4	-0.4	-0.4	-0.1	
WT#12	0.0	-0.4	-0.4	-0.4	0.1	
WT#13	0.6	0.4	0.4	0.4		
WT#14		19.3	19.3	19.3	0.0	
WT#15	0.0	-0.2	-0.2	-0.2		
WT#16	0.2	0.0		-0.2	-0.4	
WT#17	0.0	-0.3	-0.3	-0.3	-0.1	
WT#18	0.6	0.6	0.7	0.7	0.2	
WT#24	0.4	0.3	0.2	0.3	0.5	

The results in table 3 show discrepancies between the true and modeled elevations that are typically much less than 10 ft. A single discrepancy greater than 50 ft (borehole WT#6) warrants further investigation described below to determine if the discrepancy is the result of insufficient data control, inaccurate input data, side effects from non-vertical faulting, or inaccuracies in horizon grid export algorithms.

In computing the subsurface horizon models, EV employs an iterative numerical algorithm (i.e., minimum tension gridding) that attempts to fit an interpolated surface to the control points established by the well log horizon picks and fault structures. The quality, number, and spatial distribution of data points all affect the accuracy with which the model surface fits the input data. In areas of poor data control, the software algorithms tend to produce smooth surfaces that follow general trends established by the sparse control points. Likewise, the software attempts to honor the majority of densely spaced data points, but outliers may have been disregarded by EV if they fell outside the software parameter ranges specified by the DOE modelers. For example, horizon elevation extracted from the Tptpll exported horizon grid at the location of borehole WT#6 is 133.7 ft below the well-log horizon location. This means the EV software computed the elevation of the horizon to be 133.7 ft lower than the geologist picked the horizon location on the WT#6 well log. Examination of the model reveals that the Tptpll horizon is not represented in the region near well WT#6 (figure E-2), and that horizons underlying the borehole pick are drawn upwards in the immediate vicinity of the borehole

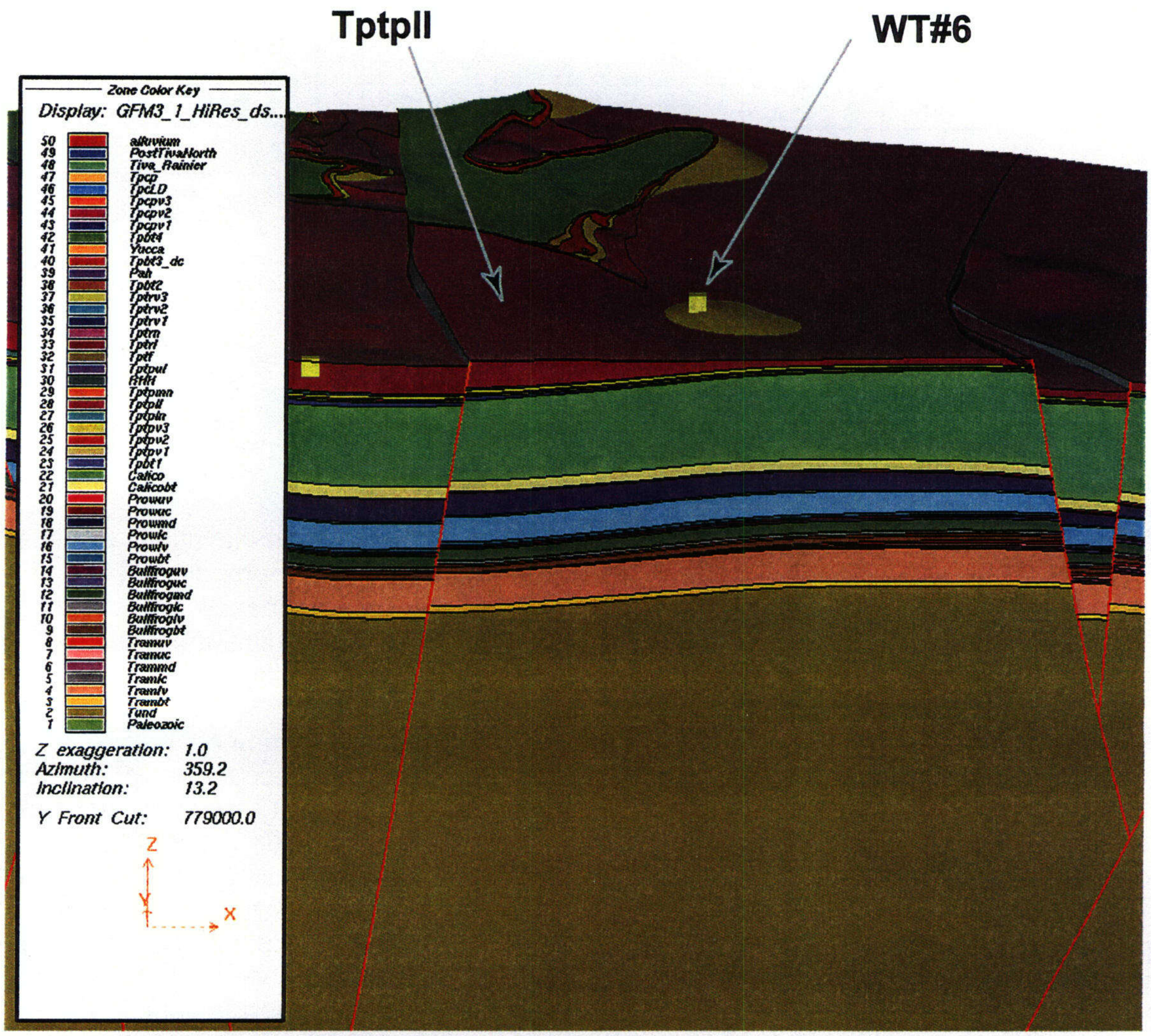

Figure E-2. Oblique view of GFM3.1 looking north. Horizons are backstripped to expose the upper surface of the Tptpll (purple) horizon near well WT#6. Yellow cube marks well pick for top of Tptpll horizon. East-west slice along 77,9000 Northing.

(figure E-3). Erroneous correlations often result when modeled faults are mis-placed relative to a borehole. However, the -133.7 ft discrepancy for the WT#6 well is not as easily explained because a fault surface is not present in the vicinity of the borehole (figure E-2). This disagreement may possibly be explained as a data outlier, poorly constrained software calculations, the presence of an unmapped fault, or incorrect horizon depth in the interpreted of actual borehole data.

EV offers several methods for horizon data extraction. The simplest method is to extract complete horizon grids from model faces files. The grids are then exported using the EV software as ASCII data files. During the export/extraction process, some data smoothing due to re-gridding can occur. The two-dimensional (2D) horizon grids and ASCII horizon data files supplied with the GFM3.1 are extracted from the GFM3.1 model faces file. An alternative method is to export ASCII data files directly from the 2D fault-block horizon grids used to construct the faces file. This method, though time-consuming, can more closely honor the input data. Where the export horizon grids produced poor correlation with the borehole horizon picks (>10 ft), the horizon elevations were also extracted from the 2D fault-block horizon grid files (table 4). The results, shown in table 5, indicate that the number or degree of erroneous correlations may be reduced but not completely eliminated using this method. In all but one horizon intersection, the erroneous correlations encountered in this analysis were minor, and do not preclude the DOE or NRC from using GFM3.1. Correlation differences of the greatest observed magnitude were associated with boreholes UZ-7a, WT6, and WT14.

(3) Are all data essential for constructing stratigraphic horizons included in the database that accompanied GFM3.1?

All data essential for constructing stratigraphic horizons are included in the database that accompanied GFM3.1. In addition, exported horizon grids and ASCII data files were supplied with the GFM3.1 submitted for analysis. As a component of DOE's ISM, horizon and fault data from GFM3.1 will be exported for use in process and design models. Evaluation of the GFM3.1 indicates that the extraction of data from fault block horizon grids provides a greater degree of accuracy than do horizons exported directly from faces files. In cases where this degree of accuracy is required, extracting horizon data from the fault-block horizon files used to construct the GFM3.1 may be the preferred extraction method. This method requires a thorough cataloguing of all fault blocks by name and extent.

Table 4. Selected GFM3.1 horizon picks computed from fault-block horizon grids with EarthVision (ft)

#wellid	Tpbt4	Tptpul	RHH	Tptpll	Tac	Tund
a#4						
a#5						
a#6						
b#1						
c#2						
G-1						
G-2						

Table 4. Selected GFM3.1 horizon picks computed from fault-block horizon grids with EarthVision (ft) (cont'd)

#wellid	Tpbt4	Tptpul	RHH	Tptpll	Tac	Tund
G-3						
G-4						
H-1						
H-3						
H-4						
H-5						
H-6						
J-13						
NRG#1						
NRG#2						
NRG#4						
NRG#5						
NRG-6						
NRG-7A						
ONC#1						
p#1						
SD-6						
SD-7						
SD-9						
SD-12						
UZ-1						
UZ#4						
UZ#5						
UZ-6						
UZ-7a	4034.3			3611.2		
UZ-14						
UZ#16						
WT-1						
WT-2						
WT#3						
WT#4						
WT#6				3929.3		
WT-7						

Table 4. Selected GFM3.1 horizon picks computed from fault-block horizon grids with EarthVision (ft) (cont'd)

#wellid	Tpbt4	Tptpul	RHH	Tptpll	Tac	Tund
WT-10						
WT-11						
WT#12						
WT#13						
WT#14		3235.7	3118.7	2976.7		
WT#15						
WT#16						
WT#17						
WT#18						
WT#24						

Table 5. Selected model to borehole miss-ties computed by subtracting the well log horizon picks in table 1 from the model fault-block horizon elevations in table 4 (ft)

#wellid	Tpbt4	Tptpul	RHH	Tptpll	Tac	Tund
a#4						
a#5						
a#6						
b#1						
c#2						
G-1						
G-2						
G-3						
G-4						
H-1						
H-3						
H-4						
H-5						
H-6						
J-13						
NRG#1						
NRG#2						
NRG#4						
NRG#5						

Table 5. Selected model to borehole miss-ties computed by subtracting the well log horizon picks in table 1 from the model fault-block horizon elevations in table 4 (ft) (cont'd)

#wellid	Tpbt4	Tptpul	RHH	Tptpll	Tac	Tund
NRG-6						
NRG-7A						
ONC#1						
p#1						
SD-6						
SD-7						
SD-9						
SD-12						
UZ-1						
UZ#4						
UZ#5						
UZ-6						
UZ-7a	4.0			-9.8		
UZ-14						
UZ#16						
WT-1						
WT-2						
WT#3						
WT#4						
WT#6				-133.7		
WT-7						
WT-10						
WT-11						
WT#12						
WT#13						
WT#14		-19.3	-19.3	-19.3		
WT#15						
WT#16						
WT#17						
WT#18						
WT#24						

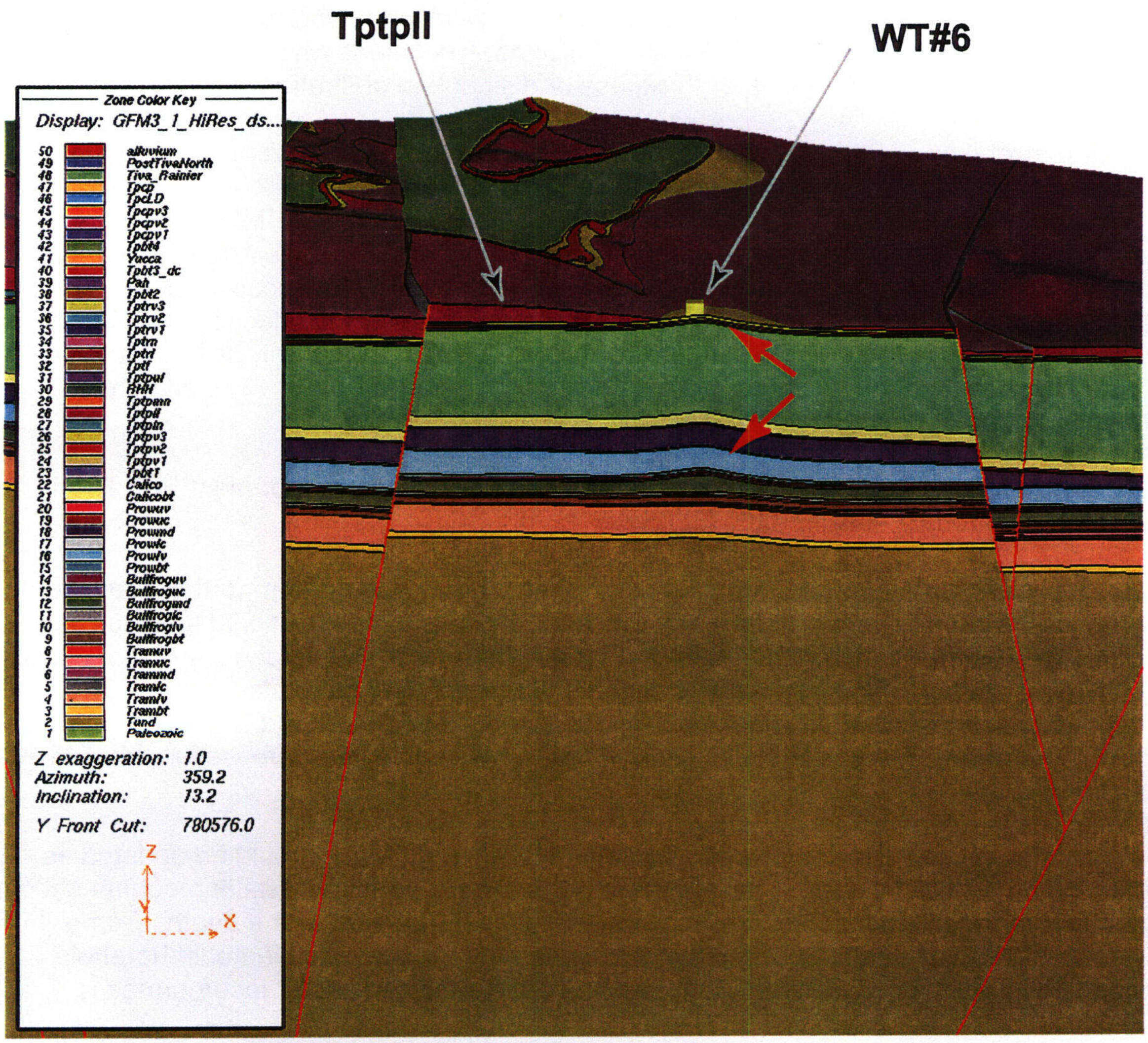

Figure E-3. Oblique view of GFM3.1 looking north. Horizons are backstripped to expose the upper surface of the Tptpll (purple) horizon at well WT#6. Yellow cube marks well pick for top of Tptpll horizon. Horizons underlying Tptpll appear drawn upward in the vicinity of the well (red arrows). East-west slice along 780576 Northing.

EarthVision constructs 3D models by building individual fault blocks, then assembling these fault blocks to form a complete model. Fault blocks are identified by user-defined names. Although a logical naming convention is followed for the GFM3.1 fault blocks, the detailed nature of the model makes it difficult to identify the location and extent of individual fault blocks by name. While all essential data required to manipulate and reproduce GFM3.1 are available, extracting data from individual fault-block horizon grids requires a complete delineation of the effective fault-block grid area, and a complete delineation and catalogued nomenclature of the model fault blocks. The sequence and faces files supplied with the GFM3.1 are not sufficient to clearly catalogue fault-block horizon grids for block-by-block horizon data extraction. This is easily solved by including a map showing GFM3.1 fault blocks by name in the GFM3.1 report. This observation in no way precludes the DOE or NRC from using the GFM3.1.

(4) Considering the technical bases for the manner in which stratigraphic horizons are represented in GFM3.1, are there alternative interpretations which should be incorporated into the model for thickness or distribution of stratigraphic horizons?

Current interpretations of thickness and distribution of stratigraphic horizons are adequate. As new data or improved interpretations are available, the GFM3.1 may benefit from the incorporation of new information and interpretations. Construction of GFM3.1 was undertaken using a reference horizon-isochore approach to modeling the subsurface horizon relationships. Alternative approaches to developing GFM3.1, through the use of balanced cross-sections, are possible and may improve the modeled distribution of horizons or modeled regions with scant borehole control. Where borehole data are available, GFM3.1 shows only scattered discrepancies between the modeled horizons and well log horizon picks. The scattered discrepancies do not prevent the DOE or NRC from using GFM3.1.

(5) Are there any observations on how stratigraphic horizons are represented in GFM3.1 that may benefit from further clarification by the DOE?

Horizon thickness variations occurring across the model may benefit from further clarification. Horizons that thicken on down-thrown sides of faults indicate syndepositional faulting (Sawyer, et al., 1994). The implication of horizons that tend to thicken or thin across the center of the model block is unclear. The thickness change relationships may be related to syn-, pre-, or postdepositional processes, or to the decrease in sub-surface data control near the model margins. Thickness changes in the volcanic stratigraphy should be addressed in the ISM description.

As new data or improved interpretations become available, GFM3.1 should be updated as required by the additional data. The integration of well bore deviation data is recommended if directional logs identify horizontal deviations of more than 1 percent of the depth. Some refinement of the fault surfaces or horizon thickness may be warranted if model-borehole discrepancies persist once the deviation data has been analyzed and/or incorporated in GFM3.1.

At this time, there are no major stratigraphic discrepancies that would preclude the NRC or the DOE from using GFM3.1.

PART II - REVIEW AND EVALUATION OF FAULT SURFACES IN GEOLOGICAL FRAMEWORK MODEL VERSION 3.1

(1) Are input data used in GFM3.1 to define faults at the surface and in the subsurface appropriate and sufficient for this purpose?

<u>Data for surface fault traces (strike) and shallow subsurface fault dips</u>

Data derived from a prepublication digital (DXF) version of the geologic map of Day, et al. (1998), the same digital database employed in construction of GFM3.0, were used to define surface traces of faults in GFM3.1. These data made it possible to represent actual mapped variations in strike of faults at the surface in GFM3.1. Reasonable interpretations of strikes of faults inferred to occur beneath alluvium were also incorporated into GFM3.1 with due consideration for location and strike of segments of mapped surface traces and inferred positions of fault traces beneath alluvium shown by Day, et al. (1998). In keeping with field observations indicating that faults do not commonly cut alluvium in the model area, fault traces were not shown cutting across alluvium in GFM3.1. Alluvium in this report follows DOE usage, but is understood to include sediments of various origins, not all of which are alluvial.

Dip measurements taken from outcrops and shown on the geologic map of Day, et al. (1998) were used to constrain fault plane orientations at the surface and in the shallow subsurface. These orientations were used to represent fault surfaces in the uppermost part of the EV-generated 2D grid (.2grd) files in GFM3.1. The dip value in the shallow sub-surface for individual faults was selected from the range of values mapped by Day, et al. (1998). The selected dip value was used to project the surface trace of the fault as mapped by Day, et al. (1998) in the updip and downdip direction to provide control points for fault plane construction (figure E-4).

<u>Data for deeper subsurface three-dimensional fault orientations (strike and dip)</u>

Based on EV-generated scattered data (.dat) files provided with GFM3.1 which contain (x, y, z) coordinates that constrain to an approximate elevation the location of faults in the subsurface, only 10 of the 42 faults in the model have some information to control their position at depth. As indicated by file names (e.g., "fmb31bow.dat" is a scattered data file [.dat] in the database for the Bow Ridge [bow] fault [f] in GFM3.1 [31] which contains both map [m] and subsurface borehole intercepts and ESF intersection [b] data), these 10 structures are the Bow Ridge, Drill Hole Wash, Dune Wash, Ghost Dance, Iron Ridge, Midway Valley, Paintbrush Canyon, Solitario Canyon, Solitario Splay G, and Sundance faults. Dip angles at depth are not quantitative, measured values but rather reflect the interpretive cross-sections of Day, et al. (1998). Dips bear a general relation to measured surface dip angles so that fault geometry and orientation are reasonably represented at depth. This is the general approach for extrapolation of fault surfaces to depth in GFM3.1. Files included with GFM3.1 make it possible to ascertain dip angles used in generation of the 2D grids for the fault surfaces.

Consideration of how faults were represented in the cross-sections of Day, et al. (1998) resulted in many of the faults in GFM3.1 being included as curved surfaces. The curved geometry was produced by purposeful manipulation of the 2D fault surface grids to produce conceptual results. This geometry does not reflect measured or calculated quantitative dip angles for faults in the subsurface. This variation in subsurface fault geometry represents the

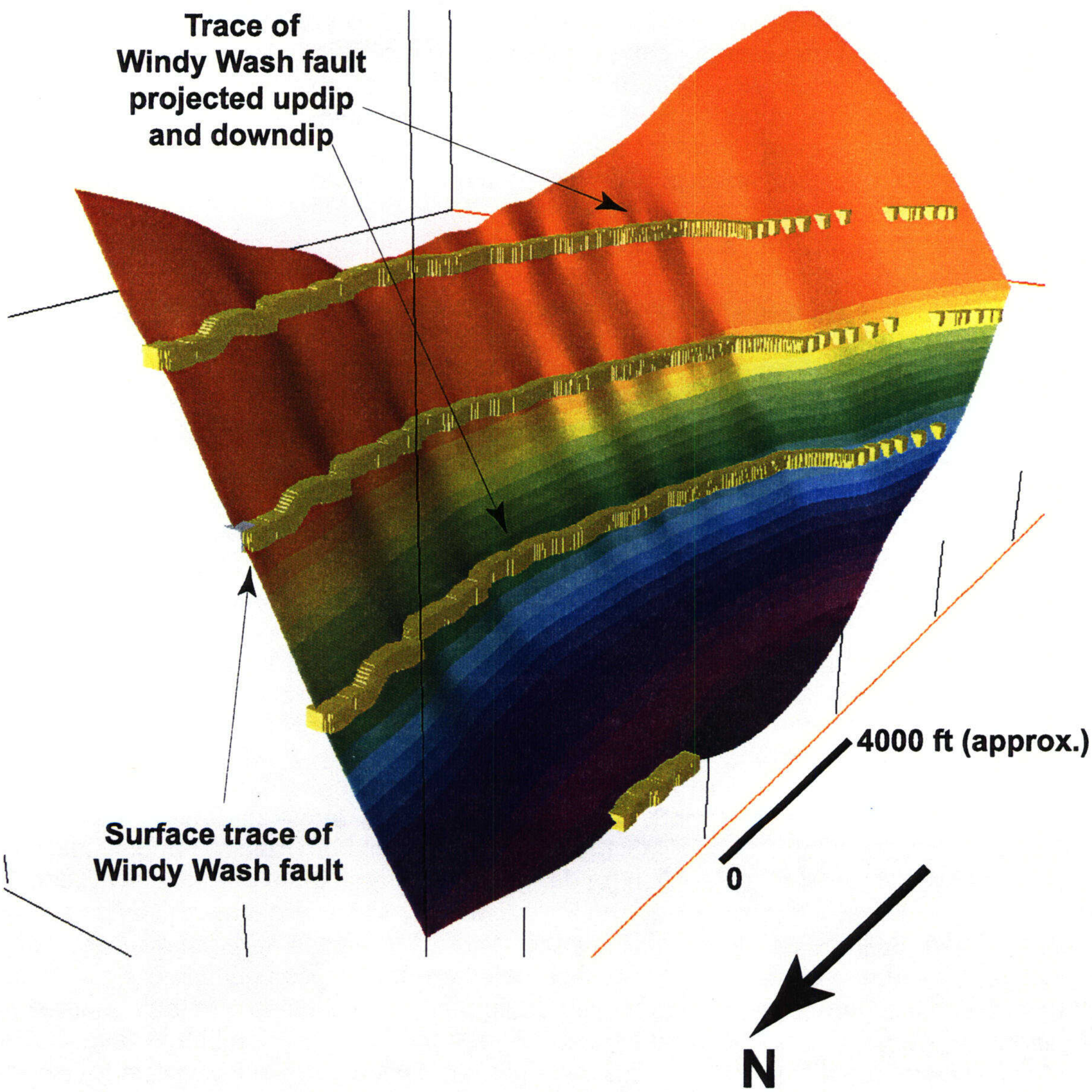

Figure E-4. View of Windy Wash fault surface from GFM3.1. Yellow cubes are data points used to define the fault surface. The central row of data points represent the surface trace of the Windy Wash fault. The trace is projected updip and downdip to provide points for definition of the fault surface.

primary difference in how fault surfaces were modeled between GFM3.0, wherein faults were planar, and GFM3.1. Figure E-5 illustrates fault surfaces as they are represented in GFM3.1. Curvature of many faults with depth is clearly shown (e.g. faults labeled in the legend as IronRidge, Ironw1, Ironw2, and Ironw3).

In summary, the data used in GFM3.1 to define geometry and orientation of faults at the surface were deemed by the NRC to be appropriate and sufficient. Although strikes and dips measured in outcrop and shown on the geologic map of Day, et al. (1998), borehole data and ESF and ECRB exposure provide the quantitative data for defining fault surfaces, the use of fault trace lines from the geologic map of Day, et al. (1998) and dips inferred from their cross sections (Day, et al., 1998) to generate 2D grid (.2grd) files in EV representing fault surfaces at depth resulted in reasonable representation of the faults included in GFM3.1. Faults were clipped with polygon (.ply) files based on the length of the mapped fault trace and on reasonable interpretations about extent at depth. Both the 2D grid (.2grd) and the polygon (.ply) files were provided in the GFM3.1 database.

(2) Do fault traces and fault surfaces as modeled in GFM3.1 fit the input data?

Fault surfaces contained in GFM3.1 as 2D grid files closely fit the field data. These data include trends of mapped surface traces from the geologic map of Day, et al. (1998) to define fault strike; dips measured along the fault trace in outcrops as recorded by Day, et al. (1998); and subsurface information on fault location and orientation for 10 of the 42 faults in the model from borehole intercepts or ESF intersections. Since little subsurface information exists for defining fault orientations at depth (the exception being the 10 faults indicated in the discussion of Item 1), strike lines were protected above and below the mapped fault trace and incorporated into the 2D grids in concert with subsurface dips suggested from the interpretive cross sections of Day, et al. (1998) as described above.

Inclusion of the qualitative interpretative cross section information resulted in many major west-dipping normal faults being modeled as curved surfaces extending to the base of the model at 8000 ft below sea level. As an example, figure E-4 illustrates the close fit between the 2D grid for the Windy Wash fault surface and all data used for construction of the grid. This structure was constructed with a dip of 60° W at the surface, shallowing to 50° W at the lower part of the 2D grid based on cross-section information.

In summary, fault traces and fault surfaces modeled in GFM3.1 closely fit the input data. Input data included field information (fault trace lines, measured dips in outcrop, and subsurface information on fault location and orientation from borehole intercepts or ESF intersections) and interpretive data from cross sections drawn by Day, et al. (1998). Polygons used to clip the fault surfaces both laterally and vertically were also considered reasonable. Quantitative observations and qualitative interpretations were used to generate the fault surfaces in a manner which the NRC considers consistent, technically reasonable, and satisfactory.

(3) Are all data essential for constructing fault surfaces and other structure models (i.e., fault blocks, zone surfaces, and zone blocks) included in the database which accompanied GFM3.1? Yes, see following basis.

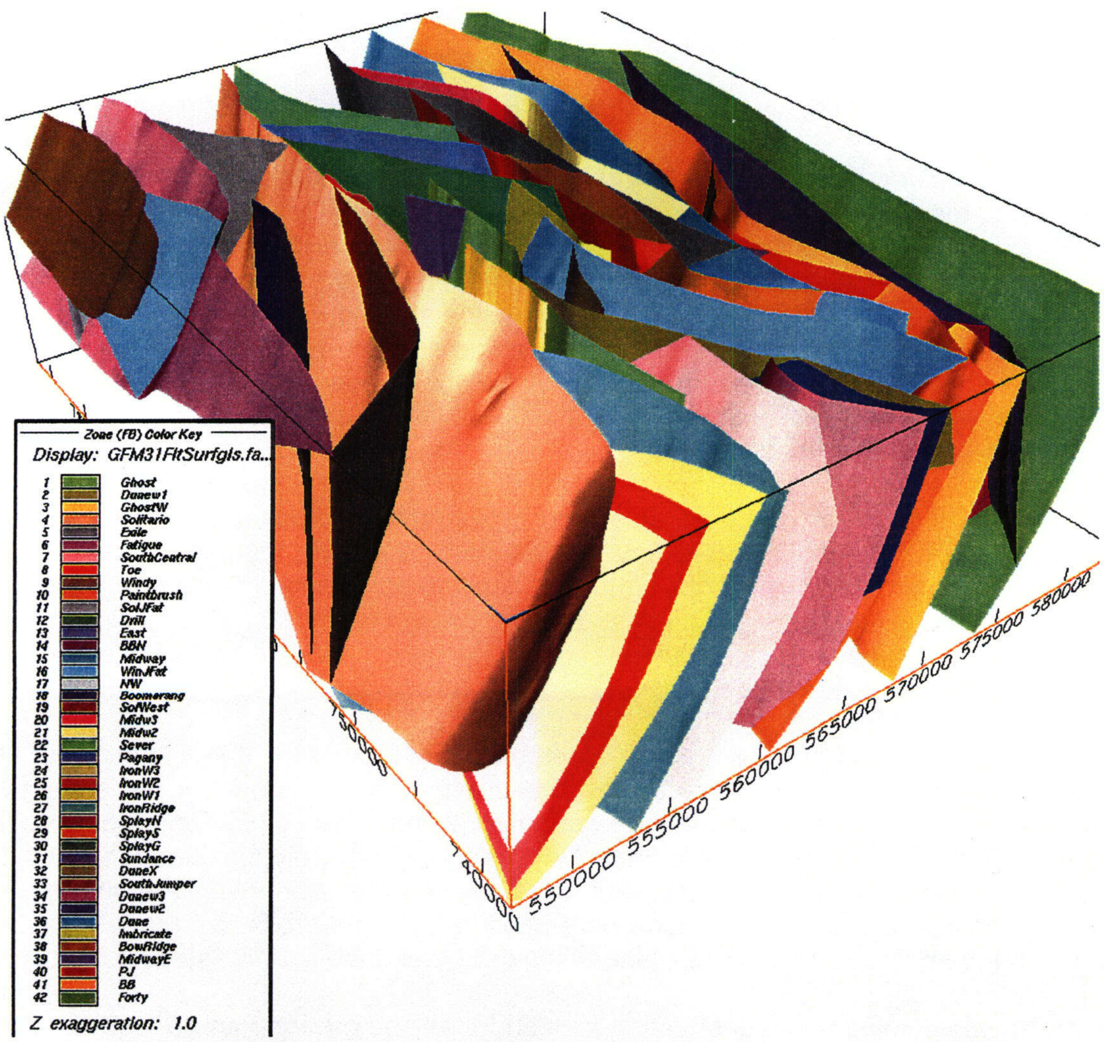

Figure E-5. Fault surface file (.faces) generated from data supplied with GFM3.1 using EarthVision software. Coordinates are Nevada State Plane (ft).

All data essential for calculating 3D structure models (i.e., four distinct models illustrating fault surfaces, fault blocks, zone surfaces, and zone blocks) using the Geologic Structure Builder (GSB) capability of EV5.0 were provided by the DOE in the GFM3.1 database submitted to the NRC. The EV-generated master sequence file (GFM31final.seq) which accompanied the original GFM3.1 database was used after only minor editorial modifications to reconstruct .faces files for the four structure models (labeled as GFM31FltSurfgls.faces, GFM31FltBlkgls.faces, GFM31ZnSurfgls.faces, and GFM31ZnBlkgls.faces). The sequence file and accompanying data in the database made it possible to reconstruct 42 faults, 43 fault blocks, and 50 stratigraphic horizons (including alluvium) for GFM3.1. It was necessary to rename select files in GFM31final.seq to provide correct path names for access. Specifically, units "Tiva_Rainier" and "alluvium" needed the directory in which they were located, horizon/, included in the path name in the sequence (.seq) file for all appropriate fault blocks, beginning with the stratigraphic sequence for fault block "aboveWindy". The modified sequence file was named GFM31FINALgls.seq and relocated to make running more efficient. This modified sequence file is included in the CRADAL database along with the original sequence file (i.e., GFM31final.seq) from the DOE.

In summary, all data essential for constructing fault surfaces and other structure models for GFM3.1 were included in the data files originally submitted to the NRC by the DOE. Only a few path names had to be altered for construction of structure models after the modified sequence file (GFM31FINALgls.seq) was relocated to a more convenient directory. To verify that all necessary data for these constructions were included and transferred to the CRADAL database, recalculation of EV-generated .faces files was accomplished for fault surfaces and fault blocks (specifically files GFM31FltSurfgls.faces and GFM31FltBlkgls.faces) and zone surfaces and zone blocks (files GFM3.1ZnSurfgls.faces and GDM31ZnBlkgls.faces) using a master sequence file (GFM31FINALgls.seq) that was only slightly modified from the original sequence file (i.e., GFM31final.seq). Figures E-5 through E-7 illustrate these reconstructed .faces files for fault surfaces and blocks and zone blocks and show the 42 faults, 43 fault blocks, and 50 stratigraphic horizons which comprise GFM3.1. The ability to readily reconstruct the four structure .faces files clearly shows that all pertinent data for doing so were provided with GFM3.1.

(4) Considering the technical bases for the manner in which fault surfaces are represented in GFM3.1, are there alternative interpretations for fault geometry which should be incorporated into the model?

During review of GFM3.0, the NRC introduced a curved geometry for fault Ironw3 (U.S. Nuclear Regulatory Commission, 1998, appendix F). This change indicated that alternative interpretations can be incorporated into the 3D geologic framework model. The changes implemented by DOE for GFM3.1 included the following:

(a) Many faults are now shown with curvature in the subsurface rather than as planar features asin GFM3.0 (see item earlier). This geometric change was in part implemented in response to observations made during review of GFM3.0. It is more realistic to represent some faults as curved rather than planar surfaces based on alternative concepts developed from field observations (Ferrill, et al., in press) and geometric analysis of balanced cross sections (Young, et al., 1993). Evaluation of cross-sections extracted from GFM3.1 indicate that alternative

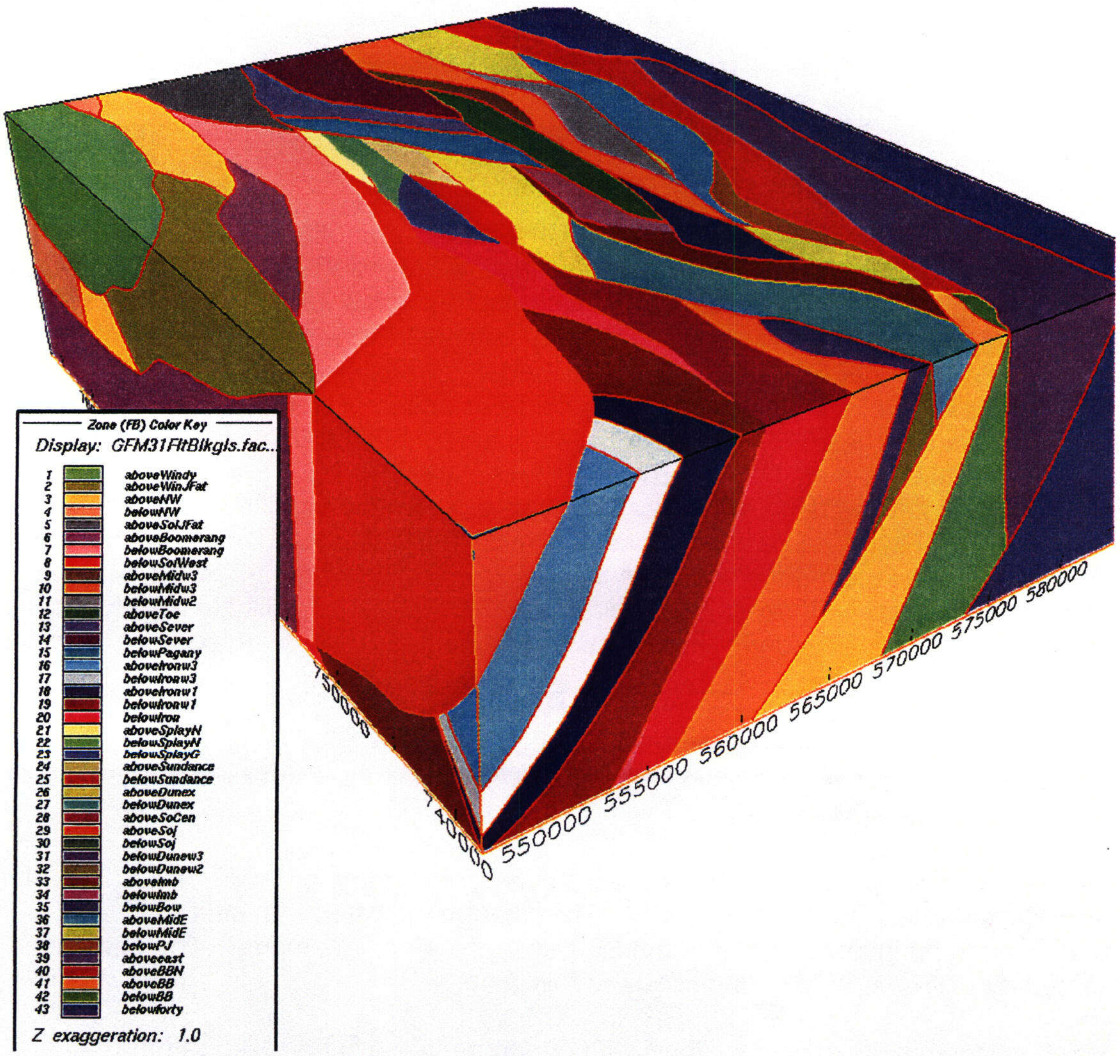

Figure E-6. Fault block file (.faces) generated from data supplied with GFM3.1 using EarthVision software. Coordinates are Nevada State Plane (ft).

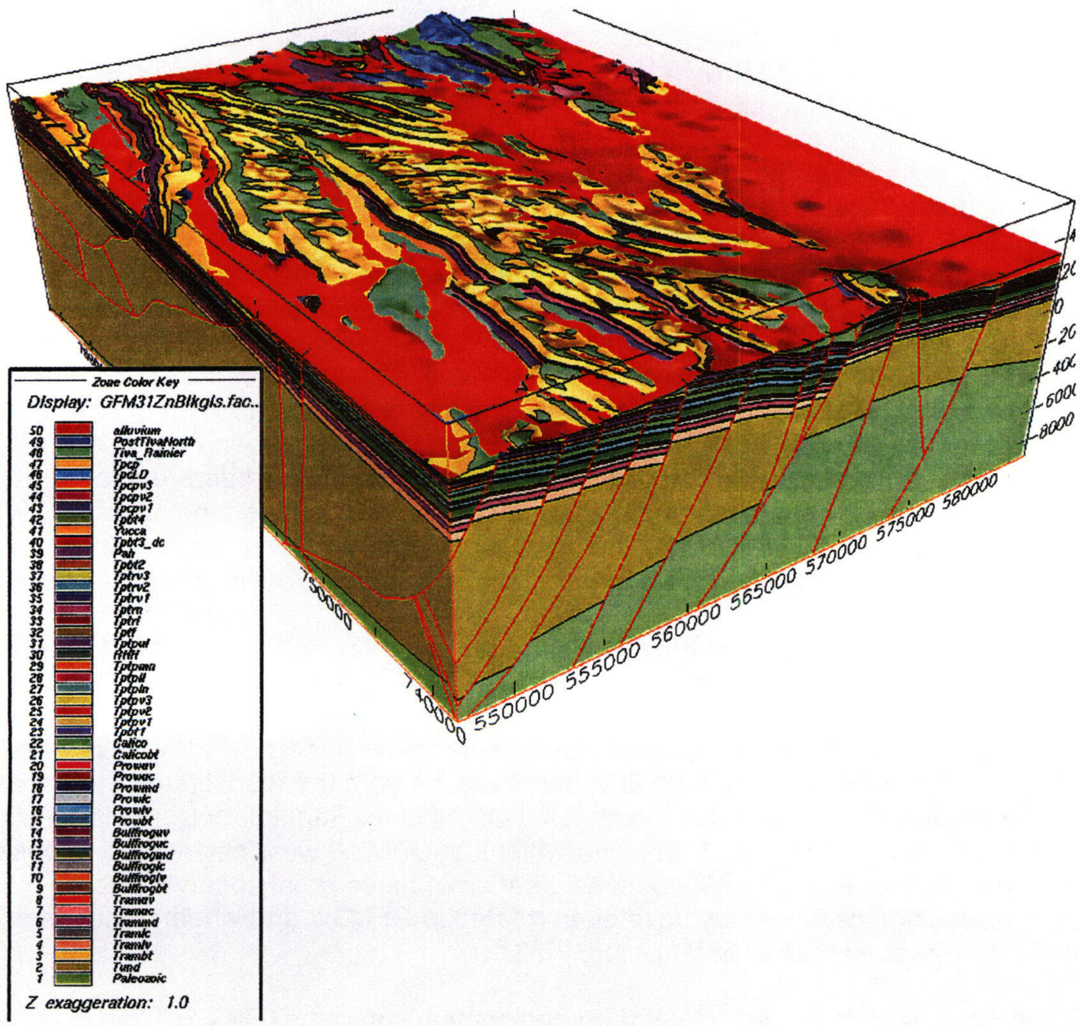

Figure E-7. Zone block file (.faces) generated from data supplied with GFM3.1 using EarthVision software. Coordinates are Nevada State Plane (ft).

interpretations of fault geometry may be indicated for some faults or fault systems (see following section (5) for explanation).

(b) A new, unnamed, east-dipping fault generalized from a family of structures shown on the geologic map of Day, et al. (1998) immediately north-northwest of The Prow, labeled as NW in GFM3.1, was added in the northwestern corner of the model between the Windy Wash, "WinJFat" (a "jumper" connecting fault between the Windy Wash and Fatigue Wash structures), and Fatigue Wash faults as shown in figure E-8. This fault was added primarily to account for the occurrence of exposed Calico stratigraphy at that location north-northwest of The Prow.

(c) Northwest-trending faults along Drill Hole Wash (Drillne and Drillsw in GFM3.0) were simplified to a single structure labeled as fault Drill in GFM3.1. These two closely-spaced, northwest trending faults were replaced by the single northwest trending structure since there appeared to be little need to retain this structural complexity at this location. That is, incorporation of faults Drillne and Drillsw in Drill Hole Wash into the model provided detail judged extraneous by DOE so the two structures were simplified to a single fault.

Currently, no additional alternative interpretations of fault geometry may need to be incorporated into GFM3.1. Inclusion of many faults as nonplanar structures at depth incorporates an alternative fault geometry which the NRC considers reasonable for certain faults in GFM3.1. This alternative subsurface geometry was suggested for inclusion in the model during review of GFM3.0. Inclusion of this alternative geometry, addition of a new fault in the northwest corner of GFM3.1 (fault NW), and deletion of one structure in Drill Hole Wash clearly indicates that EV software can be used to incorporate alternative interpretations. The modification of fault Ironw3 from planar in GFM3.0 to curved in an independent model constructed by CRADAL staff (SDS IRSR, U.S. Nuclear Regulatory Commission, 1998, appendix F) is further proof that alternative interpretations can be included using EV software.

(5) Are there any observations on how fault surfaces are represented in GFM3.1 that may benefit from further clarification by the DOE?

As part of the review of GFM3.1, it is deemed appropriate to consider previous observations made on the solid 3D model and selected 2D cross sections from the model during the review of GFM3.0, the results of which are documented in U.S. Nuclear Regulatory Commission, (1998, appendix F). Although none of the observations of GFM3.0 were considered to pose problems for NRC acceptance of GFM3.0, consideration of these initial observations is important for assessing how they may have been treated in GFM3.1 and whether they may cause concerns for representation of faults in GFM3.1.

Previous Observations from Review of GFM3.0 and comparison with GFM3.1:

a) Lack of a northwest trending structure in Antler Wash in the vicinity of borehole H-4 where a potential hydrologic connection was proposed between H-4 and the C-well complex to the southeast.

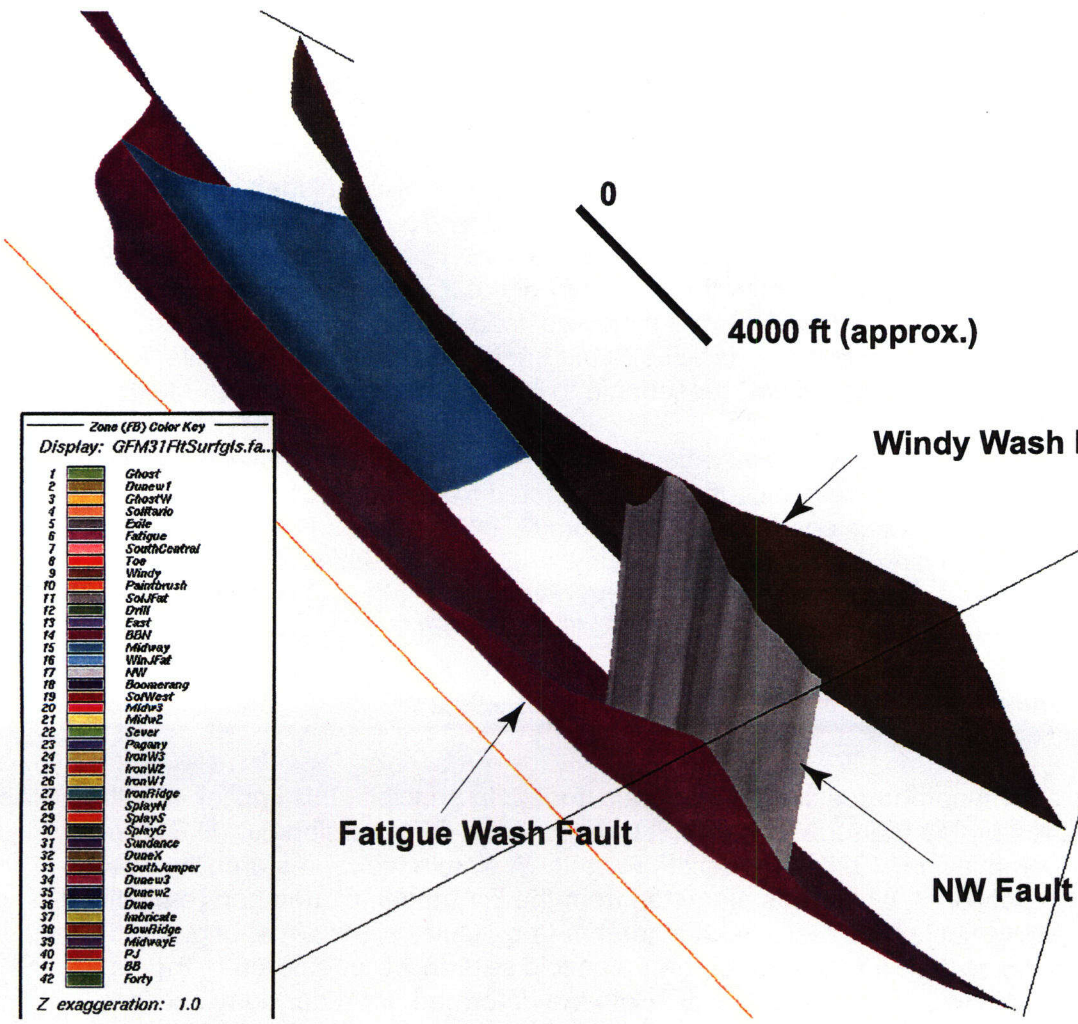

Figure E-8. New east-dipping fault "NW" (grey) between the Windy Wash (dark), WinJFat, and Fatigue Wash (purple) faults in GFM3.1

Just as for GFM3.0, GFM3.1 does not include a fault in Antler Wash. There is no geologic or geophysical evidence to support the interpretation of a buried fault paralleling Antler Wash. Lack of a northwest trending fault or fracture system in this location in no way causes the model to be unacceptable to the NRC, particularly since such a structure could be added using EV software if inclusion is deemed necessary.

b) Simplification of the imbricate fault zone to a single fault.

The single-fault geometry illustrated in GFM3.0 for the imbricate fault zone is also shown in GFM3.1. It is recognized that simplification of zones of faulting must necessarily be done to make it possible to construct a model at the scale of GFM3.1. Furthermore, additional complexity for this fault zone could be added using EV software if deemed necessary. The simplification of this zone as a single structure in no way renders GFM3.1 unacceptable to the NRC.

c) Inclusion of the Fortymile Wash fault as a prominent west-dipping structural feature even though the wash is filled with alluvium.

A west-dipping fault in Fortymile Wash, shown in GFM3.0, is also included in GFM3.1. Such a structure in the vicinity of Fortymile Wash was proposed by Young, et al. (1993) based on construction and analysis of balanced cross sections. USGS mappers (Day, et al., 1998) now consider that field data (e.g., the prevailing easterly dip of Paintbrush Group strata at Fran Ridge) strongly suggest the presence of a major west-side-down normal fault east of Fortymile Wash. This information adds new credence to the interpretation of the Fortymile Wash fault and the NRC considers it logical and reasonable to include this structure in GFM3.1.

The review of GFM3.0 included observations made from nine parallel east-west vertical 2D sections. Ten 2D east-west sections were extracted from GFM3.1 for the purpose of review (figures E-9–E21). Sections one through nine from GFM3.1 (figures E-12–E-21) parallel sections one through nine extracted for the review of GFM3.0. Section 10 from GFM3.1 (figures E-9 and E-21) was not considered in the review of GFM3.0. The following observations d. though h. are made from comparisons of GFM3.1 with GFM3.0.

d) Folding developed in the hangingwall blocks of faults that were modeled as planar at depth.

GFM version 3.1 incorporates curved fault trajectories. In principle, this implies that the sections will be more restorable than the planar fault trajectories of GFM version 3.0 (U.S. Nuclear Regulatory Commission, 1998, appendix F, Part II). A simple test of restorability was performed on section 6, which was extracted from the EV model, plotted and re-digitized. Then, using a simple vertical shear restoration algorithm (e.g., Dula, 1990; Groshong, 1990), the Tertiary volcanic section and the top of the Paleozoic section were restored to the top of unit RHH (Repository Host Horizon, GFM3.1). Both the deformed or present-day section (figure E-10) and the restored section (figure E-11) are shown. It is recognized that an east-west oriented section is not perpendicular to the more recent west-northwest–east-southeast extension direction interpreted at YM. However, the slight deviation produced by the east-west extension should be minor at the scale of restoration selected for this analysis. In addition, faulting at YM developed in an environment of east-west extension, resulting in a predominantly north-south oriented fault population (see Ferrill, et al., 1999, figure 4). Considering the

GFM version 3.1

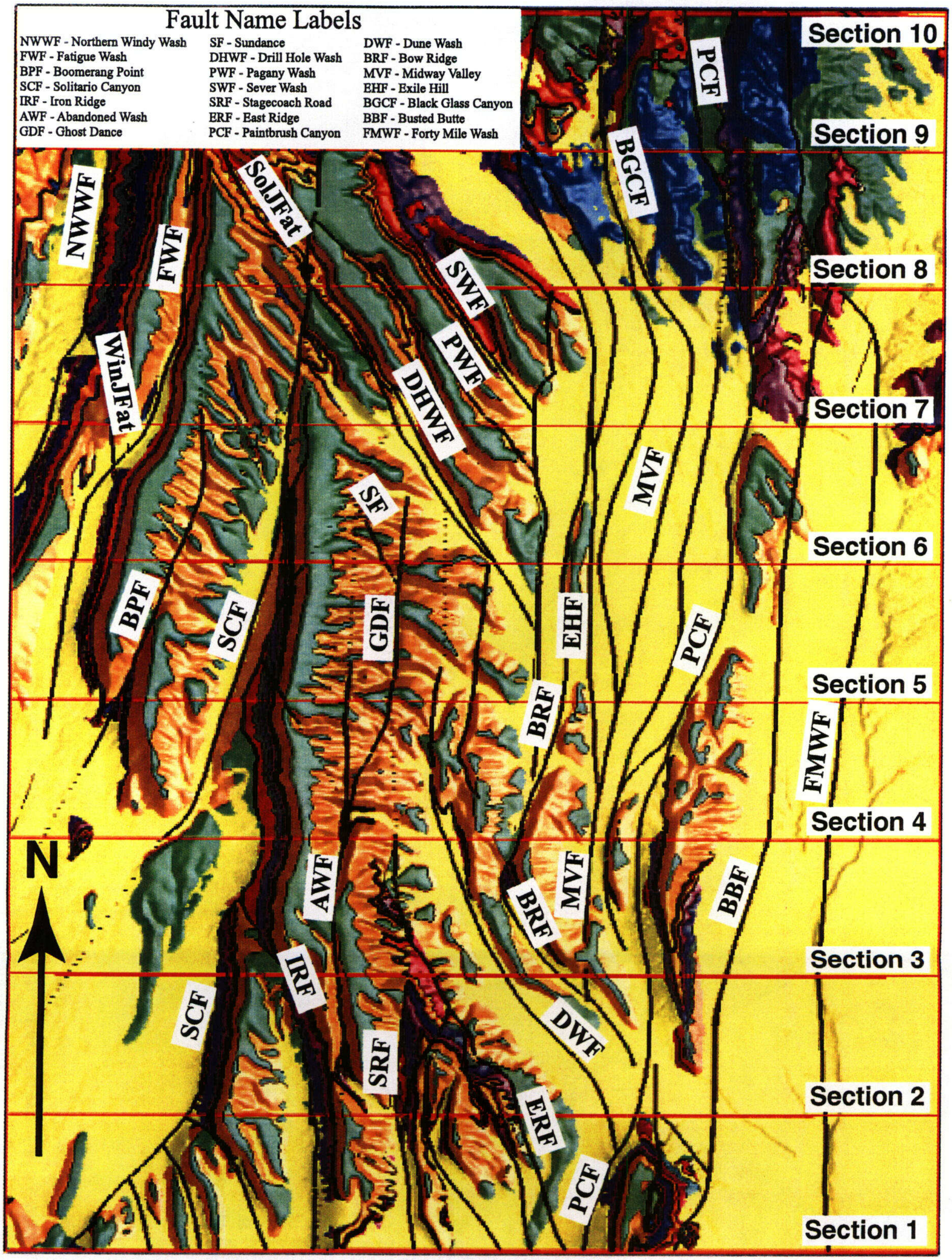

Figure E-9. Index map showing locations of sections 1 to 10 across GFM3.1 as shown in figures E-10 to E-21

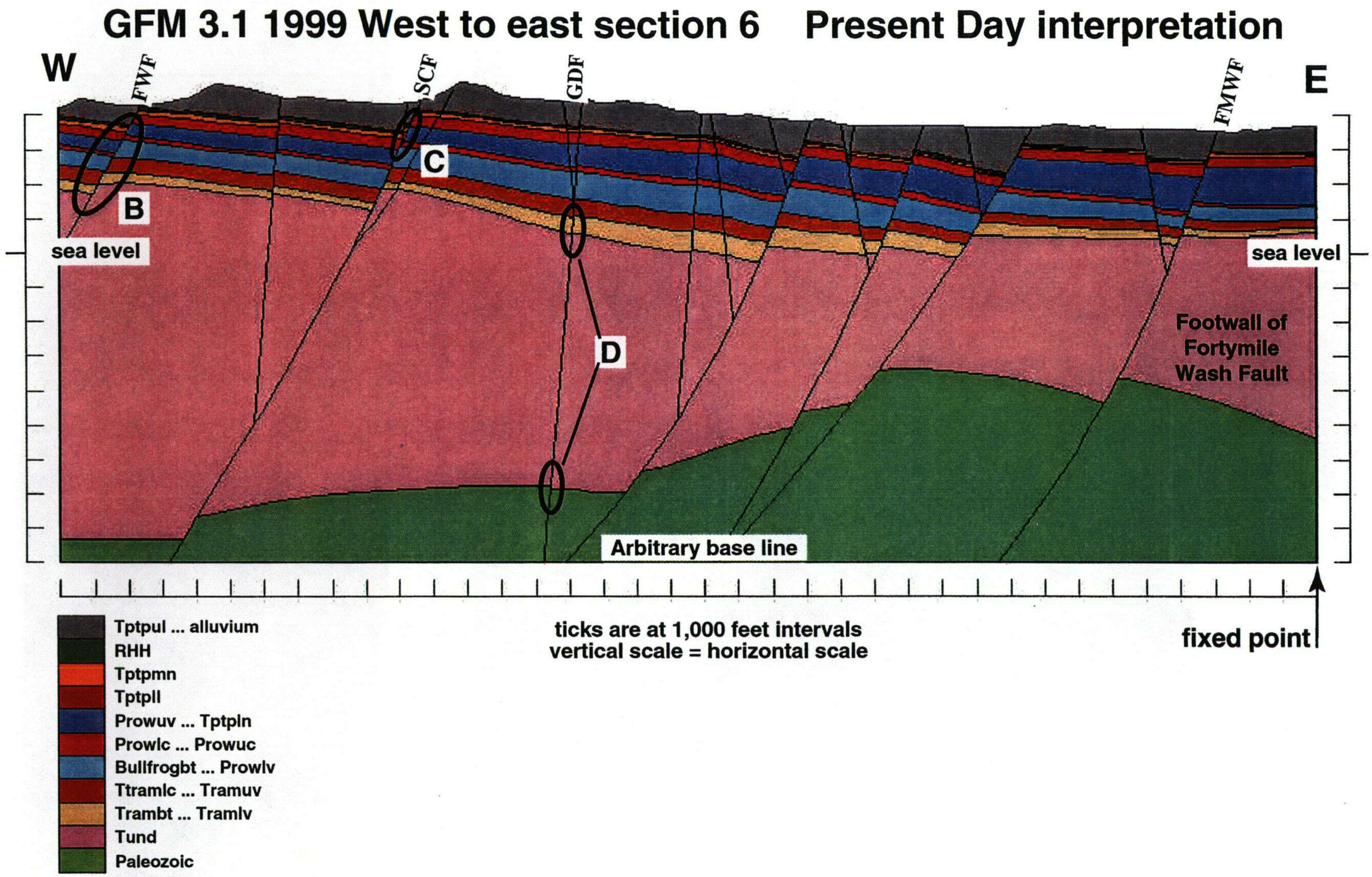

Figure E-10. Present-day interpretation along section 6 (figure E-17). Minor bed thickness/fault displacement inconsistency possibly caused by re-digitizing error. Thickness change inherent to model shown at C. Ghost Dance fault shows reversal of displacement at depth (D).

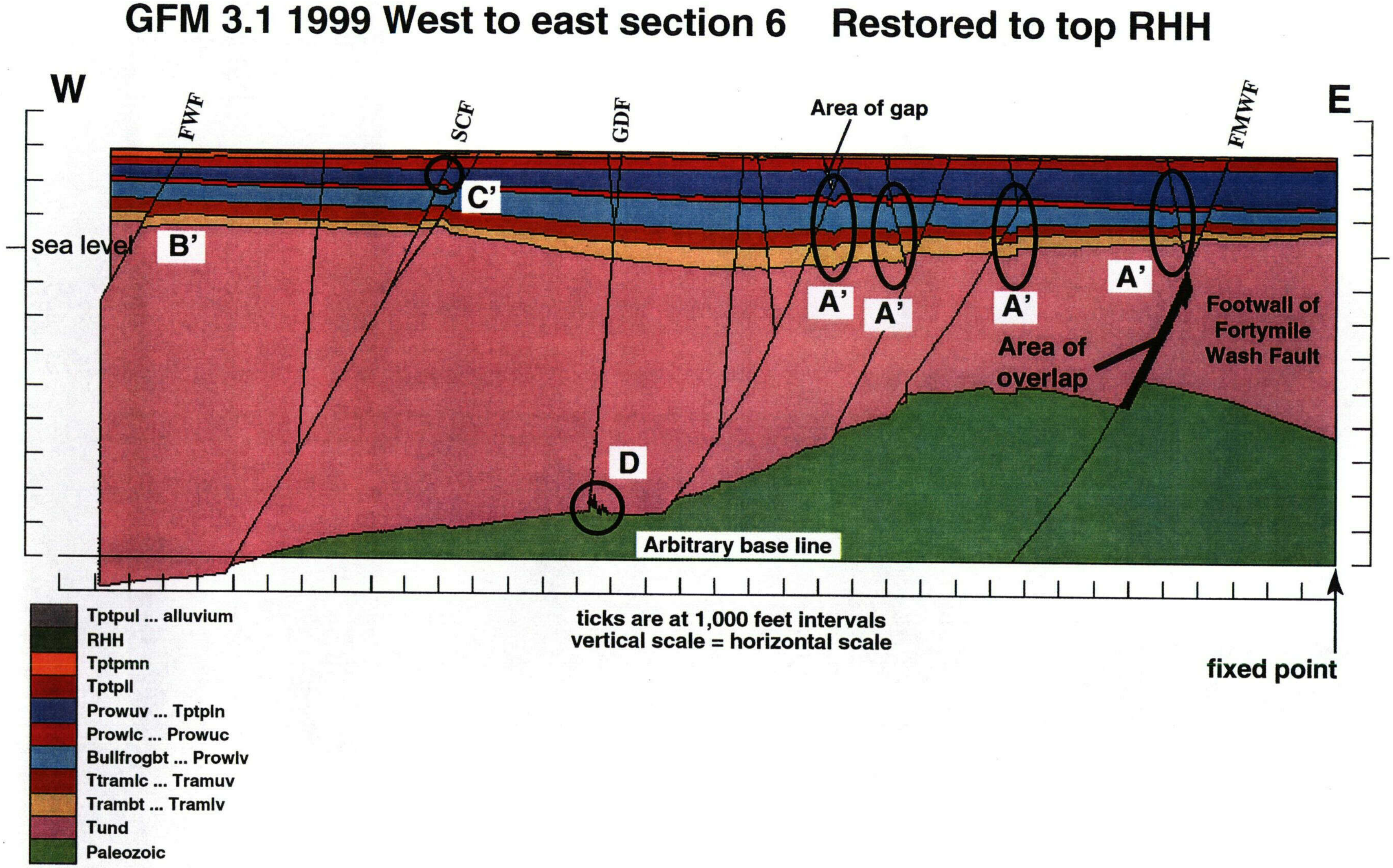

Figure E-11. Section 6 (figure E-17) restored state. Restoration by vertical shear. Mismatches at areas A' are products of vertical shear algorithm. Mismatch due to re-digitizing error at B'. Thickness change inherent in GFM3.1 produces mismatch at C'. Mismatch at D produced by displacement reversal on Ghost Dance fault (figure E-10).

Cross Section 1

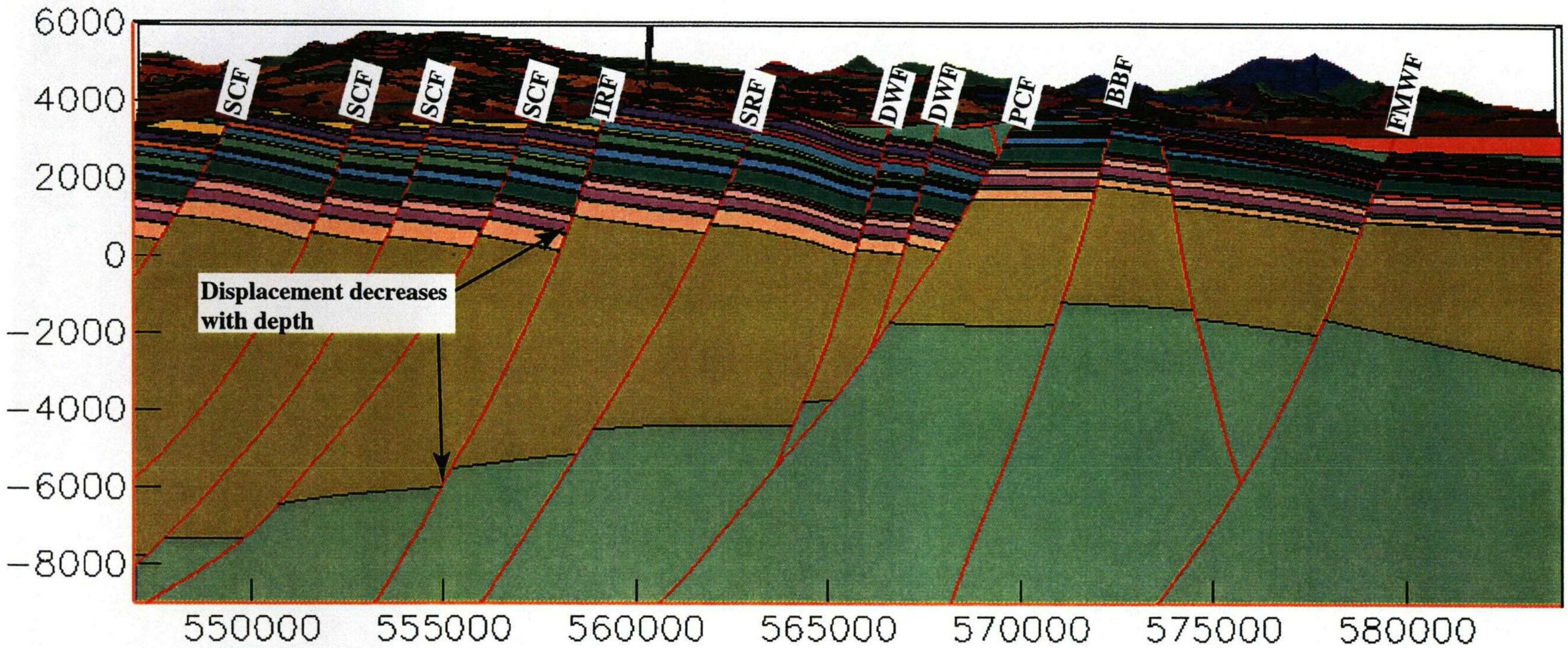

Figure E-12. Cross Section 1. Displacement on the Iron Ridge fault decreased with depth.

Cross Section 2

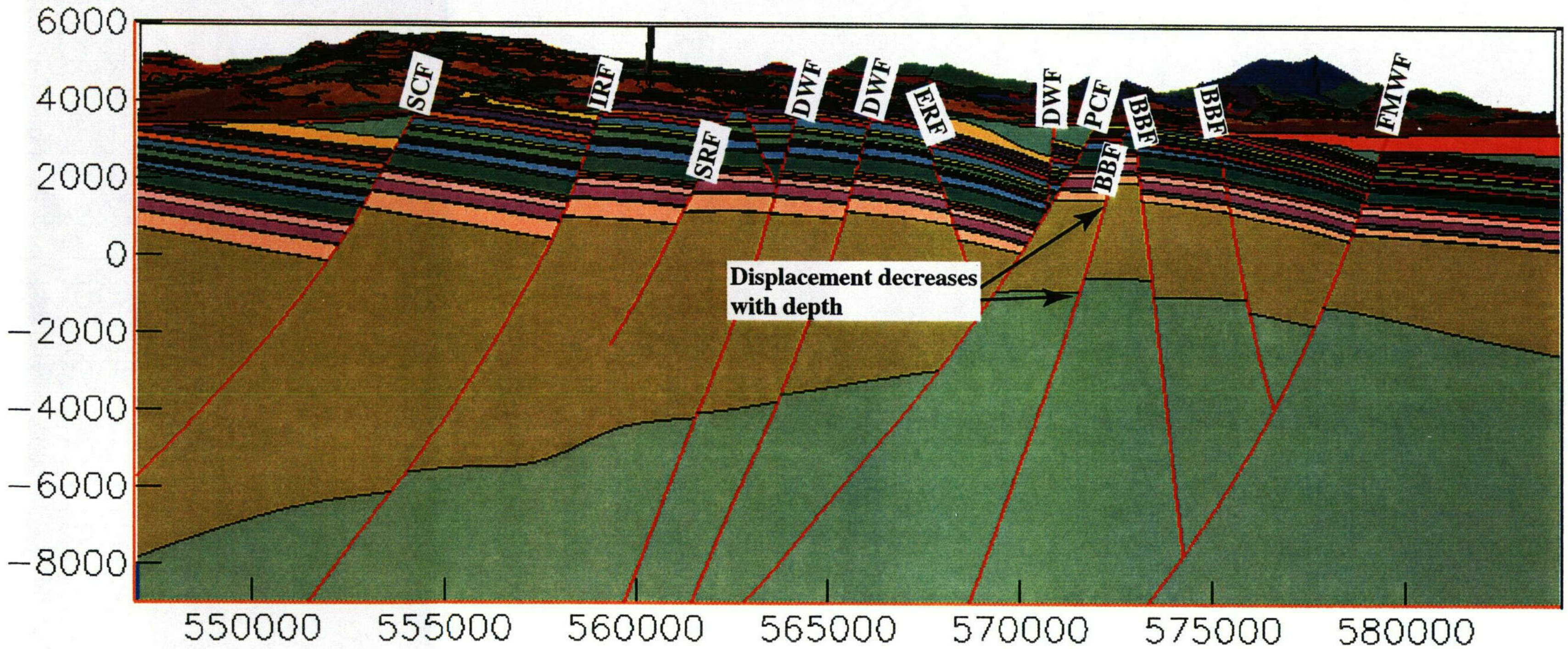

Figure E-13. Cross Section 2. Displacement on the Busted Butte fault decreases with depth.

Cross Section 3

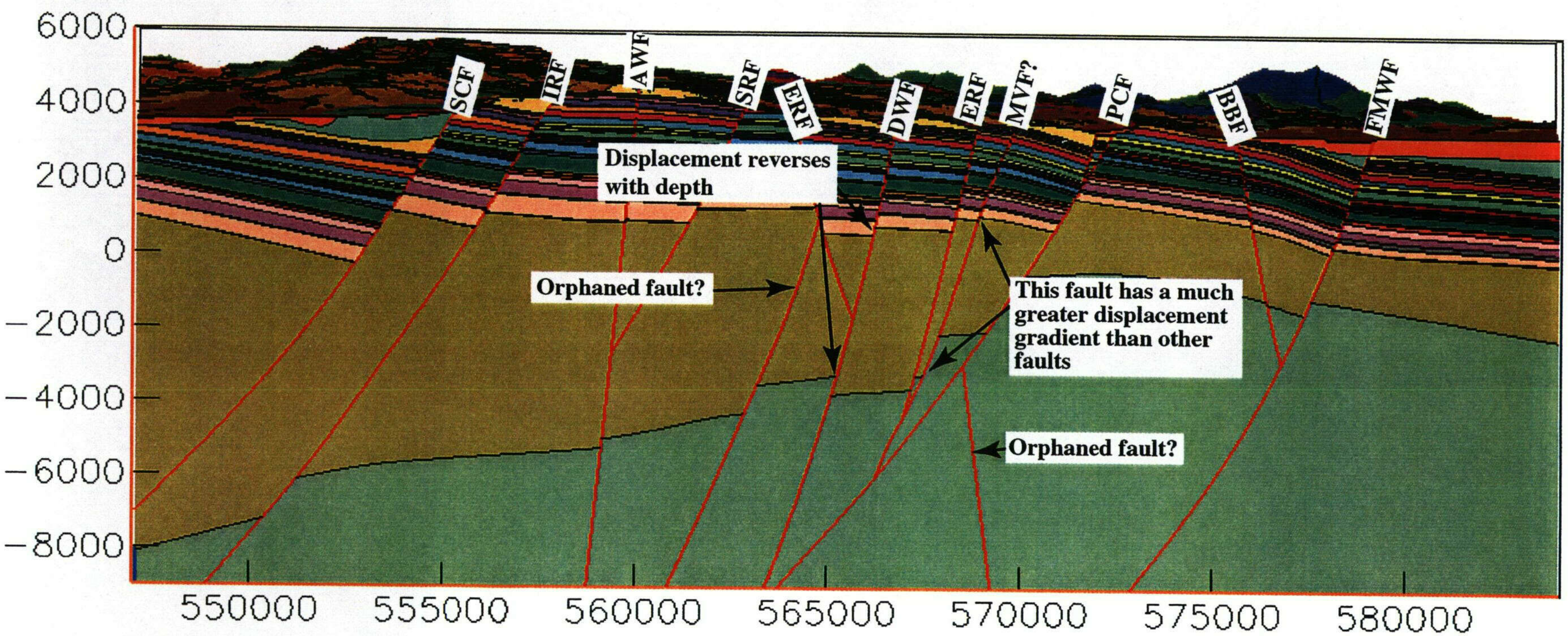

Figure E-14. Cross Section 3. Displacement on Dune Wash fault reverses at depth. Orphaned faults (see text for explanation) terminate updip. Fault labeled MVF? shows greater displacement gradient than surrounding faults.

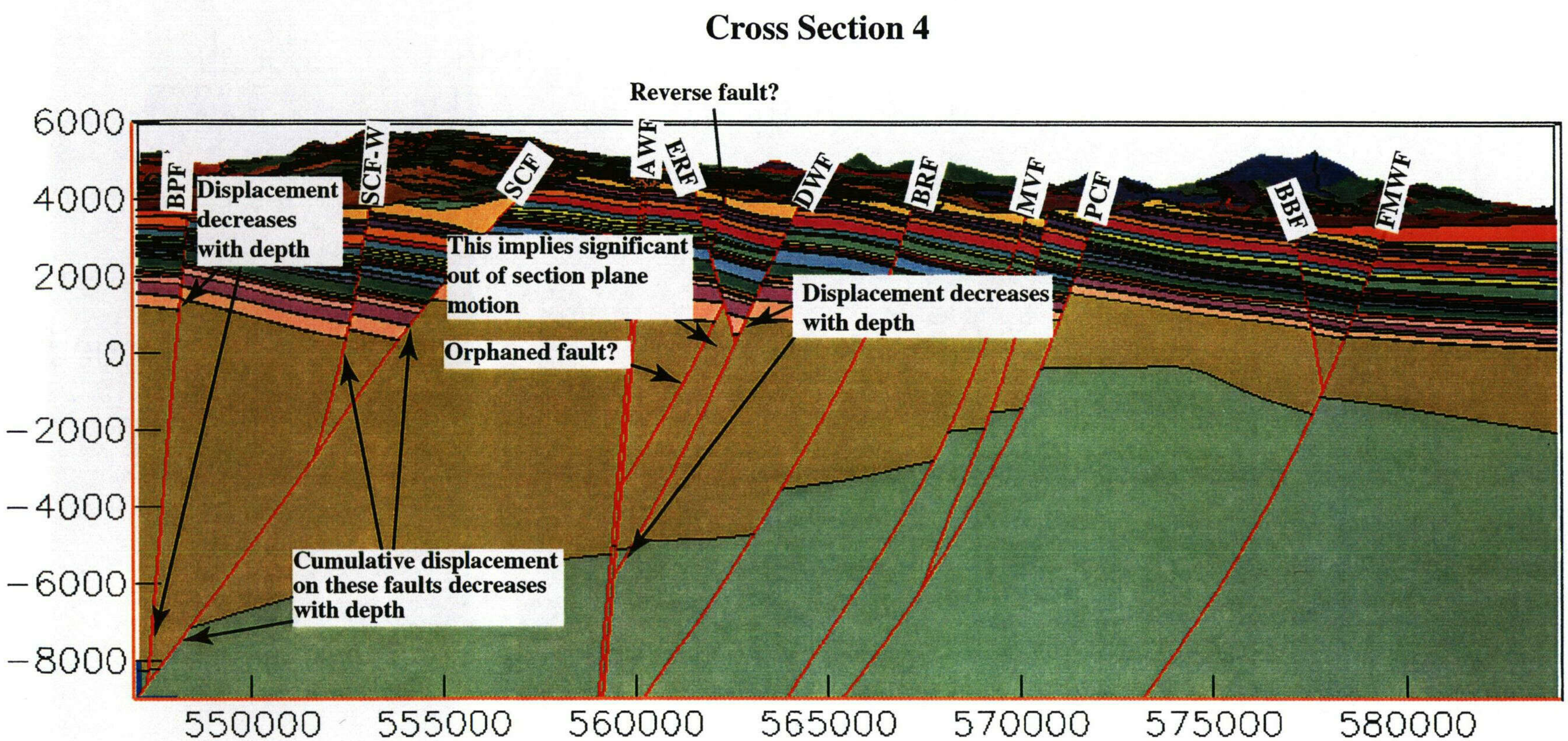

Figure E-15. Cross Section 4. Displacement on Boomerang Point and Dune Wash faults and Solitario Canyon fault system decreases with depth. Orphaned faults (see text for explanation) terminate updip. One small west-dipping fault has reverse displacement.

Cross Section 5

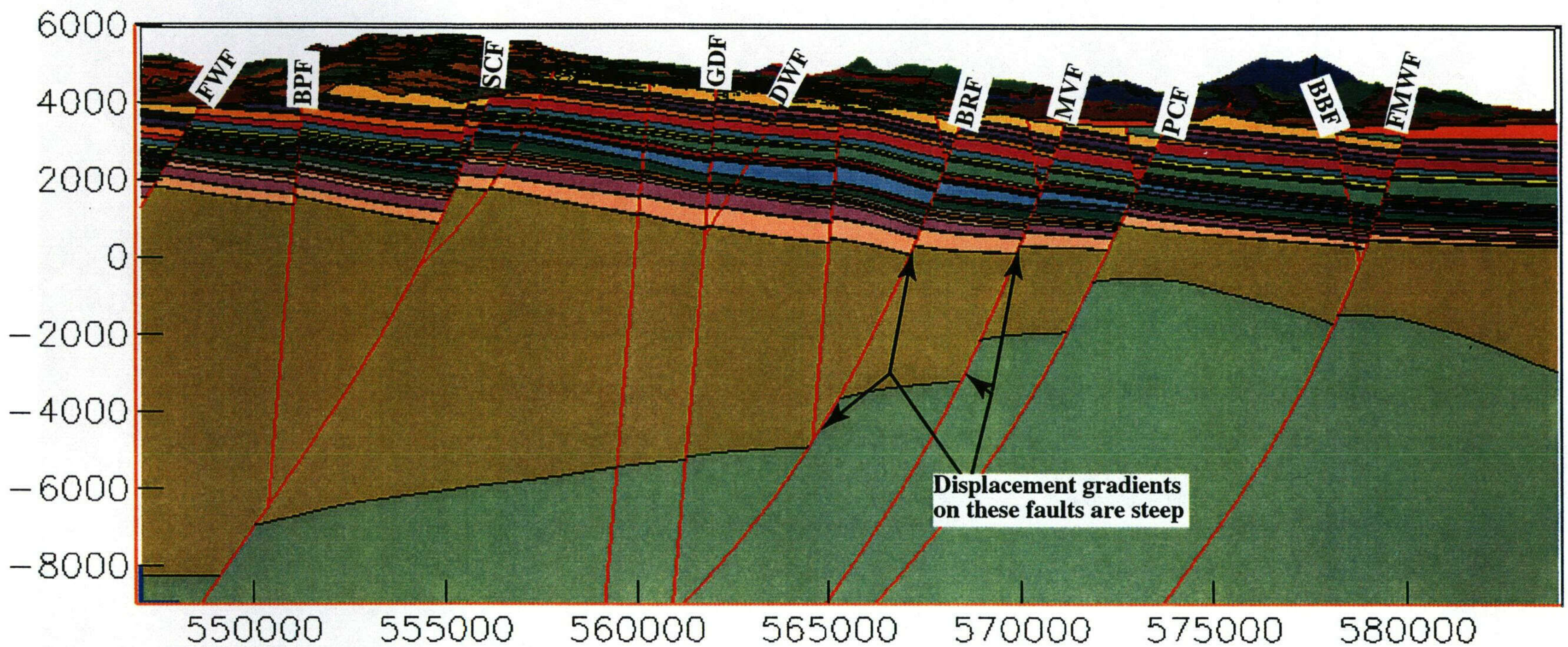

Figure E-16. Cross Section 5. Displacement increases downward on the Bow Ridge and Midway Valley fault systems, but displacement gradients are very steep in comparison with other faults.

Cross Section 6

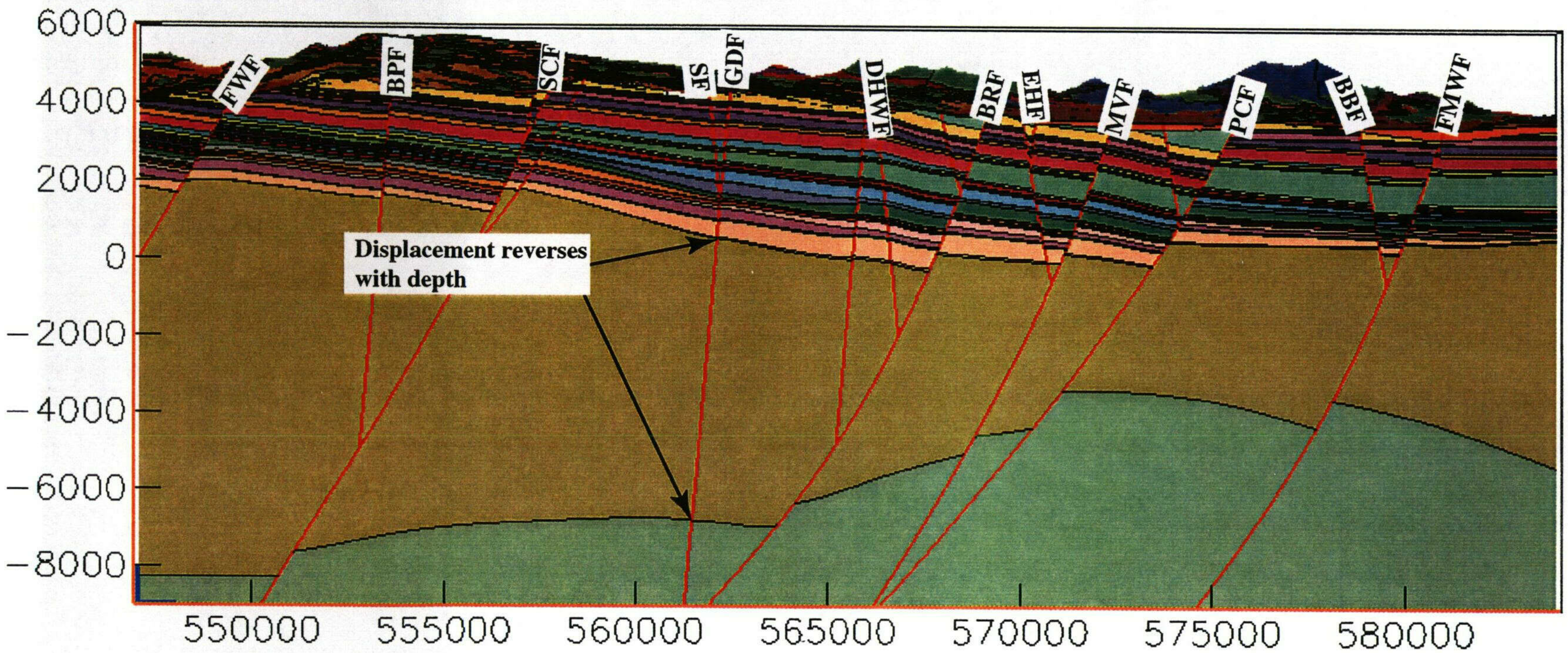

Figure E17. Cross Section 6. Displacement on Ghost Dance fault system reverses with depth.

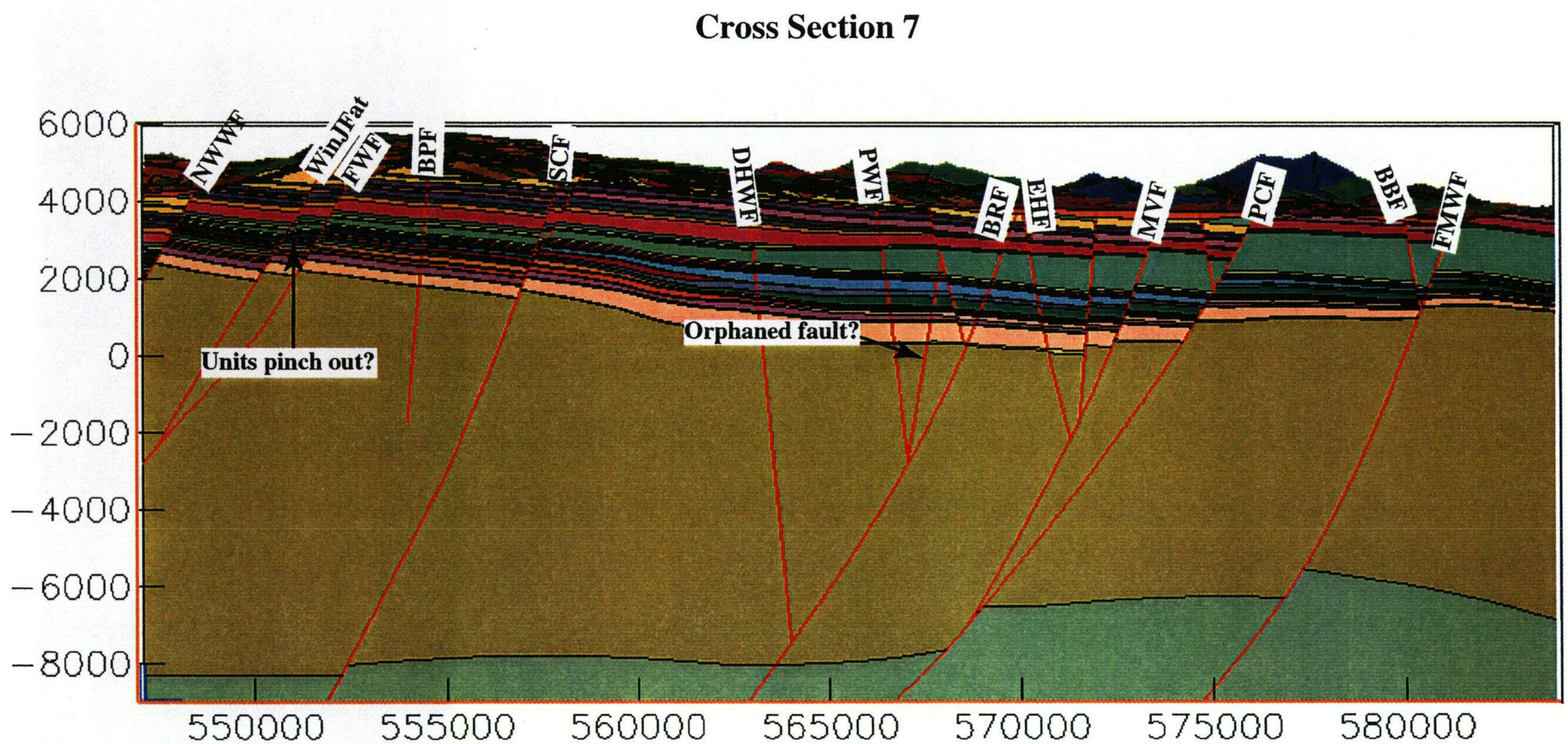

Figure E-18. Cross Section 7. Stratigraphic units appear to pinch out between the Fatigue Wash fault and the jumper fault labeled as WinJFat. An orphaned fault (truncated upward by another fault) occurs between the Pagany Wash fault and a fault within the Bow Ridge fault system.

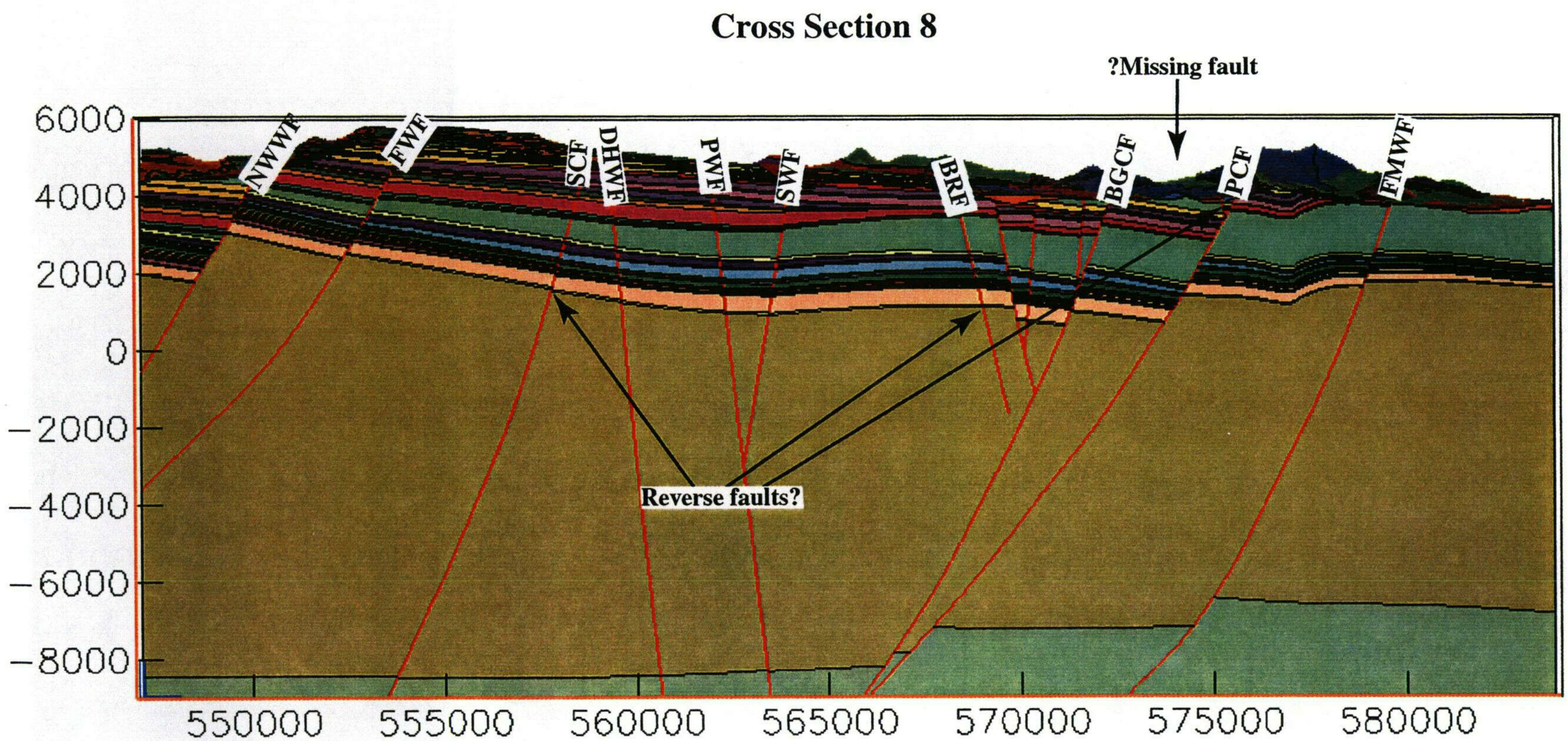

Figure E-19. Cross Section 8. Three faults, Solitario Canyon, Bow Ridge, and a small antithetic fault in the hangingwall of the Paintbrush Canyon fault, appear to have reverse motion on them. The Bow Ridge fault tips (loses all displacement) downward in this section but not in adjacent sections. Geological maps of the area (e.g., Day, et al., 1998) show another strand of the Midway Valley fault system between the Black Glass Canyon and Paintbrush Canyon faults.

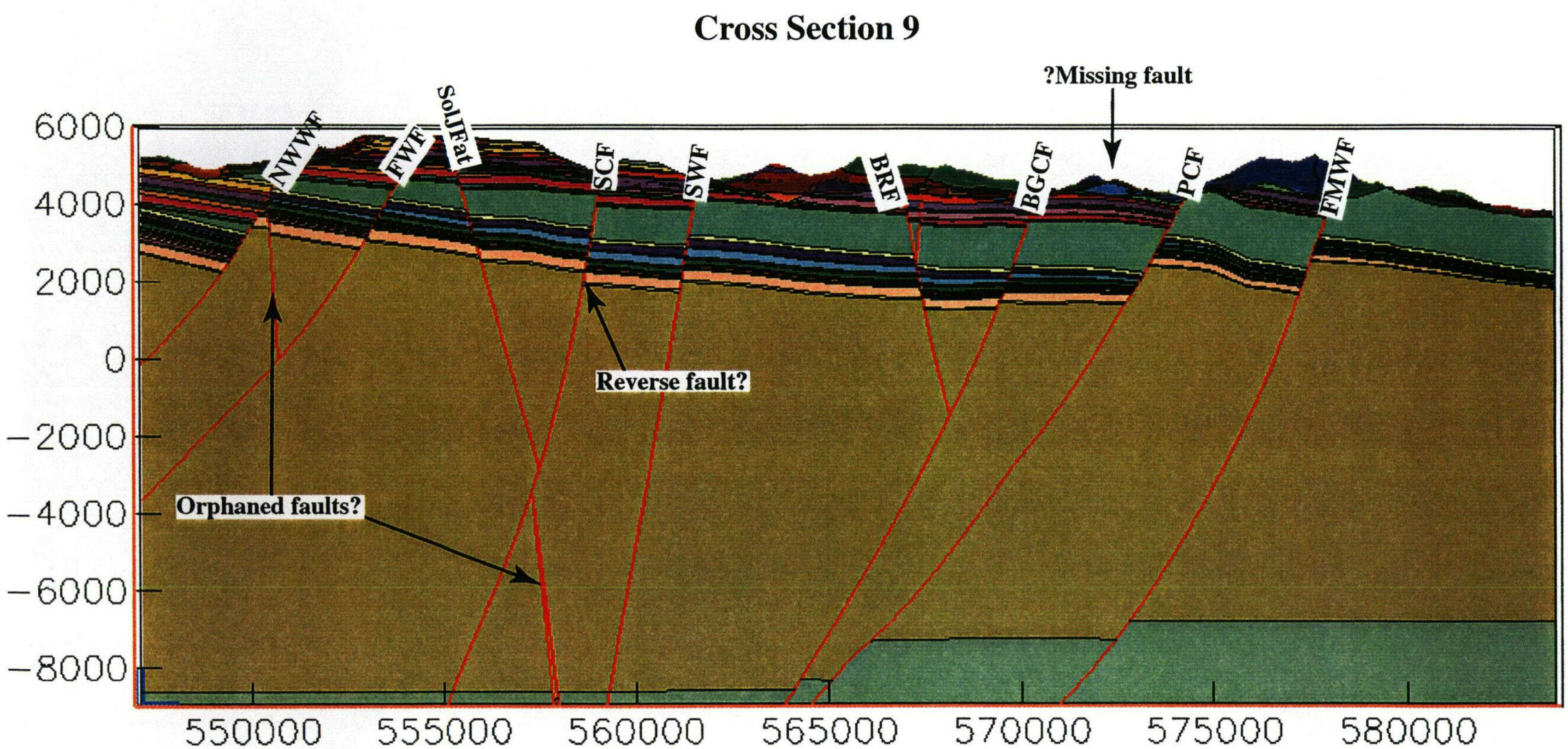

Figure E-20. Cross Section 9. The Solitario Canyon fault appears to have reverse motion. Geological maps of the area (e.g., Day, et al., 1998) show another strand of the Midway Valley fault system between the Black Glass Canyon and Paintbrush Canyon faults. Orphaned faults (truncated upward) are shown between the Northern Windy Wash and Fatigue Wash faults and the Solitario Canyon and Sever Wash faults.

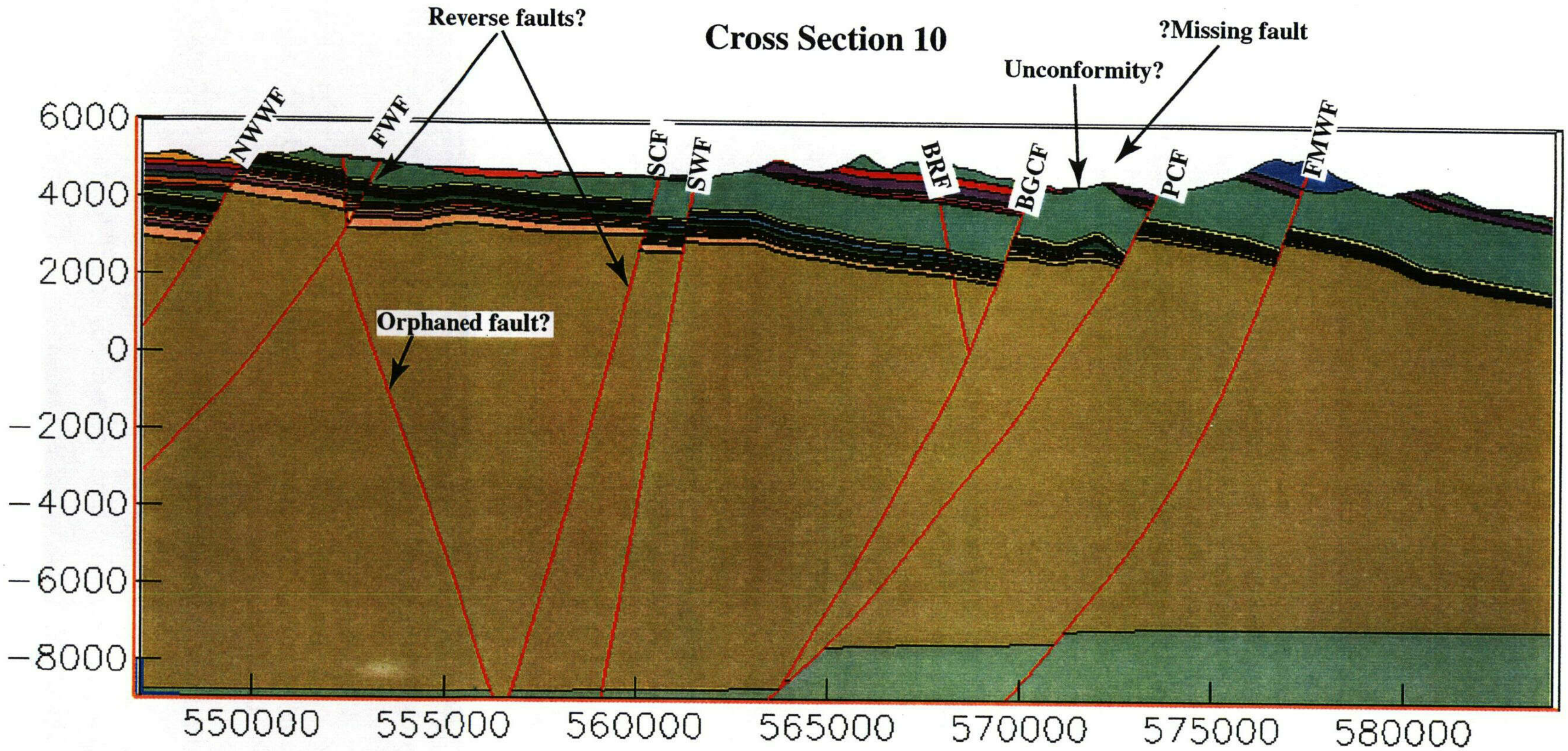

Figure E-21. Cross Section 10. The Solitario Canyon and a strand of the Northern Windy Wash faults appear to have reverse motion. Geological maps of the area (e.g., Day, et al., 1998) show another strand of the Midway Valley fault system between the Black Glass Canyon and Paintbrush Canyon faults. An orphaned fault (truncated upward) is shown between the Solitario Canyon and Fatigue Wash faults. An apparent unconformity is shown between the Black Glass Canyon and Paintbrush Canyon faults.

dominant north-south oriented fault population, and considering that much of the apparent rotation of fault trace and fault blocks can be attributed to differential dip-slip along originally north-south oriented fault traces, an east-west orientation for section restoration is preferred for analysis of the GFM3.1

Restoration indicates that the overall interpreted fault geometries are geologically reasonable. The Tertiary volcanic section restores well with minor local miscorrelations (see below). One point highlighted by this exercise is that, consistently through the model, the footwall-most portion of the fault system (footwall of the Fortymile Wash fault, c.f. figure E-20) in the present-day interpretation is lower than the hanging-wall-most portion of the fault system (hanging walls of the Fatigue Wash and Boomerang Point faults). The result is that the Paleozoic (Pz) horizon exists as a structural high in the eastern portion of the model. This is also illustrated in the restored state section where the arbitrary base line (fixed to the footwall-most block) is above the top of the undifferentiated Paleozoic section, implying that the hanging wall of the Fortymile Wash fault rose relative to its foot wall during deformation. There are two ways to resolve this:

1) Increase the displacement on the Fortymile Wash fault (or other west-dipping faults to the east) so that its footwall rises to a level at least as high as the hangingwalls of the Fatigue Wash and Boomerang faults;

2) Revise the larger (sub-regional) scale interpretation to incorporate other faults to the east, and consider the possibility of a graben situated over a basement high in the vicinity of the Fortymile Wash fault (e.g., Rahe, et al., 1997; Sims, et al., 1999).

Antithetic faults that terminate against master faults are always problematical when constructing restorable cross-sections because their displacement decreases downward to zero. The vertical shear algorithm cannot completely account for this downward decrease and generates area mismatches (for example see locations labeled A' in figure E-11). The mismatches labeled A' on the restored section (figure E-11) are a product of the restoration shear algorithm, and do not imply incorrect geometries in the deformed section (figure E-10) derived from GFM3.1.

In almost all cases, faults that intersect the top of the Paleozoic section retain displacement after restoration. This implies that there was accumulation of post-Paleozoic sedimentary/volcanic rock across these faults synchronous with fault displacement (growth). The implication that faulting was active during deposition of particular post-Paleozoic sedimentary/volcanic rock layers, as indicated by the GFM3.1, should be addressed in the GFM3.1 report.

There are a number of minor observations listed on figures E-10 through E-21 related to displacement variation along faults, thickness variation across faults, and gaps and overlaps. These observations may be attributable to one or more of three causes:

1) Inaccuracies introduced during the re-digitizing of the sections by NRC staff.

An example of a minor bed thickness/fault displacement inconsistency possibly caused by re-digitizing error is illustrated at B (present-day, figure E-10) and B' (restored, figure E-11).

2) Out of section-plane motion.

The typical assumption of constant area in restoration of cross-sections requires that no material (rock) has moved into or out of the plane of section. Restorations of the deformed brittle uppermost crust are assumed to be area constant if the section is oriented parallel with displacement. Section 6 is oriented W-E. This may be parallel to early motion on the YM faults, but not to the aggregate motion. A more likely motion direction is oriented approximately along azimuth 290° (see for example section AA' from Day, et al., 1998). However, this is an angular difference of only about 20° and, for the vertical shear algorithm used to restore fault blocks, will not cause gross distortion in the restorations of east-west section.

3) Inconsistencies observed in GFM3.1:

An example of a thickness change inherent in the model occurs at C (present day, figure E-10) and C' (restored, figure E-11). At D (figure E-10), the Ghost Dance fault shows opposite senses of motion at its intersection with the base of the Tertiary volcanic sequence and the top of the Paleozoic. This gives rise to the restoration problem at D' (figure E-11). There is a significant area of overlap across the Fortymile Wash fault (restored section, figure E-11). This is probably due in part to the presence of a synthetic fault above it, but is more likely the result of not modeling the Fortymile Wash fault trajectory using vertical shear. The small area of gap (restored section, figure E-11) is less but may have the same causes as the area of overlap.

e) In GFM3.0, the Boomerang Point fault was shown as reversing displacement at depth in the region of sections 5 (figure E-16) and 6 (figure E-17). As curved fault geometries in the GFM3.1 result in truncation of the Boomerang Point fault at depths above the Paleozoic contact, the unlikely geometry of displacement reversal at depth is not re-created in the region of sections 5 (figure E-16) and 6 (figure E-17). However, section 4 (figure E-15) does show displacement decreasing with depth along the Boomerang Point fault (see New Observations below). This apparent decrease in displacement may be due to model construction artifacts or potential uncertainty on the depth to the Paleozoic surface. Clarification in the GFM3.1 report will be helpful.

f) In GFM3.0, the Dune Wash fault was shown to be truncated against the Ghost Dance fault in the region of section 5 (figure E-16) but not in section 4 (figure E-15). This observation suggested a change in depth or "flexing" of the Dune Wash fault. In GFM3.1, dip of the Dune Wash fault has been increased so that the fault truncates against the Ghost Dance fault in both sections 4 (figure E-15) and 5 (figure E-16).

g) In GFM3.0, many faults were shown with displacement across the Paleozoic surface that was generally greater than the displacement of the base of the younger Trambt. The increase in displacement with depth indicated deposition during faulting. Most faults in GFM3.1 that cut both the top of the undifferentiated Tertiary (Tund) and Paleozoic horizons have displacements that increase with depth. However, in sections 1 (figure E-12), 2 (figure E-13), and 4 (figure E-15) there are faults that show decreasing displacement with depth. In sections 3 and 6 there are faults that reverse sense of displacement with depth. In sections 3 (figure E-14) and 5 (figure E-16) the rate of increase of displacement with depth is greater than most other faults in the model.

In Yucca Flat, the mean depth differences between depth estimates based on gravity and actual tops of the Paleozoic rock surface at 38 drill holes was 30m ± 88m. (Brethauer, et al., 1981). At YM, only a few boreholes can be used to define the Paleozoic surface. Ue25 p-1 is the only borehole that penetrates this surface. A few other boreholes, such as G-1 and Gu-3, while not penetrating the surface do constrain its depth. This information suggests that, as a minimum, only offsets greater than 100 m can be used as control for the location of faults intersecting the Paleozoic surface, and displacements of less than 100 m may be artifacts of model construction. Clarification from DOE is warranted to determine whether artifacts of modeling are an influence in this case.

h) Complex interactions between faults with opposing dip (e.g., section 3, figure E-14) are likely in the YM area (Brocher, et al., 1998) and may be important influences on groundwater flow (Ferrill, et al., 1999). Variable displacement values between different units at the same position along a given fault and beheaded (or orphaned) faults without a continuation across the offsetting fault are examples of complex fault interactions. For example, in sections 8 (figure E-19), 9 (figure E-20), and 10 (figure E-21) there are faults that show consistent reverse displacement. Are these faults interpreted as reverse faults as shown in GFM3.1, or is another interpretation warranted? Clarification from DOE is warranted to determine whether artifacts of modeling are an influence on these complex interactions.

New Observations From Geological Framework Model Version 3.1.

a) In sections 9 (figure E-20) and 10 (figure E-21), horizons in the vicinity of 572500 East show an unusual folded geometry. This may be related to a missing fault. An extension of the Midway Valley fault trace appears above this region in the map of Day, et al., (1998). The unusual folded geometry in figures E-20 and E-21 is flanked by the Black Glass Canyon and Paintbrush Canyon faults, and no fault surface corresponding to the Midway Valley fault appears between the Black Glass Canyon and Paintbrush Canyon faults in GFM3.1. Day, et al. (1998) interpret 400 ft of dip slip on the Midway Valley fault. GFM3.1 should be modified to include the extension of the Midway Valley fault.

b) In sections 3 (figure E-14), 4 (figure E-15), 7 (figure E-18), 9 (figure E-20), and 10 (figure E-21) there are faults that are orphaned. Orphaned faults in the GFM3.1 are faults that terminate updip against other faults and show no continuation of trace above the terminating fault surface. The geological significance of these orphaned faults should be discussed by the DOE. However, this does not preclude use of the affected faults or horizons from abstraction to process models.

c) In section 4 (figure E-15) an orphaned fault creates a structure that is unrestorable in the section plane. This implies significant out-of-section-plane motion. Such motion is not readily apparent in the other sections. This does not preclude use of the affected faults or horizons from abstraction to process models.

d) An important check on the validity of fault displacement interpretations is provided by distance versus displacement diagrams (see e.g., Dawers, et al., 1993; Dawers and Anders, 1995; Willemse, 1997; Ferrill, et al., in press). These diagrams graphically illustrate the variation in displacement along faults or fault systems. Steep displacement gradients on individual faults implies either (1) an adjacent or nearby fault is accommodating displacement, or (2) the fault interpretation is in error. EV models provide rich sources of fault displacement data that can be used to evaluate fault interpretations. In this analysis, we use west-east heave, the west-east horizontal component of net fault slip. All heave diagrams presented in this analysis are extracted from the exported RHH horizon. As the majority of faults are oriented approximately north-south, distance is plotted as Nevada State Plane northing (feet), and heave units as feet of horizontal displacement.

Figure E-22 shows a distance versus heave plot from displacements along the Dune Wash fault. The plot indicates a fault that truncates abruptly to the south, in this case against the Paintbrush Canyon fault. Plots of complete faults or fault systems generally show a gently parabolic curve extending from fault tip to fault tip. The heave plot of the Dune Wash fault is leptokurdic or peaked in form. This may indicate that nearby faults are accommodating horizontal displacement in areas of steep displacement gradient on the Dune Wash fault; that the fault system changes dip dramatically from center to tips along its length; that the GFM3.1 fault interpretation is incorrect; or that anomalous artifacts are present in the data extracted from GFM3.1.

Figure E-23 shows a distance versus heave plot from displacements along the Fortymile Wash fault. The plot indicates a fault that extends beyond the boundaries of the plot, with similar displacement values along its entire plotted length. Some faults in the GFM3.1 have irregular heave plots. Figure E-24 is a distance versus heave plot for the Paintbrush Canyon fault at the same scale as figures E-22 and E-23. It shows a somewhat irregular pattern with a few steep troughs (at northing 748000 and just south of 743000). The irregular pattern may indicate that faults located near the troughs are accommodating displacement corresponding to the troughs. The Paintbrush Canyon fault is plotted at full scale in figure E-25.

The Solitario Canyon fault accommodates significant displacement in the YM fault system, and is known to comprise several intersecting segments (Ferrill, et al., in press). The distance versus heave diagram, plotted at full scale in figure E-26, shows a constant displacement increase from the northern extent of the model to the center of the diagram where displacement decreases abruptly. The abrupt decrease coincides with the intersection and linkage of the Solitario Canyon fault with the Iron Ridge fault. The Iron Ridge fault (figure E-27) shows a less regular heave pattern that could indicate unmapped splays. In the simplest case, where the two linked faults represent the total displacement, summing the displacement along the southern portion of the Solitario Canyon fault with displacement on the Iron Ridge fault should produce a nearly smooth and symmetrical curve. The Iron Ridge and Solitario faults are plotted on the same diagram in figure E-28a. It is apparent from the diagram that summing the heave along the faults leaves apparent deficits along the southern (left) half of the diagram (regions A and B in figure E-28b). The southernmost portion of the Solitario Canyon fault shows a series of southeast-trending splays (figure E-9). These splays link with the main trace of the southern section of the Solitario Canyon fault to form a system of faults. Summing the heaves on the Iron Ridge and Solitario fault systems (figure E-28c) improves the smoothness of the plot and eliminates heave deficit in region B, but not region A. This may indicate the presence of unmapped faults or of faults whose relationship to the Iron Ridge–Solitario fault system is not recognized, or that displacements on these faults are incorrectly interpreted in GFM3.1.

A cumulative distance versus heave diagram is constructed by summing the heaves of all faults along the length of the fault system. Cumulative heave along the length of the GFM3.1 is

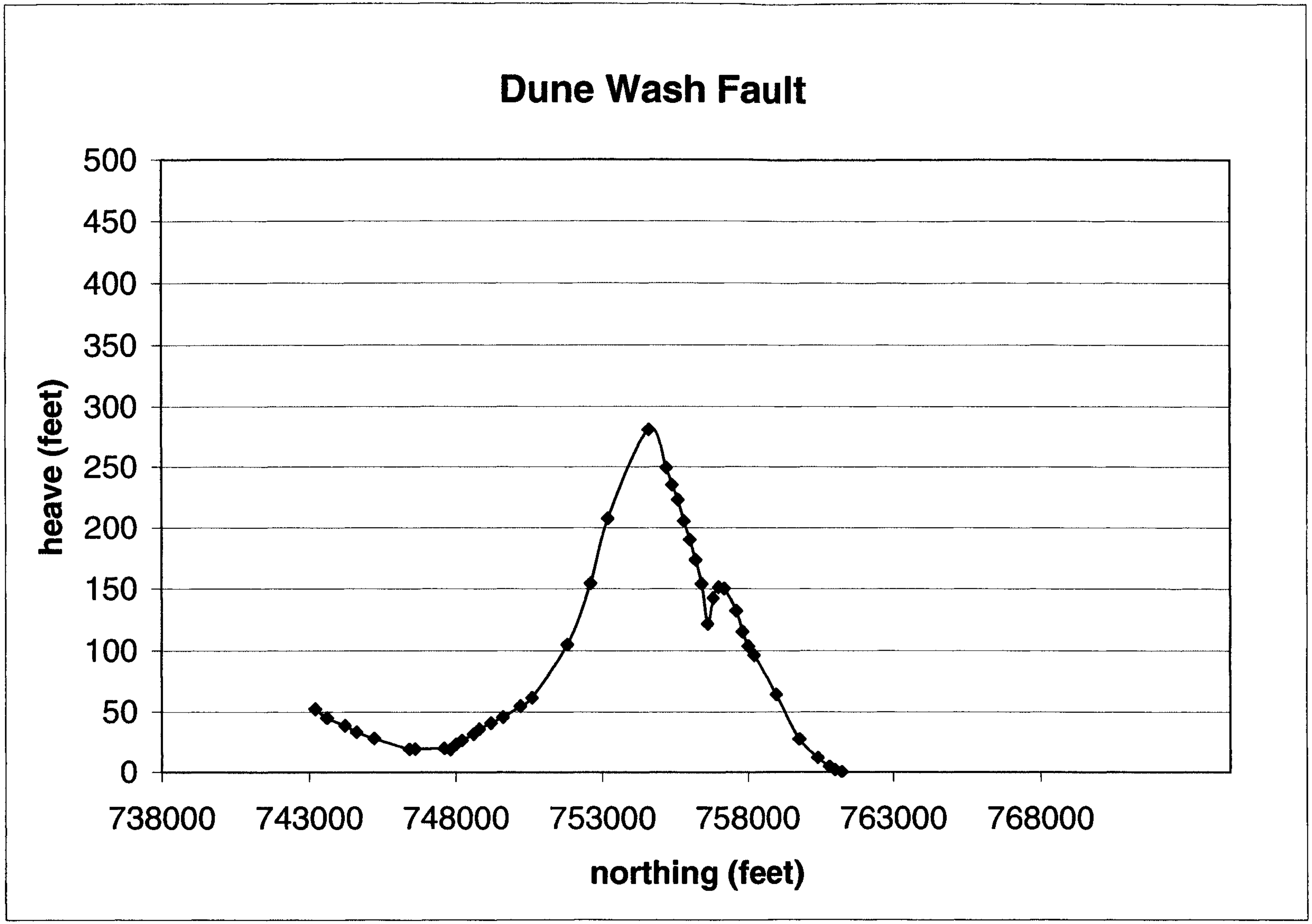

Figure E-22. Distance versus heave diagram along the Dune Wash fault. Offsets extracted from the RHH horizon. Distance given in Nevada State Plane northing (ft). The left edge of the plot fault in GFM 3.1 plot (743000N) terminates against the Paintbrush Canyon fault in GFM3.1. The right edge (761000N) terminates within the model, but does not terminate against another fault.

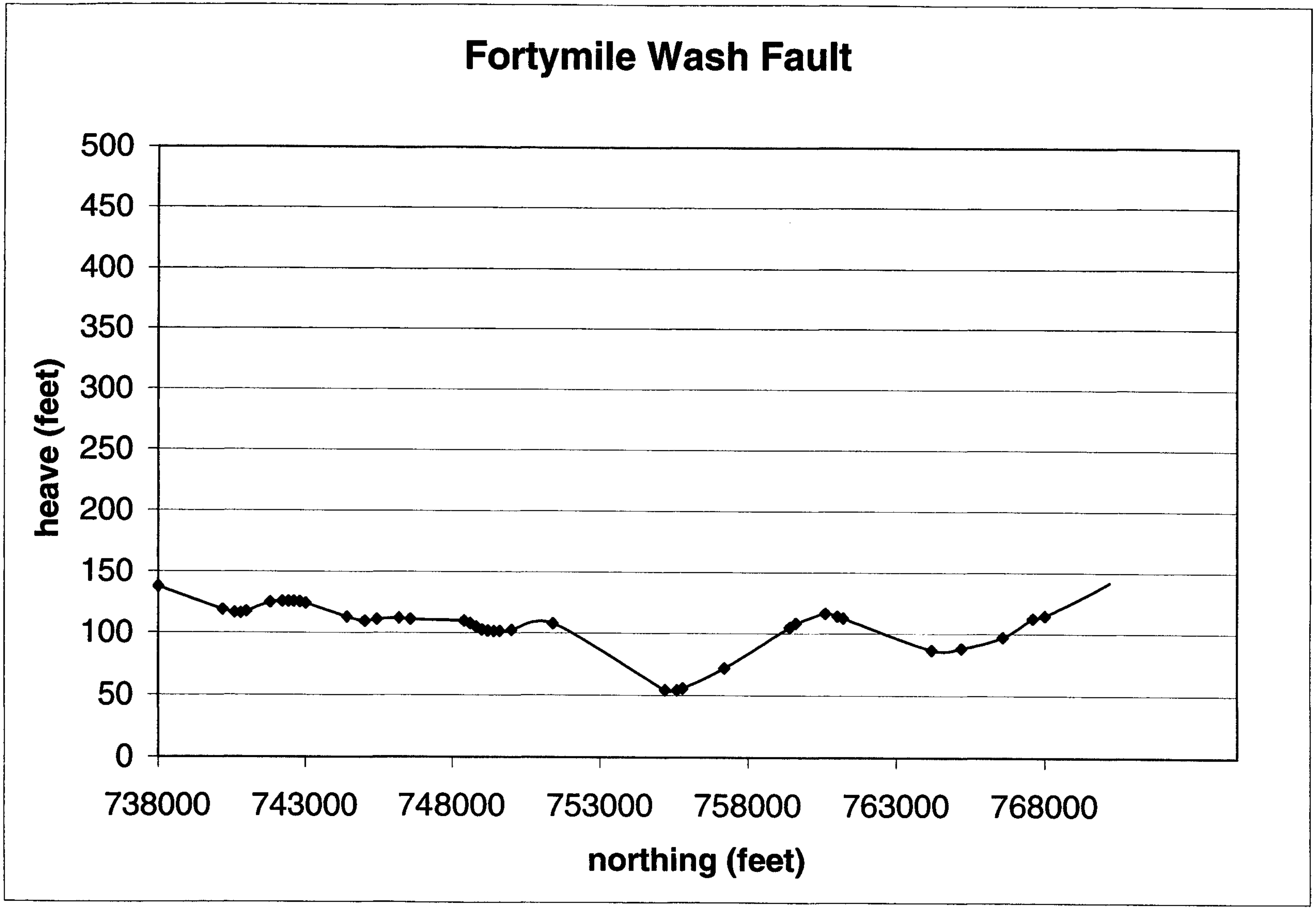

Figure E-23. Distance versus heave diagram along the Fortymile Wash fault. Offsets extracted from the RHH horizon. Distance given in Nevada State Plane northing (ft).

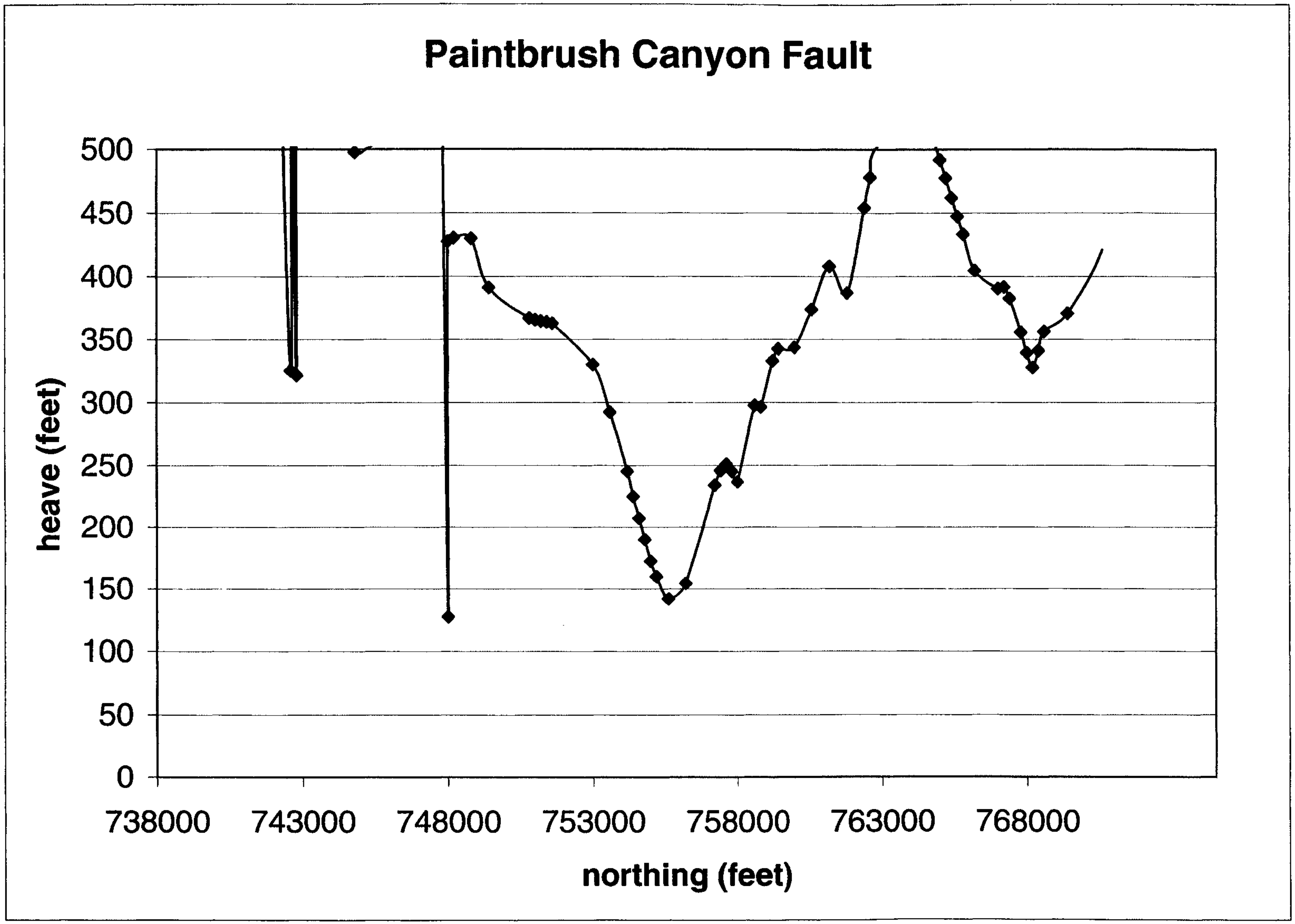

Figure E-24. Distance versus heave diagram of Paintbrush Canyon Fault. Upper limit 500 feet to preserve scale. Offsets extracted from the RHH horizon. Distance given in Nevada State Plane northing (ft).

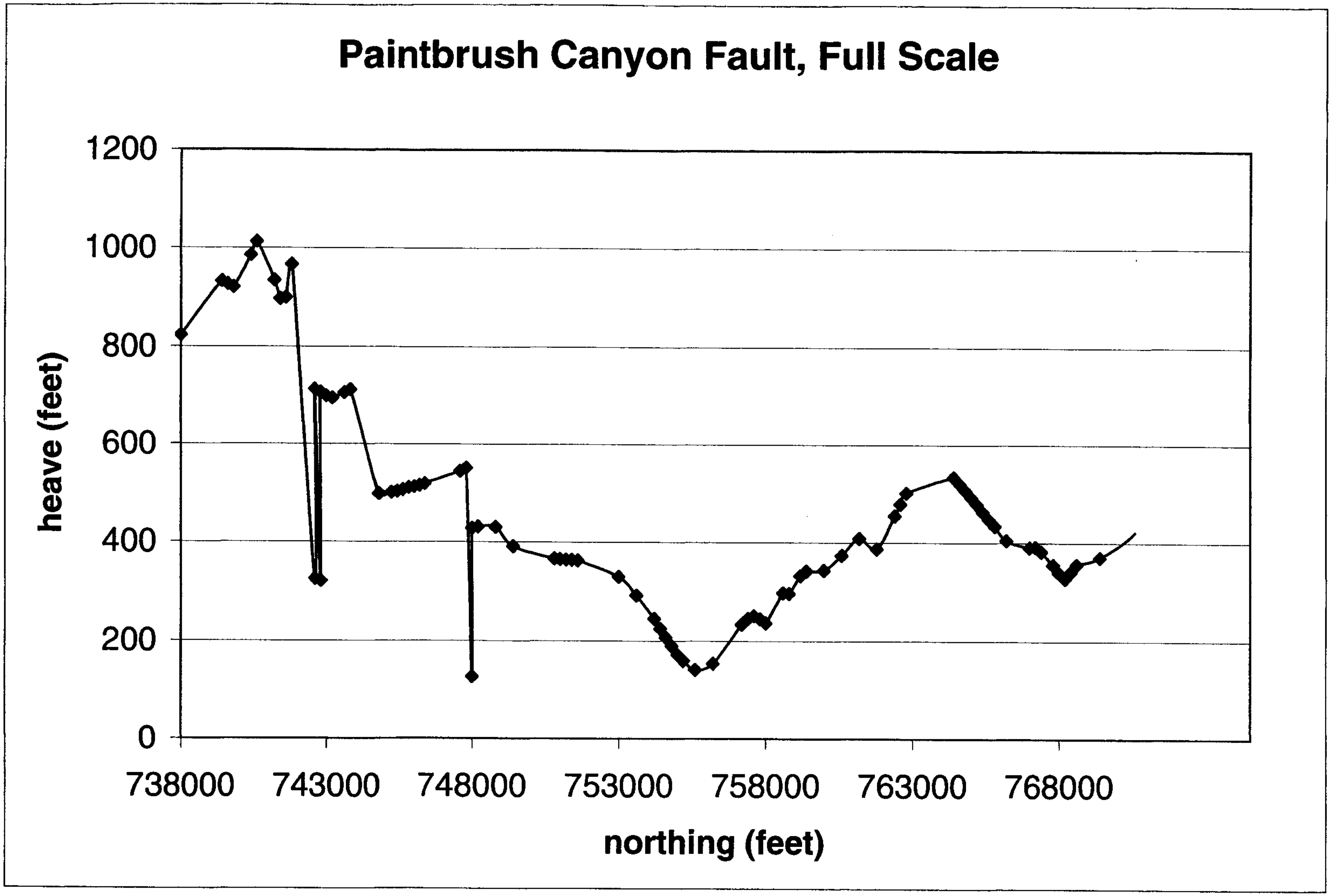

Figure E-25. Distance versus heave diagram of Paintbrush Canyon fault plotted at full scale. Offsets extracted from the RHH horizon. Distance given in Nevada State Plane northing (ft).

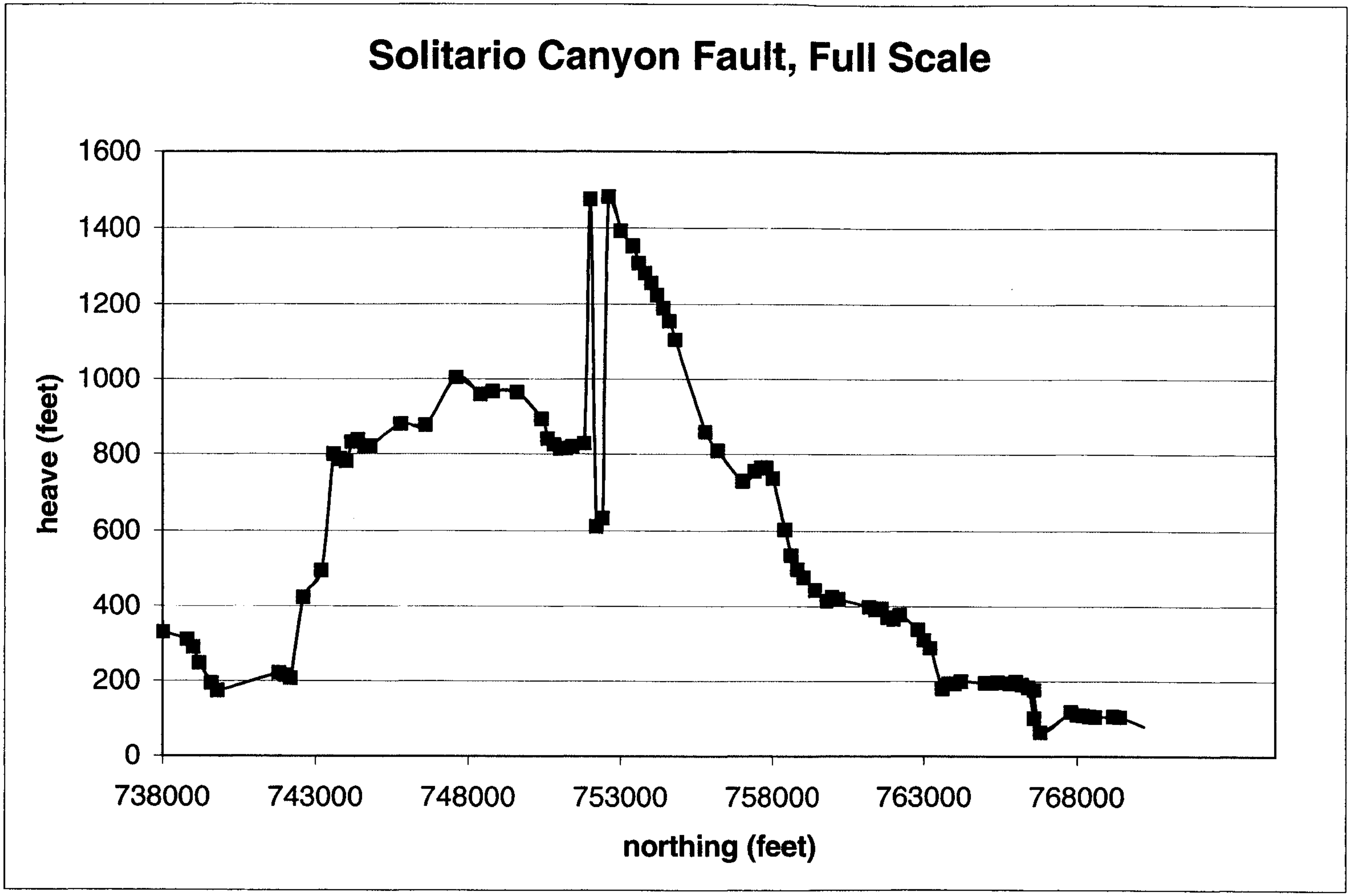

Figure E-26. Distance versus heave diagram of Solitario Canyon fault. Offsets extracted from the RHH horizon. Distance given in Nevada State Plane northing (ft).

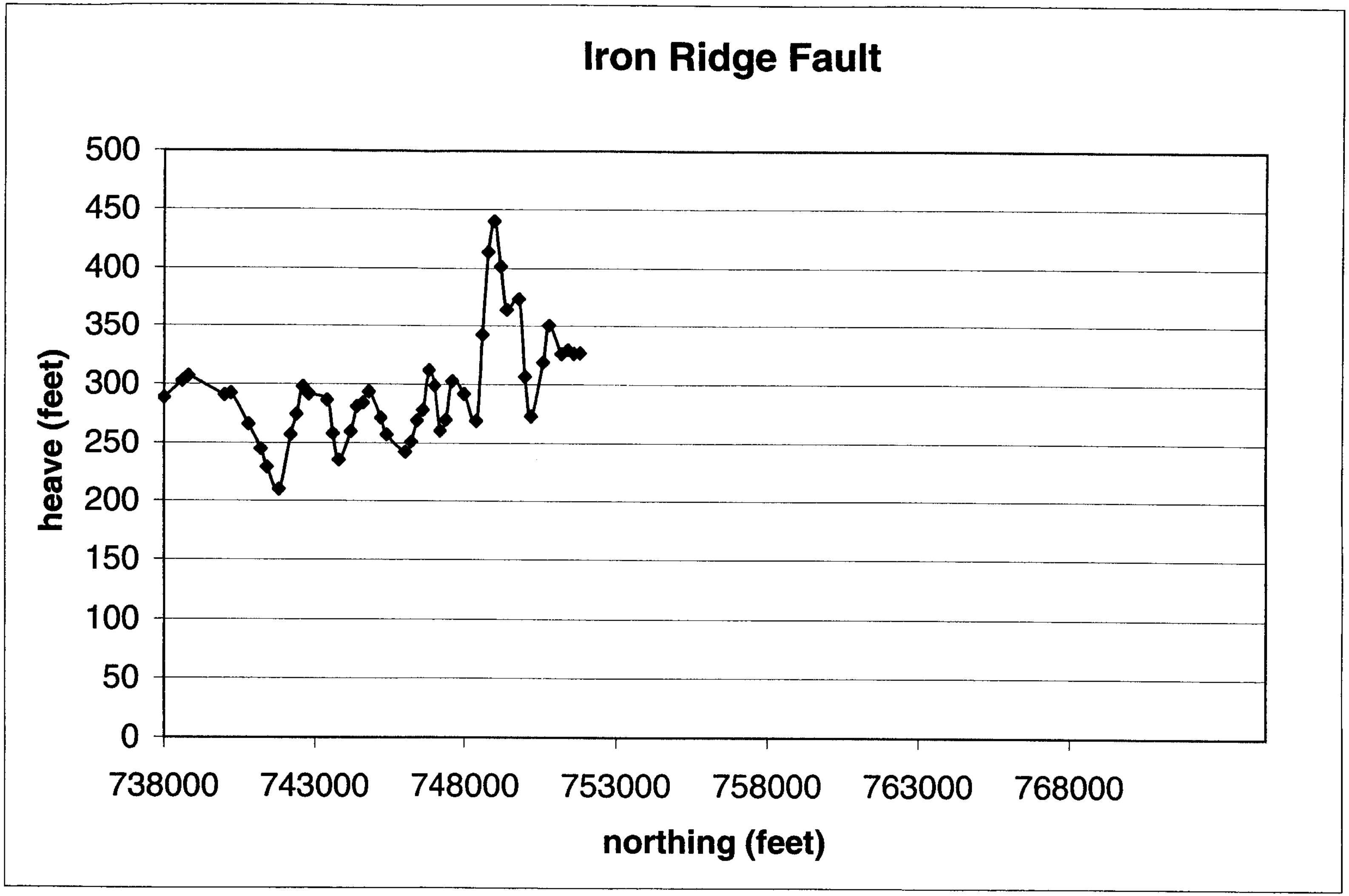

Figure E-27. Distance versus heave diagram of Iron Ridge Fault. Offsets extracted from the RHH horizon. Distance given in Nevada State Plane northing (ft).

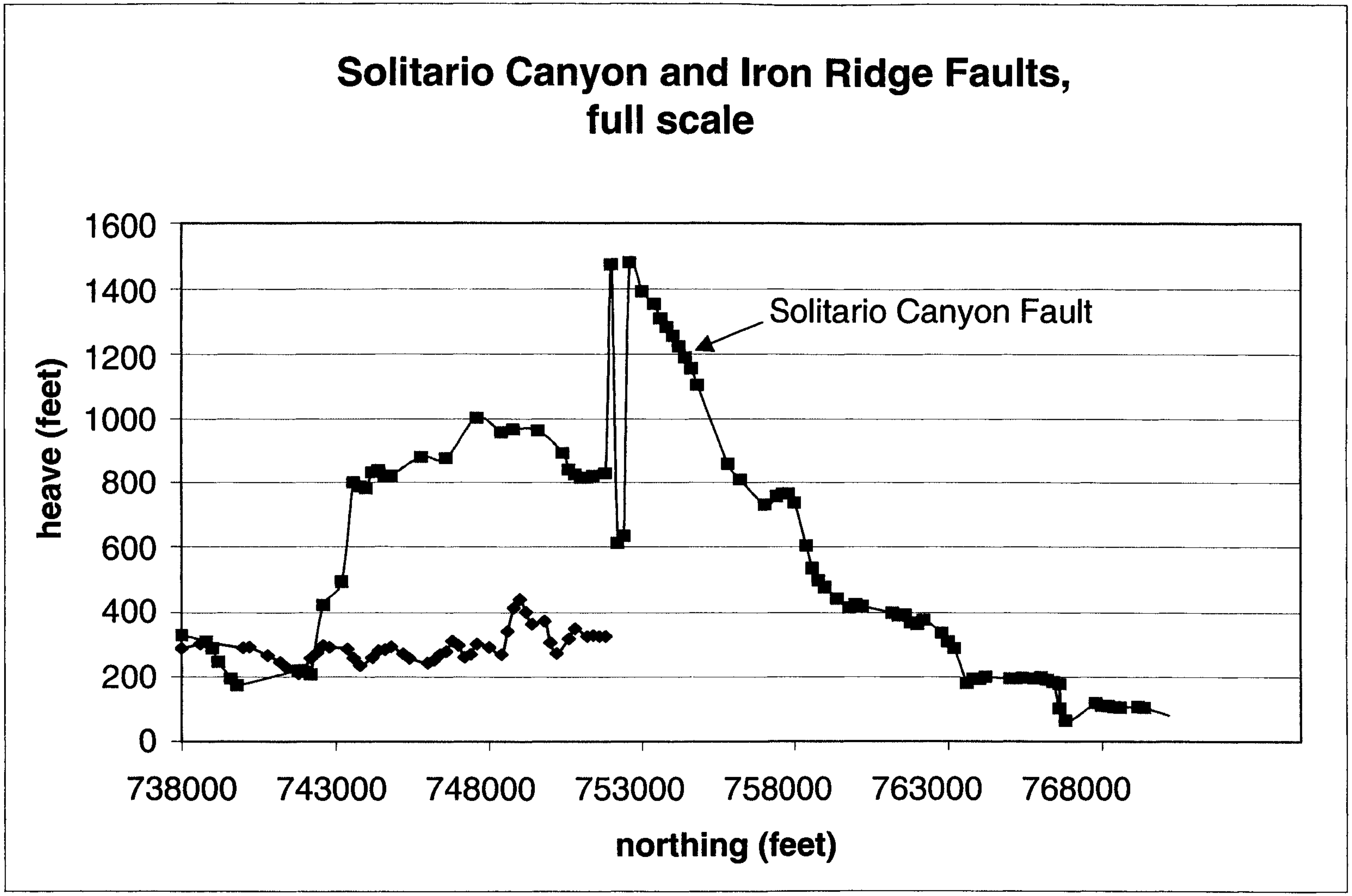

Figure E-28a. Distance versus heave diagram of Solitario and Iron Ridge faults. Offsets extracted from the RHH horizon. Distance given in Nevada State Plane northing (ft).

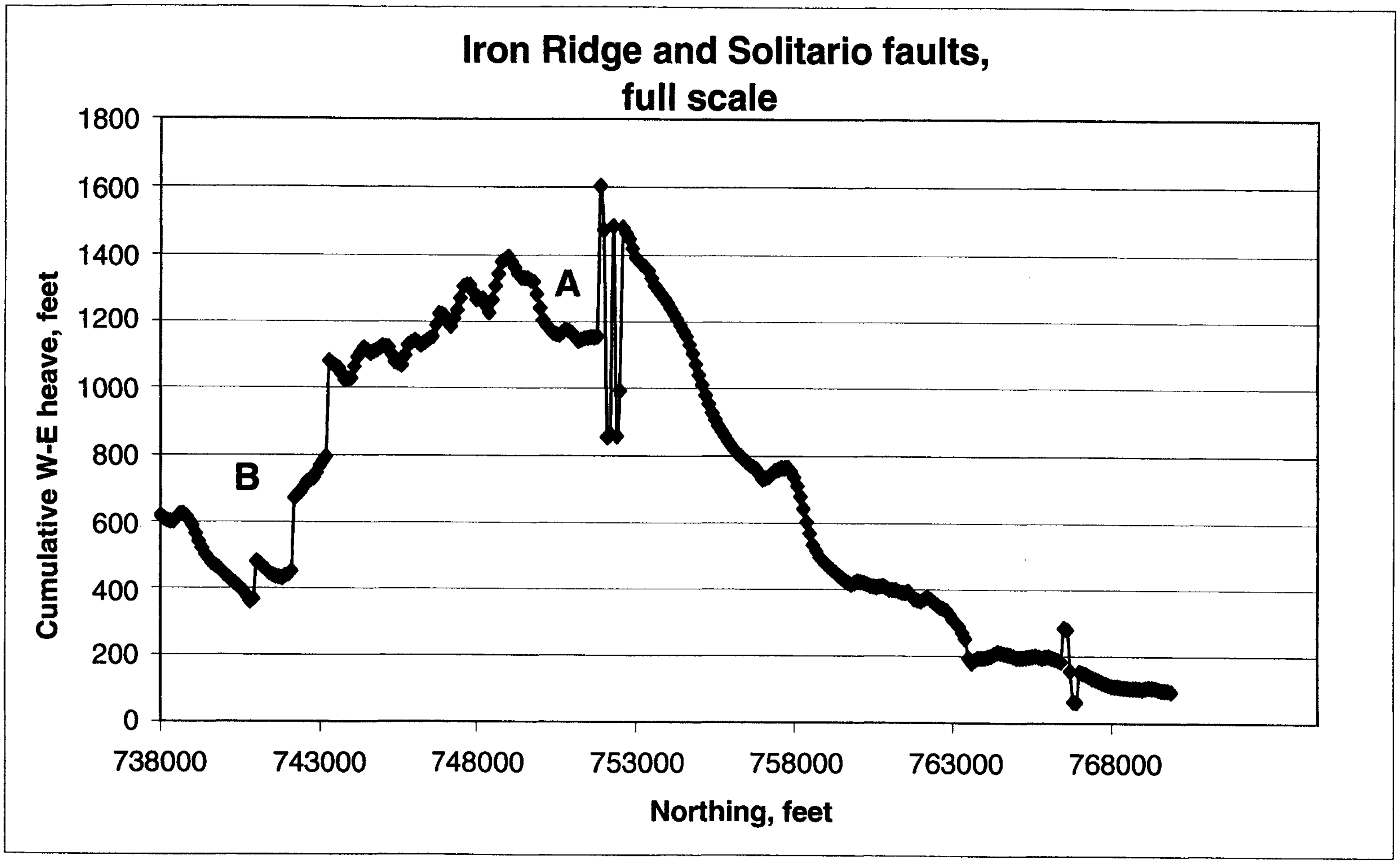

Figure E-28b. Cumulative distance versus heave diagram of Solitario Canyon and Iron Ridge faults. Offsets extracted from the RHH horizon. Distance given in Nevada State Plane northing (ft). A and B denote regions of heave deficit when only the individual faults are considered.

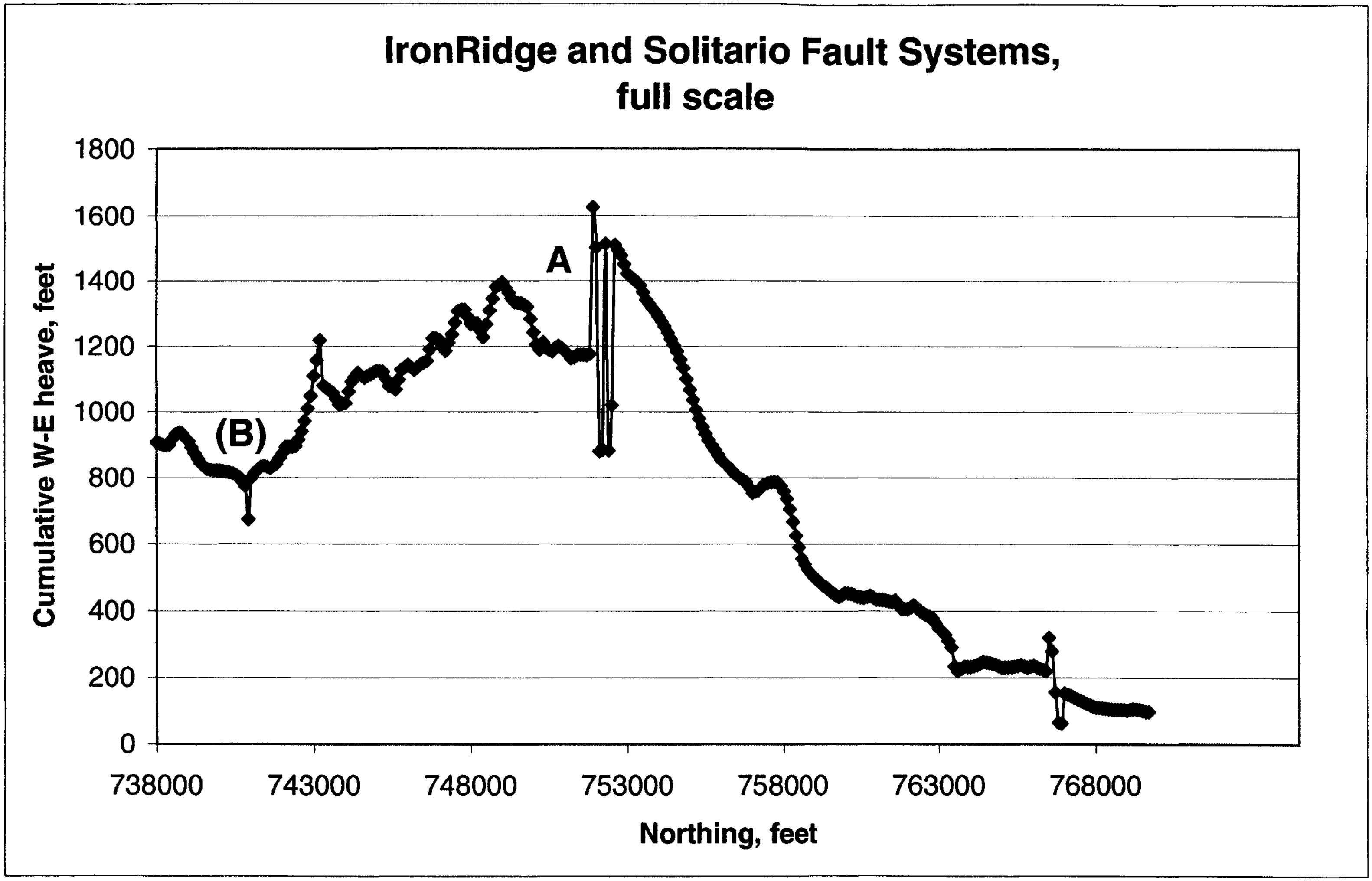

Figure E-28c. Cumulative distance versus heave Diagram of Solitario Canyon and Iron Ridge fault systems, including splays. Offsets extracted from the RHH horizon. Distance given in Nevada State Plane northing (ft). A - region of heave deficit that persists even when the two fault systems are considered together. B - region of heave deficit that is eliminated when the two fault systems are considered together.

plotted in figure E-29. Irregularities in cumulative displacement diagrams may indicate unmapped faults or faults that are not encompassed by the model boundaries, that mapped displacements are incorrect, or, in the case of heave diagrams, that fault dips are irregular or incorrect. Where dip changes with depth, as in the case of listric or curving faults, cumulative heave values mapped at depth may show values that differ from data plotted from shallow and more steeply dipping fault surfaces. These observations do not preclude abstraction of the fault surfaces in GFM3.1 to process models.

GFM3.1 shows improvements over GFM3.0, and, to our knowledge, is the best available representation of the geologic framework of YM. Though largely credible, version 3.1 of the GFM should not be considered the final version of GFM development. The Geologic Framework Model (GFM3.1) is intended to characterize site geology. The stratigraphy, fault and fault-block geometries of the YM site are products of the tectonic environment. However, the design and assembly process of GFM3.1 has to this point not been reconciled with, connected with or assimilated into the viable tectonic models.

The observations discussed above do not preclude abstraction of the GFM3.1 to process models. The level of detail and accuracy in GFM3.1 is adequate to the extent of staff's understanding of the scope of DOE's ISM3.0. Clarification in the GFM3.1 report of the above observations will be useful where process models depend upon high-resolution representations of the geologic framework at YM. The model would not be appropriate for a detailed tectonic or kinematic evaluation of YM at the site scale considering the observations above, and DOE has indicated that GFM3.1 is not intended to represent a tectonic model to be employed for such analyses.

No additional observations requiring explanation were generated from perusal of GFM3.1.

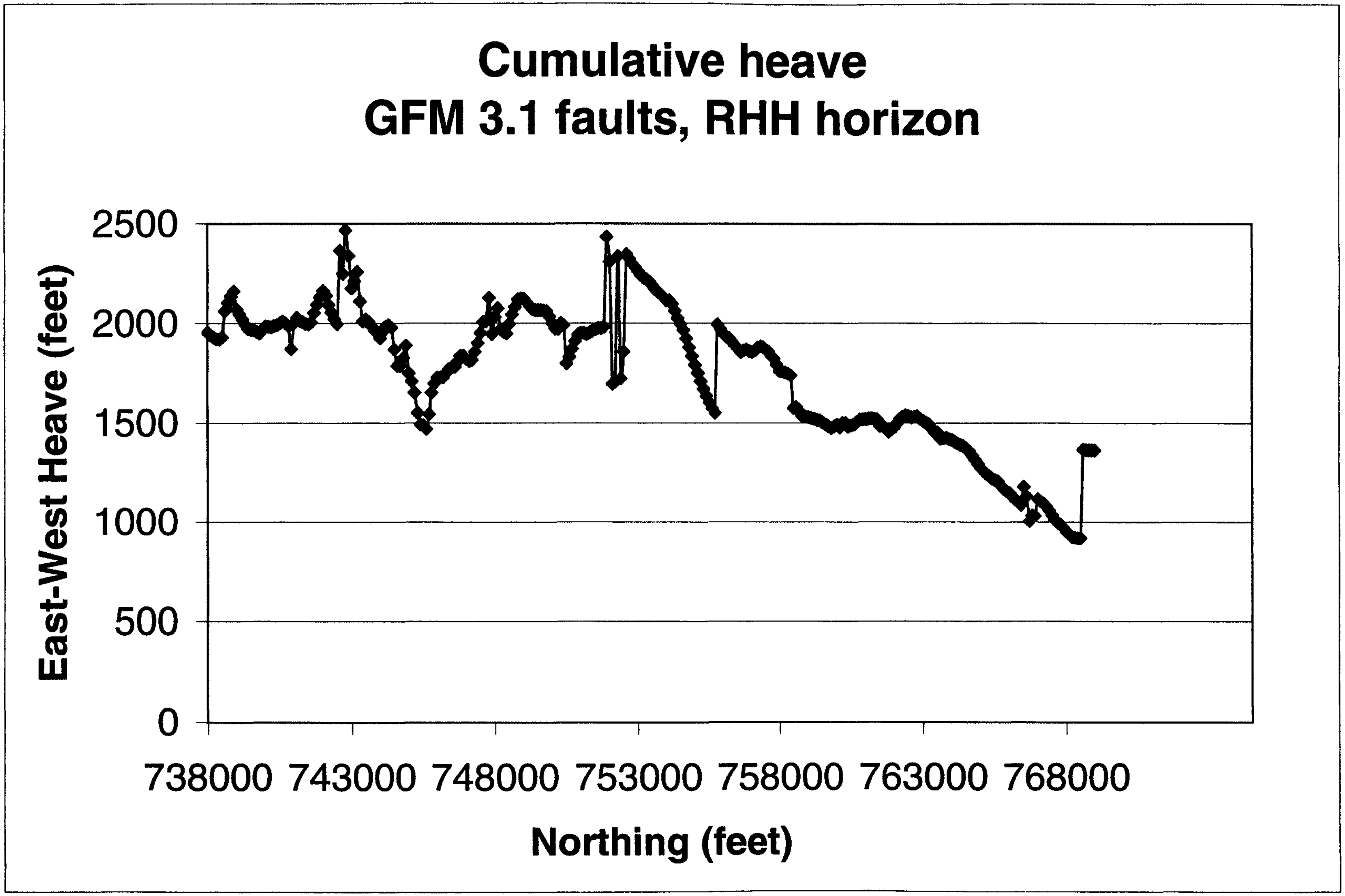

Figure E-29. Cumulative distance versus heave diagram of faults within GFM3.1 Offsets extracted from the RHH horizon. Distance given in Nevada State Plane northing (ft).

REFERENCES

Brethauer, G.E., D.L. Healy, C.H. Miller, *Statistical Analysis of the Gravity Method of Calculating the Depth of the Pre-Cenozoic Surfaces in Yucca Flat, Nevada Test Site*, Geological Prospecting, 29: 31–38, 1981.

Brocher, T.M., W.C. Hunter, and V.E. Langenheim, *Implications of seismic reflection and potential field geophysical data on the structural framework of the Yucca Mountain-Crater Flat region, Nevada*, Geological Society of America Bulletin, 110(8): 947–971, 1998.

Dawers, N.H., and M.H. Anders, *Displacement-length scaling and fault linkage*, Journal of Structural Geology, 17: 607–614, 1995.

Dawers, N.H., M.H. Anders, and C.H. Scholz, *Growth of Normal Faults: Displacement-length scaling*, Geology, 21: 1,107–1,110, 1993.

Day, W.C., R.P. Dickerson, C.J. Potter, D.S. Sweetkind, C.A. San Juan, R.M., Drake, II, and C.J. Fridrich, *Bedrock Geologic Map of the Yucca Mountain Area, Nye County, Nevada*, USGS Geologic Investigations Series, I-2627, 1998.

Dula, W.F., Jr., *Geometric models of listric normal faults and rollover folds*, American Association of Petroleum Geologists Bulletin, 75: 1,609–1,625, 1990.

Ferrill , D.A., J.A. Stamatakos, and D. W. Sims, *Normal fault corrugation: Implications for growth and seismicity of active normal faults*, Journal of Structural Geology, in press.

Ferrill, D.A., J. Winterle, G. Wittmeyer, D. Sims, S. Colton, A. Armstrong, *Stressed Rock Strains Groundwater at Yucca Mountain, Nevada*, G.S.A. Today, Geological Society of America, 9(5), 1999.

Rahe, B., D.A. Ferrill, and A.P. Morris, *Physical analog modeling of pull-apart basin evolution*, Tectonophysics, 285: 21–40, 1997.

Sawyer, D.R., R.J. Fleck, M.A. Lanphere, R.G. Warren, D.E. Broxton, and M.R. Hudson *Episodic caldera volcanism in the Miocene southwestern Nevada volcanic field: Revised stratigraphic framework, 40Ar/39Ar geochronology, and implications for magmatism and extension*, Geological Society of America Bulletin, 106: 1,304–1,318, 1994.

Sims, D., D.A. Ferrill, and J.A. Stamatakos, *Role of a ductile décollement in the development of pull-apart basins: Experimental results and natural examples*, Journal of Structural Geology, 21(5): 533–554, 1999.

Tynan, M., U.S. Department of Energy/Yucca Mountain Project, 3-D Modeling, Geologic Framework Model, *Handout at Department of Energy/U.S. Nuclear Regulatory Commission Technical Exchange*, June 3–4, 1999, Rockville, MD.

U.S. Nuclear Regulatory Commission, Issue Resolution Status Report (Revision 1) - Key Technical Issue: Structural Deformation and Seismicity, enclosure to letter dated September 30, 1998, from M.J. Bell, U.S. Nuclear Regulatory Commission, to S.J. Brocoum, U.S. Department of Energy, 1998.

Willemse, E.J.M., *Segmented normal faults: Correspondence between three-dimensional mechanical models and field data,* Journal of Geophysical Research, 102: 675–692, 1997.

Young, S.R., A.P. Morris, and G.L. Stirewalt, *Geometric Analysis of Alternative Models of Faulting at Yucca Mountain, Nevada,* International High-Level Radioactive Waste Management Conference Proceedings, LaGrange Park IL, American Nuclear Society,1,818–1,825, 1993.

APPENDIX F

GLOSSARY

[TO BE DEVELOPED FOR REVISION 3, FY2000]